Mechanisms and Regulation of Plasma Membrane-Endoplasmic Reticulum Membrane Contact Sites in *Saccharomyces cerevisiae*

by

Evan Quon

B.Sc. (Hons), Simon Fraser University, 2012

Thesis Submitted in Partial Fulfillment of the
Requirements for the Degree of
Doctor of Philosophy

in the
Molecular Biology and Biochemistry
Faculty of Science

SIMON FRASER UNIVERSITY
Fall 2018

Approval

Name:	**Evan Quon**
Degree:	**Doctor of Philosophy**
Title:	**Mechanisms and Regulation of Plasma Membrane-Endoplasmic Reticulum Membrane Contact Sites in *Saccharomyces cerevisiae***
Examining Committee:	**Chair:** Rosemary Cornell Professor
	Christopher Beh Senior Supervisor Professor
	Nicholas Harden Supervisor Professor
	Michel Leroux Supervisor Professor
	Michael Silverman Internal Examiner Professor Department of Biological Sciences
	Vanina Zaremberg External Examiner Associate Professor Department of Biological Sciences University of Calgary
Date Defended/Approved:	December 13th, 2018

Abstract

Membrane tether proteins staple the endoplasmic reticulum (ER) to other cellular membranes at Membrane Contact Sites (MCSs), as possible conduits to coordinately regulate lipid metabolism and membrane exchange. To determine the role of ER-PM MCSs in membrane regulation, I generated Δ-super-tether (Δ-s-tether) yeast cells that lack six previously identified tether proteins (the yeast E-Syts Tcb1p-3p; VAP homologs Scs2p and Scs22p; and the TMEM16 homolog Ist2p), as well as the presumptive tether Ice2p. Although Δ-s-tether cells lack direct ER-PM MCSs they were viable, albeit with severe defects in lipid homeostasis and membrane organization. To determine the role of MCSs in non-vesicular sterol transport, the bi-directional exchange of sterols between the ER-PM in Δ-s-tether cells was directly assayed *in vivo*. No significant defects in non-vesicular sterol transport were detected though lipidomic analysis revealed major dysfunction in phospholipid and sphingolipid synthesis. Based on these findings I hypothesized that Δ-s-tether growth defects might be rescued either metabolically, by increasing phosphatidylcholine synthesis through choline addition, or by overexpressing the phospholipid methyltransferase *OPI3*. These modifications did restore growth, but not by re-establishing ER-PM MCSs, suggesting that these membrane attachments are not physically required for lipid transport but rather as regulators of lipid metabolism. Phosphatidylinositol-4-phosphate (PI4P) accumulated in the PM of Δ-s-tether cells, consistent with the observed synthetic lethality between Δ-s-tether mutations and mutations in either the *SAC1* PI4P phosphatase gene or *OSH4*, which encodes a PI4P binding protein. Even though transport assays indicated that MCSs do not mediate ER-PM sterol exchange, we tested if sterols played a role in contact site generation. Cells depleted of sterols by repressing *ERG9*, which encode the sterol specific biosynthetic enzyme squalene synthase*,* exhibited nearly complete coverage of the inner cytoplasmic PM surface with cortical ER. These results support a model for ER-PM MCSs in which they collectively act as a regulatory nexus for coordinating multiple lipid metabolic pathways to control cell membrane composition.

Keywords:

endoplasmic reticulum; lipid transfer proteins; membrane contact sites; membrane lipids; membrane-tethering proteins; non-vesicular transport; plasma membrane; lipid biosynthesis; lipid homeostasis;

Acknowledgments

I would like to express my sincere gratitude to my advisor Dr. Chris Beh for the continuous support of my Ph.D. project and for his patience, motivation, knowledge, and friendship. Throughout my Ph.D. project, his guidance helped me persevere, even when mother nature was making fools of us both.

Besides my advisor, I would like to thank the rest of my thesis committee: Dr. Nicholas Harden and Dr. Michel Leroux for their insightful comments and encouragement.

I thank Dr. Jesper Johansen, Hamida Safi, Dr. Nathan Bialas, Dr. Kyla Hingwing, Dr. Laura Hilton, Julie Pike, Dr. Stephanie Vlachos, Bashe Bashe, Khang Hua, Lyssa Martin, and Sean Hoas for their support and invaluable friendship during the good time and the tough times.

I am grateful to Dr. Lynne Quarmby introducing me to the world research science and Dr. Nancy Hawkins for her guidance and support.

Thank you to my co-adventurer and loving partner, Kestrel Bailey, for supporting me, suffering me, accepting me, and loving me.

Thank you to my mother, Kathy, who has been my biggest fan and supporter my entire life. Thank you to my Father, Gavin, for your love and guidance. You always pushed me to be better.

To my sisters, Vanessa and Mikayla…. You're okay I guess.

Table of Contents

List of Tables

List of Figures

List of Acronyms

δ-ALA,	δ-aminolevulinic acid;
Δ-s-tether	Δ-super-tether
ACAT	Acetyl-CoA acetyltransferase
CDP-DAG	Cytidine Diphosphate Diacylglycerol
cER	Cortical Endoplasmic Reticulum
CRAC	Ca^{2+}-release-activated Ca^{2+}
DAG	Diacylglycerol
DHE	Dehydroergosterol
DIM	Detergent-insoluble membrane
EMC	ER membrane protein complex
ER	Endoplasmic Reticulum
ERAD	ER-Associated protein Degradation
ERMES	ER-mitochondria Encounter Structures
E-Syt	Extended-Synaptotagmins
FFAT	Two phenylalanines in an Acidic Tract
GFP	Green fluorescent protein
HPLC	High-performance liquid chromatography
IPC	Inositol-phosphoceramide
Lam	Lipid transfer proteins anchored at MCSs
LD	Lipid Droplet
LTP	Lipid Transfer Protein
MAMs	Mitochondrial Associated Membrane
MCS	Membrane Contact Site
MECA	Mitochondria-ER Cortex Anchor
MIPC	Mannosyl-IPC
mmPE	Dimethyl PE
mPE	Monomethyl PE
MSP	Major Sperm Protein
MβCD	Methyl-β-cyclodextrin
NE	Nuclear Envelope
NVJ	Nuclear Vacuolar Junction
ORP	OSBP-Related Protein

OSBP	Oxysterol Binding Protein
OSH	ORP *Saccharomyces cerevisiae* Homolog
PA	Phosphatidic acid
PAMs	PM Associated Membrane
PC	Phosphatidylcholine
PE	Phosphatidylethanolamine
PH	Pleckstrin homology
PI	Phosphatidylinositol
PIP	Phosphatidylinositol phosphate/phosphoinositide
$PI(3,4)P_2$	Phosphatidylinositol-3,4-bisphosphate
$PI(3,4,5)P_3$	Phosphatidylinositol-3,4,5-trisphosphate
$PI(3,5)P_2$	Phosphatidylinositol-3,5-bisphosphate
$PI(4,5)P_2$	Phosphatidylinositol-4,5-bisphosphate
PI3P	Phosphatidylinositol-3-phosphate
PI4P	Phosphatidylinositol-4-phosphate
PI5P	Phosphatidylinositol-5-phosphate
PM	Plasma Membrane
PS	Phosphatidylserine
RFP	Red fluorescent protein
RSR	Relative specific radioactivity
SE	Sterol ester
SGA	Synthetic Genetic Array
SMP	Synaptotagmin-like mitochondrial protein
SR	Specific radioactivity
StART	Steroidogenic Acute Regulatory Transfer
STP	Sterol Transfer Protein
STP	Sterol Transfer Protein
TAG	Triacylglycerols
TCB	Tricalbin
TULIP	Tubular Lipid Binding
UPR	Unfolded Protein Response
VAMP	Vesicle-associated membrane protein
VAP	VAMP Associated Protein
WT	wild type

Foreword

Subcellular compartmentalization with functionally distinct intracellular membranes is a defining characteristic of eukaryotic cells. Each organelle membrane within the cell has a distinct lipidomic and proteomic environment; while each compartment serves a specific purpose in the cell and is responsible for a specific set of functions. Some of these functions are restricted to specific organelles, while other cellular functions required coordination across the cell. Therefore, the cell requires precise inter-organelle communication to spatially and temporally coordinate the many intricate and complex processes. The most abundant intracellular organelle is the endoplasmic reticulum (ER) which is a vast and complex network of interconnected membrane responsible for many essential functions. To achieve this coordination, the ER membrane physically associates with every other organelle membrane to facilitate direct inter-organelle communication. These sites of heterotypic membrane association are tightly regulated ultra-structures called membrane contact sites (MCSs). These ultrastructures are relatively well conserved and are responsible for coordinating many different cellular functions depending on affixed membranes. The most abundant MCSs are between the ER and the plasma membrane (PM); there are hypothesized to be conduits for the direct exchange of material and information between opposing organelle membranes. MCSs between the PM and ER (PM-ER MCSs) have been implicated in a variety of other processes such as lipid biosynthesis, intracellular signaling, and intracellular calcium store regulation. In both yeast and mammals, PM-ER MCSs are facilitated by a large group of highly conserved PM-ER tether proteins. As detailed in this thesis, my research aimed to utilize the power of molecular genetics only available in yeast, *Saccharomyces cerevisiae* (budding yeast), to elucidate the mechanisms governing PM-ER MCS functions and regulation.

Chapter 2. Introduction

Section 1.1.2 contains excerpts modified from a manuscript in preparation. The authors and their affiliations are listed below:

Evan Quon[1], Jesper Johansen[1], Christopher T. Beh[1,2]

[1]Department of Molecular Biology and Biochemistry, Simon Fraser University, Burnaby, British Columbia V5A 1S6, Canada

[2]Centre for Cell Biology, Development, and Disease, Simon Fraser University

All conceptualization, writing, and editing were performed by Dr. Christopher Beh and myself.

Section 1.2 contains excerpts modified from the paper that has been published in Lipid Insights (Quon et al., 2016). The authors and their affiliations are listed below:

Evan Quon[1], Christopher T. Beh[1,2],

[1]Department of Molecular Biology and Biochemistry, Simon Fraser University, Burnaby, British Columbia V5A 1S6, Canada

[2]Centre for Cell Biology, Development, and Disease, Simon Fraser University

All conceptualization, writing, and editing were performed by Dr. Christopher Beh and myself.

2.1. Plasma Membrane-Endoplasmic Reticulum Membrane Contact Site function and regulation

2.1.1. The ER is a vast network of tubular and cisternae membrane that associates with every organelle in the cell

The ER is composed of a single continuous network of membrane with different domains, structures, and functions (1). This interconnected network has many diverse functions including lipid synthesis and metabolism; protein synthesis and translocation; protein folding and modifications; intracellular calcium storage and signaling; cell stress responses regulation; and organelle biogenesis (1–5). Generally, the ER can be divided into nuclear and peripheral ER. The nuclear ER (nuclear envelope; NE) is a double bilayer membrane that is contiguous with the ER and contains the cell's genomic material (6). Although the primary function of the NE is to regulate the flux of material in and out of the nucleus via pore complexes, the NE and peripheral ER do share some cellular functions, specifically lipid biosynthesis (7, 8).

The peripheral ER consists of reticulated tubule and flat cisternal membrane (1). The flat sheets of cisternae ER consist of two parallel opposing membranes approximately ~35 nm and 50 nm apart in yeast and animal cells respectively (9, 10). Historically, cisternal ER has also been called "Rough ER" for the high density of ribosomes studded in the membrane, making it the primary location for translation, translocation, post-translational modification, and protein folding (6, 11–13). The cisternae ER and NE are connected by a dynamic network of tubular ER (14). The tubular ER is also called "Smooth ER" because it lacks the ribosomal density of cisternae ER (12). Though the function of tubular ER is not well understood, its higher surface-to-volume ratio relative to cisternae ER suggest that it may be better suited for surface (bilayer) dependent processes like lipid biosynthesis (1). Recently, a trove of research has suggested that one of the primary functions of the ER is to communicate with other organelles. The dynamic and flexible nature of the ER makes it capable of physically contacting every other organelle.

MCSs are highly conserved ultra-structures that occur between two heterotypic membranes of closely opposed organelles (15). The ER has been shown to directly contact the plasma membrane (10, 16), mitochondria (17–19), Golgi (20),

vacuolar/lysosome (21), lipid droplet (LD) (22), endosomal systems (23, 24), and peroxisome (25) (**Fig 1.1**). Each different MCS governs a variety of cellular functions, some of which overlap with other MCSs. Organelles can form MCS independently of the ER. For instance, the vacuole and mitochondria form ultra structures called vacuole and mitochondria patch (vCLAMP) (26). However, ER-mediated MCSs account for most of the directed membrane association. Additionally, although some MCSs were discovered in mammals, such as ER-PM (27, 28), the genetic tools to truly study their function only exist in yeast. Therefore, the characterization and functional analysis of yeast ER-mediated MCSs, specifically PM-ER MCSs, is the primary focus of this thesis.

As discussed below, MCSs are regulated by a diverse set of membrane tethering proteins that participate in the direct membrane attachment (**Table S1**) (16, 29). To be classified as a “tether”, a protein must meet two qualifications: i) a tether must be physically localized to MCSs, and ii) a tether must functionally impact membrane association. Although all tether proteins must meet both qualifications, tethering proteins can be further subdivided based on their functional interaction with membrane association. “Primary tethers” are necessary for membrane association under normal growth conditions and their deletion, whether individually or in combination, reduces the number of discrete MCSs (30). While these primary tethers establish initial membrane contact, other proteins may maintain, stabilize, or augment, MCSs (30). I propose that “secondary tethers” are sufficient, but not necessary, for promoting MCSs. Therefore, deletion of a secondary tether may not affect membrane contact but their overexpression may enhance membrane association. It should be noted that some tether proteins may have additional roles at MCSs and may not simply be membrane staples (30). The distinction between necessary primary tethers and sufficient secondary tethers will be the focus of later chapters. Here we will discuss the various ER-mediated MCSs and the primary tethers that regulate them.

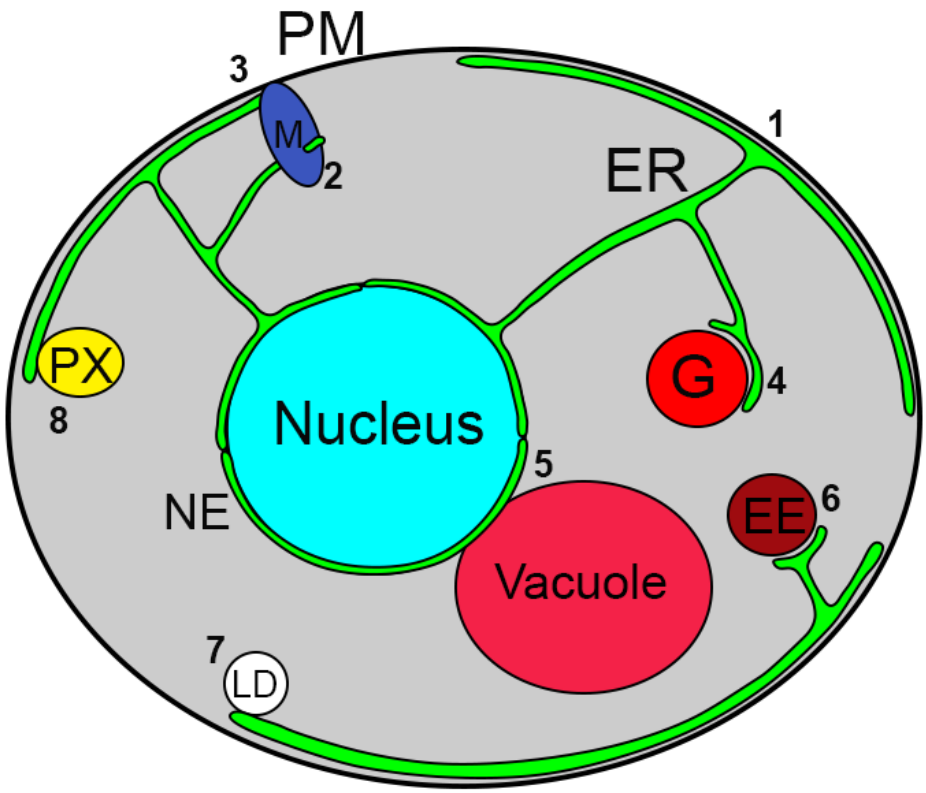

Figure 2.1. Schematic of endoplasmic reticulum (ER)-mediated membrane contact sites (MCS) in yeast.
1) Plasma Membrane (PM)-ER MCS, 2) ER-mitochondria (M), 3) mitochondria-cortex membrane anchor (MECA), 4) ER-Golgi MCS, 5) nuclear envelope (NE) vacuole junction (NVJ), 6) ER-Early endosome (EE) MCS, 7) ER-lipid droplet (LD) MCS, and 8) ER-peroxisome (PX) MCS.

1.1.1.1: Nuclear Vacuolar Junctions

One of the best characterized MCSs in yeast are between the NE and the vacuole. The vacuole is analogous to the mammalian lysosome and is involved in lipid and protein turnover, cell growth regulation, nutrient sensing, and stress responses (31). NE-Vacuole Junctions (NVJ) specifically have been implicated in nuclear microautophagy (piecemeal microautophagy of the nucleus), non-vesicular transport of lipids, lipid biosynthesis, LD biogenesis, and regulating nutrient stress response (21, 32–35). The two major NVJ primary tether proteins are the integral-NE protein Nvj1p and peripheral-vacuolar protein Vac8p which form a tethering complex that links the NE and vacuolar membranes (21, 34, 36–39). Nvj1p also recruits the yeast enoyl reductase Tsc13p and Oxysterol Binding Protein (OSBP)-Related Protein (ORP) homolog Osh1p to the NVJ (32, 36). Tsc13 is an essential outer-nuclear membrane protein required for very-long-chain fatty acid biosynthesis and is required for PMN (40, 41). Osh1p belongs

to a conserved group of lipid binding proteins which will be discussed in depth later, however, the exact role Osh1p plays at the NVJ remains unclear. Interestingly, yeast cells lacking all seven ORP homologs (*osh*Δ cells) have microautophagy defects similar to cells lacking NVJs (36). Osh1p contains an FFAT (two phenylalanines in an acidic tract) motif which binds the major sperm protein (MSP) domain of the yeast Vesicle-associated membrane protein (VAMP)-Associated Protein (VAP) homolog Scs2p (42). Although Scs2p is present throughout the entire ER, Osh1p and Scs2p physical interactions are specific to the NVJ (43). Although Scs2p has the greatest contribution to PM-ER membrane association of any tether protein (16), it is not known if Scs2p or Osh1p contributes to NVJ tethering. Mdm1p is a recently discovered NVJ tethering protein that regulates sphingolipid metabolism and LD biogenesis (35, 44). Mdm1 has a mammalian homolog, sorting nexin 14 (Snx14), but whether they are functional homologs remains to be seen (45).

1.1.1.2: ER-Endosome/Lysosome Membrane Contact Sites

Internalization of extracellular material, PM lipids and proteins is facilitated by a vesicle-mediated process called endocytosis (46). Once budded from the PM, endocytic vesicles enter the endosomal-lysosome/vacuole system, which is the complex network of organelles that regulate trafficking to the vacuole/lysosome for degradation or recycling back to the Golgi and PM (47). In mammals, it has been observed that the ER physically associates with the endosomal-lysosomal system (23, 24, 48, 49). ER-endosome MCSs have primarily been implicated in non-vesicular lipid transport and endosomal maturation, fission, and trafficking (23, 50–52). The mammalian ORP homolog ORP1L and Steroidogenic Acute Regulatory (StAR)-related lipid Transfer (StART) homologs STARD3 and STARD3NL have been shown to bind VAPA at ER-endosome MCSs and may mediate non-vesicular sterol transfer (23, 53). The integral-ER protein, Protrudin, has also been shown to be a tethering protein by binding the late-endosomal resident small-GTPase Rab7 and phosphatidylinositol 3-phosphate (PI3P) (49). Future research will likely expand the list of tether proteins and functions of ER-endosome MCSs.

1.1.1.3: ER-Golgi Membrane Contact Sites

The Golgi complex is the central hub for the secretory system, which receives and modifies newly synthesized proteins and lipids from the ER, then sorts/transports

them to their destination (54, 55). Bi-directional vesicular transport between the ER and Golgi is well understood (56). However, in absence of vesicular transport, lipids such as ceramide and phosphatidylserine (PS) can be trafficked from the ER to the Golgi (57, 58). It is hypothesized that non-vesicular lipid transport happens at ER-Golgi MCSs (59). Although the structural morphology of the Golgi varies from lower to higher eukaryotes (54, 55), there is an abundance of evidence that the ER and Golgi are physically associated. In yeast, COPII vesicle release sites called ER exit sites (ERES) contact the *cis*-Golgi (20), while in mammals, ER is closely associated with the *trans*-Golgi network (59). The role ER-Golgi MCSs play in lipid trafficking in mammals has been well established. The mammalian ceramide transfer proteins (CERT) facilitates non-vesicular ceramide transfer between the ER and *trans*-Golgi (60). *In vitro* evidence has suggested that the prototypical mammalian ORP, OSBP, and a yeast ORP homologs Osh4p, may act as sterols lipid transfer proteins (LTPs) at ER-Golgi MCSs (61, 62), however, this model remains to be confirmed *in vivo*. In contrast to their role in lipid transport, very little is known about the proteins that physically tether the ER and Golgi. Recently, the ER-resident Nvj2p was shown to tether the ER and medial-Golgi in yeast and may contribute to ER-Golgi non-vesicular ceramide transfer during cell stress (63). It has also been suggested that the VAPs may also contribute to ER-Golgi tethering (59). Future research will uncover more factors that regulate ER-Golgi MCSs and elaborate on their cellular functions.

1.1.1.4: ER-Lipid Droplet Membrane Contact Sites

Lipid droplets (LDs) are dedicated to the dynamic storage of neutral lipids, such as triacylglycerols (TAG) and sterol esters (22, 64). Rapid storage and release of lipids from LD is required to maintain membrane lipid composition and energy metabolism and prevent lipotoxicity caused by excess lipid accumulation (65, 66). LD biogenesis nucleates in the ER membrane where neutral lipids coalesce between the two membrane leaflets before budding off (67). Once LDs have separated, some remain physically associated with the ER at ER-LD MCSs (68, 69). In yeast, this process is tightly linked to the NVJ which seems to regulate LD biogenesis in response to metabolic and stress cues (35). LDs are excluded from the vesicular transport system, therefore, MCSs are essential for transferring material and information (22). Recently, the highly conserved seipins (*BSCL2* in humans; Sei1p-Ldb16p in yeast) have been implicated as ER-LD tether protein (70–73). Mutant cells, lacking seipins have LD biogenesis and

function defects (71–73). In *C. elegans,* the acyl-CoA synthase FATP1 and the diacylglycerol acyltransferase DGAT2 have been shown to act as ER-LD tethering proteins and facilitate LD expansion (74). The physiological roles of ER-LD MCSs have yet to be extensively explored, however, future research will likely uncover their role in regulating cell homeostasis.

1.1.1.5: ER-Peroxisome Membrane Contact Sites

The major functions of peroxisomes are to regulate β-oxidation of fatty acids in yeast, and hydrogen peroxide metabolism (75). ER-peroxisome MCSs are essential for peroxisome biogenesis and non-vesicular transport of lipids between the two organelles (25, 76–79). In yeast, the ER-resident Pex3p physically binds peroxisomal membrane protein Inp1p to form a tethering complex (25, 78). It has also been shown that Pex30p contributes to the formation of pre-peroxisomal vesicles during organelle biogenesis and may also function as a tether protein (80). In mammals, it has been suggested that VAP and the peroxisomal-resident Acyl-coenzyme A-binding domain protein 5 (ACBD5) form a tethering complex and facilitate lipid transfer and lipid homeostasis at ER-Peroxisome MCSs (81, 82).

1.1.1.6: ER-Mitochondria Membrane Contact Sites

MCS between the ER and mitochondria were the first identified MCS and initially characterized by electron microscopy by Willam Bernhard in 1952 (83–85). ER-MCSs were further characterized through biochemical purification of the mitochondria-associated ER membranes (MAMs), which are enriched for phospholipid enzymatic activity (86, 87). Mitochondria are required for energy production, lipid metabolism, calcium regulation, and apoptosis, however, they are excluded from the vesicular transport system. Therefore, it is hypothesized that transport of lipids to the mitochondria requires MCSs (88–90). Specifically, phosphatidylethanolamine (PE) synthesis in the mitochondria requires phosphatidylserine (PS) which is made in the ER (88). ER-mitochondria MCSs are facilitated by two separate tether complexes, namely, the ER-mitochondria encounter structures (ERMES) complex and the ER-membrane protein complex (EMC) (17, 18). Both ER-mitochondria tether complexes have functionally been implicated in the regulation of mitochondrial dynamics, inheritance, protein import, lipid transport, mtDNA inheritance, and mitophagy (19, 91, 92). The ERMES complex consists of an ER-membrane protein (Mmm1p), two outer mitochondrial membrane

proteins (Mdm10p, Mdm34p), and a cytosolic adaptor protein (Mdm12p) (17, 93). Mmm1p, Mdm12p, and Mdm34 are all hypothesized to contain synaptotagmin-like mitochondria lipid-binding protein (SMP) domains, which may facilitate non-vesicular transport of lipids (94). However, several studies have shown that in the absence of ERMES, lipid transport between the ER and mitochondria is not affected, which led to the discovery of the EMC (95, 96). The EMC was discovered by screening for mutants with mitochondrial phospholipid biosynthesis defects (18). Mutant cells lacking the six conserved tethering proteins, Emc1-6p, have significant ER to mitochondria PS transport defects (18). Importantly, cell defective for both EMC and ERMES are inviable, suggesting ER-mitochondria membrane association is essential (18). It should be noted that ERMES and EMC may be yeast specific complexes. However, mitochondria-ER MCSs are highly conserved in mammals and facilitated mitochondria-ER tether proteins (**Table S1)**.

1.1.1.7: Mitochondria-ER Cortex Anchors (MECA)

Recently, it has been shown that the ER, PM, and mitochondria can form a triple-membrane association complex called mitochondria-ER cortex anchors (MECA) (97). The main function of MECA is to control mitochondria shape and position during cell division and facilitate proper mitochondrial segregation between the mother and daughter cell (97–99). MECA are facilitated by Num1p and Mdm36p which form a tethering complex (97, 98, 100). Movement of mitochondria is facilitated by Num1p anchoring to the microtubule motor protein dynein (99). Nump1p may also affect cortical ER positioning and nuclear inheritance; potentially by binding Scs2p (99, 101, 102).

1.1.1.8: Plasma Membrane-ER MCSs

In yeast, the most abundant MCS is between the PM and the cortical ER, in that ~45% of the cytosolic face of the PM is associated with cortical ER (10). The PM associated cortical ER is a combination of cisternae and tubular ER which lack ribosomes at their interface (10). PM-ER MCSs were described soon after ER-mitochondria MCSs in the mid-1950's by Porter and Palade, who reported membrane associate between the sarcoplasmic reticulum (SR) and the PM in muscle cells (27). Similar to MAMs, *Pichler et al.* biochemically purified a Plasma membrane-Associated Membrane (PAM) subfraction which corresponded to PM-ER MCSs (103). The PAM subfraction was distinct the ER in lipid and protein composition, showing an enrichment

for phospholipid and sterol biosynthesis machinery (103). In yeast, PM-ER MCSs are mediated by a group of highly conserved primary tether proteins, consisting of the VAP homologs Scs2p/Scs22p, Extended synaptotagmin (E-Syt) homologs the tricalbins (Tcb1p-3p), TMEM16 homolog Ist2p, and Ice2p (16, 29). Each of these tether proteins will be discussed in more detail below. Functionally, PM-ER MCSs regulate lipid biosynthesis, non-vesicular lipid transport, cell signaling, and Ca2+ store regulation (16, 29, 30, 104). The accumulation of lipid biosynthesis proteins and soluble lipid binding proteins has driven the hypothesis that PM-ER MCSs are required for direct lipid exchange between the ER and PM, and the global regulation of lipid homeostasis. In this thesis, I generated a yeast model to directly test these functions.

In addition to lipid regulation, MCSs provide restricted zones for specific and efficient transfer of singling second messengers, such as calcium (105). Localized calcium signaling drive downstream responses including the regulated release of vesicles, the stimulation of mitochondrial metabolic processes, and the release of intracellular calcium stores in the ER or sarcoplasmic reticulum (SR) (106, 107). In metazoan cells, ER-PM MCSs regulate intracellular Ca^{2+}levels through store-operated Ca^{2+}entry (SOCE) (108). In SOCE, Ca^{2+}depletion in the ER triggers oligomerization of the ER-resident stromal interaction molecule 1 (STIM1), which reaches across the ER-PM gap to bind and activate the Ca^{2+}channel Orai1 at the PM. Orai1 activation drives the influx of extracellular Ca^{2+} to refill ER Ca^{2+}stores (109–119). In this regard, STIM1 and Orai1 represent a Ca^{2+}-regulated ER-PM tether complex. Nonetheless, Orai1 and STIM1 are not conserved in *S. cerevisiae* suggesting another mechanism for Ca^{2+}regulation at ER-PM MCSs serves in yeast as the functional equivalent.

Relative to other mammalian cell types, muscle cells have a high degree of PM-ER/SR membrane association (27). Junctional membrane complexes (JMC) are essential for the coupling PM electric excitation to myofilament contraction (E-C coupling) through SR Ca^{2+} release muscle cells or SOCE in non-excitable cells (120, 121). In adult mammalian ventricular cardiomyocytes, JMCs occur underneath the ER at “peripheral couplings” or “dyads” which are tubular PM invagination structures associated cytosolic SR (121). These PM-SR MCSs are mediated by a metazoan-specific class of tether proteins called junctophilins (105, 121–124).

2.1.2. PM-ER Membrane Contact Sites are regulated by a highly conserved group of primary tether proteins

The seven identified primary tethers are necessary for PM-ER contact, but the degree to which each impacts membrane association varies as does the mechanism by which they join membranes (**Fig 1.2**). All tethers are ER integral membrane proteins, but only Tcb1p-3p and Ist2p are predicted to bridge the gap between cortical ER and PM to make direct contact. Given the inherent variability in the distance between cortical ER and the PM (~15 to 60 nm) (10), there is no absolute domain length required for a tether to reach between membranes. In fact, the transverse distance between the cortical ER and PM appears to be highly dynamic and adaptable. Nonetheless, Scs2p/22p and Ice2p either lack obvious PM interaction domains or do not seem to have cytoplasmic domains long enough to span the distance between membranes. In either case, these proteins would require additional binding partners to provide membrane contacts. Forming a bridge through an extended complex of proteins to span between juxtaposed organelles is an established mode of membrane tethering. For instance, none of the four tether proteins involved in the ERMES (ER-mitochondria encounter structure) complex, can establish membrane contact alone (93). For ER-PM MCSs, Scs2p provides the greatest contribution towards establishing membrane contact (16, 125), for which Scs2p likely requires several additional interaction partners to secure tethering (126). A closer inspection of each class of ER-PM tethers reveals unique functions and activities, with the shared and surprisingly non-specific ability to tether cortical ER to the PM.

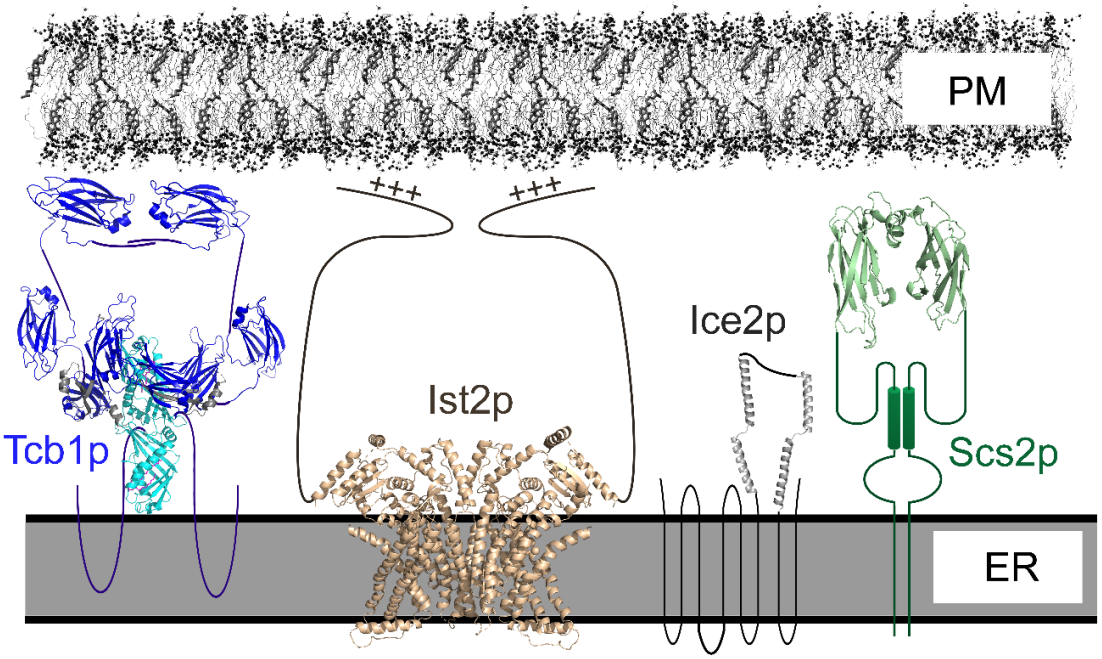

Figure 2.2. Schematic of PM-ER MCS tether proteins in yeast.
Representations of the four classes of membrane tether proteins that are required to establish ER-PM MCSs. Structures shown are based on homologous proteins in which unstructured elements are represented as simple lines. The Tcb1p dimer represents the three yeast tricalbins (Tcb1p-3p) and is shown in the "tunnel model" configuration (127) where structural elements are drawn based on mammalian E-Syt2 SMP-C2a-C2b domain (PBD ID: 4P42 and 2DMG); C2 domains are dark blue (Tcb1p has 4 C2 domains where E-Syt2 has 3 as shown) and SMP domains are light blue. The Ist2p dimer structure is based on the TMEM16 lipid scramblase (PBD ID: 4WIT) with the PM-binding C-terminal polybasic region as indicated (+++). The structure for Ice2p has not been determined though based on its four predicted helical segments and the length of the third cytoplasmic loop, it could extend ~10 nm from the ER membrane. The Scs2p dimer structure is represented by the VAPA MSP homology domain (PBD ID: 1Z9L). Scs22p shares a similar predicted structure though it probably does not extend as far from the membrane. Estimated model sizes are to scale with the ER and PM shown ~20 nm apart.

1.1.2.1: Scs2p/22p and Vesicle-associated membrane protein (VAMP)-Associated Protein (VAPs)

The elimination of the Vesicle-associated membrane protein(VAMP)-Associated Protein (VAP) Scs2p and its paralog Scs22p results in approximately a 50% reduction in ER-PM association within yeast cells, which is unmatched in its severity when compared to the consequence of removing any other tether protein (16, 42, 125). The domain architecture of all VAPs, including Scs2p/22p, consists of three major regions: (i) a Major Sperm Protein (MSP) domain, which includes the binding site for proteins containing the FFAT ("two phenylalanines in an acidic track") motif (128); (ii) a single C-terminal ER transmembrane domain; (iii) an intermediate variable linker region, which is ~ 27 nm in VAPA/B and Scs2p (**Fig 1.2**) (42, 125, 126, 129). Scs2p and Scs22p have both been

shown to bind phosphoinositides, such as PI4P, through their N-terminal MSP domain which extends out towards to PM (130). Considering that the linker region length between the transmembrane domain and the MSP domain in Scs2p could conceivably span the two membranes, it is tempting to postulate that Scs2p directly associates the two membranes. However, Scs2p or Scs22p have not been demonstrated to directly interact with the PM. Furthermore, mutations in the MSP domain that disrupt FFAT motif binding inhibit Scs2p-dependent ER-PM membrane association, suggesting that FFAT protein-MSP domain interactions are required for contact (16). The many functional and physical interactions involving VAPs and Scs2, and by extension Scs22p, suggest they act as scaffolding proteins to assemble additional tethering subunits at MCSs and physically connect organelles (126).

To establish contact between membranes, VAPs/Scs2p/22p likely interact with a bridging protein. About half of VAP interactions involve binding to FFAT-motif proteins, including a subset of the family of Oxysterol Binding Protein-Related Proteins (ORPs) homologs (126). Despite their homology to the canonical mammalian “Oxysterol-binding protein,” only a few can bind oxysterols or sterols. ORPs act as lipid transfer proteins *in vitro* and are implicated in both non-vesicular and vesicular transport pathways(61, 62, 131–137). In yeast, Scs2p, but not Scs22p, binds three of the ORP homologs (Osh1p-3p) via their FFAT motif, found within an N-terminal region aside a PI4P-binding Pleckstrin homology (PH) domain (43, 138–140). Similarly, in mammalian cells, VAPA colocalizes with most of the ORPs including the canonical OSBP (43, 135, 141, 142). These lipid and protein interaction domains dictate, at least in part, the intracellular localization of the three Osh proteins. All yeast Osh proteins are soluble, but in addition to the cytoplasm Osh2p and Osh3p can localize to the cell cortex; specifically Osh1p is targeted to sites at the nuclear-vacuole junction (NVJ) (32, 36). Osh2p and Osh3p localization with cortical ER at PM-ER membrane contact sites is dependent on PI4P and is significantly reduced by repression of Stt4p, the PM PI4P kinase (139). Scs2p/22p binding to FFAT motifs also contribute to Osh2p/3p cortical localization, as well as to Osh1p NVJ localization (42). However, in *scs2*Δ *scs22*Δ mutant cells, Osh3p colocalization with cortical ER and PM-ER MCSs is disrupted, though it remains associated with the PM (139). These results suggested that Osh3p acts as a PM-binding adaptor for a Scs2p tethering complex in the ER; Scs2p is embedded into the ER membrane where it binds to the Osh3p FFAT motif that in turn interacts with the PM via

its PH domain (139). It should also be noted that cortical localization of Osh3 is essential for its functionality while binding to Scs2 is not necessary (139). The Scs2-Osh3p ER-PM tethering complex is also proposed to include Sac1p, which mediates PI4P dephosphorylation at the PM *in trans* from its membrane localization at the ER (139). We previously suggested that this might provide a potential feedback mechanism by which Scs2p regulates MCS formation by modulating the access of Sac1p to PM PI4P (30). Sac1p turn-over of PM PI4P might then control the interaction of Osh3p, and other phosphoinositide-binding tethers, with the PM. If Osh3p acts as a tether adaptor, then elimination of Osh3p would be predicted to significantly reduce PM-ER membrane association. Unfortunately, direct experiments to quantify cortical ER-PM association in either *osh3*Δ or *osh1*Δ-*osh3*Δ cells have not been done. A recent paper reported transient interactions between Osh2p and nascent endocytic sites on the PM near associated "cortical ER rims" (143). Through interactions with the type I myosin Myo5p and Scs2p, it is proposed that Osh2p regulates cortical ER/endocytic site associations to facilitate actin patch assembly for endocytic internalization (143). These studies raise the intriguing possibility that Osh2p and Scs2p couple Myo5p-dependent actin polymerization with the clearance of cortical ER from endocytic sites undergoing membrane invagination. Even in this case, there is no evidence that Osh2p provides a stable link for ER-PM contact. Given the lack of functional data, the role of Osh proteins and other FFAT motif proteins in promoting general MCS assembly is still an important but open question.

Unlike Scs2p, the function of the other yeast VAP homolog Scs22p, is more ambiguous. Within Scs2p, a linker region of ~20 nm separates the MSP and transmembrane domains, which contributes to the overall distance Scs2p can span between the ER and PM (126). Within Scs22p, this linker region is all but absent (129), and it is unclear how this affects Scs22p tethering between the ER and PM if, in fact, Scs22p plays a role. Scs22p and Scs2p are not functionally equivalent. Unlike in *scs2*Δ cells, inositol auxotrophy and telomeric silencing defects are not observed in *scs22*Δ cells (129, 144). However, combining *scs2Δ* and *scs22Δ* mutations causes cells to be more sensitive to inositol deprivation than that in *scs2Δ* cells alone, suggesting at least a minor overlap in function. Though Yeast-two-hybrid analysis both Scs2p and Scs22p bind Osh2p/3p (145). However, when assayed *in vivo* by Bi-Fluorescent Complementation (BiFC), only Scs2p was capable of binding Osh1-3p, whereas Scs22p

did not bind any of the ORPs (43). If Scs2p and Scs22p have a shared role in membrane tethering, it is not manifested in any observed differences in cortical ER-PM association when comparing defects in *scs2Δ* and *scs2Δ scs22Δ* cells (16, 125). In fact, it is still unknown if *scs22*Δ by itself affects cortical ER-PM contact, or if *SCS22* expression rescues membrane association defects in Δtether or Δ-s-tether cells. Although *SCS22* is routinely deleted along with *SCS2* to remove all yeast VAP activity, the specific *in vivo* functions of Scs22p deserves additional attention.

1.1.2.2: Tricalbins (Tcb1p-3p) and mammalian Extended-Synaptotagmins (E-Syts)

The yeast tricalbins (Tcb1p-3p) are a class of conserved ER-PM tether proteins homologous to the extended-synaptotagmins (E-Syts) which can be found in *C. elegans* and from *D. melanogaster* to mammals (38, 146). The secondary structure of the E-Syts/tricalbins contains predicted domains consistent with tether proteins, namely: (i) an N-terminal hairpin, which inserts into the cytoplasmic leaflet of the ER; (ii) a lipid binding synaptotagmin-like mitochondrial protein (SMP) domain; and, (iii) a variable number of C-terminal C2 domains, which promote PM membrane association (**Fig 1.2**) (16, 38, 127, 147–149). Unlike VAPs/Scs2p, the E-Syts/tricalbins are anchored in the ER membrane and directly bind the opposing PM via their C2 domain. C2 domain interactions with membranes are often potentiated by cytosolic $Ca^{2+}$and/or facilitated by the presence of phospholipids, specifically $PI(4,5)P_2$ (104, 149–151). However, the role (if any) of the E-Syts/tricalbins in Ca^{2+}signalling is still unclear

Although C2 domains are often associated with Ca^{2+}-dependent membrane interactions, of the three E-Syt proteins only E-Syt1 seems affected by intracellular Ca^{2+} levels. E-Syt1 is diffusely localized throughout the ER under normal growth conditions, but its cortical localization is significantly enhanced in response to high intracellular Ca^{2+} levels associated with SOCE (104). In contrast, E-Syt2 and E-Syt3 mediate constitutive PM-ER membrane tethering irrespective of Ca^{2+}levels (104, 148, 151, 152). Even though E-Syt1 appears to be affected by SOCE, E-Syt1 plays no detectable role in SOCE regulation suggesting it represents a functionally different class of tethers from STIM/Orai (Giordano et al., 2013). Curiously, even though E-Sty1 can form heterodimers with E-Syt2 and E-Syt3, E-Syt1 exhibits a unique ER localization under normal conditions (104, 127). It is unclear if different heterodimeric combinations enable E-Syts to fulfill a broader spectrum of functional roles or to respond differentially to cellular

stimuli. However, as in yeast, the E-Syts are likely to be functionally redundant with other membrane tethers given that mice lacking all three E-Syts are normal and fertile (153, 154).

The E-Syts/tricalbins have multiple SMP (synaptotagmin-like mitochondrial lipid-binding protein) domains. These share the physical attributes of TULIP (Tubular Lipid Binding) domains that contain deep hydrophobic channels capable of lipid binding (94, 127, 155). It is of no surprise then that E-Syts are implicated in the Ca^{2+}-induced non-vesicular transfer of neutral glycerolipids, such as DAG, between membranes (156, 157). In the "tunnel model," E-Syts are proposed to facilitate direct lipid transfer between membranes by forming a lipid tunnel between membranes (127). In this structural conformation model, the E-Syt SMP domains dimerize to form a long singular channel that binds lipids. However, the length of the SMP dimer tunnel (~9 nm) is less than the observed minimum distances between the ER and PM suggesting that the tunnel is too short to directly span between the ER and PM. Therefore the lipid tunnel model might not faithfully represent the *in vivo* conformation of E-Syts (10, 30, 127, 155, 158, 159). Alternatively, in the "shuttle model," E-Syts act as membrane-anchored lipid transfer proteins (127). Neither of these structural models have been definitively proven, and the precise role of Ca^{2+} in E-Syt/tricalbin-dependent lipid transfer remains to be elucidated. Recent evidence suggests that E-Syt2 may also regulate PI4P by recruiting the mammalian Sac1 to the cortex and modulating its dynamic localization (160). Considering that the tether proteins in yeast were in part discovered through their physical interactions with Sac1p, this dynamic interaction might represent an important function of E-Syts/tricalbins (16).

1.1.2.3: Ist2p and TMEM16

Like the tricablins, Ist2p (increased sodium tolerance 2) is a primary tether that has extended sequences long enough to directly form a bridge between the ER and PM (161). Ist2p consists of: an ER transmembrane region that shares homology with the anoctamin (ANO/TMEM16) protein family; a C-terminal cortical sorting sequence; and a cytosolic inter-membrane linker (**Fig 1.2**). The cortical sorting sequence is a lysine-rich domain of low complexity that mediates direct PM binding by interacting with $PI(4,5)P_2$ (161–164). Ist2p plays a major role at PM-ER MCSs because the deletion of IST2 alone causes a significant reduction in membrane association (16, 161). Indeed, in *scs2*Δ

*scs22*Δ cells, the additional deletion of *IST2* has a greater impact on cortical ER-PM association than the deletion of all three tricalbins (16). Unlike the tricalbins and Scs2/22p, the domain of Ist2p that extends from the ER to the PM has little-defined structure, seemingly serving the simple requirement of being long enough to bridge the inter-membrane distance.

The bulk of Ist2p homology to ANO/TMEM16 proteins is located within its multipass transmembrane domain region (162, 165). Of the ten human ANO proteins (ANO1-10), Ist2p shares the greatest similarity to ANO10 (TMEM16K) (166). Most of the human ANO proteins, such as ANO1/2 (TMEM16a/b), localize to the PM and act as Ca^{2+}-activated Cl^- ion channels. Still, other ANO homologs, such as human ANO6 (TMEM16f) or *A. Fumigatus* and *N. haematococca* TMEM16, appear to have phospholipid scramblase activities (165, 167–173). However, Ist2p does not seem to have a similar scramblase activity when directly assayed (167). Because Ist2p shares a similar Ca^{2+}-dependent sorting pathway to the cortical ER with the mammalian ER Ca^{2+} sensor STIM1, it has been proposed that Ist2p might be a functional equivalent of STIM1 for yeast regulation of cytoplasmic Ca^{2+} (166, 174). The precise function of the homologous Ist2p ER-transmembrane domain remains unknown.

1.1.2.4: Ice2p

Already fulfilling a major role in mediating inter-organelle contact in yeast, Ice2p also has a minor but important role as a primary tether required for ER-PM association (29, 125, 175–179). Ice2p is an ER Type III transmembrane protein that plays two distinct roles in organelle associations depending on cellular growth phase (**Fig 1.2**). When cells exit from stationary phase, Ice2p facilitates a direct physical interaction between the ER and lipid storage droplets, where it regulates the flow of neutral lipids from lipid droplets into the ER (178). As cells re-enter exponential growth, Ice2p rapidly re-localizes to the ER (29, 175, 178). During the normal mitotic cell cycle, Ice2p is found on cortical and perinuclear ER, where it maintains ER network architecture and promotes cortical ER inheritance along the PM from mother cells into growing buds (29, 125, 175, 177, 179). These results reveal a function in both stationary and exponential cells in which Ice2p mediates ER association either with lipid droplets or the PM, suggesting a role as a tether or a regulator of organelle contact to multiple membranes.

At first glance, Ice2p does not meet simplistic expectations presumed of a tether. Unlike the tricalbins or Ist2p, Ice2p likely contains no large cytoplasmic domain or defined lipid binding domains capable of bridging across membrane gaps (178). Nonetheless, the third cytoplasmic loop of Ice2p is predicted to have four amphipathic helices that together with unstructured linker regions might, in fact, extend the same distance as the proposed E-Syt “tunnel model” (~9 nm). This third Ice2p loop appears to be particularly important for its function at lipid droplets, where it might mediate a physical interaction with other organelles either directly or through other proteins (178). When expressed alone the Ice2p cytoplasmic loop localizes to LDs and to a lesser degree the ER (178). Whether this loop is necessary for ER-PM association remains to be seen, though its estimated length is just under the smallest observed distance (16 nm) between cortical ER and the PM (10). Based on these considerations, Ice2p probably acts together with adaptor proteins to contact membrane targets, as proposed for Scs2p and Scs22p. It should be noted that artificial PM-ER tether proteins (artificial staples) that functionally complement some defects associated with loss of directed PM-ER membrane association is only predicted to extend ~10 nm from the ER to the PM (see below). It is therefore naive to think that tethering capability can be prejudged solely based on estimated trans-membrane linker lengths.

In *ice2*∆ cells, most small budded cells show significant cortical ER-PM association defects, with a significant percentage of cells showing no ER within daughter buds at all (175). In *ice2*∆ mother cells, less continuous peripheral ER was also observed suggesting that Ice2p maintains ER at the cortex for its delivery into the bud (175, 179). Functional interactions between *ICE2* and *SCS2* suggest that *ICE2* acts in parallel with *SCS2,* most likely to further support ER inheritance by mediating its localization at the cell periphery (125, 129, 177). These effects appear to be specific to the cortical ER network, given that the absence of *ICE2* and *SCS2* does not affect nuclear or cytoplasmic ER (177). More to the point, the residual ER-PM association that persists in Δtether cells (16) is all but eliminated when *ICE2* is deleted in these cells (29). The deletion of all seven tethers has severe functional consequences that were not observed when *ICE2* was unaffected in ∆tether cells. The generation of ∆-s-tether cells revealed specific lipid defects and surprising genetic interactions that were formerly masked by the presence of the Ice2p tether. With the ∆-s-tether strain, we have the

means to test how ER-PM MCSs functionally contribute to the regulation of membrane growth.

2.2. PM-ER Membrane contact sites facilitate direct lipid exchange through a non-vesicular transport mechanism

Two general modes of transfer dictate lipid exchange between membranes within the cell: vesicular and non-vesicular lipid transport (180–182). Given that secretory vesicles are inherently composed of lipids, it is not surprising that vesicles mediate the bulk of lipid transport. In contrast, lipid transfer can also occur in the absence of vesicles through mechanisms that are less well defined. This transfer could happen spontaneously (Passive) or may require the aid of LTPs or lipid tunnels (Facilitated) (**Fig 1.3**). In addition to *bona fide* soluble LTPs that shuttle lipids between membranes, lipid exchange also involves specific sites where intracellular membranes are closely apposed. In fact, LTPs and MCSs appear to be inter-related mechanisms that together mediate non-vesicular transport. In this section, I will discuss the plausibility of various non-vesicular lipid transport mechanisms.

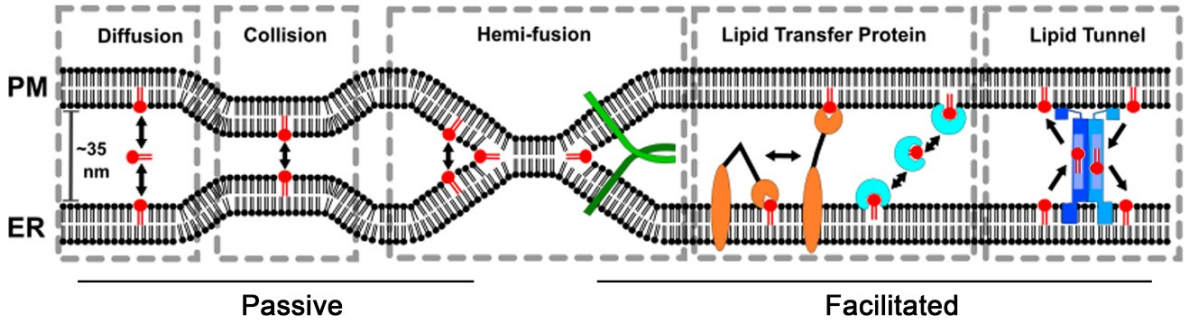

Figure 2.3. Mechanistic models for non-vesicular lipid transport between the ER and PM at membrane contact sites.

Hypothetically, lipids exchange (red) between membranes involves passive or facilitated mechanisms. Overcoming a large energy barrier due to lipid exposure to the aqueous cytoplasm, passive lipid exchange models (left) involves spontaneous lipid transfer in the absence of a protein intermediate. “Diffusion” occurs when a lipid is ejected into the aqueous phase, followed by its diffusion and re-insertion to an acceptor membrane. “Collision” of membranes might permit a direct exchange of lipids when bilayers transiently collide, thereby minimizing exposure to the aqueous cytoplasm. “Hemi-fusion” might involve a more persistent collision whereby direct lipid exchange occurs by cis-leaflet fusion between the PM and ER membranes. The hemifusion intermediate might also be facilitated by proteins (green), leading to incomplete SNARE-mediate fusion (*e.g.* between the ER-resident R-SNARE Sec22p and a PM-localized Q-SNARE). Facilitated mechanisms might also involve the active exchange of lipids between membranes via

membrane-bound or soluble “Lipid Transfer Proteins” (LTPs), or “Lipid Tunnels” (blue) that contain putative hydrophobic channels mediating a rapid lipid flux between membranes.

2.2.1. Passive lipid transport happens independently of any proteins

The physical properties and morphological architecture of membranes at contact sites are conserved from yeast to humans (105). In yeast, PM-ER contact is extensive where ~45% of the inside surface of the cortex is covered with ER tubules, and PM and ER membranes are separated on average by 33 nm (10). Given that calcium can readily traverse this negligible distance at membrane contact sites in muscle cells, it is tempting to speculate that lipids might as well. Without the assistance of an associated protein transporter, spontaneous lipid exchange between two membranes could theoretically occur through several mechanisms: (i) aqueous diffusion; (ii) membrane collision; and (iii) transient bilayer hemifusion (**Fig 1.3**).

As one of the least hydrophobic lipids, unesterified cholesterol is arguably a prime candidate for a lipid that can be transferred by aqueous diffusion between membranes at contact sites. Aqueous diffusion involves the first-order kinetics of lipid desorption from a donor membrane into the aqueous cellular milieu, followed by diffusion and re-insertion of the lipid into an acceptor membrane (**Fig 1.3**) (181). However, because the step of lipid desorption from the donor membrane is rate-limiting, this type of spontaneous lipid transfer is not contingent on membrane proximity to the acceptor. As determined *in vitro*, the half-time of spontaneous cholesterol transfer between donor (20 mol % cholesterol) and acceptor vesicles is 2.3 h (183), but *in vivo,* the approximate half-time of cholesterol exchange between the ER and PM is 4 min (184). Thus, the amount of cholesterol that is spontaneously ejected into the aqueous phase can only account for 3% of the observed amount transferred *in vivo*. For more hydrophobic lipids, half-times for transfer are much longer (185), precluding aqueous diffusion as a general mode of lipid transfer. For example, the half-times for spontaneous transfer between membranes for phospholipids such as 1-palmitoyl-2-oleoyl PC and dipalmitoyl PC are 48 and 83 h, respectively (183, 186). It is true that for measurements involving biological membranes containing embedded proteins, the physiochemical nature of the bilayer might have an unpredicted effect on lipid ejection. However, the data suggest that even for less-hydrophobic lipids aqueous diffusion across the aqueous gap at contact sites is insufficient to meet the cellular requirement for lipid exchange.

In contrast to aqueous diffusion, a direct exchange of lipids might result from stochastic collisions of two membranes, without exposing hydrophobic lipid side chains to the cytoplasm (**Fig 1.3**). Contact sites could promote direct membrane interactions as required by both lipid collision and facilitated collision models (90). In these models, lipid exchange proceeds either though superficial surface interactions or partial fusion between donor and acceptor membranes (181). Facilitated collision also involves stressing the packing order of lipids to cause their protrusion from the bilayer, thereby decreasing the energy required for transfer. Through facilitated or passive mechanisms, donor and acceptor membranes might completely or partially (hemifusion) fuse, allowing lateral diffusion of lipids between bilayers (**Fig 1.3**) (90). For instance, it has been shown that the ER-resident R-SNARE Sec22p interacts with the PM-localized Q-SNARE to facilitate an interaction between PM and ER membranes, which based on known SNARE interactions could be postulated to promote partial membrane fusion(187). However, Sec22p was experimentally shown not to mediate partial fusion because membranes at contact sites where it is present do not get closer than ~15 nm apart and lipid mixing does not occur (187). Although these facts alone do not preclude the existence of short-lived membrane fusion bridges, the inability to detect them suggests that they cannot be major conduits for lipid exchange. More likely are models in which lipids are actively transported by protein shuttles, such as LTPs, or possibly through proteinaceous tunnels that span the gap between membranes at contact sites (Fig 1.2). In agreement with these models, isolated PM-ER membrane contact sites from “unroofed cells” (where the cell membrane is sheared away, dispersing the cytoplasm and leaving the inner face of the cell surface) exhibited no detectable passive sterol or phospholipid transfer (188). However, these results would also seem to preclude the possibility of any lipid-transferring tunnels or membrane-bound LTPs, which ought to have been present and active in these isolated contact sites (assuming that sterol transfer occurs at these contact sites in the first place). Unfortunately, soluble ancillary regulators required by membrane-bound transfer proteins would also be lost using this experimental approach. These results notwithstanding, several membrane-associated lipid transfer proteins are found at membrane contact sites.

2.2.2. Facilitated non-vesicular lipid transport is mediated by soluble and membrane-bound LTPs and possibly lipid tunnels

Soluble LTPs such as the ceramide transfer protein CERT and the sterol carrier STARD4 represent paradigms for non-vesicular lipid transport. As reviewed by others (189, 190), their mechanisms of lipid capture, lipid shielding from the aqueous cytoplasm, and trafficking to target membranes are well described. CERT and other soluble LTPs are also enriched at membrane contact sites, suggesting an additional complexity in the mechanism of non-vesicular lipid transport (32, 36, 42, 139, 176, 191).

The ORPs represent a potential class of LTPs (133, 135, 192). In yeast and mammalian, many ORPs are recruited to MCSs, specifically PM–ER contacts (**Table S5** and **Table S6**) (42, 62, 131, 136, 137, 139, 191). Humans have twelve ORP homologs with 16 different isoforms, while yeast have seven ORPs homologs called the "*OSHs";* all of which are related to one another through their ORP Related Domain (ORD) (**Fig 1.4**). Several *OSHs* have variable N-terminal extensions and are referred to as the "Long" *OSHs*, while the "Short" *OSHs* consist of only an ORD (*OSH4-7*) (133). The major characteristic of the ORD is the presence of a lipid binding pocket (134, 136, 193). Although, ORPs were initially discovered for their ability to bind oxysterols and sterols, not all ORPs bind sterols (**Table S6**). In fact, several of the Osh proteins only bind phospholipids, such as Osh3, Osh6, and Osh7 (140, 194). Because all *OSHs* are capable of binding lipids in an aqueous environment, it has been hypothesized that all ORPS represent a class of soluble LTPs. Recent *in vivo* evidence has suggested that Osh6p and Osh7p and their mammalian homologs ORP5 and ORP8, are capable of binding PS and PI4P and act as PS/PI4P counter-transporters (**Fig 1.5**) (136, 195).

Figure 2.4. Yeast Osh protein domains and structure of Osh4p.
Upper, domains of the canonical mammalian OSBP compared with all seven yeast Osh proteins. ORPs are defined by the ORD (highlighted in yellow), within which is the SEQVSHHPP signature motif found in all ORPs. The ORP superfamily can be divided into short and long subgroups. The latter contains protein-binding domains including a FFAT motif, ankyrin repeats (ANK), or a Golgi dynamics (GOLD) domain. Long Osh proteins also contain a PH domain that binds PIPs. In Osh4p (green), a conserved region (orange) corresponds to the surface region that associates with anionic lipids, such as PI(4,5)P2. The corresponding sterol-bound (red) and PI4P-bound (purple) structures of Osh4p show the relative positions of these domains on the folded protein (lower). This Figure and text was originally published in the Journal of Biological Chemistry. Beh, C T., McMaster, C.R., Kozminski, K.G., and Menon, A.K. Detour of Yeast Oxysterol Binding Proteins. J. Biol. Chem. 2012; Vol 287(14):11481-8(133).

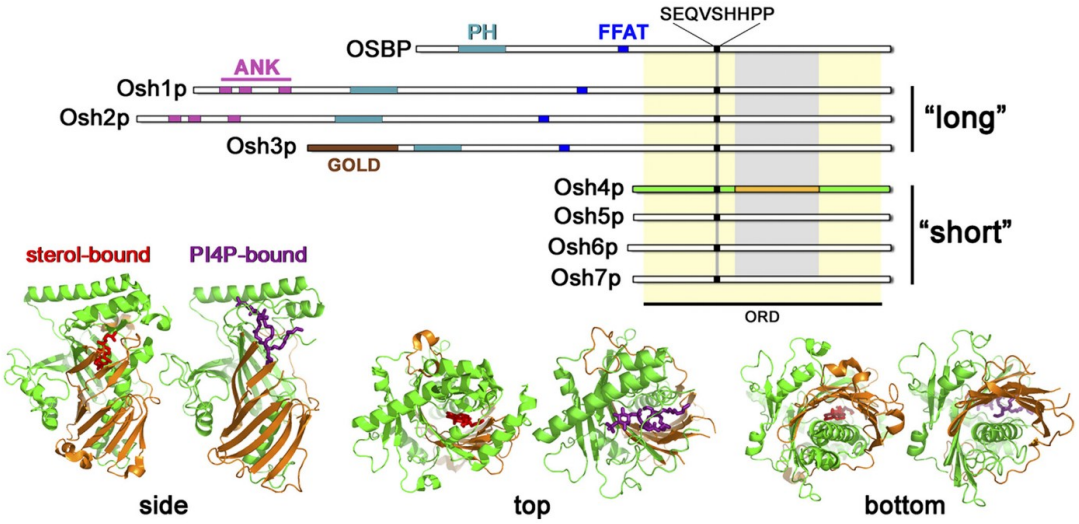

The largest concentration of PS is on the PM cytoplasmic leaflet, while the source of PS in the ER has relatively low PS concentrations (196). Therefore, Osh6p/7p and ORP5/8 must "anterograde" transport PS against its concentration gradient from the ER to the PM. The current model suggests the anterograde PS transport is "powered" by coupling "retrograde" counter-transport of PI4P from the PM back to the ER (**Fig 1.5**) (197). PM PI4P is also relatively high compared to the ER (198). Once in the ER membrane, PI4P is rapidly dephosphorylated by phosphatidylinositol phosphate (PIP) phosphatase Sac1p to maintain a steep PI4P concentration gradient. This model has been suggested to also be true for other ORPs such as Osh4p and Osh1p in yeast and OSBP in mammals (**Fig 1.5**) (61, 62, 199, 200).

Although proof of concept has been shown *in vitro* for Osh4p and Osh1p to act as a sterol/PI4P counter-transporter between the ER and Golgi or vacuole, respectively (61, 62, 199), this model remains to be confirmed *in vivo*. It should be noted that deletion of *OSH4,* or elimination of all seven *OHSs* (*osh*Δ cells), has no impact on non-vesicular sterol transport from the ER, where sterols are synthesized, to the PM where sterols are concentrated (184). In hypoxic cells forced to take up exogenous sterols, the redistribution of sterols from the PM to internal lipid droplets (involving several intermediary steps, including ER sterol esterification) slows by ~50% when ORPs are eliminated (184). This small effect was suggested to be a downstream consequence of eliminating Osh protein function. In contrast, the elimination of all yeast ORPs greatly increases PI4P levels, which led to the proposal that the primary and collective function

of yeast ORPs actually involves phosphoinositide regulation (131, 184). Phosphoinositides play an important role in regulating membrane contact by tethering proteins, as discussed later. Regardless of how sterol distribution is affected, LTPs, like the ORPs, seem to regulate lipid transfer and phosphoinositide metabolism, which affect the bilayer properties of the PM and ER membranes.

Additionally, the counter-transporter model has put into question the ability of Sac1p to work *in trans* at the PM (139). Zewe *et al*. showed that the mammalian Sac1 poorly dephosphorylates PM PI4P (201), however, the PM activity of Sac1 can be significantly enhanced if an extended trans-membrane linker region is added to the cytosolic phosphatase domain of Sac1. This suggests that Sac1 is capable of dephosphorylating PM PI4P directly but is physically inhibited by its reach. However, it should be noted that PM-ER MCSs exist in a range of distances between ~15-60 nm. It is possible that the PM activity of Sac1 could be regulated by an unknown mechanism that regulates PM-ER MCS distance (202). Additionally, models in which Sac1 works *in trans* or *in cis* are not mutually exclusive, though a *trans* activity exclusive model does preclude the PS-PI4P counter-transport models.

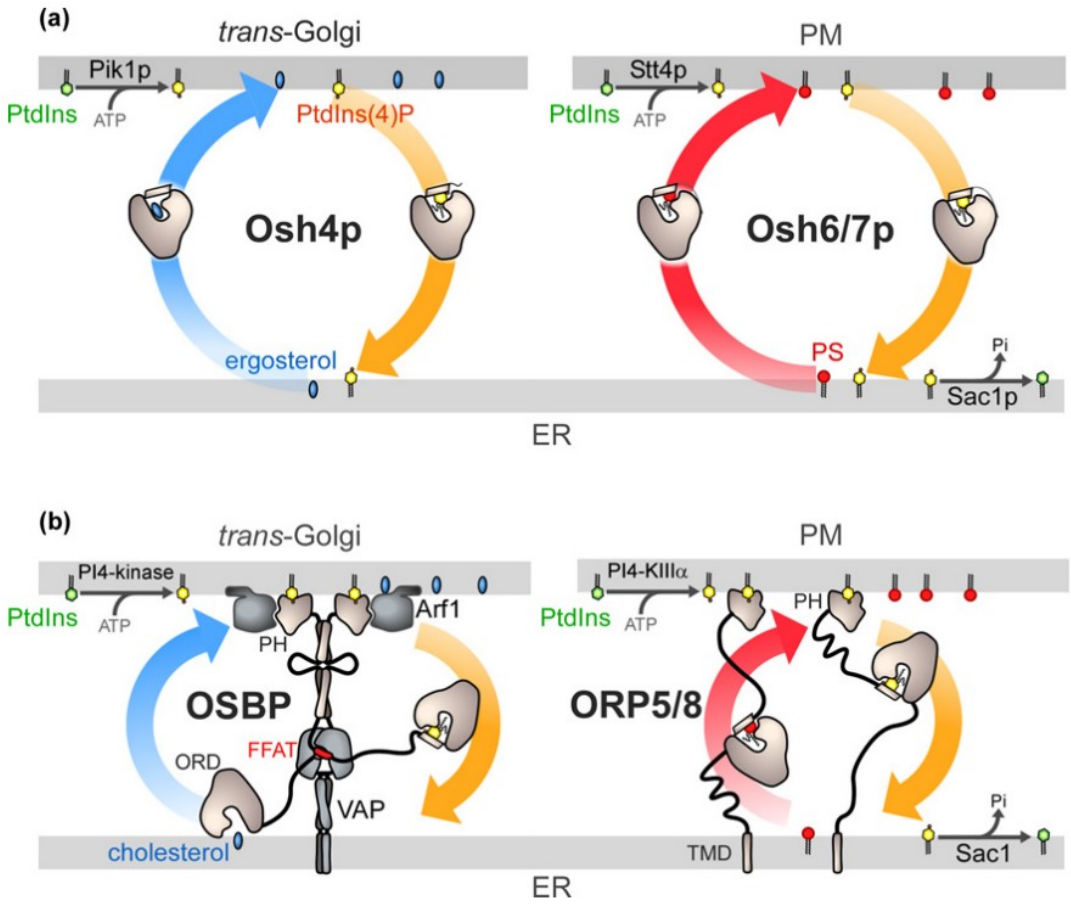

Figure 2.5. Lipid exchange by ORP/Osh proteins at membrane interfaces
(a) Sterol and PS are synthesized in the ER. Osh4p and Osh6/Osh7p transport ergosterol or PS from the ER to the trans-Golgi or the PM, respectively, and PI4P in the backward direction. PI-4 kinases ensure the ATP-dependent phosphorylation of PI into PI4P. At the ER, Sac1p hydrolyzes PI4P into PI. Maintenance of the PI4P gradient would allow the vectorial transport of sterol or PS, thereby generating a gradient for these lipids. (b) OSBP interacts via its FFAT motif with the VAP receptors and, via its PH domain, with GTP-bound Arf1 and PI4P. ORP5/8 are anchored to the ER by TMDs and bind to the PM PI4P with PH domains. These multidomain ORPs must bind the ER and a second membrane to exchange lipids. This figure and text was originally published in Drin G., Moser von Filseck J., and Copic A., Biochemical Society Transactions, 2016. (200)

An example of such a membrane-bound LTP is the mammalian integral membrane protein, STARD3 (Steroidogenic Acute Regulatory (StAR)-related lipid Transfer (StART) domain protein 3) (190). STARD3 is a representative of a large protein family in which the prototypical member, StAR, transfers cholesterol from the outer to the inner-mitochondrial membrane (190, 203–205). STARD3 is tethered to the late endosomal membrane through its MLN64 N-terminal (MENTAL) domain. It uses its C-terminal StART domain to capture cholesterol from the late endosomal membrane and then to transfer it to the ER (53, 190, 206–208). For STARD3, the StART domain has

been proposed to swing between these membranes to mediate sterol transfer (190), though direct experimental evidence is needed (209). Even though STARD3 transfers cholesterol *in vitro* (208, 210), disruption of its StART domain *in vivo* has modest physiological consequences (209). In this regard, STARD3 might be functionally redundant for cholesterol transport *in vivo*, or STARD3 might have another important function independent of its StART domain. STARD3 has a close homolog called "STARD3 N-terminal Like" (STARD3NL), which completely lacks a StART domain (207). Through their FFAT domains, both STARD3 and STARD3NL bind VAPA and VAPB, two mammalian "VAMP/synaptobrevin-associated protein" homologs (53). The FFAT motif links STARD3 and STARD3NL to the ER via VAP and the MENTAL domain anchors STARD3 and STARD3NL to late endosomes. Recently, several yeast StART protein homologs, Ysp1p, Ysp2p, Sip3p, and Lam4p-Lam6p, have been identified (211, 212). All members contain one or more ER-transmembrane domains and several have PH domains permitting *trans* association with other membranes. These properties suggest a mechanism of action similar to STARD3, where LTP function is coupled with the capability as "secondary" tether proteins to bring acceptor membranes closer for direct lipid transfer. In fact, it has been shown that Lam6p regulates the size and expansion of membrane contact sites for multiple inter-organelle associations (213). As far as some StART domain proteins are concerned, it is clear that they have a complex range of functions.

In contrast to LTPs, the "Tunnel model" postulates that protein bridges span the distance between the PM and ER and facilitate direct lipid transfer through a hydrophobic channel (**Fig 1.3**) (127). Examples of potential tunnel proteins include the E-Syts, a family of "extended synaptotagmin-like proteins" anchored to the ER membrane (104, 149, 214). E-Syts are integral membrane proteins that contain multiple Ca^{2+} binding C2 domains involved in phospholipid binding (149). and a synaptotagmin-like mitochondrial lipid-binding protein (SMP) domain that forms a hydrophobic groove when dimerized (94, 104, 127, 149, 151, 214). Similar SMP domains are also found in the Mmm1p/Mdm12p/Mdm34p core components of ERMES complex (94), which tethers the ER and outer mitochondrial membranes together and is implicated in direct phospholipid exchange between these membranes (17), It was initially proposed that the ERMES complex forms a lipid-binding tunnel for shuttling lipids between the ER and mitochondria (93, 127), but an in-depth structural analysis of the core ERMES complex

components sheds doubt on whether any contiguous tunnel or channel can form through these proteins (127, 215). In so far as the E-Syts are concerned, it was argued that the tunnel structural conformation might be too short to span the observed gap between the PM and ER but in an alternative “shuttle conformation” the E-Syts might reach across (127). These structural models suggest that the ERMES complex and the E-Syts might act more like transmembrane domain-tethered shuttles/LTPs than tunnels (**Fig 1.3**).

2.3. Regulation of lipid biosynthesis in yeast

Lipids are organic molecules which are soluble in non-polar organic solvents. As one of the four classes of biological macromolecules they are an essential component of all cells. Eukaryotic cells invest a great deal of energy in synthesizing thousands of different lipid species with varying degrees of complexity (216). Therefore, from an evolutionarily perspective there must be a reason for the cell to dedicate so much energy to synthesize lipids. Each organelle membrane has a distinct lipid composition which is maintained by integrating lipid biosynthesis, transport, and degradation/turnover (196). Each distinct lipid composition functionally accommodates the corresponding organelle membrane requirements. Lipids serve many functions in the cell including acting as energy reservoirs, cell signaling molecules, protein localization markers, and cell membranes matrices (196).

There are eight major classes of lipids: i) fatty acyls, ii) glycerolipids, iii) glycerophospholipids, iv) sphingolipids, v) sterol lipids, vi) prenol lipids, vii) saccharolipids, and viii) polyketides (216). The main structural lipids in eukaryotic membranes are glycerophospholipids, sphingolipids, and sterols; these will be the focus of this thesis. Yeast are an optimal system to study lipid metabolism because they use a relatively simple and conserved network of lipid biosynthesis pathways that only produce several hundred lipid species, as opposed to the tens of thousands in mammals (196, 216). Considering the enrichment of lipid biosynthesis enzymes at PM-ER MCSs, I hypothesized that PM-ER MCSs regulate lipid biosynthesis by coordinating the interconnected biosynthetic pathways. Here I will discuss the major lipid classes and how their synthesis and regulation are interconnected.

2.3.1. The basic components of complex lipids are fatty acids (FA)

Despite the large chemical variety of lipids in yeast and mammals, they all have the same key carbon precursor, is Acetyl-Coenzyme A (CoA). Acetyl-CoA is the primary building block used to make fatty acids (FA), which ultimately becomes complex glycerophospholipids and sphingolipids, or are used to make sterols (217). FA are carboxylic acids of varying carbons chain lengths (4-26) and degrees of saturation (217, 218). An organism's FA repertoire is the main contributor to lipidome diversity and complexity. FA can be acquired by *de novo* synthesis, hydrolysis/turnover of complex lipids/lipidated proteins, or exogenous uptake (219). Yeast have a relatively simple FA repertoire producing only saturated or mono-unsaturated FAs between 10-26 carbon long chains (220). The major classes of FA are C16:1 (palmitoleic acid), and C18:1 (oleic acid), C16 : 0 (palmitic acid) and C18:0 (stearic acid); while the minor FA are C14:0 (myristic acid) and C26:0 (cerotic acid) (220).

In yeast, *de novo* synthesis of FA is initiated in the cytosol and mitochondria by Acc1p and Hfa1p, respectively, by converting acetyl-CoA to malonyl-CoA. Malonyl-CoA serves as the building block for further elongation by FA synthase (FAS) (221, 222). Most medium and long chain FA are produced by the cytosolic FAS complex, consisting of six Fas1p and six Fas2p subunits (223). In contrast, the mitochondrial FAS complex (Cem1p, Oar1p, Htd2p, Etr1p and Ppt2p) plays a smaller role in FA synthesis (217). Synthesis of very long chain FA (VLCFA) occurs in the ER membrane by the elongases, Elo1-3p, which are required for sphingolipid production (224, 225). Desaturation of FA is catalyzed by the acyl-CoA Δ9-desaturase Ole1p in the ER (226). Through these processes, yeast can produce many different FA species which contribute to a diverse lipidome.

2.3.2. Glycerophospholipid biosynthesis and regulation

Glycerophospholipids are amphipathic molecules consisting of two fatty acids and a phosphate head group attached by a glycerol backbone. In an aqueous environment, glycerophospholipids form bilayers with the hydrophilic head groups facing the aqueous environment and the hydrophobic FA tails forming the membrane core (196). In yeast and mammals, the major glycerophospholipids (phospholipids) are phosphatidylcholine (PC), phosphatidylethanolamine (PE), phosphatidylinositol (PI),

phosphatidylserine (PS) and their precursor phosphatidic acid (PA) (218). Each of the major phospholipids have a distinct molecular geometry depending on i) FA tail length, ii) saturation, and iii) head groups size (196). These properties affect the width, curvature, and fluidity of lipid bilayers (227). For instance, PC and PI are primarily cylindrical lipids that form a flat lipid bilayer; PE, PS, and PA are instead conically shaped, inducing negative curvature (11, 196, 227, 228). For this reason, PE and PS are primarily found on the inner leaflet of organelle membranes (**Fig 1.6**) (196, 229–231).

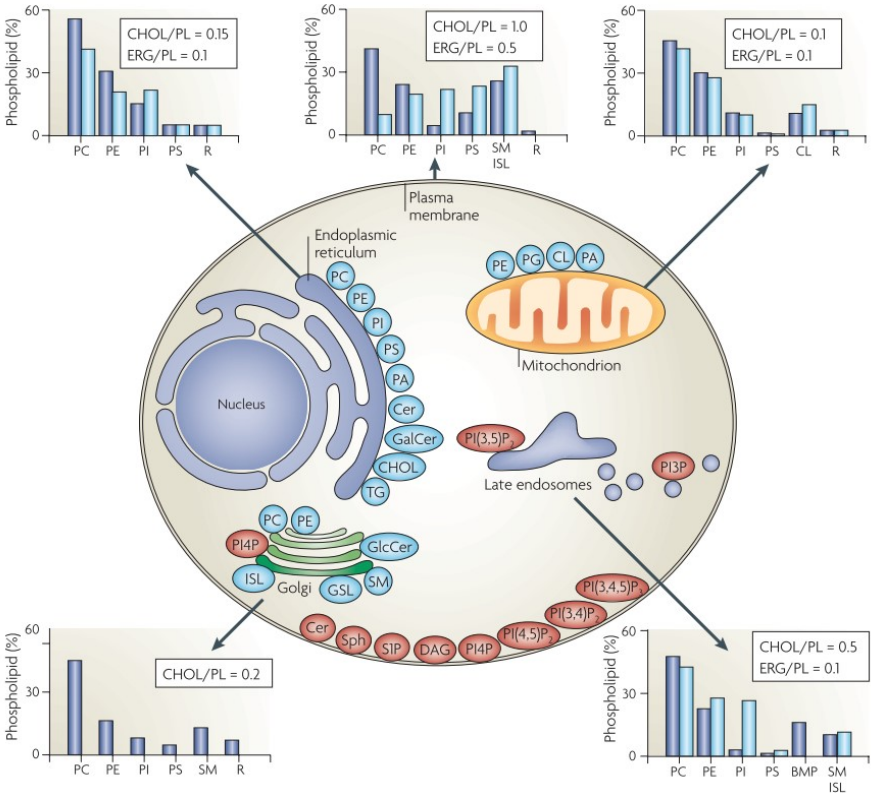

Figure 2.6. Lipid synthesis and steady-state composition of cell membranes.

The lipid composition of different membranes varies throughout the cell. The lipid compositional data (shown in graphs) are expressed as a percentage of the total phospholipid (PL) in mammals (blue) and yeast (light blue). As a measure of sterol content, the molar ratio of cholesterol (CHOL; in mammals) and ergosterol (ERG; in yeast) to phospholipid is also included. The figure shows the site of synthesis of the major phospholipids (blue) and lipids that are involved in signaling and organelle recognition pathways (red). The major glycerophospholipids assembled in the endoplasmic reticulum (ER) are PC, PE, PI, PS, and PA. In addition, the ER synthesizes ceramide (Cer), galactosylceramide (GalCer), cholesterol and ergosterol. The Golgi lumen is the site of synthesis of sphingomyelin (SM), complex glycosphingolipids (GSLs) and yeast inositol sphingolipid (ISL) synthesis. Approximately 45% of the phospholipid in mitochondria (mostly PE, PA, phosphatidylglycerol (PG), and cardiolipin (CL)) are autonomously synthesized by the organelle. Bis-monoacylglycerol-phosphate (BMP) is a major phospholipid of mammalian late endosomes. PI(3,5)P_2; PI(4,5)P_2, PI(3,4,5)P_3, PI4P, PI3P has distinct organelle localizations. Reprinted by permission from Springer Nature, Nature Review Molecular Cell Biology, Membrane

lipids: where they are and how they behave, van Meer G., Voelker D., and Feigenson G. W., 2008 (196).

Each organelle membrane has a different glycerophospholipid composition, which can change based on growth conditions and cell cycle (**Fig 1.6**) (217, 232). Under standard growth conditions, whole cell homogenate normally consist of 20.3% PI, 14.0% PE, 14.3% PC, 8.3% PA, and 1.8% PS (220). Intracellularly, PC is a major lipid in the ER, nuclear envelope, mitochondrial, vacuole, and endosomal membranes; in contrast the PM has relatively low amounts of PC (**Fig 1.6**) (233). In fact, the PM is highly enriched for PS, and the primary store of PS in the cell (217). It was commonly believed that PC was the dominate glycerophospholipids in yeast (233); however, PI has also been shown to be the major lipid, constituting up to 30% of the entire lipidome (220, 232). This revelation is mirrored in the functional importance of PI, which will be discussed in depth later. In addition to the subcellular lipidomes, each bilayer leaflet has a specific lipid environment. For example, the PM outer leaflet consists primarily of sphingolipids and PC, while the inner leaflet consists of PE, PS, PIPs (234). Even though there is a broad diversity of lipid concentrations across the cell, most glycerophospholipids, are synthesized in the ER. The two main *de novo* synthesis pathways are the CDP-DAG pathway and the Kennedy pathway; both are highly conserved and interconnected (**Fig 1.7**).

1.3.2.1: Dynamic balance of PA and DAG regulates glycerophospholipid biosynthesis

In eukaryotic cells, PA is an essential precursor to glycerophospholipids and stored neutral lipids (235). The CDP-DAG pathway uses PA as a precursor to produce PS, PC, PE, PI, cardiolipins (CL) and complex sphingolipids (**Fig 1.7**). However, PA is also rapidly and reversibly dephosphorylated to diacylglycerol (DAG) which is either converted to TAG for lipid storage or used to make PE and PC via the Kennedy pathway (**Fig 1.7**). Therefore, the dynamic balance of PA and DAG is tightly linked to membrane composition and energy storage regulation.

In yeast, PA synthesis occurs in two steps: i) first Sct1p and Gpt2p convert Glycerol-3 Phosphate to lyso-PA (236), ii) then Slc1p, or its homolog Ale1p, convert lyso-PA to PA (237) (**Fig 1.7**). PA can be dephosphorylated to produce DAG by the PA phosphatase Pah1p, or the broader lipid phosphatases Lpp1p and Dpp1 (238–241).

Pah1p accounts for nearly all PA phosphatase activity related to glycerophospholipid and TAG synthesis (239). Under normal conditions, Pah1 is phosphorylated by the Pho85p-Pho80 protein kinase-cyclin complex or the cyclin-dependent kinase Cdc28p, causing it to be cytosolically localized (242). Dephosphorylation of Pah1p by the ER-resident Nem1p/Spo7p phosphatase complex causes Pah1p to become membrane-bound and activate (241, 243, 244). Phosphorylated Pah1p is normally rapidly degraded, allowing for stringent enzymatic regulation (245). DAG levels are also modulated by the DAG kinase, Dgk1p, which phosphorylates DAG back to PA (246). Although, PA (CDP-DAG pathway) and DAG (Kennedy pathway) both contribute directly to PC/PE synthesis pathways, growth conditions and available nutrients (ie. choline/ethanolamine) determine which pathways are more active (247).

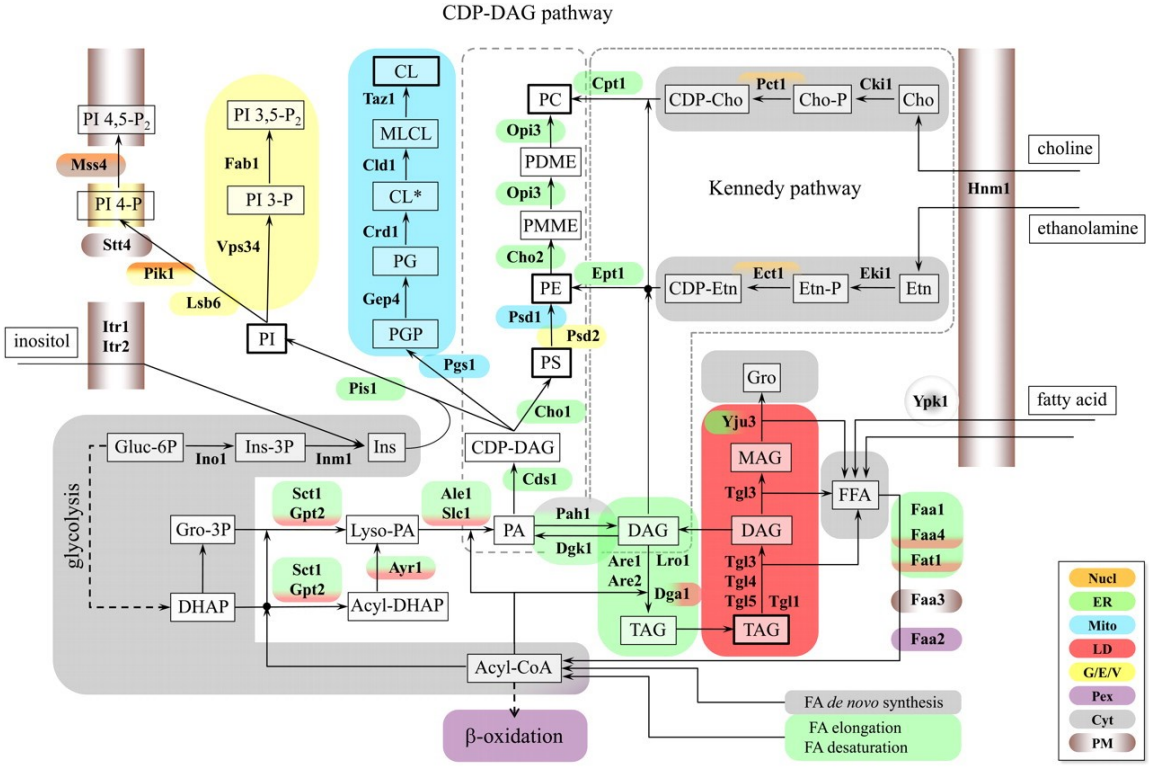

Figure 2.7. Phospholipid and triacylglycerol biosynthesis in the yeast.
Pathways for the synthesis of glycerolipids and their subcellular localization. Phospholipids and TAG share DAG and PA as common precursors. In the *de novo* synthesis of phospholipids, PA serves as the immediate precursor of CDP-DAG, a precursor to PI, PG, and PS. PS is decarboxylated to form PE, which undergoes three sequential methylations resulting in PC. PA also serves as a precursor for PGP, PG, and ultimately CL. Alternatively, PA is dephosphorylated, producing DAG, which serves as the precursor of PE and PC in the Kennedy pathway. DAG also serves as the precursor for the TAG and can be phosphorylated, regenerating PA. The names of the enzymes discussed are summarized in **Table S2**. Lipids and intermediates are boxed, with the most abundant lipid classes boxed in boldface type. Enzyme names are indicated in boldface type. The abbreviations not found in the text are: MAG,

monoacylglycerol; Gro, glycerol; DHAP, dihydroxyacetone phosphate, PG, phosphatidylglycerol; PGP phosphatidylglycerol phosphate; CL* precursor cardiolipin; MLCL, monolyso-cardiolipin; CL, mature cardiolipin; PMME, phosphatidylmonomethylethanolamine; PDME, phosphatidyl-dimethylethanolamine; FFA, free fatty acids; Cho, choline, Etn, ethanolamine, Ins, inositol; Cho-P, choline phosphate; CDP-Cho, CDP-choline; Etn-P, ethanolamine phosphate; CDP-Etn, CDP-ethanolamine; Nucl, nucleus; Mito, mitochondria; G/E/V, Golgi, endosomes, vacuole; Pex, peroxisomes; Cyt, cytoplasm. Reprinted by permission from Genetics Society of America, *Genetics*, Henry S., Kohlwein S. D., and Carman G. M., 2012.

1.3.2.2: CDP-DAG pathway

The CDP-DAG pathway can generate all the major yeast glycerophospholipids and is the main source of PE and PC under standard growth conditions (in nutrient-rich media at 30°C) (**Fig 1.7, 1.8; Table S2**) (247). Because some lipids are synthesized outside of the ER membrane, the CDP-DAG pathway requires the rapid flow of lipids between organelles (248). Therefore, the CDP-DAG pathway is heavily integrated with MCSs and non-vesicular lipid transport. In the first enzymatic step, PA is converted to CDP-DAG by the CDP-DAG synthase, Cds1p in the ER membrane (**Fig 1.7, 1.8**) (249–251). CDP-DAG is then used to generate, PS by the PS synthase Cho1p, or PI which will be elaborated on below (58, 252, 253). PS is then either trafficked to its destination – primarily the PM – or it can be converted to PE. The latter reaction occurs in the mitochondrial or Golgi/vacuolar membranes and is catalyzed by the PS decarboxylase Psd1p or Psd2p, respectively (254). The transfer of PS to the mitochondria occurs at ER-Mitochondria MCSs and may be redundantly facilitated by the EMC and ERMES tether complexes (**Fig 1.8**) (18). The majority of PE is produced in the mitochondria while ~30% is synthesized in the Golgi/vacuole (255, 256). PE is then transferred back to the ER membrane where it can be methylated thrice to produce PC. The first methylation is catalyzed by Cho2p while the second and third methylations are carried out by Opi3p (257–260). In yeast, Opi3 localizes to PM-ER MCSs and it has been proposed to work *in trans* to the PM membrane to rapidly adjust PM PC levels in an Osh3p dependent manner (177).

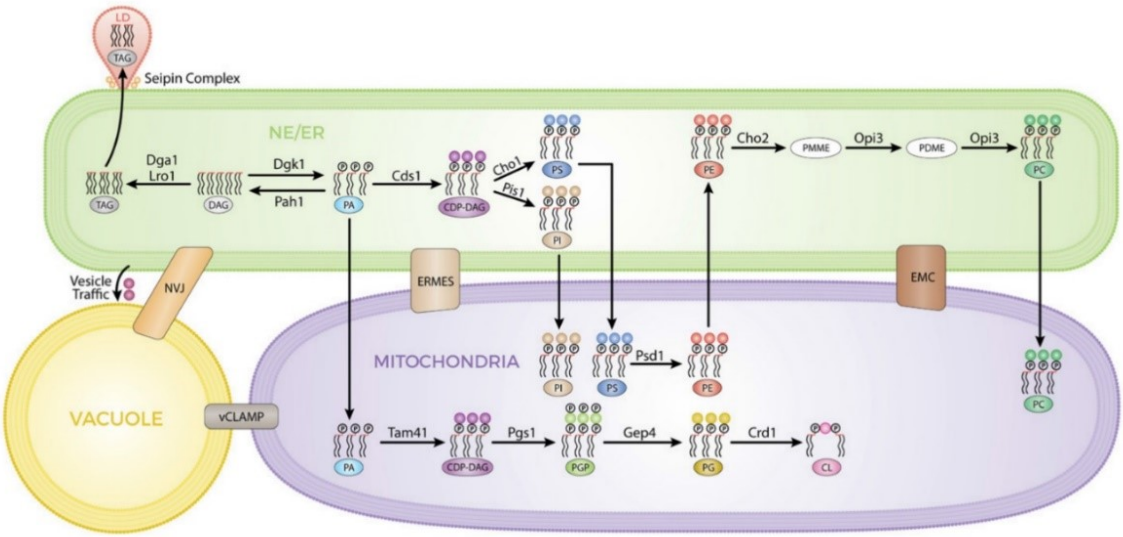

Figure 2.8. MCSs enable metabolic flux through different compartments for PL and TAG syntheses.

This figure outlines several lipid biosynthetic pathways and their locations. The MCSs bridging the gaps between the different compartments are indicated. PA is the key lipid precursor for the synthesis of TAG and PLs taking place at the nuclear envelope (NE)/ER (green). TAG is sorted into LDs (pink) connected to the ER by the seipin complex. Most of the reactions for PL synthesis take place at the ER. PS decarboxylation mediated by Psd1 and generating PE occurs in the mitochondria (purple) with transport of PS and PE indicated by arrows across these compartments. Transports of PI, PC, and PA (for the synthesis of the specific mitochondrial lipids PG and CL) into mitochondria are also indicated by arrows from the ER and into mitochondria. ER-mitochondria encounter structure (ERMES) and ER membrane protein complex (EMC) are represented as boxes connecting both compartments. An alternate route through the vacuole (yellow) bridging ER and mitochondria is shown. Vacuole and NE/ER are connected indirectly by vesicle traffic through the endomembrane system, as well as by the NVJ contact site. The vacuolar and mitochondrial patch (vCLAMP) contact site is represented as a box connecting both compartments. Reuse of JLR content must include the following: This research was originally published in the *Journal of Lipid Research*. Fernández-Murray, J. P., McMaster, C. R. Lipid synthesis and membrane contact sites: a crossroads for cellular physiology. J. Lipid Res. 2016; Vol 54 (10):1789-1805. © the American Society for Biochemistry and Molecular Biology or © the Authors.

1.3.2.3: Kennedy pathway

CDP-DAG pathway mutants have choline and ethanolamine auxotrophy phenotypes, which lead to the discovery of an alternative PE and PC synthesis pathway dependent on choline and ethanolamine (256, 260). The Kennedy pathway is an alternative PC and PE biosynthesis pathway that utilizes choline and ethanolamine (**Fig 1.7, 1.8; Table S2**). Exogenous choline and ethanolamine are imported by the PM choline/ethanolamine transporter Hnm1p (261). In the cytosol, the choline kinase Cki1p and the phosphocholine cytidylyltransferase Pct1p convert free choline to CDP-choline (262, 263). The final and rate-limiting step of the Kennedy pathway is the conjugation of

DAG to CDP-Choline to produce PC , catalyzed by the choline phosphotransferase, Cpt1p (264). Similarly, in PE synthesis, ethanolamine is converted to CDP-ethanolamine by Eki1p and Ect1p (265, 266), then conjugated to DAG to make PE by Ept1 (267). PE synthesized by the Kennedy pathway can enter the CDP-DAG pathways to generate PC via Cho2p and Opi3p. Mutant cells which are defective for both PE and PC branches of the Kennedy pathway can only produce PC and PE through the CDP-DAG pathway (247). However, unlike CDP-DAG mutants, Kennedy pathway mutants do not have any auxotrophic phenotypes (247, 267). In the absence of exogenous choline and ethanolamine the Kennedy pathway still produces PC and PE albeit at a reduced rate (268). In this case, the choline required for PC synthesis is derived from the yeast phospholipase D homolog, Spo14p (Pld1p), by hydrolysis of PC into choline and PA (269–271). Currently, a corresponding PE specific phospholipase enzyme has yet to be described, though CDP-ethanolamine is a byproduct of sphingolipid metabolism and will be discussed more later (218).

1.3.2.4: Phosphatidylinositol biosynthesis

The CDP-DAG pathway also contributes to PI synthesis. The phosphatidylinositol synthase Pis1p completes with Cho1p for CDP-DAG in the ER membrane (272, 273). Pis1p generates PI by attaching inositol to CDP-DAG (**Fig 1.7**). Inositol is obtained either exogenously by the myo-inositol transporters Itr1/2p, or by *de novo* synthesis (274). Inositol is synthesized by the inositol-3-phosphate synthase Ino1p, and by the inositol monophosphatase Inm1p, converting glucose-6-phosphate into inositol (275–277). PI can be further modified by kinases and phosphatases to produce phosphatidylinositol phosphates (PIPs), which have a variety of functions (**Fig 1.10**). Additionally, PI is used as a substrate to synthesize complex sphingolipids (**Fig 1.11**).

1.3.2.5: Cardiolipin synthesis

Mitochondria have their own specific subset of lipids which are locally synthesized from precursors acquired from the ER. PA generated in the ER is transported to the mitochondria, then used to make the mitochondria specific phosphatidylglycerol (PG) and cardiolipin (CL) (**Fig 1.7, 1.8**) (248). In the mitochondria, PA is converted to CDP-DAG by the mitochondrial CDP-DAG synthase TAM41. CDP-DAG is then converted to PG by Psg1p and Gep4p (278, 279). PG is converted to CL by the CL synthase Crd1p, Cld1p, and Taz1p (248, 280, 281).

1.3.2.6: Glycerophospholipid turnover

Turnover of lipids is an important component to lipid homeostasis; and essential process that maintains membrane composition and energy stores. The majority of phospholipid turnover is catalyzed by phospholipases and lipid phosphatases. The four yeast phospholipase B homologs, Plb1p-3p and Nte1p, removed fatty acids from glycerophospholipids with varying degrees of specificity (282–285). Nte1p primarily targets PC in the ER membrane; throughout the cell, Plb1 and Plb3p target PC and PE, and PI, respectively. The glycerophosphocholine (GroPCho) produced by Nte1p, is further metabolized by the GroPCho-phosphodiesterase Gde1p to produce choline, which is recycled back into the Kennedy pathway (286). The soluble phospholipase C homolog Plc1p, central to many signaling pathways, targets $PI(4,5)P_2$ to produce DAG and Inositol 3-phosphate (287, 288). As previously discussed, the phospholipase D homolog, Spo14p, which catalyzes the hydrolysis of PC to produce choline and PA.

1.3.2.7: Neutral lipid synthesis and turnover

Shuttling lipids into LDs is an important biological process helping to maintain cellular energy stores and membrane lipid concentrations. When cells enter stationary phase they no longer require lipids for growth; to avoid waste, lipid biosynthesis is turned off and lipids are shuttled into LD for storage (64, 217, 218). This process is tightly regulated by the dynamic balance of PA and DAG in the ER membrane. After PA is converted to DAG by Pah1p, DAG is acylated by the ER-resident acyltransferases, Dga1p and Lro1p, to produce TAG (**Fig 1.7**) (289–292). Dga1p uses a diverse subset of acyl-CoA species to esterify DAG, whereas Lro1p transfers acyl chains from PE and PC to DAG producing TAG and lyso-PE/lyso-PC, respectively (67, 290, 291, 293, 294). The ER resident sterol acyltransferases, Are1p and Are2p, marginally contribute to TAG synthesis, however, their primary role is to produce sterol esters (295–297). Cells incapable of generating TAG and sterol esters (*dga1*Δ *lro1*Δ *are1*Δ *are2*Δ*;* 4Δ) are completely devoid of LDs but are viable, suggesting that lipid storage is dispensable in dividing cells (64, 244, 297). When cellular conditions change, and TAG must be liberated from LD, it is converted to back to DAG to be circulated back into lipid biosynthesis or converted to monoacylglycerol (MAG) for further metabolism (**Fig 1.7**). It is hypothesized that DAG recirculation occurs during the transition from stationary to logarithmic growth phases by Ice2p, the ER transmembrane protein and PM-ER tether protein, suggesting a dual role for Ice2p and possible coordination between MCSs (178).

1.3.2.8: Transcriptional regulation of glycerophospholipid biosynthesis

In yeast, many glycerophospholipid biosynthesis genes are controlled by the UAS_{INO} promoter element which is regulated by lipid precursor levels, such as inositol, choline, and PA (**Fig 1.9**) (218, 235, 298–302). Ino2p and Ino4p form a heterodimer transcription factor which binds to the UAS_{INO} sequence and induces transcriptional activation (303–307). In the presence of inositol and choline Opi1p translocates to the nucleus, repressing UAS_{INO} by inhibiting Ino2p-Ino4p activation (298, 300, 301, 304, 308). In the absence of inositol, Opi1p is physically sequestered to the ER by binding Scs2p, thereby allowing transcription from the UAS_{INO} promoter(42, 301). Of all the UAS_{INO} containing genes, *INO1* is the most stringently regulated (218, 298–300). Considering Ino1p facilitates inositol synthesis, *ino1*Δ mutant cells have inositol auxotrophy phenotypes (303, 309). Similarly, mutant cells missing UAS_{INO} transcriptional activation machinery (ie. *ino2*Δ and *ino4*Δ) or proteins required for Opi1p nuclear exclusion (ie. s*cs2*Δ) also have inositol auxotrophy phenotypes (42, 301, 303, 309–312). Inversely, *opi1*Δ mutant cells have increased *INO1* transcription and overproduce inositol (303, 309).

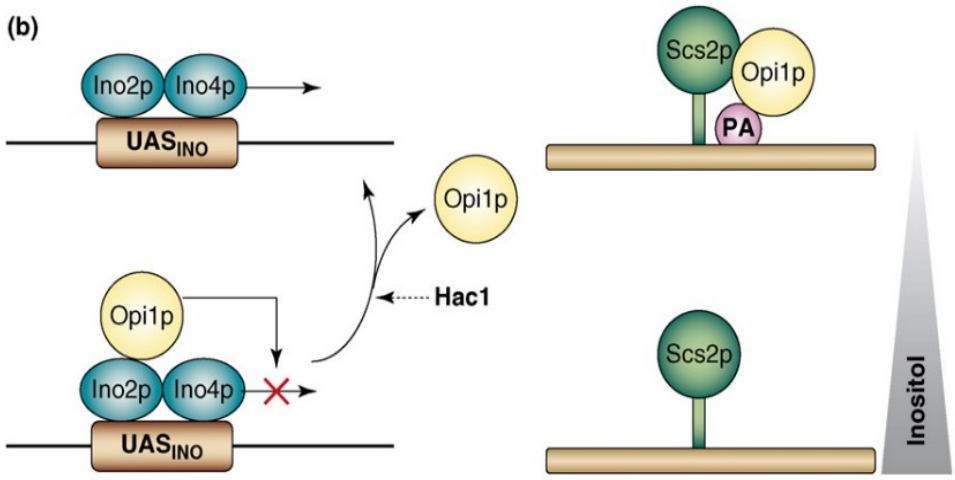

Figure 2.9. Regulation of phospholipid biosynthesis in yeast.
Regulation of INO1 transcription. Transcriptional activation of INO1, as with that of other phospholipid biosynthesis enzymes (e.g. as depicted in Figure 1.8), requires the cis-regulatory element UAS_{INO}, which serves as a binding site for the Ino2p–Ino4p activator complex. In the presence of inositol, the Opi1p repressor suppresses INO1 transcription by binding to the DNA-bound Ino2p. Dissociation of Opi1p from Ino2p relieves its inhibitory effect and promotes transcriptional activation. This occurs upon inositol deprivation or under UPR-inducing conditions, that stimulate Hac1 synthesis (see text). It seems that the signal for repression is not inositol itself but rather phosphatidic acid (PA) levels. PA accumulates in the absence of inositol and stabilizes the localization of Opi1p in the ER, where it interacts with Scs2p. Upon inositol addition, PA levels

decrease, and Opi1p is released from the ER and rapidly translocates to the nucleus, where it inhibits transcription. Thus, the translocation of Opi1p to and from the nucleus is crucial for INO1 transcription. Sequestering of Opi1p by Scs2p would, therefore, relieve the inhibitory effect that Opi1 has on INO1 transcription. Reprinted by permission from Elsevier, *Trends in Cell Biology*, Lev S., Halevy D. B., Peretti D., and Dahan N. 2008.

Glycerophospholipid biosynthesis regulation is also tightly linked to the unfolded protein response (UPR), a conserved intracellular signaling cascade activated by ER stress (313). In response to ER stress, such as an accumulation of misfolded proteins in the ER lumen, the UPR increases lipid synthesis and the expression of ER protein folding machinery to restore ER homeostasis (314). Prolonged activation results in cell death (314). In yeast, ER stress is monitored by the transmembrane sensor Ire1p which senses the levels of unfolded proteins in the ER lumen (315). Upon activation, Ire1p cleaves the *HAC1* pre-mRNA intron permitting the translation of the Hac1p transcription factor, in turn activation transcription of UPR target genes (316, 317). Deletion of many lipid biosynthesis genes or the restriction of inositol causes UPR induction in yeast and mammals (318–324). It has been shown that *ire1*Δ and *hac1*Δ mutant cells, which have defective UPR activation, cannot sustain *INO1* expression in media lacking inositol (322). This defect can be suppressed by the deletion of *OPI1* suggesting that the UPR regulates the UAS_{INO} transcription system (**Fig 1.9**) (322). However, cells treated with tunicamycin, which stimulates the UPR, or with constitutively active UPR, do not increase *INO1* transcription in the presence of inositol (325). It should be noted that the UPR program appears to be adaptable and might remodel differently to different stresses (326). Interestingly, cells lacking six of the PM-ER tether proteins (Δ-tether) have significant lipid defects and show constitutive UPR activation (16, 29). Therefore, the link between the UPR and lipid biosynthesis is highly complex and requires further exploration.

2.3.3. Phosphatidylinositol Phosphates regulation in yeast

PI is a major structural lipid to all membranes in the cell. However, PI is unique because it can be phosphorylated and dephosphorylated at the *D-3, -4,* and *-5* carbons of the inositol ring to generate 7 distinct phosphatidylinositol phosphate (PIP) species. Yeast only produce four of the possible species: phosphatidylinositol-4-phosphate (PI4P), phosphatidylinositol-4,5-bisphosphate ($PI(4,5)P_2$), phosphatidylinositol-3-phosphate (PI3P), and phosphatidylinositol-3,5-bisphosphate ($PI(3,5)P_2$) (**Fig 1.10**).

PI3P, PI4P, and PI(4,5)P_2 are the major species and account for ~30% of total PIPs each, while PI(3,5)P_2 makes up less than ~5% (327, 328). Mammals produce all seven species with each PI4P and PI(4,5)P_2 accounting for approximately 40-45% of total PIPs, while PI3P, phosphatidylinositol-5-phosphate (PI5P), phosphatidylinositol-3,4-bisphosphate (PI(3,4)P_2), PI(3,5)P_2, and phosphatidylinositol-3,4,5-trisphosphate PI(3,4,5)P_3 make up the remaining 10-20% (**Fig S1**) (328). This thesis focuses on PIP regulation in yeast, however, the regulation and synthesis of the remaining metazoan-specific PIPs are summarized in **Table S3** and **Fig S1**.

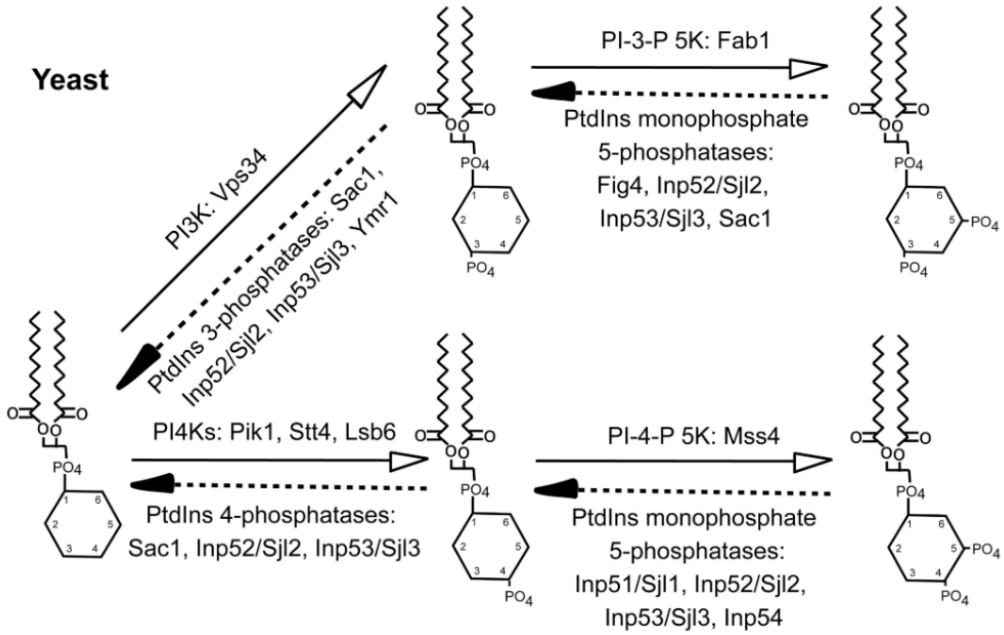

Figure 2.10. Phosphatidylinositol phosphates (PIP) synthesized in yeast and the corresponding phosphatases and kinases.
PIP metabolism in the yeast *Saccharomyces cerevisiae*. The execution points of the yeast PI kinases and PI phosphatases that regulate the synthesis and turnover of PIPs, respectively, are identified. Reprinted by permission from Elsevier, Progress in Lipid Research, Phosphoinositide phosphatases in cell biology and disease, Liu Y., and Bankaitis V. A., 2010.

The interconversion of PIP species is tightly regulated by PIP kinases and phosphatases. Because PIPs are precisely spatially and temporally controlled, they act both as area codes for different organelle membranes and as time stamps for various processes (**Fig 1.6**). Many proteins physically interact with PIP headgroups using conserved PIP-binding domains, such as the PH and C2 domains previously discussed, which regulate protein localization and activity (329). For example, the PM-ER tether proteins Tcb1p-3p and Ist2p are embedded in the ER and bind to PI(4,5)P_2 at the PM to facilitate membrane tethering (38, 161). Additionally, some PIPs are metabolized by

phospholipases, generating second messenger molecules during signaling cascades (330). Collectively, PIP diversity and regulation allows them to dually act as membrane structure components as well as regulators of many biological processes and signaling pathways.

1.3.3.1: Phosphatidylinositol-4-phosphate (PI4P)

PI4P is primarily concentrated in the Golgi and PM, the bulk of which is generated by PI 4-kinases that phosphorylate PI at *D4* (**Fig 1.6, 1.10**)(327, 331). Yeast have three PI 4-kinases, Pik1p, Stt4p, and Lsb6p, which all have mammalian homologs (PI4KIIIb, PI4KIIIa, PI4KII respectively) (331–334). Stt4p and Lsb6p localize to the PM while Pik1p primarily localizes to the Golgi and, transiently, to the nucleus (327). It has been proposed the Pik1p and Stt4p are the major PI 4-P kinases, accounting for 45% and 40% of PI4P in the cell respectively, while Lsb6p plays a minor role (327, 331, 333).

Although each PI 4-kinase performs the same enzymatic reaction, each affects distinct cellular processes. Pik1p activity regulates Golgi and endosomal PI4P levels, and is essential for vesicular trafficking (333, 335–340). Lsb6p has been implicated in regulating the yeast endocytosis and actin patch formation (341). Stt4p is responsible for generating PM PI4P and regulates cell polarization, protein recruitment, cell signaling and non-vesicular transport of lipids (52, 62, 133, 200, 338). Stt4p activation is regulated by the peripheral PM protein Efr3p, the scaffolding protein Ypp1p, and the PM transmembrane protein Sfk1p, all of which are conserved in mammals (342–344). Efr3p and Ypp1p are required for Stt4p PM recruitment, then Ypp1p is replaced with Sfk1p to facilitate Stt4p activation (345).

PI4P turnover is mediated by the ER-resident PIP phosphatase Sac1p, and the soluble synaptojanin phosphatases Inp52p-53p (Sjl2-3p) (139, 327, 332, 346, 347). In yeast, loss of *SAC1* results in accumulation of PI4P at the PM and increase total PI4P levels 8-fold (139). Interestingly, cells lacking the major primary PM-ER tether proteins (Δtether) have a 10-fold increase in PI4P (16). Considering that deletion of all synaptojanins in yeast (*inp51Δ inp52Δ inp53Δ*) does not affect levels (348), this strongly suggests that PM-ER MCSs are regulators of Sac1p. It has been shown that Osh4p is an activator of Sac1p, and deletion of *SAC1* can suppress the synthetic lethality caused by hyperactivating Osh4p ($OSH4^{Y97F}$) (131, 139). Furthermore, cells lacking all seven *OSHs* (*oshΔ*) or all PI 4P-phosphatases (*sac1Δ inp52Δ inp53Δ*) yield a 21 fold and 28

fold increase in PI4P levels, respectively (139). This suggests that *OSHs* are not just regulators of Sac1p, but the global regulators of PI4P. It has been proposed that Sac1p can directly regulate PM PI4P by reaching across PM-ER MCSs and working *in trans* at the PM (139). However, this mechanism has recently been contested with evidence suggesting that the flexible linker region of the mammalian *SAC1* is not long enough to work *in trans* and can only facilitate *cis* activity at the ER membrane (201). The previously discussed counter-transport model postulates that anterograde lipid transport is powered by retrograde PI4P transport to the ER (**Fig 1.5**) (200). In this model, Sac1p rapidly metabolized ER PI4P to maintain a steep concentration gradient. Although the *trans* vs *cis* activity models are inherently not mutually exclusive, the counter-transport model is dependent on the latter.

1.3.3.2: Phosphatidylinositol-4,5-bisphosphate (PI(4,5)P2)

In both yeast and humans, PI(4,5)P_2 is primarily localized to the PM cytoplasmic leaflet (**Fig 1.6, 1.10**) (328). Yeast can only generate PI(4,5)P_2 through the PM resident PI4P 5-kinase Mss4p (349, 350), which is conserved in mammals (PIP5Kα, PIP5Kβ, and PIP5Kγ) (327, 331). In yeast, PI(4,5)P_2 is either dephosphorylated by the soluble PIP 5-phosphatases (Inp52p, Inp53p), or metabolized by phospholipase C (330, 347, 348). PI(4,5)P_2 is required as a second messenger in many different signaling pathways which regulate cell growth, polarization, movement, stress response, cell survival and endocytosis (351–355). Many of these functions are facilitated by lipid-protein interactions with PI(4,5)P_2 (329, 331). Alternatively, PI(4,5)P_2 can be metabolized by phospholipase C during Ca^{2+} signaling. In response to a variety of stimuli, Plc1p or PLCδ1, in yeast and humans respectively, hydrolyzes the inositol headgroup from PI(4,5)P_2 to generate 1,4,5-triphosphate (IP3) and DAG (330, 356). Both act as second messengers (330). IP3 has many downstream effectors, the best characterized being interactions with calcium channels in the ER (330). Upon IP3 binding the channels rapidly released of Ca^{2+} into the cytosol (330). In higher metazoans, PI(4,5)P_2 is also essential for the PI3K/Akt signaling cascade (357).

1.3.3.3: Phosphatidylinositol-3-phosphate (PI3P) and Phosphatidylinositol-3,5-bisphosphate (PI(3,5)P2)

PI3P is essential for mediating endosomal trafficking, and so is primarily found in the early/late endosome and vacuolar/lysosomal membranes (**Fig 1.6**) (327, 328). In

yeast, PI3P is generated by the conserved PI 3-kinase Vps34p which phosphorylates PI at *D3* (**Fig 1.10**) (358, 359). Vps34p activation is dependent upon binding the protein kinase Vps15p (359, 360). The Vps34-Vps15 complex then recruits other proteins to regulate endosomal sorting and autophagy (361, 362). In yeast, PI3P is dephosphorylated to PI by the myotubularin PIP 3-phosphatase Ymr1p and the synaptojanins (Inp52p, Inp53p) (363).

PI3P can also be phosphorylated by the PI 5-kinase Fab1p (PIKfyve in mammals) to make PI(3,5)P_2, which is reversed by the PIP 5-phosphatase Fig4 (**Fig 1.10**) (364–368). PI(3,5)P_2 is a minor PIP species (0.1% of total PI) and is strictly localized to the vacuole/lysosome where it regulates endosomal trafficking and vacuolar/lysosomal function (**Fig 1.10**) (196, 369–372) Fab1p kinase activity is dependent on the physical interaction with the scaffolding protein Vac14p and regulator Atg18p (371, 373, 374). Although Fig4 mediates PI(3,5)P_2 turnover, *FIG4* mutants show reduced PI(3,5)P_2 levels suggesting that Fig4p is required for Fab1p activation (368, 371, 375, 376). It has been suggested that Fig4p physically interacts with the Fab1-Vac14 kinase complex which couples PI(3,5)P_2 synthesis and turnover (371).

2.3.4. Sphingolipid biosynthesis and regulation in yeast

Sphingolipids play essential roles as membrane structural elements and signaling molecules (377). Sphingolipids are primarily localized to the extracellular leaflet of the PM where they modulate lipid bilayer chemical properties or serve as secondary messengers for several signaling pathways that regulate cell-cell communication, cell cycle and growth, ER stress response, apoptosis, autophagy, and protein stability and localization (66, 377–379). Like glycerophospholipids, sphingolipids consist of two fatty acid tails but instead of glycerol, serine is used to generate the sphingiod base backbone (196). Sphingolipids tend to have longer saturated or *trans*-unsaturated FA tails - relative to glycerolphospholipids - that form tall, narrow cylinders causing them to pack tightly and leave interdigitation between leaflets which favor sterol binding (196). Also, it is hypothesized that sphingolipid headgroups shield sterols from the aqueous environment which cause them to preferentially mix (380). Sphingolipids and sterols have a higher packing density than glycerophospholipids resulting in a more rigid membrane (196). *In vitro,* sphingolipids and sterols can laterally segregate in lipid bilayers and self-assemble into microdomains (381). This suggested that sterols, sphingolipids and specific

transmembrane/lipidated proteins may form similar micro-domains called lipid rafts *in vivo* (382, 383). However, the explicit existence of lipid rafts, as well as their regulation and function are still debated. In addition to establishing membrane rigidity and lateral segregation, sphingolipids and sterols also contribute to membrane curvature and have been shown to affect vesicular membrane trafficking (384). Although yeast and mammals have a divergent set of complex sphingolipid species, many of the biosynthetic pathways and their downstream regulatory functions are conserved (378).

1.3.4.1 Sphingolipid biosynthesis in yeast

The first step in sphingolipid synthesis is the production of long-chain bases (LCB) (**Fig 1.11**). LCB *de novo* synthesis beings in the ER by the serine palmitoyltransferase (SPT) complex consisting of Lcb1p and Lcb2p which conjugates serine to palmitoyl-CoA to produce 3-ketohidydrosphingosine (3-KDS) (**Table S4**)(217, 385, 386). This reaction can be inhibited by the antibiotic drug myriocin (387). SPT is part of the larger conserved SPOTS complex (SPT, Tsc3p, Orm1p/2p, Sac1p) which regulates this initial step of sphingolipid biosynthesis (388). Orm1p and Orm2p are negative regulators of SPT, while Sac1p is a repressor of Orm1p and Orm2p resulting in SPT activation (377, 388).

LCBs are intermediate sphingolipid metabolites and essential regulators of sphingolipid biosynthesis (378). 3-KDS is reduced by Tsc10p to produce the LCB, dihydrosphingosine (DHS) (**Fig 1.11**) (389). DHS is hydroxylated by Sur2p to produce phytosphingosine (PHS) (390). Both DHS and PHS can be phosphorylated for degradation or converted to ceramide. LCB phosphorylation is mediated by the sphingoid kinases Lcb4p or its homolog Lcb5p (391). LCB-phosphates can be degraded by Dpl1p, forming an ethanolamine-1-phosphate by-product that can enter PE synthesis via the Kennedy pathway (217, 392). The conversion of LCBs to ceramide also takes place in the ER. The ceramide synthase complex, consisting of Lag1p, Lac1p, and Lip1p, catalyze an acyl-CoA-dependent acetylation of DHS or PHS with very long chain fatty acids (VLCFA) to yield dihydroceramide (DHCer) and phytoceramide (PHCer), respectively (393, 394).

Ceramides are simple sphingolipids which lack headgroups (378). The transition from ceramide to complex sphingolipids occurs in the Golgi, therefore, ceramide must be transferred from the ER to the Golgi. It has been hypothesized that ceramide transfer

occurs at ER-Golgi MCSs (57). In mammals, non-vesicular transport of ceramide is mediated by the well-characterized ceramide LTP, CERT (90, 189, 395). A non-vesicular transport mechanism exists in yeast, however, the regulatory mechanisms surrounding it remains largely unknown. Yeast also heavily rely on COPII-mediated vesicular transport of ceramide which may be regulated by Osh proteins (57, 396). Mutant cells lacking all *OSHs* (*osh*Δ) or have defective COPII-mediated vesicular transport (*sec18-1*^{ts}) show significant decreases in complex sphingolipids (396).

In yeast, complex sphingolipids are generated by the sequential addition of inositol headgroups to ceramide. This reaction catalyzed by the inositol phosphorylceramide (IPC) synthase complex consisting of Aur1p and Kei1p (**Fig 1.11**) (397–400). The Aur1p-Kei1p complex transfers the inositol headgroup from PI to PHCer which produces IPC and DAG (400). IPC is then mannosylated by the mannosyl-IPC (MIPC) complex consisting of Sur1p, Csg2p, and Csh1p (401). Finally, MIPC can have another inositol phosphate group attached by Ipt1p to produce M$(IP)_2$C (402). All complex sphingolipids are metabolized by the inositolphosphosphingolipid phospholipase C, Isc1p, which produces ceramide (403). Cells lacking the PI4P phosphatase *SAC1* or cells starved from inositol have decreased complex sphingolipid levels and accumulate LCBs and ceramide suggesting a block in biosynthesis (404, 405). This may be caused by an insufficient amount of PI substrate for complex sphingolipid biosynthesis (404). Interestingly, both *sac1* and *osh3* mutant cells are resistant to myriocin which inhibits the first step of sphingolipid synthesis (29, 388, 396, 406). This resistance may be caused by an accumulation LCB and ceramide precursors, reducing the need for additional LCB synthesis.

The initial steps of sphingolipids synthesis are well conserved between yeast and mammals, however, after the production of LCBs, mammalian and yeast sphingolipid biosynthesis diverge. In the ER ceramide either be converted to ceramide phosphoethanolamine and galactosylceramide (GalCer) in the ER membrane, or it can be transported to the Golgi to make sphingomyelin (SM) and glucosylceramide (GluCer) (60, 196, 407). Mammalian cells have a significantly broader diversity of sphingolipids species, producing over a 1000 different sphingolipid species, while yeast only produce three different complex sphingolipids with limited chain length and saturation diversity (379, 408, 409). However, many of the biosynthetic steps are functionally conserved and

combined with their genetic tool and relative simplicity, yeast is still an optimal system to study sphingolipid biosynthesis.

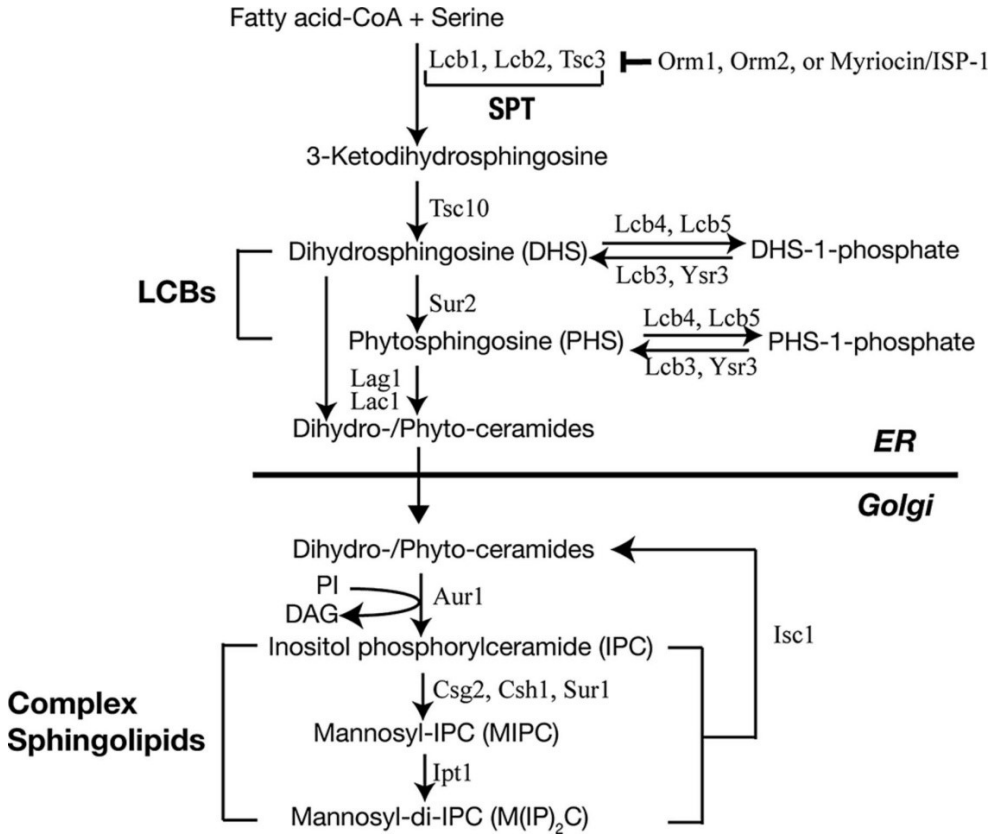

Figure 2.11. Schematic of sphingolipid metabolism in the yeast.
The biosynthetic network of sphingolipid synthesis in the yeast with the most important intermediates, end products, and enzymes is shown. For a detailed description, see text. P, phosphate; PP, pyrophosphate; CoA, Coenzyme A; VLCFA, very long-chain fatty acid. Reprinted by permission from American Society of Cell Biology, Molecular Biology of the Cell, TORC1-regulated protein kinase Npr1 phosphorylates Orm to stimulate complex sphingolipid synthesis. Shimobayashi M., Oppliger W., Moes S., Jeno., P., and Hall M., 2013.

1.3.4.2: Target of Rapamycin Complex (TORC) signaling network regulation of sphingolipid biosynthesis

One of the most well-defined mechanisms of regulating sphingolipid biosynthesis is through the Target of Rapamycin Complex (TORC) signaling network. The TORC network is a highly conserved signaling pathway which regulates cell growth, protein/lipid biosynthesis, and metabolism in response to intracellular and extracellular cues (410). This network is nucleated by the Ser/Thr kinase Tor1p or its homolog Tor2p. Tor1p/2p are a part of two distinct complexes: i) TORC1, which is sensitive to rapamycin, and ii) TORC2 which is not (410). TORC1 and TORC2 independently and

distinctly regulate sphingolipid biosynthesis through Orm1p/2p (411, 412). TORC1 acts as a negative regulator of sphingolipids biosynthesis while TORC2 is a positive regulator (389, 413–416). In response to low ceramide or LCB levels, TORC2 activates the downstream kinase Ypk1p which directly phosphorylates and inhibits Orm2p and in turn activates the SPT (388, 417–420). TORC1 inhibits Orm1p and Orm2p phosphorylation by inactivating the starvation-activated kinase Npr1p (411, 412, 416).

As will be discussed in later chapters, cells lacking all PM-ER MCSs have significant sphingolipid defects. Considering the role Sac1p and PIPs play in phospholipid regulation, and the role PIPs play in TORC pathways regulation, it is possible that PM-ER MCS may regulate sphingolipid synthesis by modulating Sac1p activity and/or TORC pathway activation (404, 421). For instance, the primary tethers *TCB3* and *ICE2* genetically interact with Rag small GTPase homolog and TORC activator *GTR2,* and the TORC2 nucleating kinase *TOR2* (422). Future research will elucidate how PM-ER MCSs regulate sphingolipid biosynthesis and if they interact with the sprawling TORC signaling network.

2.3.5. Sterols biosynthesis and regulation in yeast

Sterols are synthesized in the ER; however, ER sterols account for only 0.5-1% of total cellular sterols (423). Most sterols are concentrated in the PM, where they form complexes with sphingolipids and proteins as previously discussed (**Fig 1.6**). Sterols are also well established as regulators of vesicular trafficking, cell signaling and transcriptional activation (133, 338, 424, 425). It is well established that sterols are rapidly trafficked in the absence of vesicular transport (425), though the mechanisms and regulation surrounding this non-vesicular transport pathway remain to be eluded (425). Sterols have important structural roles in maintaining membrane integrity and manipulating bilayer chemical properties (196). The major membrane sterol in mammals is cholesterol, while the major yeast sterol is ergosterol (196). The structure of cholesterol differs from ergosterol by two additional C4-C7 and C22-C23 double bonds, and a methyl group at C24 (426). With that in consideration, in the absence of ergosterol yeast can use cholesterol with no aberrant growth defects (29, 427–429).

1.3.5.1: Sterol uptake pathways

Cellular sterol levels are maintained through *de novo* synthesis, internalization or a combination of both depending on the organism. Several steps of sterol synthesis are dependent on oxygen or heme, which also requires oxygen for synthesis (428–430). Therefore, *de novo* sterol synthesis is an aerobic process and under normal growth conditions, all sterols are *de novo* synthesized in yeast (429). If yeast cells are grown anaerobically or no longer produce heme, by mutating the heme biosynthesis enzyme *HEM1,* then the yeast will internalize extracellular sterols to compensate (429, 431, 432). Internalization is regulated by the PM ABC transporters, Aus1p, and Pdr11p (433, 434).

Inversely, insects do not synthesize sterols at all and solely rely on sterol internalization (435). Mammalian cells are somewhere in between, and simultaneously use both pathways to accommodate their sterol requirements. Mammals can uptake sterols in low-density lipoprotein (LDL) LDL-particles from the extracellular space which is dependent on LDL-receptors at the cell surface (424). LDL is internalized by receptor-mediated endocytosis and is eventually transported to the lysosome(436). Once in the lysosome, sterol are released from the LDL particles and distributed throughout the cell.

1.3.5.2: Sterols biosynthesis in yeast

De novo Synthesis of ergosterol from acetyl-CoA requires sixteen successive enzymatic reactions facilitated by twenty-three ergosterol biosynthesis enzymes called Erg proteins (**Fig 1.12**). This pathway is remarkably well conserved between humans, *S. cerevisiae* (Budding yeast) *and* S. *pombe* (fission yeast), except for several enzymatic steps which result in cholesterol production instead of ergosterol (**Fig 1.12**). Fission yeast are an important system to study sterol biosynthesis because they share a conserved regulatory mechanism with metazoans, that is not present in budding yeast (discussed below) (426).

Ergosterol synthesis begins with the condensation of three acetyl-CoA molecules into 3-hydroxy-3-methylglutaryl-CoA (HMG-CoA) by Erg10p and Erg13p (**Fig 1.12**) (437, 438). HMG-CoA is then reduced to mevalonate by the HMG-CoA Reductase, Hmg1p, and Hmg2p (426, 439). HMG-CoA reduction to mevalonate is the first rate-limiting step and major checkpoint of ergosterol synthesis (426). Mevalonate is then converted to the isoprenoid farnesyl pyrophosphate (FPP) by Erg8p, 12p, 19p, 20p and Idi1p (**Fig 1.12**).

FPP is an essential isoprenoid precursor which can be converted to sterols, dolichols, and ubiquinones, or for protein prenylation (440).

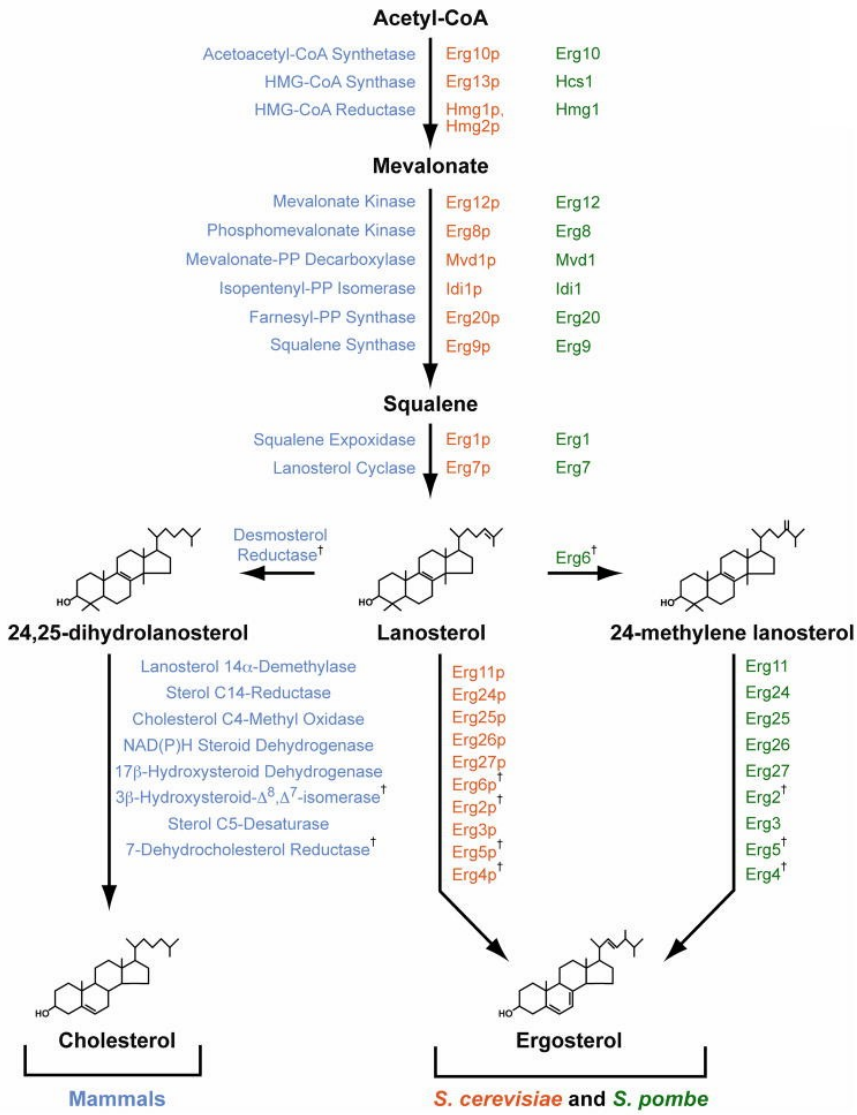

Figure 2.12. Schematic of yeast and mammalian sterol biosynthesis:
Schematic of mammalian cholesterol biosynthesis and *S. cerevisiae* and *S. pombe* ergosterol biosynthesis with major landmark derivatives depicted. Mammalian enzyme names are in blue*, S. cerevisiae* are in orange, *S. pombe* are in green. Reprinted by permission from Elsevier, Progress in Lipid Research, Regulation of HMG-CoA reductase in mammals and yeast, Burg J., and Espenshade P., 2011

The conversion of FPP to squalene (SQ) is the first sterol-specific enzymatic step. Two FPP molecules come together to form SQ by the SQ synthase Erg9 (441). Inhibition of Erg9p specifically blocks ergosterol synthesis and leads to cell death (442). However, lethality can be rescued by inducing exogenous sterol uptake (29). Therefore,

cells which can transcriptionally modulate *ERG9* are utilized to study the specific effects of sterol depletion (443). Through a variety of demethylations, reductions, and desaturations, SQ is converted to ergosterol by Erg1-7p, Erg11p, and Erg24-28p (426, 444, 445). At this point, ergosterol is rapidly transported throughout the cell, specifically to the PM, which was discussed previously.

As discussed previously, PM-ER MCSs and PAMs were defined as contaminating microsomal membrane factions enriched for phospholipid and sterol biosynthesis enzymes (103). Therefore, in addition to potentially regulating non-vesicular sterol transport, PM-ER MCS may also regulate sterol biosynthesis. One would postulate that sensing sterol levels at the PM and transferring that information would be essential for facilitating sterol homeostasis. Future research will determine if PM-ER MCSs help facilitate that process.

1.3.5.3: Divergent models of sterol biosynthesis regulation

In mammals, sterol synthesis is regulated by the well-characterized Sterol Regulatory Element Binding Protein (SREBP) complex (426, 446). In the absence of cholesterol, SREBP transcriptionally upregulates more than 30 genes required for sterol synthesis and sterol uptake, such as HMG CoA reductase and LDL-receptor, respectively (426). SREBP is an integral ER protein which possesses a cleavable N-terminal transcription factor domain. SREBP complexes with SREBP cleavage Activating protein, Scap, and under normal sterol conditions, SREBP-Scap complex is retained in the ER by Insig (426, 446). When sterols are low, the SREBP-Scap complex is transported to the Golgi where SREBP is cleaved allowing its transcription factor to translocate to the nucleus and activate transcription. While fission yeast have a homologous system, budding yeast does not have an SREBP homolog.

Instead, in budding yeast, ergosterol biosynthesis regulation is mediated by the transcription factors Hap1, Upc2p, and Emc22p. As previously mentioned, *de novo* ergosterol synthesis is dependent on oxygen and heme. In response to oxygen and heme level, Hmg1p is transcriptionally regulated by Hap1p (447). Hmg2p protein levels are normally low and tightly controlled post-translationally by the ER-associated degradation (ERAD) system (448, 449). Upc2p and Emc22p redundantly regulate sterols by physically sensing sterol concentrations (450). Upon sterol binding, Upc2 and Emc22 are transcriptionally repressed (450). In sterol-depleted cells there are no sterols to bind

Upc2p; therefore Upc2p undergoes conformational activation, translocates to the nucleus and activates transcription (450).

2.4. Membrane Contact Sites in health and disease

Recently many components and regulators of PM-ER MCSs have been implicated in human disease. Here I will discuss genes specifically associated with PM-ER MCSs and disease, however, other MCSs have well-characterized roles in disease. Interestingly, deletion of all E-Syts in mice resulted in no deleterious effects suggesting that it is either working redundantly with other proteins or plays a minor role in membrane association or lipid transfer relative to other systems (153, 157). Like in yeast, the human VAPs are involved in many different cellular functions, therefore, their association with several different human diseases is unsurprising (451). Genes associated with lipid biosynthesis and regulation, particularly the regulation of PIPs, have well-established roles in human disease but will not be discussed in depth. Interestingly, all the human ORPs seem to be associated with human diseases, as summarized in **Table S5** (452). I will focus on the roles of ORP3, ORP5, ORP6 and ORP8 in human disease because they distinctly localize to PM-ER MCSs.

2.4.1. Mutations in VAPB and ORPs associated with Amyotrophic lateral sclerosis (ALS) 8

Protein aggregation is a common feature of many neurodegenerative diseases, such as Alzheimer's disease, Parkinson's disease, Huntington's disease, and Amyotrophic lateral sclerosis (ALS) (453). Recently, several studies have linked MCSs with neurodegenerative diseases, such as ER-mitochondrial MCSs in Alzheimer's and Parkinson's disease (454, 455); NVJ in spinocerebellar ataxia 20 (SCAR20) (45) and ER-endosome MCSs in Niemann Pick Type C (NPC) (456). PM-ER MCSs have been specifically associated with an autosomal dominant form of ALS (ALS8). ALS is a heterogeneous progressive motor neuron degeneration disease characterized by loss of motor neurons in the spinal cord, brainstem, and motor cortex (457). ALS8 is a slow and progressive disorder characterized by fasciculation, cramps and postural tremor (457). A common driving mutation found in ALS8 has been mapped to the highly conserved P56 residue of VAPB ($VAPB^{P56S}$) (457). $VAPB^{P56S}$ is a dominant negative mutation and has been suggested to sequester wild type VAPB into insoluble aggregates (458). Several

independent studies have shown that expression of VAPB^{P56S} in cultured cells cause the formation of insoluble aggregates that localized to the cytosol (457), non-ER compartments (459), or immobile tubular ER clusters (458, 460). Photobleaching experiments suggest that the VAPB^{P56S} proteins are mostly immobile in these aggregates while ultrastructural analysis revealed that the VAPB^{P56S} aggregates consist of tubules continuous with the ER (458). Considering the universal function of the VAPs, the precise pathology of ALS8 is still debated. It has been suggested that VAPB^{P56S} mediated aggregation causes neurodegeneration through UPR desensitization, or though chronic and progressive lipid biosynthesis/transport defects (451).

Recently, it has been shown that overexpression OSBP and ORP3, which both bind VAPB (43), can suppress phenotypes associated with the VAPB^{P56S} mutation (461, 462). Although OSBP has a well-established intracellular localization, ORP3 can localize to PM-ER MCSs (463). ORP6 also localizes to PM-ER MCSs, has been associated with Alzheimer's disease, however the extent of this association is unknown (463, 464). Further investigation into ORP and VAP function at PM-ER MCSs will likely provide insight into neurodegenerative diseases.

2.4.2. Mutations in VAP and ORPs are associated with cancer

PIP regulation is essential for many different cellular functions, including cell growth, proliferation, and survival (347, 465). It is clear that MCSs, specifically between the PM and ER, play a large role in regulating the interconversion of PIPs (16, 29, 139). Therefore, it is unsurprising that PM-ER MCSs are associated with some cancers. Overexpression of VAPB has been shown to promote breast tumor cell proliferation, by inappropriately activating the commonly mutated oncogenic PI3K/Akt signaling network (466). PI4P levels at the Golgi cause by defective SAC1 has been associated with breast cancer cells progression (467). Both PM-ER MCS resident ORPs and proposed PS/PI4P counter-transporters, OPR5 and ORP8, have been implicated in cancer. ORP8 may act as a tumor suppressor by suppressing the Wnt pathways gastric cancer cells (468). Loss of ORP8 is also associated with apoptosis resistance caused by reduced Fas-ligand receptors at the cell surface (469). Inversely, overexpression ORP5 is associated with metastatic pancreatic and lung cancer development (470, 471). ORP3, which binds VAPA, has been demonstrated to stimulate the oncogenic R-Ras signaling network (141). Additionally, there has been a swell of evidence showing that

misregulation of lipid metabolism and biosynthesis has severe implications on cancer progression and metastasis (472). Collectively, this suggests that PM-ER MCSs can affect cell growth, proliferation, invasiveness, and survivability; all of which can be exploited by a cancer cell.

2.4.3. PM-ER MCSs exploited in viral entry and replication

During viral infection, viruses exploit endomembrane to build complex viral replication machinery and facilitate viral expansion. Some of the proteins exploited also facilitate PM-ER MCS. Positive-sense RNA viruses, such as Hepatitis C virus (HCV) and human rhinoviruses (HRV) can manipulate PI4P and cholesterol regulation to facilitate virus entry and replication (465, 473, 474). HCV, specifically, can displace SAC1 and recruit PI4 kinases to increase local PI4P concentration necessary for viral replication (475). Several mammalian ORPs, namely OSPB and ORP4, are required for enterovirus and HCV replication (476, 477). OSBP, SAC1, and both VAPs (VAPA/B) are implicated in Aichi Virus replication (478). Ishikawa-Sasaki *et al.* suggest that Aichi Virus directly target and recruit cholesterol transport machinery through protein-protein interaction resulting in the formation of MCS between the ER and Aichi virus replication organelles (478). Recent evidence has shown that E-Syt1 and E-Syt3 negatively modulate Herpes Simplex Virus-1(HSV-1) viral release into the extracellular milieu, cell-to-cell viral spread, and viral entry (479). These phenomena are also seen in plant positive-strand RNA viruses (480). While using yeast as a tombusvirus infection model, it was shown that viral replication requires the glycerophospholipid biosynthesis machinery, namely the Scs2p and Opi1p transcriptional regulation complex; and *OSHs* (480, 481). Considering the direct role PM-ER MCS play in regulating lipid homeostasis, membrane structure, and association, and PIP regulation, they present an attractive target to exploit during membrane dependent processes.

2.5. Hypothesis and specific aims:

The primary goal of this thesis is to experimentally test the functions of PM-ER MCSs, specifically their role in the non-vesicular transport of sterols and regulation of lipid homeostasis. Previous work performed by the Emr lab identified the first six primary tether proteins in yeast (16). In their work, they generated a strain lacking the genes for all six tether proteins (∆tether) (16). However, by their own admission, ∆tether cells still had detectable directed membrane association. This suggested the existence of another undiscovered tether protein. I hypothesized that the ER-resident transmembrane protein Ice2p was the undiscovered primary PM-ER MCS tether protein and that deleting *ICE2* in ∆tether cells would significantly reduce the remaining directed membrane association. We predicted that *ice2*∆ ∆tether (∆-s-tether) cells would lack all directed membrane association and pose an optimal system to test PM-ER MCSs functions.

In collaboration with the Menon lab at Weill Cornell Medical College, we hypothesized that PM-ER MCSs are regulators for lipid biosynthesis and non-vesicular transport of sterols. We predicted that in the absence of all directed PM-ER membrane association, non-vesicular transport of sterols and lipid biosynthesis would be reduced. To test these hypotheses, our collaborators and I used a combination of cell biological, genetic, and biochemical approaches.

Additionally, the current definition of what constitutes a tether protein is ambiguous. To clarify this definition, I propose that tethers can be defined as either “Primary” or “Secondary” tethers proteins. Primary tether proteins are necessary for membrane association under normal growth conditions; secondary tether proteins are sufficient to induce membrane association when overexpressed but are otherwise dispensable. As proof of concept, I hypothesized that the ER-resident Yeast Start Homolog, Ysp2p, and the PA phosphatase Pah1p are secondary tethers. To test this hypothesis, I used a combination of cell biology and genetics to determine the affect *YSP2* and *PAH1* overexpression had on PM-ER membrane association, and growth defects, in cells lacking PM-ER MCSs.

Chapter 3. Endoplasmic reticulum-plasma membrane contact sites integrate sterol and phospholipid regulation

This chapter is a modified version of a paper that has been published in PLOS Biology (29). The authors and their affiliations are listed below:

Evan Quon[1†], Yves Y. Sere[2†], Neha Chauhan[2], Jesper Johansen[1], David P. Sullivan[2], Jeremy S. Dittman[2], William J. Rice[3], Robin B. Chan[4], Gilbert di Paolo[4,5], Christopher T. Beh[1,6‡], Anant K. Menon[2‡]

[1]Department of Molecular Biology and Biochemistry, Simon Fraser University, Burnaby, British Columbia V5A 1S6, Canada

[2]Department of Biochemistry, Weill Cornell Medical College, 1300 York Avenue, New York, NY 10065, USA

[3]Simons Electron Microscopy Center at the New York Structural Biology Center, 89 Convent Ave., New York, NY 10027

[4]Department of Pathology and Cell Biology, Columbia University College of Physicians and Surgeons, 630 West 168th St, New York, NY 10032, USA

[5]Denali Therapeutics, South San Francisco, CA 94080, USA

[6]Centre for Cell Biology, Development, and Disease, Simon Fraser University

[†]co-first author

[‡]co-corresponding author

I am a co-first author of this manuscript with Dr. Yves Sere who was under the supervision of Dr. Anant Menon.

I performed genetic manipulations to generate all recombinant yeast strains which served as the basis for this publication (**Table 2.1** and **2.2**). I performed fluorescent microscopy and data analysis in Figure 2.4A-B, 2.5C, 2.5D, 2,5F, 2.17A-C. I performed yeast kinetic growth assays in Figure 2.5B, 2.6, 2.7, 2.12, 2.14, 2.15A-B, 2.15E, 2.18, 2.19A-C. I performed an analysis of lipidomic data on Figure 2.5G, 2.8A-C. I also contributed to the experimental conceptualization of the project and writing/editing of the manuscript.

Dr. Yves Sere performed biochemical analysis of sterol transport in Figure 2.9, 2.10, 2.11, 2.13, 2.19E-G. Dr. Sere performed 3D modeling of FIB-SEM in Figure 2.1F.

Dr. Jesper Johansen performed fluorescent microscopy and data analysis, kinetic growth analysis in Figure 2.1B-C, 2.1E, 2.5E, 2.21B-F, 2.22, and 2.23.

Dr. Christopher Beh performed transmission electron microscopy in Figure 2.23 and contributed to writing and editing of the manuscript.

Statistical analysis of PM-ER membrane association and lipidomic data was performed by Dr. Anant Menon in Figure 2.1E, 2.2 and 2.5G and contributed to the writing and editing of the manuscript.

Dr. Neha Chauhan performed fluorescent microscopy and data analysis, and western blot analysis in Figure 2.3 2.9B-G, 2.16.

Dr. William Rice performed transmission electron microscopy and focused ion beam scanning electron microscopy in Figure 2.1D-F.

Dr. Robin Chan and Dr. Gilbert di Paolo performed lipidomic analysis and data acquisition in Figure 2.5G, 2.8, 2.20.

Abstract

Tether proteins attach the endoplasmic reticulum (ER) to other cellular membranes, thereby creating contact sites that are proposed to form platforms for regulating lipid homeostasis and facilitating non-vesicular lipid exchange. Sterols are synthesized in the ER and transported by non-vesicular mechanisms to the plasma membrane (PM) where they represent almost half of all PM lipids and contribute critically to the barrier function of the PM. To determine whether contact sites are important for both sterol exchange between the ER and PM and inter-membrane regulation of lipid metabolism, we generated Δ-super-tether (Δ-s-tether) yeast cells that lack six previously identified tethering proteins (yeast extended synaptotagmin (E-Syt), VAP, and TMEM16-anoctamin homologs) as well as the presumptive tether Ice2. Despite the lack of ER-PM contacts in these cells, ER-PM sterol exchange is robust, indicating that the sterol transport machinery is either absent from or not uniquely located at contact sites. Unexpectedly, we found that the transport of exogenously supplied sterol to the ER occurs more slowly in Δ-s-tether cells than in wild-type cells. We pinpointed this defect to changes in sterol organization and transbilayer movement within the PM bilayer caused by phospholipid dysregulation, evinced by changes in the abundance and organization of PM lipids. Indeed, deletion of either *OSH4*, which encodes a sterol/phosphatidylinositol-4-phosphate (PI4P) exchange protein, or *SAC1* which encodes a PI4P phosphatase, caused synthetic lethality in Δ-s-tether cells due to disruptions in redundant PI4P and phospholipid regulatory pathways. The growth defect of Δ-s-tether cells was rescued with an artificial "ER-PM staple," a tether assembled from unrelated non-yeast protein domains, indicating that endogenous tether proteins play non-specific bridging functions. Finally, we discovered that sterols play a role in regulating ER-PM contact site formation. In sterol-depleted cells, levels of the yeast E-Syt tether Tcb3 were induced and ER-PM contact increased dramatically. These results support a model in which ER-PM contact sites provide a nexus for coordinating the complex inter-relationship between sterols, sphingolipids, and phospholipids that maintain PM composition and integrity.

3.1. Introduction

Most lipids are synthesized in the endoplasmic reticulum (ER) and distributed to other membranes by non-vesicular mechanisms. These mechanisms act in conjunction with lipid metabolic networks to maintain the unique lipid profile of the plasma membrane (PM) and subcellular organelles and enable rapid membrane lipid remodeling in response to signals and stresses (181, 482, 483). An attractive hypothesis is that non-vesicular lipid transport and lipid biosynthetic and regulatory pathways intersect at ER-PM membrane contact sites (MCSs), where protein tethers retain the ER and PM within ~15-60 nm of each other (16, 30, 103, 202, 484, 485). In this view, ER-PM MCSs would serve as a nexus, coordinating requirements in the PM for lipids with their production in the ER (202, 483). How this coordination is accomplished is not well understood. Here we report on the interplay between sterol and phospholipid homeostasis at ER-PM MCSs.

Cholesterol - and its yeast counterpart ergosterol - are synthesized in the ER and transported by non-vesicular mechanisms to the PM (486, 487) where they are found at high concentrations corresponding to ~40 mole percent of PM lipids, i.e. one out of every 2-3 lipids in the PM is a sterol. The spontaneous exchange of sterols between membranes is slow *in vitro* and undetectable *in vivo*, primarily because sterol desorption from the membrane is energetically expensive (183, 488, 489). To move sterols efficiently between the ER, PM and other membranes, cells make use of sterol transport proteins (STPs) whose proposed function is mainly to reduce the energy barrier for sterol desorption, thereby extracting sterols into a binding pocket within the protein for transit through the cytoplasm (488). STPs may operate freely in the cytoplasm, or at MCSs. Soluble and membrane-bound STPs might work in parallel to provide redundant mechanisms for sterol exchange. As transport is predicted to be rate-limited by the desorption step rather than diffusion of the STP-sterol complex through the cytoplasm of (488), the proximity of the ER to the PM at an MCS may not determine the sterol transport rate unless STPs are restricted to these sites. Because a number of sterol biosynthetic enzymes are enriched in PM-associated ER membrane fractions (103) it is attractive to consider that the biosynthetic and transport machinery may co-localize to ER-PM MCSs, effectively channeling sterol between compartments (202) to facilitate sterol homeostasis.

The identity of STPs is controversial and the role of MCSs in sterol transport is unexplored. STP candidates in yeast include members of two protein families: soluble Osh proteins (related to mammalian oxysterol-binding protein (OSBP)(133)) and membrane-bound Lam proteins (members of the StARkin superfamily of Steroidogenic Acute Regulatory Transfer (StART) proteins (190, 490)). Osh4 binds sterols and phosphatidylinositol-4-phosphate (PI4P) (132) and by toggling between its sterol and PI4P bound states, it has been shown to transport sterol against a concentration gradient between vesicle populations *in vitro* (62). While this activity may account for certain aspects of sterol homeostasis, Osh4p is not required for retrograde sterol transport (491), nor is it essential for the high rate of sterol exchange between the ER and PM as evinced by robust sterol transport in cells where all seven *OSH* genes are inactivated (*osh*Δ) (184). The seven Osh proteins share overlapping essential activities (192), but because Osh6 and several other Osh proteins do not bind sterols (136, 140, 194), sterol transport is not a function shared by the entire family. Lam proteins each have one or two sterol-binding StARkin domains. The purified domains have been shown to catalyze sterol exchange between vesicles *in vitro* (212, 492). Lam1p-Lam4p are integral ER membrane proteins located at the cell cortex where they might function as sterol transporters similar to the mammalian StARkin STARD3, which is anchored to endosomal membranes and has been suggested to facilitate endosome-ER cholesterol transfer (493). Although elimination of Lam proteins does not inhibit the bidirectional transport of newly synthesized ergosterol between the ER and PM, sterol organization at the PM is altered (211). If Osh and Lam proteins catalyze ER-PM sterol transport then they must do so redundantly with each other and/or with additional STPs yet to be identified. Our results address this point.

In addition to their proposed role in sterol homeostasis, ER-PM MCSs are known to be involved in phospholipid biosynthesis and turnover. Phosphatidylcholine (PC) is synthesized via Cho2p and Opi3p-mediated methylation of phosphatidylethanolamine (PE). Opi3p is an ER-localized membrane protein in yeast that has been proposed to act *in trans* at ER-PM MCSs to convert PM-localized PE to PC (177). In the absence of Opi3p function (either through lack of the enzyme or disruption of ER-PM MCSs), cells rely on the Kennedy pathway through which PC is synthesized from choline taken up from the growth medium. It has been proposed that phosphoinositide turnover also occurs at ER-PM MCSs, where the ER-localized PI4P phosphatase Sac1 may act *in*

trans to turnover PI4P synthesized in the PM (16). These examples highlight the possibility that ER-PM MCSs may contribute to a wide range of reactions that underlie cellular phospholipid homeostasis.

In yeast, ~45% of the PM retains a closely associated cortical ER (cER) membrane (10, 16), and this association requires a number of tethering proteins that staple the ER and PM together (16, 38, 125, 161, 177). Six ER-PM tethering proteins are currently known (Fig 1A): the three tricalbins (Tcb1p-3p), which are yeast homologues of the extended synaptotagmin (E-Syt) family of membrane tethers; Ist2p, a member of the TMEM16-anoctamin family of ion channels and phospholipid scramblases; and the yeast VAP (VAMP-associated protein) homologues Scs2p and Scs22p. Several of these tethers appear to be Ca^{2+}-regulated in mammalian cells, and from their embedded location within the ER membrane, a number of them make contact with the PM through associations with phosphoinositides and/or other phospholipids (30, 104, 130, 160, 163, 485, 494). By eliminating all six of these tethering proteins, Manford et al. (16) created ∆tether yeast cells in which large sections of the PM are devoid of cortically associated ER membrane. However, as these authors noted, additional unknown tethers must still exist in ∆tether cells given that small regions of cER were still associated with the PM (16). Consistent with this conclusion, the localization of Lam1p-Lam4p close to the PM near presumptive MCSs is unaffected in ∆tether cells (211). These results suggest that the elimination of the six tether proteins is not sufficient to remove all ER-PM contacts, and that additional proteins/mechanisms must exist to account for the remaining ER-PM association.

In order to eliminate residual cER in ∆tether cells, we focused on Ice2p, an integral ER membrane protein (Fig 1A) with established roles in cER inheritance (125, 175), ER-PM contact (125, 177), phospholipid synthesis from stored neutral lipid (177, 178) and ER quality control (495). Ice2p was first shown to facilitate cER redistribution and inheritance along the PM from mother cells into daughter buds (175). In cells lacking both *ICE2* and *SCS2*, cER association at the PM is disrupted more than for each of the single mutants (125, 177). The defect in ER-PM membrane association in *scs2*∆*ice2*∆ cells is linked to dysfunctional PC synthesis, likely because the Opi3p methyltransferase is no longer able to act on its PM-localized lipid substrate *in trans* at contact sites (177). When cells enter stationary phase, Ice2p has another function in which it generates a bridge between the ER and lipid droplets (178). This membrane attachment has been

proposed to play a role in channeling droplet-generated diacylglycerol to the ER for phospholipid synthesis when cells resume growth (178). Curiously, the ERAD substrate CPY* is stabilized in *ice2*Δ cells compared with wild-type (WT) cells, pointing to a direct or indirect role for Ice2p in ER-associated degradation (495). We reasoned that because of its various ER functions, specifically including the generation of ER-PM contacts during mitosis, Ice2p might account for the residual cER in Δtether cells.

If ER-PM contact is necessary for non-vesicular sterol transfer, the rate of ER-PM sterol exchange and/or PM sterol organization would be inhibited by the elimination of all ER-PM MCSs. Likewise, if MCSs serve as regulatory interfaces to coordinate pathways for phospholipid metabolism in the ER and PM, then removing ER-PM MCSs would be predicted to alter cellular phospholipid profiles. We now report that disruption of *ICE2* in Δtether cells sharply reduces ER-PM associations to the predicted frequency of randomly finding untethered ER in the vicinity of the PM. The availability of these Δ-super-tether (Δ-s-tether) cells now permits direct tests of hypotheses concerning how ER-PM MCSs impact non-vesicular sterol exchange and inter-membrane lipid regulation.

We now report that the bidirectional movement of sterols between the ER and PM is unaffected in Δ-s-tether cells, indicating clearly that the sterol transfer machinery in yeast is either absent from or not uniquely localized to ER-PM MCSs. Nonetheless, sterol pools within the PM bilayer of Δ-s-tether cells are dramatically altered, and the rate of transbilayer sterol movement within the PM is slowed. We discovered that these defects were associated with changes in the organization and composition of PM lipids and could be largely reversed by supplementing cells with choline, or by expressing a non-specific artificial ER-PM tether. Phospholipid dysregulation in the PM was revealed by changes in the levels of sphingolipids and other PM lipids, as well as by the accumulation of PI4P at the PM of mother Δ-s-tether cells. Interestingly, Δ-s-tether cells were inviable when they also lacked Osh4p or Sac1p. After testing the associated roles of Osh6p and the ER-membrane association of Sac1p, we conclude that Osh4p and ER-PM MCSs are redundant regulators of PI4P and phospholipid homeostasis. Finally, we found that ER-PM MCS formation is responsive to cellular sterol levels, whereby the tether protein Tcb3p is induced in sterol-depleted cells resulting in a dramatic increase in membrane association. These results suggest that ER-PM contact sites are dynamic

interfaces that adjust and respond to lipid metabolism to maintain PM composition and organization.

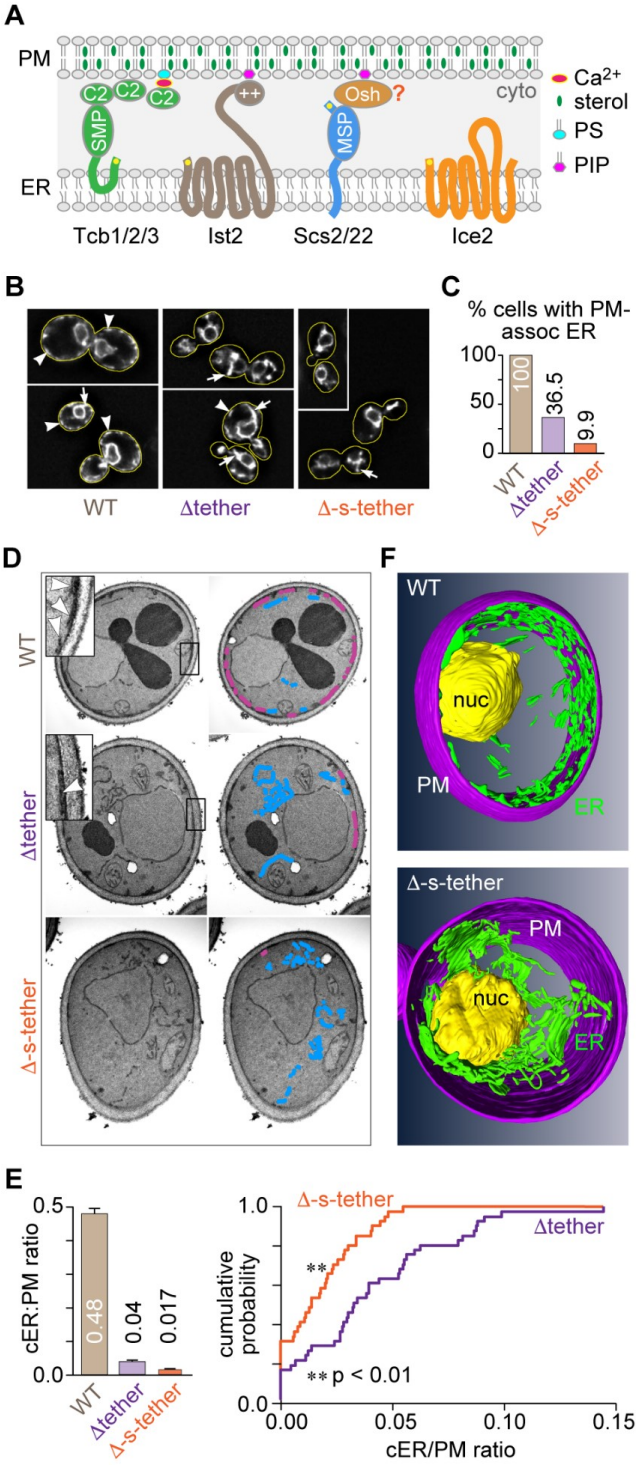

Figure 3.1. Quantitative disruption of ER-PM contacts in ∆-s-tether cells.
A. Proposed topology of ER membrane proteins involved in establishing ER-PM contact sites. The yellow dot indicates the N-terminus of the protein. The tricalbins (Tcb1p/2p/3p) associate with the PM through lipid-binding C2 domains and possess a synaptotagmin-like mitochondrial-lipid-binding protein (SMP) domain that is implicated in the exchange of phospholipids and diacylglycerol between the PM and ER (104). Ist2 is a member of the TMEM16 family of ion channels and lipid scramblases. It interacts with the PM via its C-terminal PI(4,5)P2-binding polybasic region (++)(161). The yeast VAMP (vesicle-associated membrane protein)-associated proteins (VAPs) Scs2p/22p interact with the PM indirectly, likely through Osh proteins (or other proteins) that possess an FFAT motif capable of binding to the major sperm protein (MSP) domain of the VAPs (42, 128, 129), and a PH domain that interacts with phosphoinositides at the PM. Ice2p facilitates cER inheritance from the mother cell along the PM into the bud (125, 175); the ICE2 and SCS2 genes have a negative genetic interaction (177). **B**. Representative images of WT (SEY6210), ∆tether (ANDY198), and ∆-s-tether (CBY5838) cells expressing the ER marker RFP-ER (pCB1024). The PM-associated ER (arrowheads) at the cell cortex (outlined in yellow) observed in WT cells was largely absent in the ∆tether and ∆-s-tether mutants, which exhibited prominent extra-nuclear cytoplasmic ER (arrows). Scale bar = 2 µm. **C**. Quantification of RFP-ER localization comparing the percentage of WT and mutant cells exhibiting cortical ER-PM fluorescence (n > 140 cells). **D**. Electron micrographs of WT, ∆tether, and ∆-s-tether cells. Inserts correspond to magnifications of boxed regions at the cell cortex, showing PM-associated ER (arrowheads). Cortical PM-associated ER (magenta) was reduced in ∆tether cells and all but eliminated in ∆-s-tether cells. Extra-nuclear/cytoplasmic ER (blue) is prominent in the tether mutant cells. **E**. Left; Quantification of cER expressed as a ratio of the length of PM-associated ER per circumference of PM in each cell (n = 41 cells; bars are mean ± S.E.M.). Right; Comparison of the cumulative distribution of cER/PM ratios for ∆tether (purple) versus ∆-s-tether (red) shows a significant decrease in cER across the entire population of cells. ** $p < 0.01$ by Kolmogorov-Smirnov (KS) and by Wilcoxin Rank Sum tests. See Supplementary Fig S1 for further details. **F**. Models of the 3-D organization of ER membranes within WT and ∆-s-tether cells constructed from sections imaged by focused-ion beam tomography: cER (green) in association with the PM (magenta); and nuclear ER (yellow).

3.2. Results

3.2.1. Yeast cells without ER-PM contact sites

Despite the dramatic reduction in ER-PM contact sites caused by the elimination of six tether proteins, the extent of cER in ∆tether cells (16) is both significant and heterogeneous, with >35% of the cells possessing fluorescently labeled ER in the vicinity of the PM (**Fig 2.1B, 2.1C**) and individual cells displaying as much as 20% of the average cER found in WT cells (**Fig 2.1D, 2.1E** and **Fig 2.2**). Residual cER in ∆tether cells is also evinced by the cortical localization of GFP-tagged Ysp2p/Lam2p/Ltc4p (hereafter called Lam2p; **Fig 2.4**) and other Lam proteins (211). These observations suggest that there are additional mechanisms for generating ER-PM association (485). Because the gene encoding the ER membrane protein Ice2 (**Fig 1A**) has a negative genetic interaction with *SCS2*, and Ice2p plays roles in maintaining cER structure and mediating the inheritance of cER from mother cells into daughter buds (125, 175), we

hypothesized that Ice2p may contribute to ER-PM association and that its presence in Δtether cells could account for the residual cER seen in these cells.

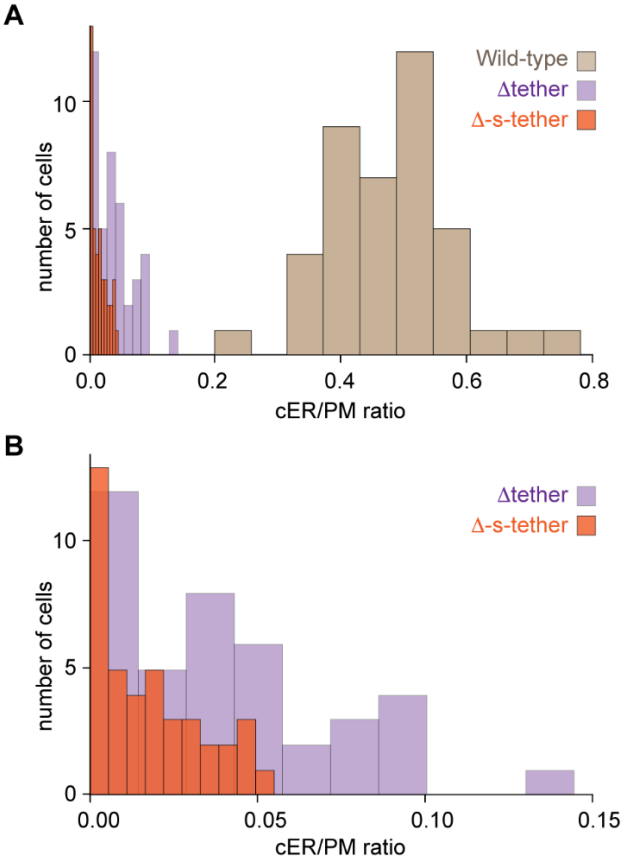

Figure 3.2. Histograms of the cER/PM ratio for WT, Δtether, and Δ-s-tether cells. WT (SEY6210), Δtether (ANDY198), and Δ-s-tether (CBY5838) cells were processed for electron microscopy and the cER/PM ratio was measured for each cell as described in Fig. 1 (panels D and E). Frequency distributions were obtained using 10 bins in each case. **A** compares all three strains, whereas **B** expands the region 0 < cER/PM < 0.15 to highlight significant differences between the tether mutants. Note that the cumulative distributions shown in Fig. 1E are derived from the raw, unbinned data with N = 41 for both mutants. The Kolmogorov–Smirnov (KS) test gave Dmax = 0.41 and P = 0.001. The Wilcoxin Rank Sum test gave U = 1681 and a two-tailed P-value of 0.0006.

To explore this possibility, we used confocal fluorescence microscopy to determine the subcellular distribution of Ice2p-GFP in Δtether cells (**Fig 2.3**). Ice2p-GFP was observed throughout the ER, including cytoplasmic strands radiating from nuclear ER towards the cell periphery (**Fig 2.3A**). Notably, Ice2p-GFP fluorescence was observed at the cell cortex, visualized by co-expressing the PM marker RFP-Ras2 (**Fig 2.3A**). Optical sections focused at the cell surface showed a concentration of Ice2p-GFP fluorescence at remaining ER cortical spots that were visualized using the fluorescent pan-ER marker RFP-ER (dsRED-*SCS2*$^{220\text{-}244}$) (**Fig 2.3B**). This localization pattern

resembles that of Scs2p, and differs from that of the tricalbins and Ist2p that are restricted to ER-PM MCS spots (16, 38, 125, 496). These data suggest that Ice2p is correctly localized to contribute to ER-PM tethering. To eliminate residual cER in ∆tether cells we therefore deleted *ICE2* in tandem with the other ∆tether mutations. We predicted that the resulting ∆-s-tether cells would be largely devoid of ER-PM contact sites and this was indeed the case.

We confirmed the near absence of PM-associated cER in ∆-s-tether cells as follows. *First*, expression of the pan-ER marker RFP-ER revealed that, unlike WT and ∆tether cells where cortical fluorescence was observed in 100% and >35% of cells, respectively, fewer than 10% of Δ-s-tether cells had fluorescence at the cell cortex (**Fig 2.1B, 2.1C**). Whereas cortical fluorescence in WT cells and many Δtether cells occurred in the form of linear strands running parallel to the cell perimeter in equatorial views (**Fig 2.1B**, arrowheads), the occasional fluorescence seen at the cortex of a small fraction (<10%) of Δ-s-tether cells was in the form of punctae, possibly corresponding to the ends of ER tubules or coincidental positioning of the ER near the PM in the focal plane chosen for imaging (**Fig 2.1B**, arrows). *Second*, whereas GFP-Lam2p is localized exclusively in cortical punctae in WT and ∆tether cells (~15 cortical punctae per cell, on average, for both strains), cortical expression of Lam2p is considerably reduced in ∆-s-tether cells (~4 cortical punctae per cell, on average; **Fig 2.4A, 2.4B**) even though the expression level of the protein is unaffected (**Fig 2.4C**). *Third*, cER association along the PM in ∆-s-tether cells was all but absent as quantified by measuring the cER/PM length ratio in equatorial views of individual cells obtained by transmission electron microscopy (**Fig 2.1D**). The average cER/PM ratio was 0.48 and 0.04 in WT and Δtether cells, respectively (16), but only 0.017 in Δ-s-tether cells (**Fig 2.1E**). The decrease in the cER/PM ratio in Δ-s-tether versus Δtether cells was statistically significant (**Fig 2.1E**, right panel), representing not only a ~60% lower average value but also a considerable tightening of the distribution of cER/PM values (**Fig 2.1E** and **Fig 2.2A**). *Finally*, we generated 3D models of WT and Δ-s-tether cells by reconstructing images obtained with a focused ion beam-scanning electron microscope (FIB-SEM). These models (**Fig 2.1F**) illustrate that the extensive cER coverage of the PM in WT cells is clearly absent in Δ-s-tether cells where a spaghetti-like accumulation of cytoplasmic tubular ER is observed instead. We estimate that the low amount of cER in Δ-s-tether cells (**Fig 2.1E** and **Fig**

2.2B) can be accounted for by the random chance of finding untethered ER at the cortex (Materials and Methods).

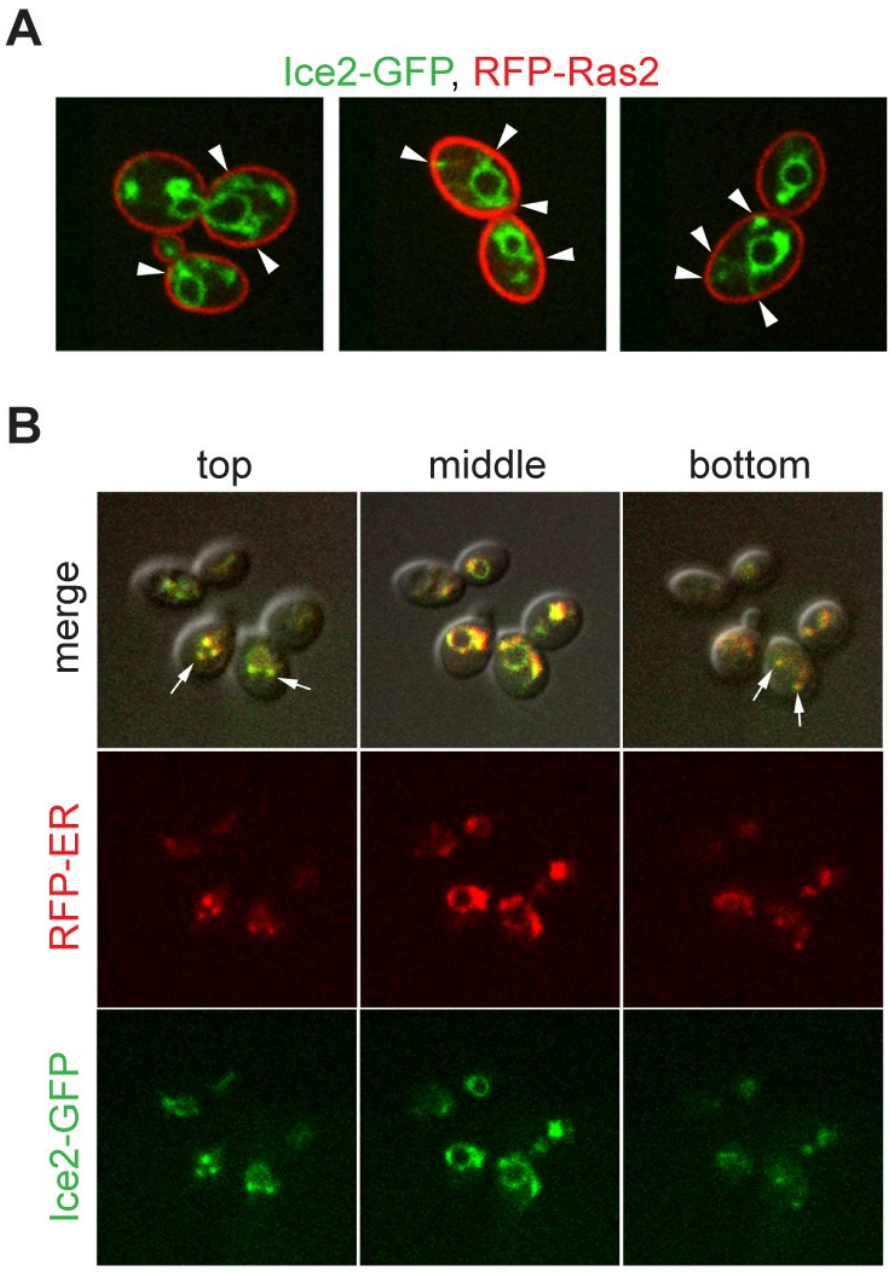

Figure 3.3: Ice2 localizes to the ER and is found at cortical ER sites.
A. Ice2-GFP in Δtether cells (CBY6220) was observed at nuclear ER and in ER tubules that extend to the cell periphery, as demarcated by RFP-Ras2 (pCB1204). In this strain, the remaining cortical attachments of ER to the PM contain Ice2-GFP (arrowheads). **B**. Serial optical sections focused at the top, middle, and bottom of Δtether cells expressing Ice2-GFP and the ER marker RFP-ER (pCB1024). The merged images of Ice2-GFP and RFP-ER fluorescence superimposed onto corresponding DIC whole cells images indicates complete co-localization. At optical sections near the cell cortex, Ice2-GFP was present as discrete spots (arrows) in equal or greater fluorescence relative to RFP-ER, consistent with ER-PM MCSs.

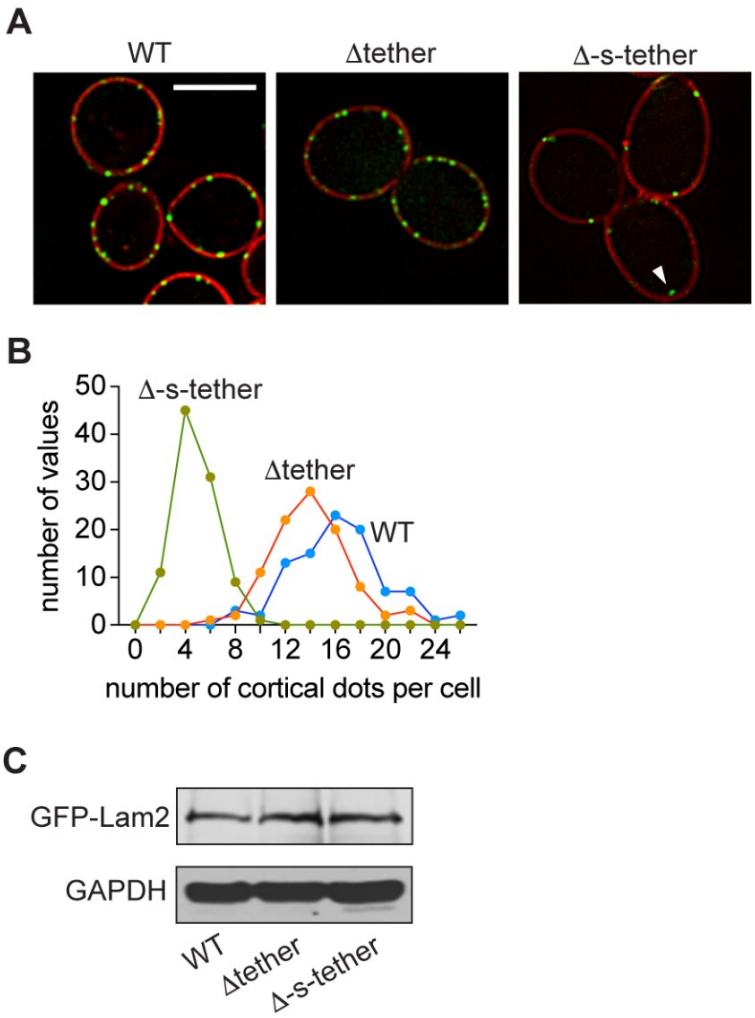

A.

Figure 3.4. Localization of Lam2 in WT and tether mutants.
A. GFP-Lam2 was expressed from a plasmid (pGFP-Lam2) in WT (SEY6210), Δtether (ANDY198), and Δ-s-tether (CBY5838) cells. The cells were stained with CellMaskTM Orange for 5 min to mark the PM before fluorescence microscopy. Arrowhead: fluorescence in the cell interior. Scale bar = 5 μm. **B.** Frequency distribution indicating the number of fluorescent cortical dots in WT, Δtether), and Δ-s-tether cells expressing GFP-Lam2. More than 90 cells of each strain were scored and the distribution was plotted using a bin size of 2. The average number of cortical dots per cell was 16, 14 and 4 for WT, Δtether and Δ-s-tether, respectively. **C.** Anti-GFP immunoblots indicated that GFP-Lam2 levels were unaffected in Δtether and Δ-s-tether cells as compared to wild type, using anti-GAPDH as the loading control.

Δ-s-tether cells grow normally on rich media but poorly on minimal media (**Fig 2.5B, 2.5E**), suggesting that the lack of ER-PM contact sites disrupts cell metabolism. If this were indeed the case, then an artificial ER-PM tethering protein might allow the cells to grow normally. Several of the natural ER-PM tethers, e.g. Tcb1p-3p and Ist2p (**Fig 2.1A**), have a modular architecture and we used this design principle to assemble an artificial tether ("ER-PM staple") from unrelated non-yeast proteins. As building blocks

for the ER-PM staple we used: (i) two ER-anchoring trans-membrane domains from herpes virus mK3 E3 ubiquitin ligase; (ii) extended helices from mammalian mitofusin 2 to span the gap between the PM and ER; and (iii) the C-terminal polybasic region from mammalian Rit1 (RitC) that targets the PM (**Fig 2.5A**). We fused green fluorescent protein (GFP) to the *N*-terminus in order to visualize the ER-PM staple in cells. Expression of the ER-PM staple from the yeast actin promoter largely rescued the growth defect of Δ-s-tether cells cultured on solid medium (**Fig 2.5B**), indicating that the artificial staple is a functional substitute for the endogenous tether proteins. Fluorescence microscopy revealed that the ER-PM staple localizes to cER in both WT and Δ-s-tether cells, consistent with the idea that it generates ER-PM contact sites albeit fewer than endogenous tethers (**Fig 2.5C, 2.5D**). The overall distribution of the ER-PM staples was similar in WT and Δ-s-tether cells, although the staples in Δ-s-tether cells aggregated in larger spots with greater fluorescence. The finding that a wholly heterologous construct can replace endogenous tether proteins in rescuing the poor growth of Δ-s-tether cells indicates importantly that the tethers (**Fig 2.1A**) perform a non-specific bridging function relevant to cell growth that is exclusive of any tether-specific activities. A further conclusion from this result is that the proposed lipid transfer function of the SMP domains of the tricalbins (**Fig 2.1A**)(155) is not required for cell growth, consistent with observations in HeLa cells and mice lacking E-Syts (153, 157).

Figure 3.5. Slow growth of ∆-s-tether cells is rescued by expression of an artificial ER-PM tether or choline.

A. The “ER-PM staple" has a modular architecture consisting of an N-terminal GFP, an ER anchor comprising two transmembrane domains and a lumenal loop from herpes virus (MVH68) mK3 E3 ubiquitin ligase, two helices from mitofusin 2 that are predicted to adopt an antiparallel arrangement ~9 nm long, and the polybasic domain from RitC that targets the PM.**B.** Tenfold serial dilutions of WT (SEY6210) and ∆-s-tether (CBY5838) cells, transformed with either the vector control (YCplac111) or a plasmid expressing the artificial staple (pCB1185), spotted on solid growth medium and incubated for 2 days at 30˚C.**C**. Differential Interference Contrast (DIC) images of WT and ∆-s-tether cells and the corresponding spinning disc confocal fluorescence microscopy images showing the co-localization of RFP-ER (pCB1024) and the GFP-marked artificial staple (pCB1185) at three different optical focal planes. Scale bar = 5 µm. **D**. Quantification of the staple distribution within mother and buds, and at cortical ER (cER) versus internal cytoplasmic ER.**E**. Choline-dependent growth of ∆-s-tether cells. WT, ∆tether (ANDY198), and ∆-s-tether (CBY5838) cells were streaked onto solid growth medium supplemented with 1 mM choline chloride as indicated, and incubated for 3 days at 30°C.**F**. Quantification of ER-RFP localization in WT and ∆-s-tether cells with and without 1 mM choline represented as a ratio of the length of PM-associated ER per circumference of PM in each cell (n > 50 cells; error bars represents S.E.M.).**G**. Lipid composition of WT, ∆tether and ∆-s-tether cells represented as a normalized mole percentage relative to WT (set to 1.0). The data represent the mean ± s.e.m. derived from the analysis of 5 independent samples.

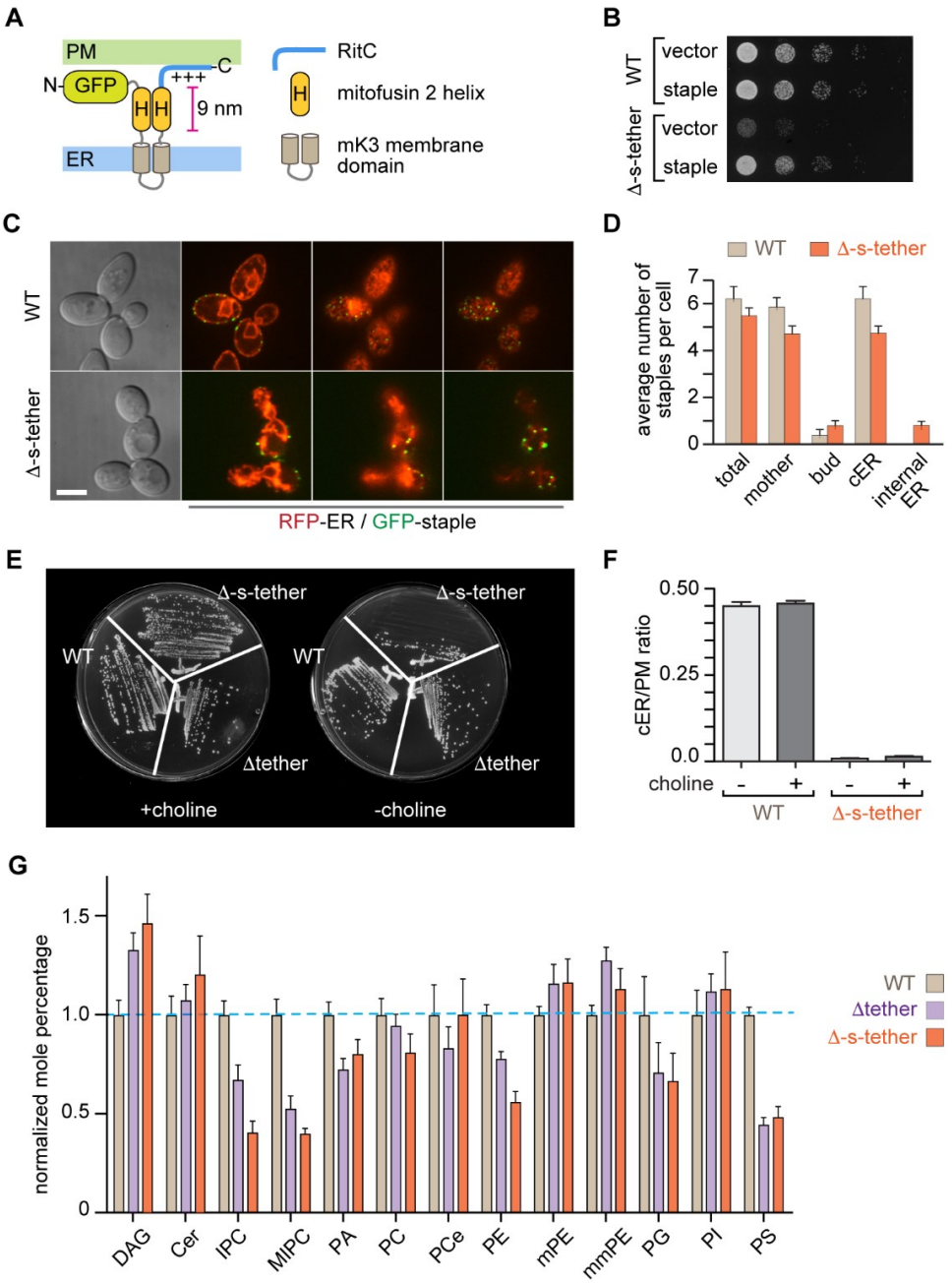

3.2.2. ER-PM contacts have multifactorial effects on several lipid biosynthetic pathways

Why would the absence of ER-PM tethers cause cells to grow slowly, with growth rescue being achieved by an artificial tether? Tavassoli et al. (177) suggested that the ER-anchored phospholipid methyltransferase Opi3p acts at ER-PM contact sites, *in trans*, to generate a pool of PC at the PM that is necessary for growth. If Opi3p is unable

to act on the PM, as would be expected for cells lacking ER-PM contact sites, then a choline supplement must be provided to generate the necessary PC via the Kennedy pathway (177). Indeed, we found that ∆-s-tether cells achieve normal growth when the medium is supplemented with choline (**Fig 2.5E**). Importantly, the extent of cER was not detectably different in choline-grown ∆-s-tether cells (**Fig 2.5F**). We conclude that choline supplementation bypasses the requirement for ER-PM contact sites to support cell growth.

Figure 3.6. *OPI3* and *CHO2* affect choline-sensitive growth defects of ∆-s-tether cells.

A. Deletion of CHO2 or OPI3 in ∆-s-tether cells results in a synthetic growth defects when the cells are cultured without addition of choline to the growth medium. WT (SEY6210), ∆-s-tether (CBY5838), cho2∆ ∆-s-tether (CBY6267) and opi3∆ ∆-s-tether cells (CBY6271) were streaked onto selective solid media with or without 1 mM choline, and incubated for 2 days at 30°C. **B**. Increased expression of Opi3 suppresses choline-sensitive ∆-s-tether growth defects. WT and ∆-s-tether cells transformed with either the vector control (pRS416) or a plasmid expressing OPI3 from a constitutively active promoter (pOPI3) were streaked onto solid growth media supplemented with or without 1 mM choline as indicated, and incubated for 2 days at 25°C.

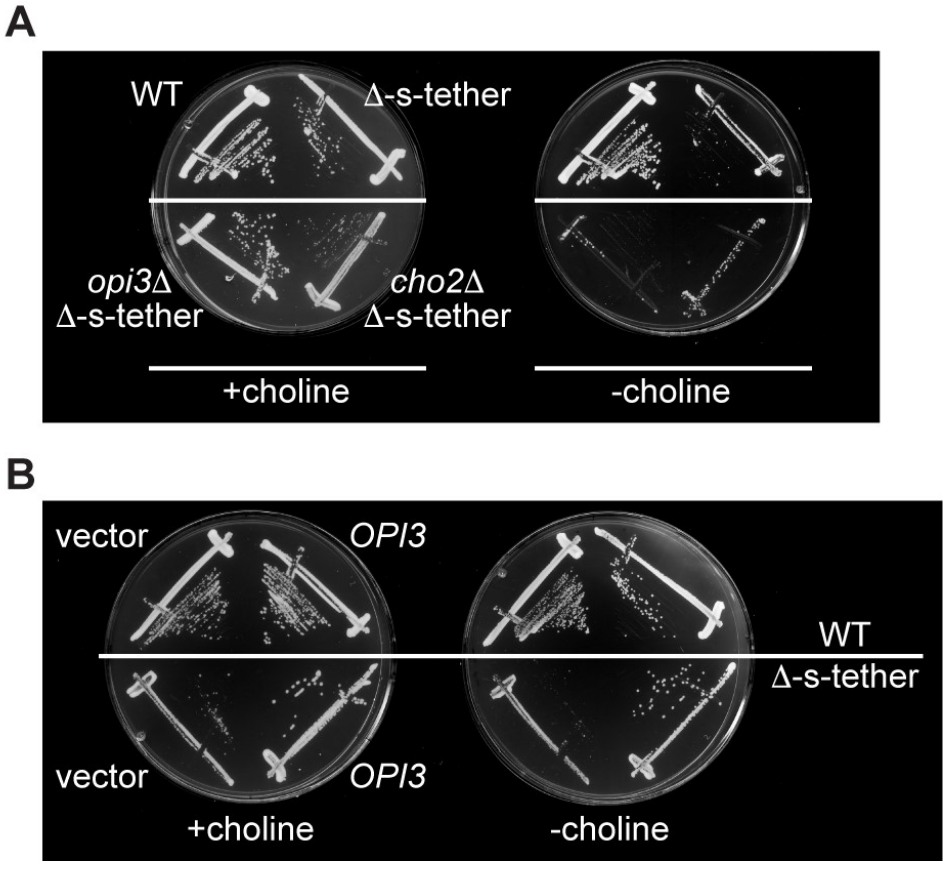

Consistent with these findings, the deletion of either *OPI3* or *CHO2* in ∆-s-tether cells severely exacerbated the growth defect of the cells unless choline was provided

(**Fig 2.6**). However, in the absence of choline, *OPI3* overexpression effectively suppressed the choline-dependent growth defect of ∆-s-tether cells (**Fig 2.6B**), potentially by providing an alternative route to generate PC pools at the PM. Unlike choline supplementation to the growth medium, the addition of ethanolamine or inositol, which promote PE and PI synthesis respectively, did not rescue ∆-s-tether growth defects (**Fig 2.7**).

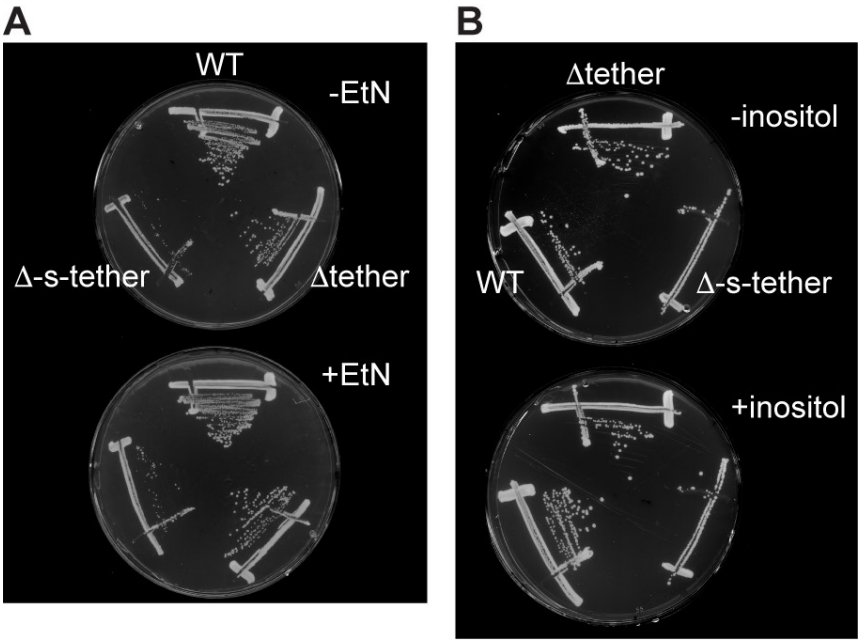

Figure 3.7. Ethanolamine and inositol supplementation do not suppress ∆-s-tether growth defects.
WT (SEY6210), ∆tether (ANDY198), and ∆-s-tether (CBY5838) cells were streaked onto solid growth media supplemented with 1 mM ethanolamine (**A**) or 75 µM inositol (**B**) as indicated, and incubated at 30°C for 2 or 3 days, respectively.

The ability of choline to rescue the poor growth of Δ-s-tether cells, and the functional requirements of ∆-s-tether cells for *CHO2* and *OPI3*, suggested that PC synthesis/levels might be dysregulated in these cells. Surprisingly, whole cell lipidomics (**Fig 2.5G**) revealed that PC levels were only ~20% lower in ∆-s-tether cells compared with WT cells, but the relative amounts of a number of other lipids, notably PE, PS and the yeast sphingolipids IPC and MIPC were considerably reduced. Reduced levels of these lipids were also found in ∆tether cells that grow almost as well as WT cells, but the lipid compositional effects were generally more pronounced in ∆-s-tether cells. For example, we found the mole percentage of IPC content in ∆tether cells to be ~67% of that in WT cells, whereas in ∆-s-tether cells the level of this lipid fell to ~40% of that in

WT cells. Increases in some lipids were also measured, most notably DAG which was 1.3-fold higher in Δ-s-tether compared with WT cells. These results suggest a possible threshold effect in which the lipid compositional changes in Δ-s-tether cells have a severe impact on growth, whereas the somewhat lesser changes in Δtether cells do not.

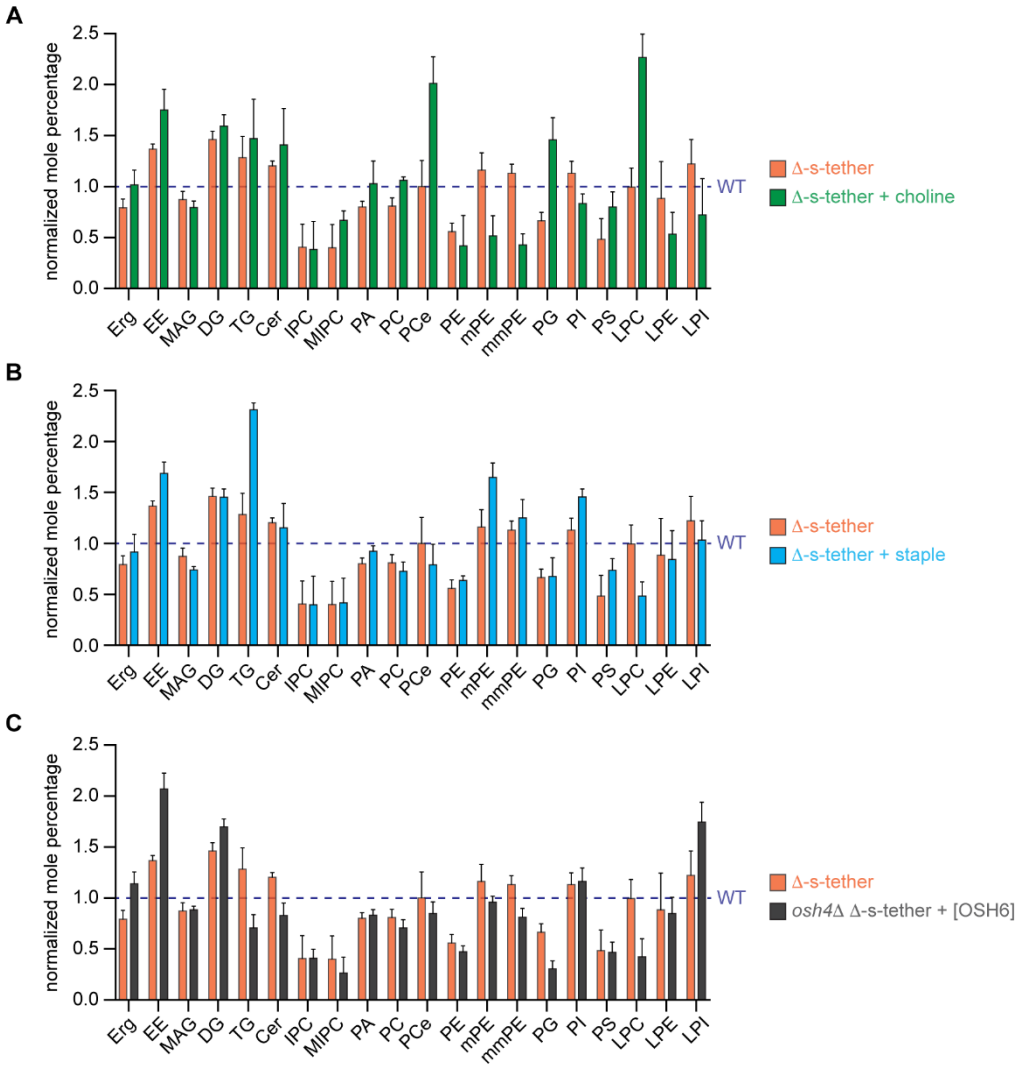

Figure 3.8. Lipidomics analyses of Δ-s-tether cells.
A. Comparison of the lipid composition of Δ-s-tether cells grown in the absence or presence of 1 mM choline. **B**. Comparison of the lipid composition of Δ-s-tether cells and Δ-s-tether cells expressing an artificial tether ('staple'). The cells were grown in synthetic medium without choline. **C**. Comparison of the lipid composition of Δ-s-tether cells and osh4Δ Δ-s-tether expressing Osh6. In all panels, lipid compositions are presented as a normalized mole percentage relative to WT (blue dotted line set to 1.0). The data represent the mean ± s.e.m. derived from the analysis of 5 independent samples. Erg, ergosterol, EE, ergosteryl ester, MAG, monoacylglycerol, DG, diacylglycerol, TG, triacylglycerol, Cer, ceramide, IPC (inositol phosphorylceramide); MIPC (mannosylinositol phosphorylceramide); PA (phosphatidic acid); PC (phosphatidylcholine); PCe (ether phosphatidylcholine); PE (phosphatidylethanolamine); mPE (monomethyl PE); mmPE (dimethyl PE); PG (phosphatidylglycerol); PI (phosphatidylinositol); PS (phosphatidylserine), LPC (lyso PC), LPE (lyso PE), LPI (lyso PI).

Comparison of the lipid composition of ∆-s-tether cells cultured with or without choline supplementation revealed changes that could be predicted based on the deployment of the Kennedy pathway because of the availability of choline (**Fig 2.8A**). Thus, PC and PS levels increased in the choline-supplemented cells, bringing the levels of these lipids closer to those in WT, whereas levels of mono- and dimethyl-PE (mPE, and mmPE, respectively) fell. Choline supplementation of ∆-s-tether cells also resulted in an increase in MIPC levels, though other sphingolipids and their precursors were only slightly affected. Unlike lipid compositional changes seen upon choline addition, rescue of ∆-s-tether growth defects by the artificial tether indicated a different mechanism. The lipidomic profile of ∆-s-tether cells expressing the artificial tether was more consistent with a restoration of normal phospholipid synthesis through the CDP-DAG pathway (**Fig 2.8A**). The artificial tether increased PS, PI, and mmPE levels, though levels of PC were not appreciably changed from ∆-s-tether cells cultured without choline. The artificial tether also affected storage lipids: esterified ergosterol and triacylglycerol (TG) showed especially large increases as a proportion compared to WT. To our surprise, expression of the artificial tether in ∆-s-tether cells did not restore levels of sphingolipids or their immediate precursors. We conclude that the molecular basis of growth rescue in Δ-s-tether cells by choline and the artificial tether is multifactorial and is likely finely tuned to the precise pools and relative abundance of several lipids depending on the mode of suppression.

3.2.3. Retrograde transport of sterols is defective in ∆-s-tether cells

To determine whether ER-PM contact sites play a role in sterol exchange between the two membranes, we compared the rate of retrograde transport of dehydroergosterol (DHE) from the PM to the ER in WT, ∆tether and ∆-s-tether cells using a previously described assay (**Fig 2.9A**) (184, 497). DHE is a fluorescent sterol that is widely used as a reporter of intracellular sterol transport and distribution (498); it is particularly appropriate as a sterol reporter in yeast cells as it is a closely related to ergosterol, and as effective as ergosterol in supporting the growth of *hem1Δ* cells that cannot synthesize sterols (184). To load DHE into the PM, the cells are incubated under hypoxic conditions to overcome "aerobic sterol exclusion" which represses endogenous sterol synthesis in favor of exogenous sterol import. When the DHE-loaded cells are transferred to aerobic conditions, ergosterol synthesis resumes and DHE is displaced

from the PM. On reaching the ER, DHE becomes esterified by ER-localized sterol acyltransferases. The extent of esterification - detected by the appearance of lipid droplets containing fluorescent DHE or direct measurement of DHE esters by HPLC analysis of lipid extracts from the cells (184) - provides a measure of retrograde transport.

Figure 3.9. Retrograde transport of exogenously supplied DHE is slowed ~4-fold in ∆-s-tether cells; rescue by expression of an artificial ER-PM tether or choline.

A. Schematic illustration of the retrograde sterol transport assay. The assay measures transport-coupled esterification of exogenously supplied dehydroergosterol (DHE). Cells are incubated with DHE for 36 h under hypoxic conditions to load the sterol into the plasma membrane (PM)(step 1, mediated by the ABC transporters Aus1 and Pdr11). Further incubation (chase period) after exposing the cells to air results in the exchange of DHE between pools in the PM (step 2) and its transfer to the endoplasmic reticulum (ER) (step 3) where it is esterified (step 4) by the sterol esterification enzymes Are1 and Are2. DHE esters that are sequestered in lipid droplets (LD). **B**. Representative images of WT, ∆tether and ∆-s-tether cells obtained immediately after DHE loading (chase time = 0 h) and 2 h after incubation under aerobic conditions. The puncta seen in the 2 h chase images correspond to LDs. Scale bar = 10 µm. **C**. DHE esters were quantified at different times during the aerobic chase period by analyzing hexane/isopropanol extracts of the cells by HPLC equipped with an in-line UV detector. The data are represented as percentage of DHE ester recovered (= DHE ester/(DHE + DHE ester)). Linear regression of the data points between 1-2 h indicates relative slopes of 1 (for WT and ∆tether cells) and 0.24 ± 0.05 for ∆-s-tether cells (also see panel D). **D**. Transport-coupled esterification of exogenously supplied DHE. The bar chart presents the mean ± S.E.M. (n = 3) of the relative rate of DHE esterification after the 1 h lag period at the start of the aerobic chase. The mean esterification rate for WT cells is set at 1.0. **E**. Incorporation of DHE into the PM (corresponding to step 1 in panel A), quantified using fluorescence images acquired immediately after the hypoxic incubation period. The area, integrated fluorescence and the Corrected Total Cell Fluorescence (CTCF) was calculated for individual cells using Image J. At least 40 cells were analyzed. CTCF = integrated density - (area of selected cell x mean fluorescence of background reading). The box and whiskers plot shows the mean of the measurements, with whiskers ranging from the minimum to the maximum value measured. **F**. Microsomes from WT and ∆-s-tether cells were assayed for their ability to esterify [3H]cholesterol (supplied as a complex with methyl-β-cyclodextrin) on addition of oleoyl-CoA. Esterification, assessed by organic solvent extraction and thin layer chromatography, proceeded linearly for at least 10 min. The bar chart shows the mean ± S.E.M. (n = 4) of ACAT (acyl CoA: cholesterol acyl transferase) activity as the rate of production of cholesteryl ester (CE) per mg microsomal protein per minute. This measurement corresponds to step 4 in panel A. **G**. The amount of ergosterol in WT and ∆-s-tether cells (nmol per OD600 of cell suspension) was measured by lipid extraction and HPLC at the start and end of the aerobic chase period. This measurement corresponds to step 3a in panel A (see text for details).

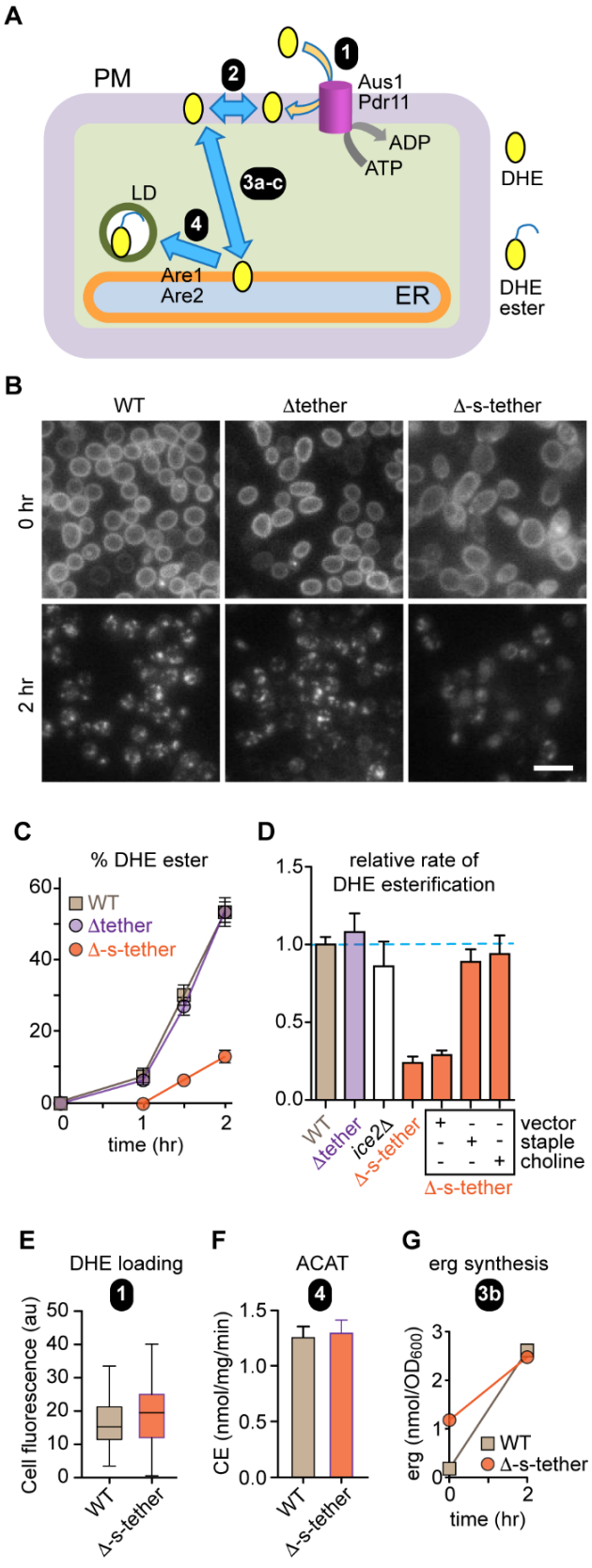
A
PM
1
2
Aus1
Pdr11
ADP
ATP
3a-c
LD
4
Are1
Are2
ER
DHE
DHE ester
B
WT
Δtether
Δ-s-tether
0 hr
2 hr
C
% DHE ester
WT
Δtether
Δ-s-tether
time (hr)
D
relative rate of
DHE esterification
WT
Δtether
ice2Δ
Δ-s-tether
vector
staple
choline
Δ-s-tether
E
DHE loading
1
Cell fluorescence (au)
WT
Δ-s-tether
F
ACAT
4
CE (nmol/mg/min)
WT
Δ-s-tether
G
erg synthesis
3b
erg (nmol/OD600)
WT
Δ-s-tether
time (hr)

At the start of the chase period, DHE fluorescence was observed as a 'ring stain' in WT, ∆tether and ∆-s-tether cells (**Fig 2.9B**), indicating insertion of the fluorescent sterol into the PM (184, 434). After a 2 h incubation ('chase') under aerobic conditions, fluorescence was concentrated in lipid droplets in WT and ∆tether cells, but the same punctate fluorescence was not observed in ∆-s-tether cells (**Fig 2.9B**). To quantify retrograde transport, the amount of imported DHE that was converted into DHE esters was measured at different times following the aerobic chase (**Fig 2.9C**). DHE esterification proceeds linearly after a lag period of ~1 h during which the cells adapt to aerobic conditions allowing resumption of ergosterol synthesis (184). Compared to WT or ∆tether cells, we observed a ~4-fold decrease in the rate of transport-coupled esterification of DHE in ∆-s-tether cells (**Fig 2.9B, C**). This reduction in esterification rate was not seen in the progenitor strains ∆tether or *ice2*∆, and could be restored to WT levels by expressing the ER-PM staple, or by growing the cells in choline (**Fig 2.9D**, **Fig 2.10**). The latter result (i) suggests that sterol transport between the PM and ER does not depend on ER-PM MCSs as these structures are equally absent in ∆-s-tether cells grown with or without choline (**Fig 2.5F**), and (ii) argues against a recent proposal [54] that the sterol acyl transferases Are1p and Are2p act *in trans* at ER-PM MCSs, directly receiving sterols from the ABC transporters Aus1p and Pdr11p, thereby eliminating the need for STP-mediated sterol transport between the PM and ER.

Figure 3.10. Retrograde transport of exogenously supplied DHE in ∆-s-tether cells supplemented with choline.

A. Representative images of choline-grown WT and ∆-s-tether cells obtained immediately after DHE loading (chase time = 0 h) and 2 h after incubation under aerobic conditions. The puncta seen in the 2 h chase images correspond to LDs. **B**. DHE esters were quantified at different times during the aerobic chase period by analyzing hexane/isopropanol extracts of the cells by HPLC equipped with an in-line UV detector. The data are represented as percentage of DHE ester recovered (= DHE ester/(DHE + DHE ester)). **C**. Incorporation of DHE into the PM of choline-grown cells, quantified using fluorescence images acquired immediately after the hypoxic incubation period as detailed in Fig 3E. 50 cells were analyzed. The box and whiskers plot shows the mean of the measurements, with whiskers ranging from the minimum to the maximum value measured. **D**. Microsomes from choline-grown WT and ∆-s-tether cells were assayed for their ability to esterify [3H]cholesterol on addition of oleoyl-CoA as described in Fig 3F. The bar chart shows the mean ± S.E.M. (n = 3) of ACAT (acyl CoA: cholesterol acyl transferase) activity as the rate of production of cholesteryl ester (CE) per mg microsomal protein per minute. **E**. The amount of ergosterol in choline-grown WT and ∆-s-tether cells (nmol per OD600 of cell suspension) was measured by lipid extraction and HPLC at the start and end of the aerobic chase period. Each data point represents a triplicate measurement (the error bars are contained within the symbol used for plotting).

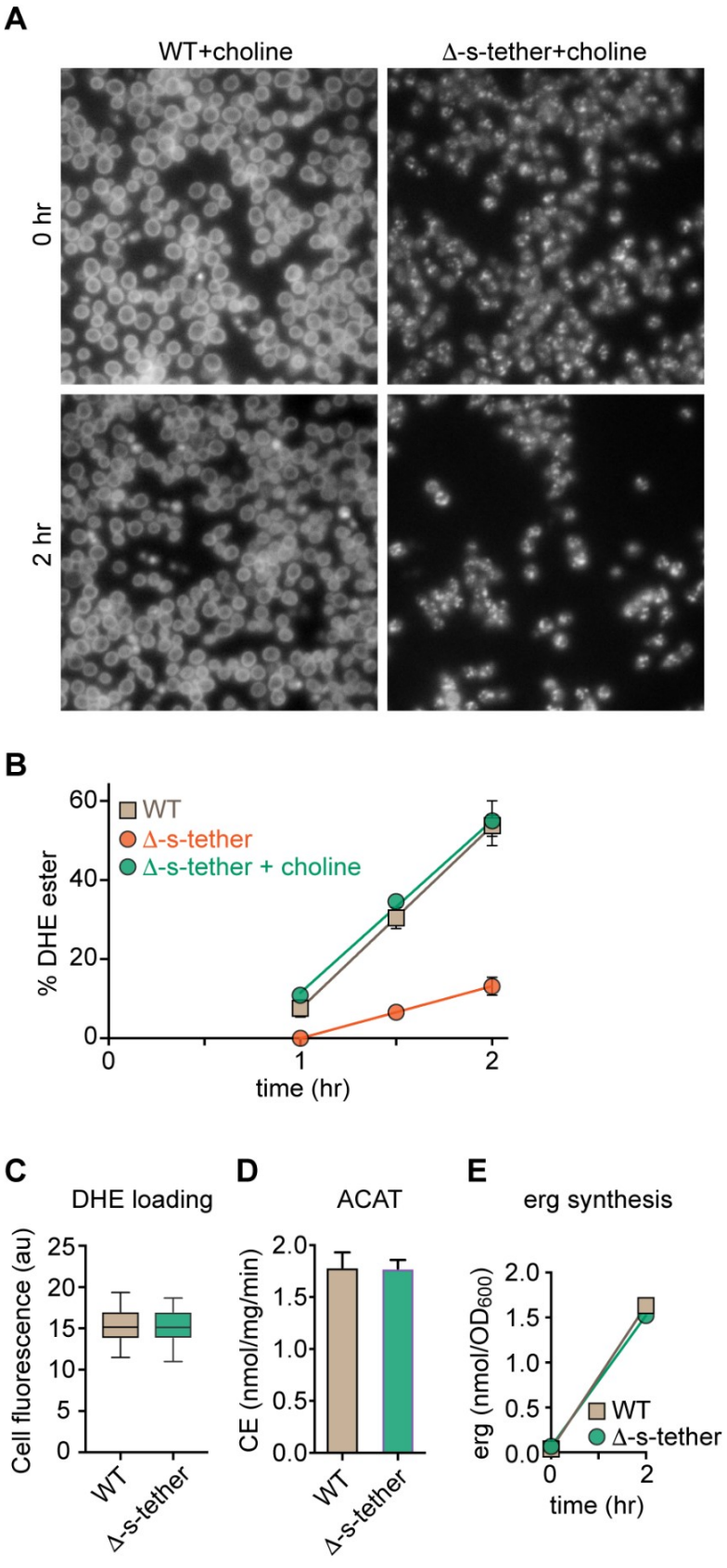
A
WT+choline
Δ-s-tether+choline
0 hr
2 hr
B
WT
Δ-s-tether
Δ-s-tether + choline
% DHE ester
time (hr)
C
DHE loading
Cell fluorescence (au)
WT
Δ-s-tether
D
ACAT
CE (nmol/mg/min)
WT
Δ-s-tether
E
erg synthesis
erg (nmol/OD600)
WT
Δ-s-tether
time (hr)

Transport-coupled esterification of DHE is a complex process that can be separated into a series of discrete mechanistic steps (**Fig 2.9A**): **1** - insertion of DHE into the PM, requiring the ABC transporters Aus1p and Pdr11p; **2** - equilibration of DHE amongst PM sterol pools, *e.g.* pools located in the outer and inner leaflets; **3** - non-vesicular transport of DHE from the cytoplasmic face of the PM to the ER (**3a**), a process that requires resumption of ergosterol synthesis (**3b**) as the cells recover from hypoxia, and transport of ergosterol to the PM (**3c**); and finally, **4** - esterification of DHE at the ER by the ACAT enzymes Are1p and Are2p. Defects in one or more of these steps could account for the slow-down in DHE esterification seen in ∆-s-tether cells. We verified that DHE loading (step **1**) (**Fig 2.9E**) and ACAT activity (step **4**) (**Fig 2.9F**) were similar in WT and ∆-s-tether cells grown in the absence of choline, and the same was true when the cells were grown in the presence of choline (**Fig2.10C, D**). However, the level of endogenous ergosterol in ∆-s-tether cells at the start of the aerobic chase was higher than in WT cells on a per cell basis, although it reached the same value at the end of the chase indicating that ergosterol re-synthesis (step **3b**) occurs normally (**Fig 2.9G**). No difference between ergosterol content and re-synthesis was seen when the cells were grown in the presence of choline (**Fig2.10E**). As ergosterol synthesis is largely abolished under hypoxic conditions, the ergosterol content of each cell diminishes with each cell division and is replaced in our protocol by DHE. Because ∆-s-tether cells grow slowly in the absence of choline, the ergosterol 'wash-out' is less complete for these cells than for WT cells. The presence of a significant amount of residual ergosterol in ∆-s-tether cells at the start of the aerobic chase could conceivably reduce the rate at which newly synthesized ergosterol is able to displace DHE from the PM, resulting in an apparently slower DHE esterification rate and obscuring information on whether sterol transport between the PM and ER is indeed affected. Thus, our results suggest that the slow rate of esterification observed in ∆-s-tether cells could be due to a defect in steps **2** (DHE equilibration within the PM) and/or **3** (sterol (DHE and ergosterol) exchange between the PM and the ER) (**Fig 2.9A**).

3.2.4. Bidirectional exchange of newly synthesized ergosterol between the ER and PM is normal in ∆-s-tether cells

To test directly whether sterol exchange between the ER and PM is affected in ∆-s-tether cells, one of the possibilities suggested by our results on retrograde sterol transport (**Fig2.9C, D**) we used a pulse-chase protocol (**Fig 2.11A**) to compare the rate

at which newly synthesized ergosterol is transported from the ER to the PM (184, 489). The assay was performed as described previously, using [^{3}H]methyl methionine to pulse-radiolabel ergosterol in the ER (184). Aliquots of cells taken at different chase time points were homogenized, and the PM was separated from the ER and other internal membranes by sucrose gradient centrifugation. For each time point, the specific radioactivity of [^{3}H]ergosterol (SR = scintillation counts (cpm) ÷ absorbance at 280 nm) was determined for the unfractionated cell homogenate and specific fractions after resolving the corresponding lipid extracts by HPLC, and the relative specific radioactivity for each fraction ($RSR_{fraction} = SR_{fraction} \div SR_{cell}$) was calculated.

Figure 3.11. Bidirectional transport of ergosterol from the ER to the PM is unaffected in ∆-s-tether cells.

A. Outline of the transport assay. **B**. Characterization of sub-cellular fractions. Top, Immunoblots using antibodies against Pma1 (PM), Dpm1 (ER) and Vph1 (vacuole). Fraction 2 is designated ER* to indicate that it contains membranes in addition to ER membranes. Data correspond to fractionation of a homogenate of WT cells prepared at the end of the labeling pulse. Middle, Quantification of Dpm1 and Pma1 in fractions prepared from homogenates of WT and ∆-s-tether cells taken after a 30-min chase period. The blots were quantified by ImageJ. Bottom, Quantification of ergosterol in the different fractions from the middle panel. **C**. WT and ∆-s-tether cells were processed as in panel A. The specific radioactivity (SR) of ergosterol in each fraction ([3H]ergosterol (cpm) ÷ ergosterol mass as determined from HPLC-UV absorbance) was normalized to the SR of the total homogenate at each time point to obtain a relative specific radioactivity, RSR. The figure shows RSR versus time (t = 0 min is the start of the labeling pulse). The lower portion of the graph (solid symbols) is based on 3-4 independent experiments); the upper portion (open symbols) is based on 2-5 independent experiments). The lines are mono-exponential fits of the data that plateau at RSR = 1. **D**. Transport of ergosterol in ∆-s-tether cells with block in vesicular transport. Mid-log cultures of WT, sec18-1ts (CBY2859), ∆-s-tether (CBY5838) and ∆-s-tether sec18-1ts (CBY5851) cells were grown at 24°C, shifted to the restrictive temperature of 37°C for 20 min, pulse-labeled with [3H]methyl-methionine for 4 min and chased for 15 min at the same temperature. The bar chart shows the RSR of the PM fraction from samples taken at the end of the pulse and chase periods. Data are mean ± S.E.M. (n = 3).

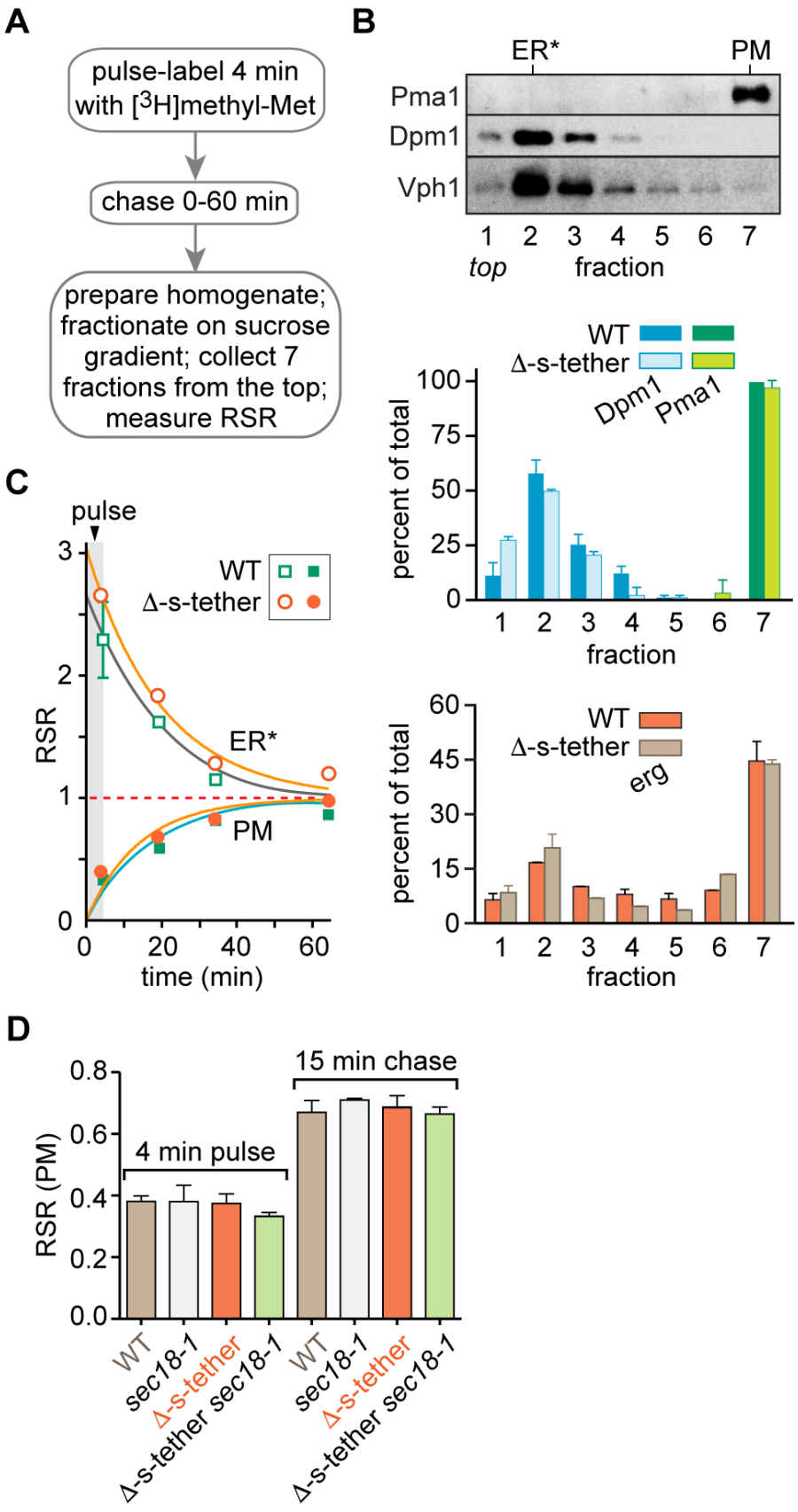
A
pulse-label 4 min with [3H]methyl-Met
chase 0-60 min
prepare homogenate; fractionate on sucrose gradient; collect 7 fractions from the top; measure RSR
B
ER*
PM
Pma1
Dpm1
Vph1
1 2 3 4 5 6 7
top
fraction
WT
Δ-s-tether
Dpm1
Pma1
percent of total
100
75
50
25
0
1 2 3 4 5 6 7
fraction
C
pulse
RSR
3
2
1
0
WT
Δ-s-tether
ER*
PM
0 20 40 60
time (min)
WT
Δ-s-tether
erg
percent of total
60
45
30
15
0
1 2 3 4 5 6 7
fraction
D
RSR (PM)
0.8
0.6
0.4
0.2
0.0
4 min pulse
15 min chase
WT
sec18-1
Δ-s-tether
Δ-s-tether sec18-1
WT
sec18-1
Δ-s-tether
Δ-s-tether sec18-1

Identical subcellular fractionation profiles were obtained with WT and ∆-s-tether homogenates (**Fig 2.11B**), displaying clear separation of the PM from internal membranes as judged by immuno-blotting using antibodies against organelle-specific proteins. The quality of the fractionation was exactly as reported in a previous study where a wide spectrum of antibodies was used to confirm the separation of the PM from other membranes (184). The majority of ergosterol was recovered in the PM fraction from WT cells, as expected, and this was also the case for ∆-s-tether cells indicating that the subcellular distribution of ergosterol is not affected by the absence of ER-PM contact sites (**Fig 2.11A, bottom panel**).

We analyzed fractions 7 (PM) and 2 (ER-enriched; we designated this fraction ER* to indicate that it contains other intracellular membranes (**Fig 2.11B**). The results are shown in **Fig 2.11C**. For both WT and Δ-s-tether cells, RSR for ER* was high (>2.0) on completion of the labeling pulse because [^{3}H]ergosterol is synthesized in the ER, before declining over the chase period to reach a value of 1.0. Conversely, RSR for the PM started at a low level (<0.5; the non-zero value indicates that [^{3}H]ergosterol is transported to the PM even as it is being synthesized during the pulse-labeling period) and increased to 1.0 by the end of the chase. The final RSR values of 1.0 for both fractions indicate equilibration of the ergosterol pulse between the ER and PM as previously reported (184, 489, 499). Mono-exponential fits of the data indicate that [^{3}H]ergosterol is exchanged between the ER and PM with a half time of ~10 min for both WT and Δ-s-tether cells. Thus, the exchange of newly synthesized ergosterol between the ER and PM is normal in ∆-s-tether cells.

We considered the possibility that conventional vesicular transport might deliver sterols to the PM to compensate for the possible failure of non-vesicular modes of transport in ∆-s-tether cells. To test this possibility, we constructed a ∆-s-tether *sec18-1*^{ts} strain that eliminates both exocytosis and ER-PM contact at elevated temperatures. Sec18p is required for exocytosis and most modes of vesicular trafficking (500, 501) and the *sec18-1*^{ts} conditional mutation blocks vesicular transport of secretory proteins and lipids to the PM (500, 502). Whether on its own or in the context of the ∆-s-tether mutations, the *sec18-1*^{ts} allele does not allow cells to grow at 37˚C, and ∆-s-tether *sec18-1* cells do not even grow at 30˚C (**Fig 2.12**). However, the combined growth defects of the ∆-s-tether mutations and *sec18-1* at 30˚C are additive as would be predicted for unrelated pathways, and do not correspond to a synergistic interaction as

would have been observed between mutations disrupting convergent pathways. After culturing at 23˚C, strains were incubated for 20 min at 37˚C and pulse labeled with [^{3}H]methyl-methionine followed by a 15 min chase. The calculated RSRs of [^{3}H]ergosterol in PM fractions showed no significant differences between WT, *sec18-1*, ∆-s-tether, or ∆-s-tether *sec18-1* cells, indicating that ergosterol exchange between the ER and PM is unaffected in all of these strains (**Fig 2.11D**). These results indicate that secretory vesicles do not provide a compensatory sterol transport mechanism in Δ-s-tether cells.

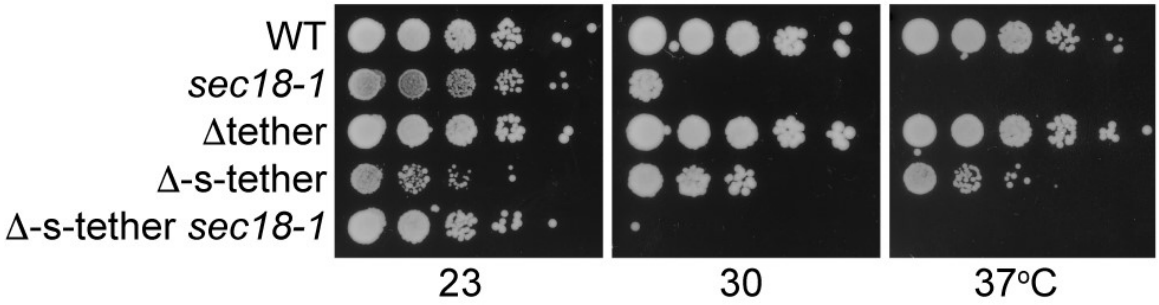

Figure 3.12. Growth of strains carrying the *sec18-1^{ts}* allele.
Tenfold serial dilutions of WT (SEY6210), sec18-1ts (CBY2859), ∆tether (ANDY198), ∆-s-tether (CBY5988) and ∆-s-tether sec18-1ts (CBY5851) cultures were spotted on synthetic complete medium and incubated at the indicated temperatures for 3 days.

We conclude that the exchange of newly synthesized ergosterol between the ER and PM does not require ER-PM contact sites. This result has two clear implications. *First*, the sterol transfer machinery in yeast is either absent from or not uniquely localized to ER-PM MCSs. This suggests that contact site-localized proteins such as Lam1-Lam4 are not essential for sterol exchange between the PM and ER; these proteins may act redundantly with soluble STPs or play other roles in intracellular sterol homeostasis (211). *Second*, yeast cells do not possess soluble STPs capable of lowering the energy barrier for sterol desorption by >10 k_BT, which would make intracellular sterol transport diffusion-limited rather than desorption-limited (488). Thus, non-vesicular sterol transport in yeast is likely mediated by cytoplasmic STPs that lower the energy barrier for desorption by a more typical ~2-3 k_BT (488) and that are present in a sufficient number per cell to account for the measured sterol exchange rate (488).

3.2.5. Does Osh4 account for sterol transport in the absence of ER-PM contact sites?

Osh4p is one of the subset of Osh proteins capable of binding sterols, and it is present in high levels in yeast at >30,000 copies per cell (503). Although elimination of Osh4p had no effect on sterol transport as measured via assays of sterol import (491) or ER-PM sterol exchange (**Fig 2.13**), we tested whether Osh4p might nevertheless provide a compensatory sterol transport mechanism to allow normal ER-PM sterol exchange in ∆-s-tether cells where the absence of ER-PM contact sites would prevent any putative membrane-bound STPs from reaching their target membrane. Consistent with a possible redundancy between Osh4p and ER-PM contact sites in sterol transport, we discovered that *osh4*∆ ∆tether cells grew poorly and *osh4*∆ ∆-s-tether cells were inviable (**Fig 2.15A**). In contrast, deletion of the putative sterol transporter encoded by *LAM2* had no impact on ∆-s-tether cells whether cultured with or without added choline (**Fig 2.14**). This result is consistent with the fact that the ∆-s-tether mutations compromise Lam2p function by eliminating its proximity to the cell cortex (**Fig 2.2**), and therefore no further effect would be anticipated on eliminating expression of the protein itself. Expression of Scs2p from a plasmid rescued *osh4*∆ ∆-s-tether cell lethality, but choline supplementation did not (**Fig 2.15A**). This result suggests that an ER-PM tether is required to restore viability to these strains; tether-independent, choline-induced, phospholipid synthesis is either irrelevant to *osh4*∆ ∆-s-tether synthetic lethality or choline supplementation is simply insufficient to overcome the severity of the phospholipid defect.

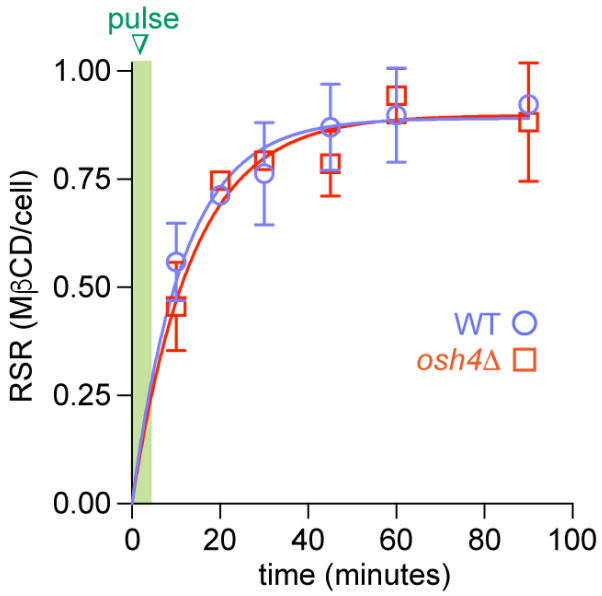

Figure 3.13.Normal transport of newly synthesized ergosterol to the PM in *osh4*Δ cells.

Transport of newly synthesized ergosterol to the PM in WT (SEY6210) and osh4Δ (HAB821) cells was measured by pulse-chase radiolabeling as described in Fig. 3, using MβCD extraction rather than PM isolation to quantify transport. A pulse of [3H]ergosterol was generated in the ER by labeling cells for 4 min with [3H-methyl]methionine. Samples were chased for the indicated times. At each chase point, an aliquot of cells was removed, dosed with energy poisons, placed on ice and incubated with MβCD. Following incubation, the sample was centrifuged and the MβCD-containing supernatant was removed from the cell pellet. Ergosterol was recovered from MβCD-ergosterol complexes as well as from the cell pellet by extraction with hexane/isopropanol, and its specific radioactivity was determined by HPLC (UV detection). The ratio of the specific radioactivity of ergosterol in MβCD-ergosterol complexes versus the cell homogenate (relative specific radioactivity, RSR) provides a measure of transport. Data points represent the mean ± S.E.M of three independent experiments, each of which comprised duplicate measurements at the indicated time points.

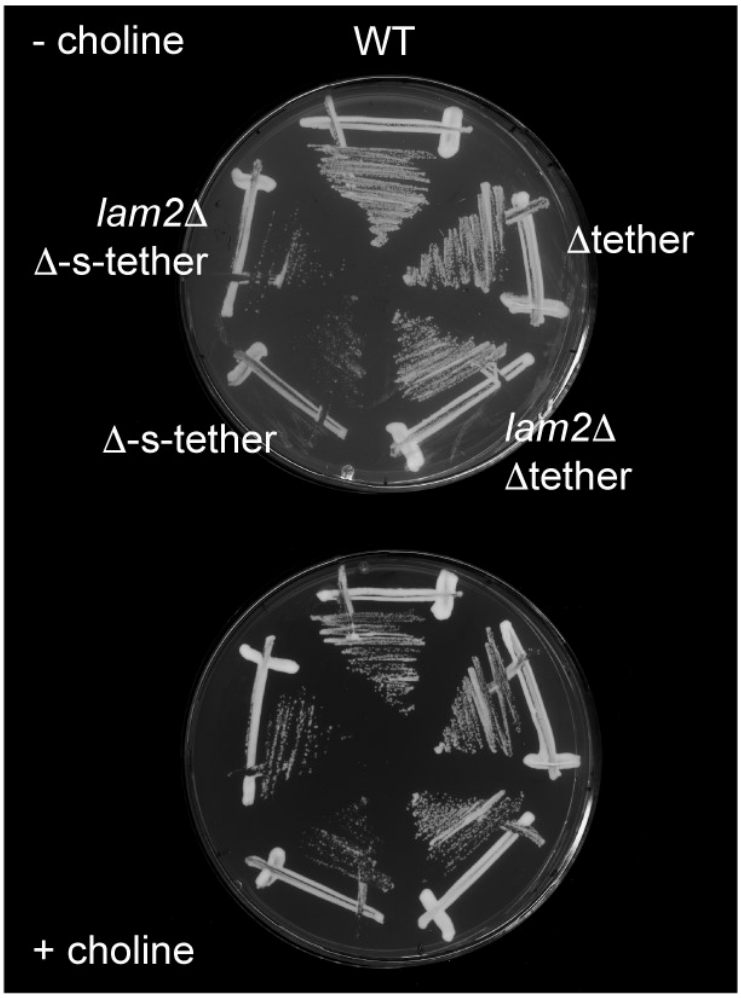

Figure 3.14. *LAM2* deletion does not impact growth of Δtether or Δ-s-tether.
WT (SEY6210), Δtether (ANDY198), Δ-s-tether (CBY5838), lam2Δ Δtether (CBY6150), and lam2Δ Δ-s-tether cells (CBY6150) were streaked onto selective solid media with and without 1 mM choline and incubated for 2 days at 30˚C.

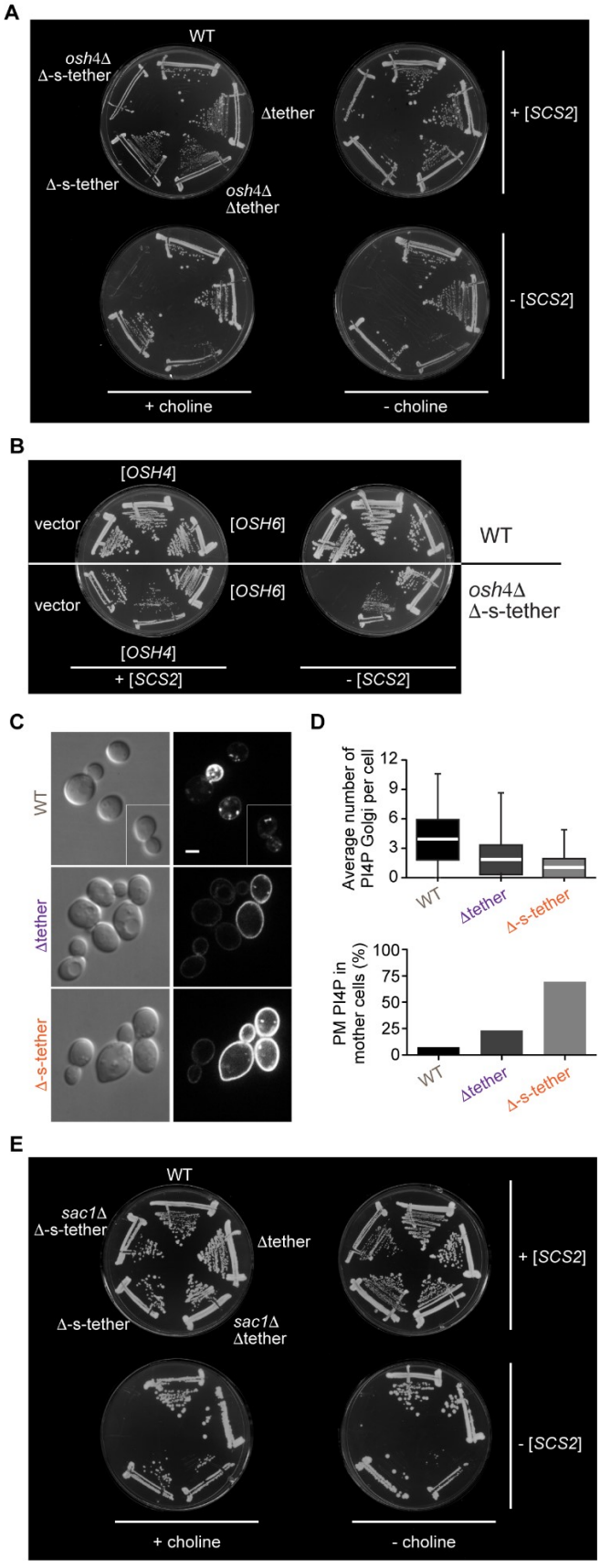
A
WT
osh4Δ
Δ-s-tether
Δtether
Δ-s-tether
osh4Δ
Δtether
+ [SCS2]
- [SCS2]
+ choline
- choline
B
[OSH4]
vector
[OSH6]
WT
[OSH6]
vector
osh4Δ
Δ-s-tether
[OSH4]
+ [SCS2]
- [SCS2]
C
WT
Δtether
Δ-s-tether
D
Average number of PI4P Golgi per cell
12
9
6
3
0
WT
Δtether
Δ-s-tether
PM PI4P in mother cells (%)
100
75
50
25
0
WT
Δtether
Δ-s-tether
E
WT
sac1Δ
Δ-s-tether
Δtether
Δ-s-tether
sac1Δ
Δtether
+ [SCS2]
- [SCS2]
+ choline
- choline

Figure 3.15. Functional interactions between ER-PM tethers and PI4P regulators
A. OSH4 deletion in Δ-s-tether cells results in synthetic lethality. WT (SEY6210), Δtether (ANDY198), Δ-s-tether (CBY5838), osh4Δ Δtether (CBY5940), and osh4Δ Δ-s-tether cells (CBY5988) were transformed with an episomal copy of the SCS2 tether gene (+ [SCS2]; pCB1183) and streaked onto selective solid media with and without choline supplementation. The presence of the SCS2 gene provides an ER-PM tether that confers robust growth, even in the absence of all other tether genes. On growth medium selecting against the SCS2 plasmid (- [SCS2]), osh4Δ Δ-s-tether cells were inviable with or without choline. **B**. OSH6 expression suppresses the synthetic lethality of osh4Δ in Δ-s-tether cells. WT and osh4Δ Δ-s-tether cells containing an episomal copy of SCS2 were transformed with either the high-copy vector control (YEplac181), OSH4 (pCB598), or OSH6 (pCB1266) and streaked onto solid growth media. On a medium selecting against the SCS2 plasmid, OSH4 or OSH6 expression suppressed osh4Δ Δ-s-tether synthetic lethality, whereas vector control did not. **C**. Representative images of WT, Δtether, and Δ-s-tether cells by DIC with corresponding fluorescence microscopy showing the localization of the PI4P sensor GFP-2xPHOSH2 (pTL511). Scale bar = 2 μm. **D**. Bar graphs quantifying the number of GFP-2xPHOSH2 fluorescent Golgi spots (lower and upper boundaries of boxes correspond to data quartiles; the white bar indicates the median; lines represent the range of spots/cell) and the percentage of GFP-2xPHOSH2 fluorescent mothers detected in WT, Δtether and Δ-s-tether cells. **E**. SAC1 deletion in Δ-s-tether cells results in a synthetic lethal interaction. WT, Δtether, sac1Δ Δtether (CBY6142), Δ-s-tether and sac1Δ Δ-s-tether cells (CBY6146) were transformed with an episomal copy of SCS2 and streaked onto selective solid media with and without choline supplementation. On a medium that selects against the SCS2 plasmid, sac1Δ Δ-s-tether cells were inviable whether or not choline was added.

To test if *osh4*Δ Δ-s-tether synthetic lethality results from defects in intracellular sterol transport, we generated a conditionally viable strain that combines Δ-s-tether mutations with a temperature-sensitive *osh4-1* allele (443). At 36˚C, *osh4-1 osh4*Δ Δ-s-tether cells do not grow, and so we measured DHE transport from the PM to the ER 1 hour after switching to the inactivating temperature. When *OSH4* is inactivated in Δ-s-tether cells in this manner, DHE transfer and esterification were found to be the same as in Δ-s-tether cells (**Fig 2.16**). We conclude that the elimination of *OSH4* has no further impact on sterol transport from the PM to the ER in Δ-s-tether cells.

Each of the seven *OSH* genes can provide the essential requirement for the entire family of *OSH* genes (192). Even though they are defined as 'oxysterol-binding protein homologs', not all Osh proteins are able to bind sterols but all likely bind PI4P (134, 197). Thus, Osh6 binds PI4P and PS in a mutually exclusive fashion, but cannot bind sterols (136, 194). As another way to determine if the *osh4*Δ Δ-s-tether synthetic lethality relates to the sterol- versus PI4P-binding activities of Osh4, we therefore tested if Osh6p could functionally replace Osh4p in this context. As shown in **Fig 2.15B**, expression of Osh6p from a multi-copy plasmid rescued the growth defect of *osh4*Δ Δ-s-tether cells. Plasmid-based expression of Osh6p was important for growth rescue as the chromosomally expressed protein, present at fewer than 2000 copies per cell (503), was

not able to support growth. Lipidomics analysis of *osh4*Δ Δ-s-tether cells rescued with multicopy *OSH6* did not reveal an obvious mode of suppression by changes in lipid metabolism (**Fig 2.8C**). Compared to Δ-s-tether cells, levels of most sphingolipid precursors and phospholipids (including PS) were unchanged in the *OSH6*-rescued cells or showed minor reductions. The minor reduction in free ergosterol measured in Δ-s-tether cells was restored to WT levels in *OSH6*-rescued *osh4*Δ Δ-s-tether cells, and ergosterol ester levels doubled over WT. These results are consistent with a model in which Osh4p and ER-PM tethers function redundantly and independently, but in an important function revolving around PI4P with indirect effects on sterol metabolism.

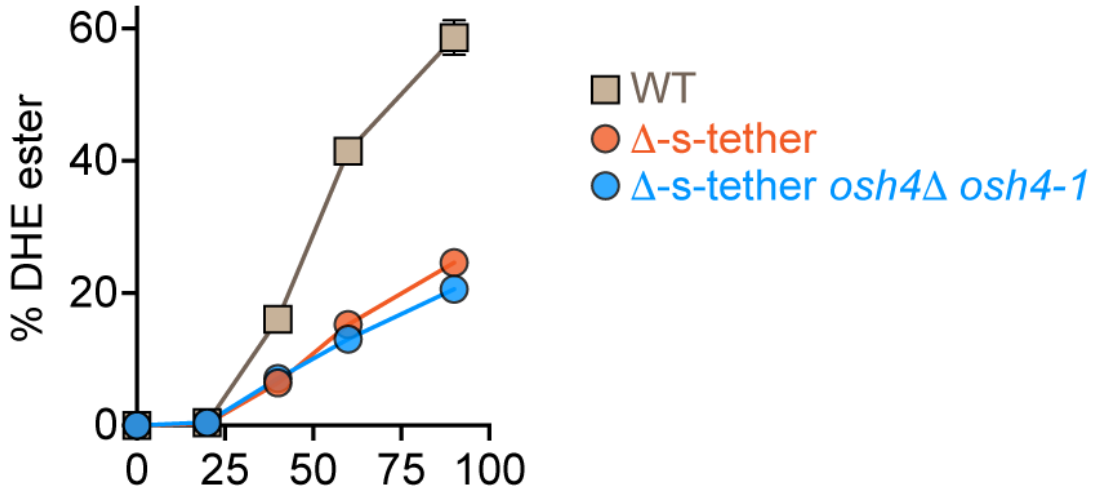

Figure 3.16. Elimination of Osh4 function in the Δ-s-tether strain does not exacerbate the slow rate of esterification of exogenously supplied DHE.

WT (SEY6210), Δ-s-tether (CBY5838) and osh4-1 osh4Δ Δ-s-tether (CBY6031) were inoculated from a saturated overnight culture into fresh media (complete synthetic media for WT and Δ-s-tether and the same medium without leucine for osh4-1 osh4Δ Δ-s-tether) supplemented with 20 μg/ml DHE and 0.5% Tween:ethanol. The cells were incubated under hypoxic conditions for 36 h at 30°C, before being transferred to 37°C for 1 h (continuing in hypoxic conditions) and then chased aerobically for the indicated time-points at 37°C. DHE esterification was measured as described in Fig 3.

To explore this model further, we used the PI4P marker GFP-PH^{Osh2} to compare the distribution of PI4P in WT and Δ-s-tether cells. It had been previously reported that PI4P was dysregulated in Δtether cells (16) and we anticipated that this phenotype might be exacerbated in Δ-s-tether cells. WT cells showed PI4P concentrated at the PM only in buds and also localized to the Golgi apparatus (**Fig 2.15C, D**); this distribution, was disrupted in Δ-s-tether cells where PI4P was evenly distributed throughout the PM in

both mother cells and buds (**Fig 2.15C, D**). The intensity of PI4P staining in the PM of ∆-s-tether mother cells was greater than that seen for ∆tether cells (**Fig 2.15C, D**). To test if the artificial staple could correct the PI4P accumulation/depolarization phenotype, GFP-PH^{Osh2} and the ER-PM staple were both expressed in ∆-s-tether cells (**Fig 2.17**). Although at a gross level the artificial tether did not restore normal PI4P polarization, PI4P was absent at the immediate cortical sites where the staple interacted with the PM, suggesting a potentially local corrective effect. The addition of choline to ∆-s-tether cells had no impact on GFP-PH^{Osh2} depolarization (100% of ∆-s-tether cells cultured with or without choline had equal GFP-PH^{Osh2} fluorescence in mother and bud PM, compared to 4.7% of WT cells grown with no added choline and 3.6% of WT cells with choline; n >104 cells), indicating that ER-PM MCS regulation of PI4P in the PM is distinct from the role of MCSs in PC metabolism. Taken together, our results suggest that the synthetic lethality of the ∆-s-tether mutations with *osh4*∆ is associated with dysregulation of PI4P homeostasis.

Figure 3.17. Altered PI4P distribution in ∆-s-tether cells is not corrected by expression of the artificial ER-PM staple.

A. Wild-type (SEY6210) cells expressing an mCherry-tagged version of the artificial RFP-staple (RFP-staple; pCB1188) and co-transformed with the PI4P sensor GFP-2xPHOSH2 (pTL511), as shown by DIC and fluorescence confocal microscopy. Scale bar = 5 µm. **B**. Fluorescent images of ∆-s-tether cells (CBY5838) co-expressing GFP-2xPHOSH2 and the artificial RFP-staple. The boxed region represents an enlarged region shown in the inset where gaps in the uniform PM PI4P fluorescence coincide with the presence of the artificial RFP-staple. Scale bar = 5 µm. C. Quantification of mother cell GFP-2xPHOSH2 fluorescence at the PM observed as a percentage of all wild-type and ∆-s-tether cells (n > 100 cells).

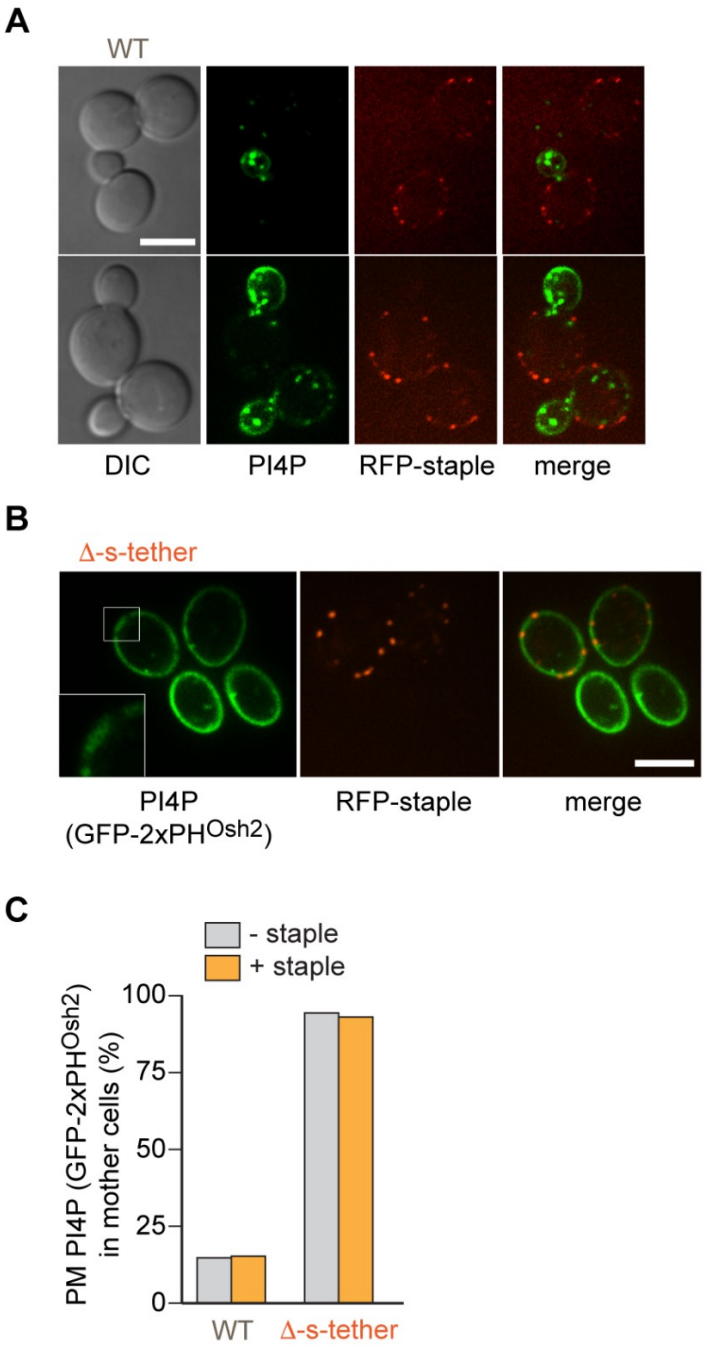

Osh4p and several other Osh proteins have been shown to be upstream regulators of the PI4P phosphatase Sac1p, inducing its activity and thereby affecting PI4P levels in several cellular membranes including the PM (131). Sac1p is an ER-membrane protein that interacts with most of the ER-PM tethers deleted in the Δ-s-tether strain (16), placing it in a position to act across ER-PM contact sites to dephosphorylate PM-localized PI4P. If Osh4p acts through Sac1p in the same pathway, then *sac1*Δ might also be synthetically lethal in Δ-s-tether cells. This was indeed the case (**Fig 2.15E**),

consistent with the model that Osh4p and Sac1p function in a PI4P regulatory pathway operating alongside ER-PM tethers. One possibility is that Sac1p itself provides limited tethering, a function that might be induced by the absence of the other tethers in Δ-s-tether cells. However, expressing the soluble enzymatic domain of Sac1p (Sac1$^{1-522}$p) without its ER membrane-binding domain suppressed *sac1*Δ Δ-s-tether lethality (**Fig 2.18**). This result indicated that Sac1p does not act as a tether, and that Sac1 dependence on MCSs can be partially bypassed if Sac1p is released from the membrane so that it can access PI4P in the PM. Because Osh4p acts *in vitro* as a soluble PI4P transport protein (62), it might function in cells to extract and transport PI4P from the PM to Sac1 in the ER. We tested if the requirement for Osh4-mediated PI4P transport could be circumvented if Sac1p was freed from the ER membrane to diffuse to the PM to dephosphorylate PI4P. However, soluble Sac1$^{1-522}$p expressed from a multicopy plasmid did not rescue *osh4*Δ Δ-s-tether lethality, indicating that the requirement for Osh4p cannot be bypassed by liberating Sac1p from the ER (**Fig 2.18**). Thus, in the context of ER-PM MCSs, Osh4p might play an important role in Sac1 regulation, but clearly has other independent functions as well.

Figure 3.18. The membrane-detached enzymatic SAC1$^{1-522}$ domain suppresses the synthetic lethality of *sac1*Δ Δ-s-tether but not *osh*Δ Δ-s-tether cells.

(**A**) WT (SEY6210) and sac1Δ Δ-s-tether (CBY6146) cells expressing an episomal copy of SCS2 (pSCS2) were transformed with the vector control (YCplac111) or plasmids expressing SAC1 (pRS415 SAC1), SAC11-522 (pRS415 SAC11-522), or SAC11-522expressed from a high-copy plasmid (pRS425 SAC11-522). Cells were streaked onto solid growth media containing 5'-FOA (to select against strains that cannot growth without SCS2), supplemented with and without 1 mM choline, for 3 days at 30°C; SAC1 and high-copy SAC11-522suppressed sac1Δ Δ-s-tether synthetic lethality, regardless of choline addition. (**B**) WT and osh4Δ Δ-s-tether (CBY5988) cells containing an episomal copy of SCS2 were transformed with the vector control, or plasmids expressing SAC1, SAC11-522, or high-copy SAC11-522. Cells were streaked onto solid 5'-FOA-containing media with and without 1 mM choline and incubated for 3 days at 30°C. In the absence of SCS2, neither SAC1 nor SAC11-522 expression suppressed osh4Δ Δ-s-tether synthetic lethality.

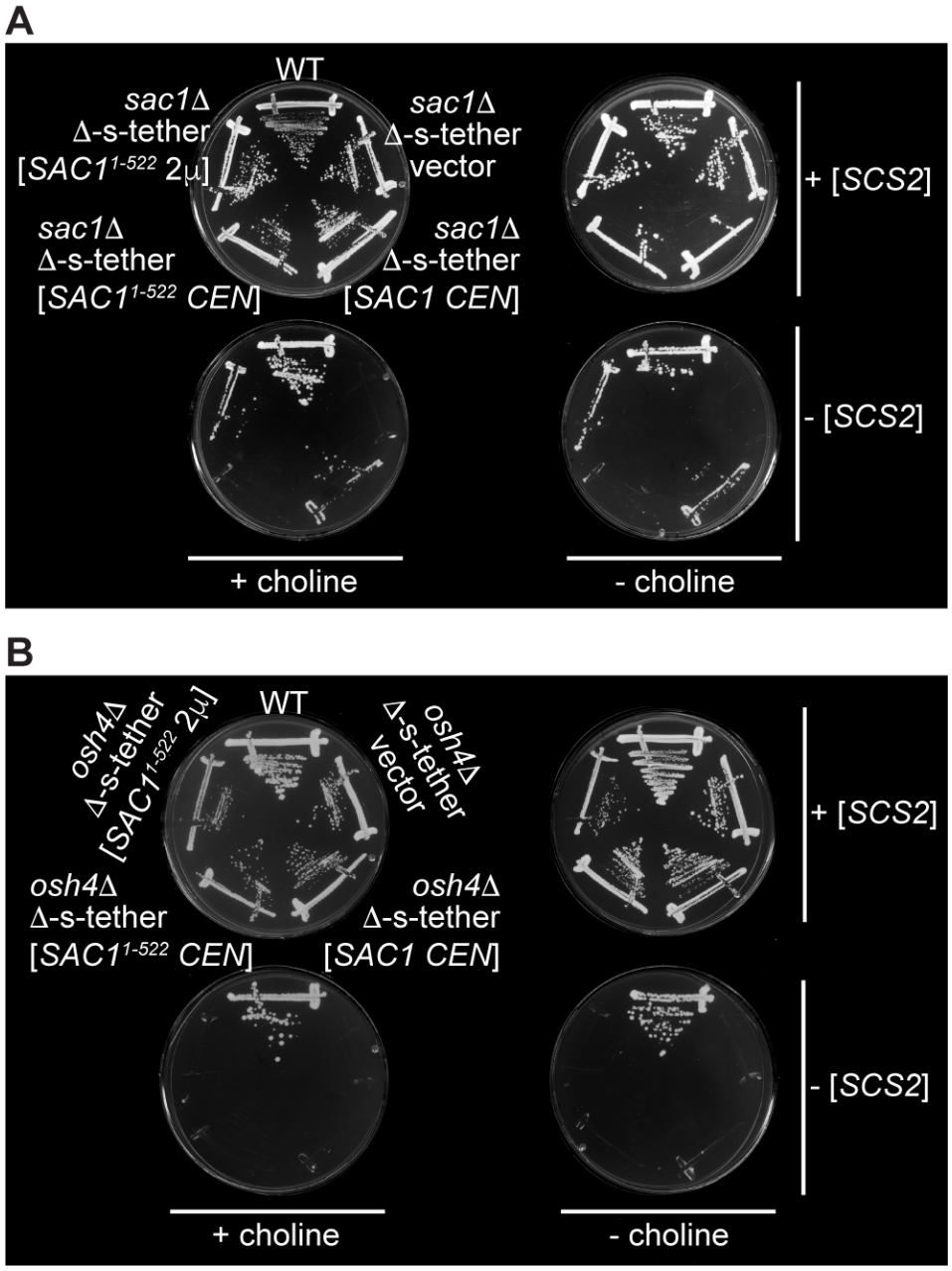

3.2.6. Altered lipid organization in the PM of Δ-s-tether cells

We have shown that the absence of ER-PM contact sites does not affect sterol exchange between the ER and PM (**Fig 2.11C**), and that this lack of effect is not due to compensatory sterol transport by secretory vesicles (**Fig 2.11D**) or by the single most abundant sterol binding protein in yeast, Osh4p (**Fig 2.15B**). We can therefore pinpoint the cause of slow transport-coupled esterification of exogenously supplied DHE in Δ-s-tether cells to step **2** in the scheme depicted in **Fig 2.9A**, i.e. the exchange of sterol

between sterol pools within the PM lipid bilayer. To investigate this point, we tested the growth of ∆-s-tether cells in the presence of three drugs that report on the lipid organization of the PM: nystatin, duramycin, and edelfosine.

Nystatin is an ergosterol-binding polyene antimycotic compound. Nystatin resistance is observed in viable sterol biosynthesis mutants and some mutants, such as *osh4*∆ (497), that disrupt sterol organization within the PM. Conversely, many mutants with altered lipid composition and/or PM organization exhibit nystatin sensitivity (497, 504). On nystatin-containing medium, ∆-s-tether cells exhibited an exacerbated growth sensitivity compared to ∆tether cells, and both strains were more sensitive than WT or nystatin-resistant *osh4*∆ cells (**Fig 2.19A**).

Figure 3.19. Alterations in ergosterol pools and dynamics at the PM in ∆-s-tether cells.

A. Sensitivity of ∆-s-tether cells to nystatin. Tenfold serial dilutions of WT (SEY6210), osh4∆ (HAB821), ∆tether (ANDY198) and ∆-s-tether (CBY5838) cultures spotted onto solid rich medium containing no nystatin, 1.25 µM (+), or 2.5 µM (++) nystatin, and incubated for 3 days at 30˚C. **B**. Tenfold serial dilutions of WT, ∆tether, and ∆-s-tether, lem3∆ (CBY5194) cultures were spotted onto solid rich media containing no drug, 5 µM duramycin, or 60 µM edelfosine, and incubated for 2 days at 25˚C and 30˚C. The lem3∆ strain is known to be duramycin-sensitive and was used as a positive control. **C**. Tenfold serial dilutions of WT, ∆tether, ∆-s-tether, and osh3∆ (JRY6202) cultures were spotted onto solid rich media containing no drug or 0.5 µg/mL myriocin, and incubated for 2 days at 30˚C. The osh3∆ strain is known to be myriocin-resistant and was used as a positive control. **D**. Assay to measure the proportion of cellular ergosterol that is extracted by MβCD. The PM of a yeast cell is shown, with outer (green) and inner (blue) leaflets delineated. Incubation of cells with MβCD on ice results in extraction of ergosterol from the outer leaflet. The sample is centrifuged to recover MβCD-ergosterol complexes in the supernatant. Ergosterol is extracted from the cell pellet and supernatant with hexane/isopropanol and quantified by HPLC (UV detection). **E**. The MβCD-accessible pool of ergosterol (quantified as in panel D) is ~20-fold greater in ∆-s-tether cells versus WT cells, and partially restored to WT levels in cells expressing the 'ER-PM staple'. The statistical significance of the difference between the measurement of WT cells and each of the different ∆-s-tether samples is $p < 0.0001$, and between the ∆-s-tether samples is $p = 0.0205$ (*) and 0.436 (not significant, ns). **F**. Assay to measure transport of newly synthesized ergosterol from the ER to the MβCD-accessible pool. Cells are pulse-labeled with [3H]methyl-methionine to generate [3H]ergosterol in the ER, and chased as described in Fig 3. After a 30-min chase period, energy poisons are added and cells are placed on ice and incubated with MβCD. The ratio of the specific radioactivity of ergosterol in MβCD-ergosterol complexes versus that of the cell homogenate (relative specific radioactivity, RSR) provides a measure of transport. **G**. Transport of newly synthesized ergosterol from the ER to the MβCD-accessible pool. The bar chart shows RSR values for the different samples. The dotted line indicates the average RSR (~0.82, averaged over both WT and ∆-s-tether samples) after 30 min of chase for the PM fraction as described in Fig 3. The statistical significance was determined by one-way ANOVA (***$p = 0.0003$, **$p = 0.0027$, *$p = 0.043$).

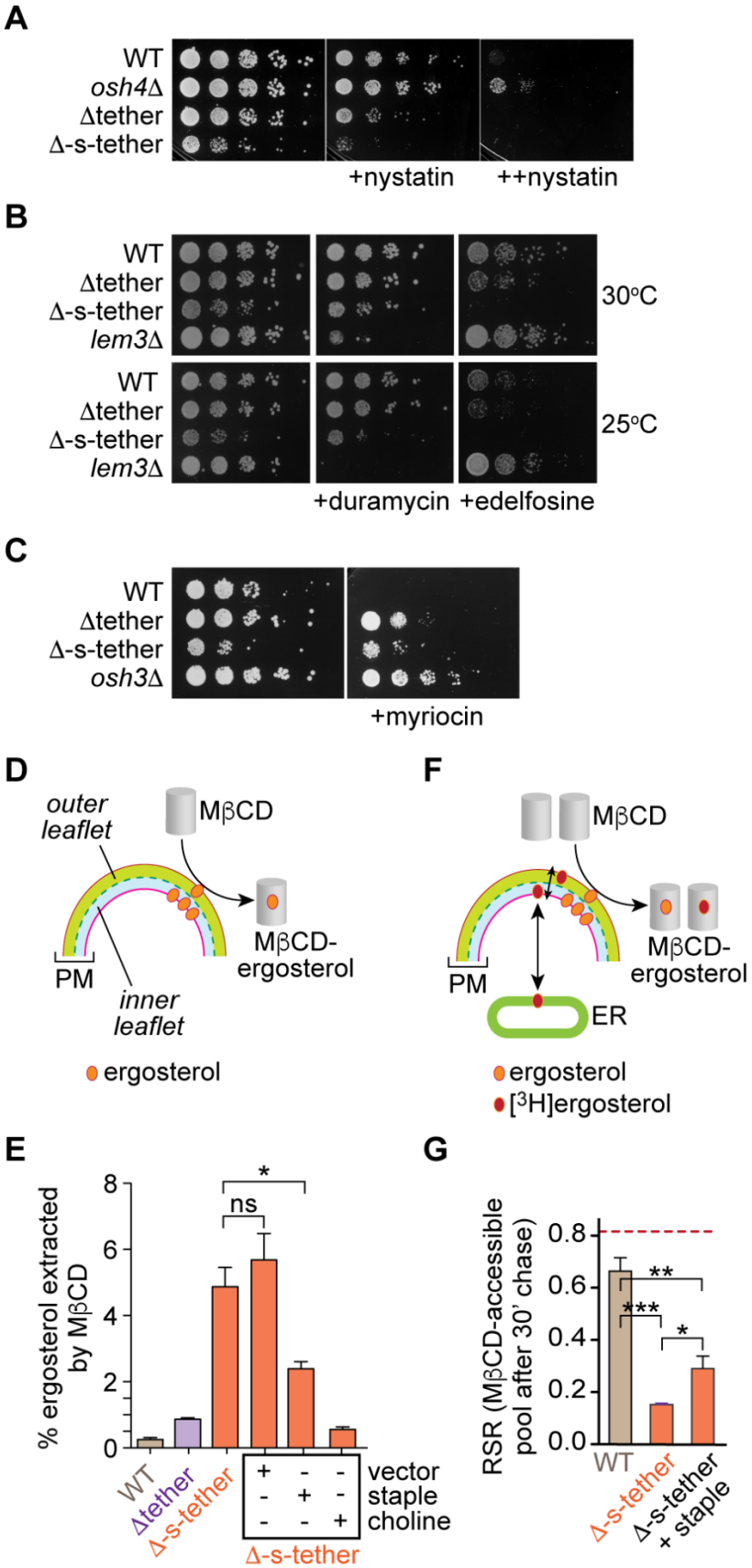
A
WT
osh4Δ
Δtether
Δ-s-tether
+nystatin
++nystatin
B
WT
Δtether
Δ-s-tether
lem3Δ
30°C
25°C
+duramycin
+edelfosine
C
WT
Δtether
Δ-s-tether
osh3Δ
+myriocin
D
outer leaflet
MβCD
MβCD-ergosterol
PM
inner leaflet
ergosterol
F
MβCD
MβCD-ergosterol
PM
ER
ergosterol
[3H]ergosterol
E
% ergosterol extracted by MβCD
ns
*
WT
Δtether
Δ-s-tether
vector
staple
choline
Δ-s-tether
G
RSR (MβCD-accessible pool after 30' chase)
**
***
*
WT
Δ-s-tether
Δ-s-tether + staple

Duramycin is a lantibiotic that disrupts cell growth by directly binding PE in the outer leaflet of the PM. As PE is principally located in the cytoplasmic leaflet of the PM, duramycin sensitivity indicates changes in PE bilayer asymmetry as seen in the phospholipid-flippase mutant *lem3*Δ. The growth of WT, Δtether, and Δ-s-tether cells was not significantly affected by duramycin (**Fig 2.19B**) indicating that transbilayer phospholipid asymmetry is unaffected. We next tested edelfosine, a cytotoxic lysophosphatidylcholine analogue whose activity in yeast is modulated by PM phospholipid flippase activity, and by sterol and sphingolipid pathways. A flippase defect confers edelfosine resistance (505), whereas changes in the lipid composition and physical properties of the PM confer edelfosine sensitivity (506). Δ-s-tether cells displayed acute cytotoxicity to edelfosine compared to WT or even Δtether cells (**Fig 2.19B**) consistent with changes in PM properties.

Based on the sensitivity of Δ-s-tether cells to edelfosine (**Fig 2.19B**), as well as the significant reductions in their sphingolipid levels revealed by lipidomics analyses (**Fig 2.5G**), we considered the possibility that the cells would exhibit a growth phenotype in response to the sphingolipid synthesis inhibitor myriocin (**Fig 2.19C**). Indeed, previous work had shown that elimination of the three tricalbins alone causes myriocin sensitivity (38). Unexpectedly, both Δtether and Δ-s-tether cells were myriocin-resistant (**Fig 2.19C**). These results suggest that myriocin toxicity in Δ-s-tether cells is mitigated by compensatory alterations either in membrane composition or in the sphingolipid biosynthesis apparatus. Taken together, the results of our drug screening experiments indicate that changes in PC and sphingolipid organization in Δ-s-tether cells might indirectly modulate sterol pools within the PM.

The perturbation in PM lipid organization revealed by drug tests (**Fig 2.19A-C)** was not evident in measurements of the ergosterol 'status' of the cell (**Fig 2.20**). Thus, when comparing WT and Δ-s-tether cells, we found no significant difference in the fraction of total cellular ergosterol that was recovered in detergent-insoluble membranes (DIMs) (**Fig 2.20F**), a crude read-out of the extent to which ergosterol associates with phospholipids and sphingolipids containing saturated acyl chains (184, 489). Likewise, there were no significant differences in the total ergosterol content of the cells (**Fig 2.20A**), the ergosterol/phospholipid ratio (**Fig 2.20B**) or the fraction of cellular ergosterol located in the PM (**Fig 2.11B**). Because these bulk measurements are unlikely to be

responsive to nuanced changes in lipid composition and organization, we chose a more sensitive technique to probe ergosterol organization at the PM.

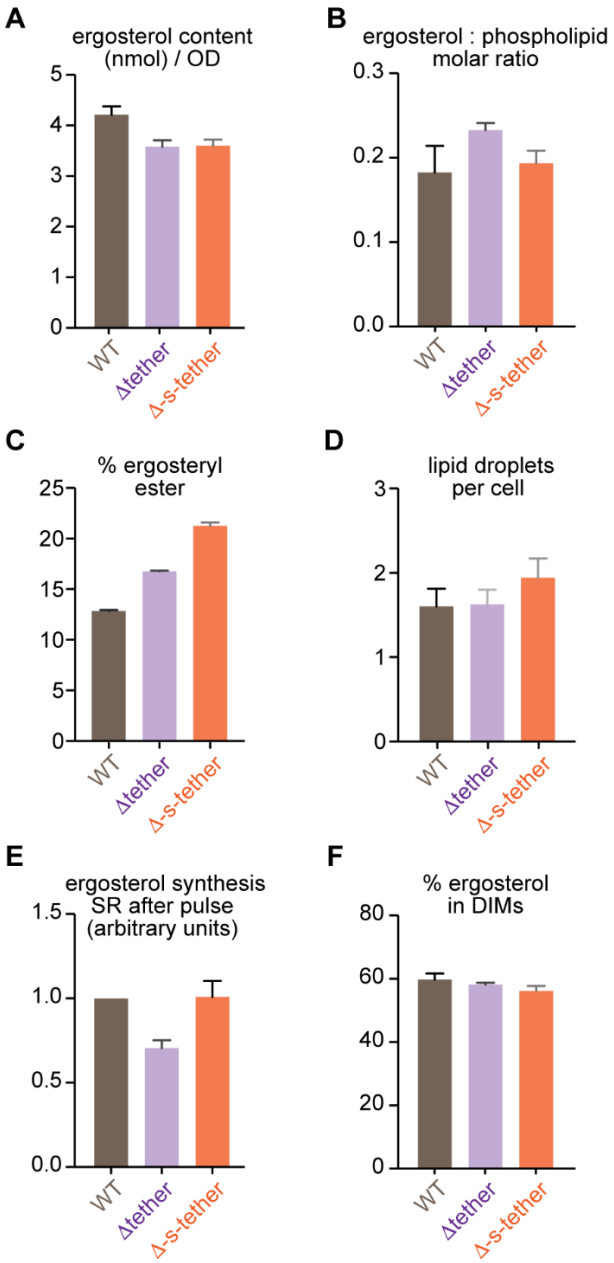

Figure 3.20. Analysis of bulk lipids in WT, Δtether and Δ-s-tether cells.
A-C. Quantification of ergosterol, ergosterol:phospholipid molar ratio and ergosteryl ester in WT (SEY6210), Δtether (ANDY198), and Δ-s-tether (CBY5838) cells. Lipids were extracted and quantified as described in Materials and Methods. D. Quantification of the number of lipid droplets per cells (n > 100 cells counted for each strain). E. The specific radioactivity (SR) of ergosterol after labeling cells for 4 min with [3H-methyl]methionine was determined by HPLC as described in Fig. 3 and normalized to that of WT cells (set arbitrarily to 1.0). F. Detergent-insoluble membranes (DIMs) were prepared by incubating cells with ice-cold Triton X-100. The proportion of ergosterol in DIMs versus whole cells was quantified solvent extraction followed by HPLC analysis.

Methyl-β-cyclodextrin (MβCD) extracts only a very small fraction, <0.5%, of total cellular ergosterol from the outer leaflet of the PM of WT cells under our standard conditions (184, 489), indicative of the unusual physical properties of the yeast PM (184, 489, 507–509). When PM lipid organization is perturbed, then the amount of MβCD-extractable sterol can increase dramatically as seen as in *osh*Δ *osh4-1*^{ts} cells and sphingolipid-deficient *lcb1-100*^{ts} cells at the non-permissive temperature (184, 489). We compared the MβCD-extractability of ergosterol in WT cells versus the tether mutants (**Fig 2.19D**). As reported previously, the proportion of ergosterol extracted from WT cells by MβCD is ~0.25% of total cellular ergosterol (184, 489); a similarly low level of extraction (<1%) was obtained with Δtether cells (**Fig 2.19E**). However, in Δ-s-tether cells, the MβCD-accessible ergosterol pool in the PM was >5%, ~20-fold greater than for WT cells, consistent with a major change in the PM lipid bilayer that enabled greater extraction of ergosterol. This effect was largely reset by expression of the ER-PM staple and completely restored to WT levels by supplementing the growth medium with choline (**Fig 2.19E**). The ability of both the ER-PM staple and choline to restore PM lipid organization as revealed by MβCD-extractability of ergosterol parallels their ability to correct the slowdown in retrograde transport of DHE (**Fig 2.9D**). Thus, these results are consistent with the idea that the reduced rate of transport-coupled esterification of DHE is due to perturbations of the PM lipid bilayer that delay the access of exogenously supplied DHE to cytoplasmic STPs (**Fig 2.9D**, step **2**). The ability of choline to provide the same corrective effect as the ER-PM staple without inducing membrane contacts indicates that the role of tethers in this context is to support normal phospholipid and/or sphingolipid homeostasis, and thereby membrane organization.

Although the exchange of ergosterol between the ER and PM as a whole was unchanged in Δ-s-tether cells (**Fig 2.11C, D**), we investigated if the movement of ergosterol within the PM bilayer might be affected. Non-vesicular transport of newly synthesized [^{3}H]ergosterol deposits ergosterol molecules in the cytoplasmic leaflet of the PM. At a minimum, these molecules must exchange with the outer leaflet pool of ergosterol before they fully equilibrate with PM ergosterol pools and become accessible to MβCD (**Fig 2.19F**). We tested if the exchange of ergosterol within the PM was affected in ∆-s-tether cells by measuring the rate at which newly synthesized ergosterol becomes accessible to MβCD extraction. We used [^{3}H]methyl-methionine to pulse-label ergosterol in the ER and then chased the cells for 30 min. The samples were subjected

to MβCD extraction and, in parallel, samples were taken for subcellular fractionation to isolate the PM (as in **Fig 2.11B**). Both the MβCD extract and the PM fraction were processed with organic solvents to extract ergosterol for HPLC analysis and measurement of RSR. The RSR for the PM fraction after a 30-min chase was ~0.8 for both WT and Δ-s-tether cells (**Fig 2.19G, dashed line**), as expected (**Fig 2.11C**). However, the RSR for MβCD-extracted ergosterol in WT cells was ~0.65 (**Fig 2.19G**, WT), indicating a slight delay in the transport of ergosterol within the PM to the MβCD-accessible pool in the outer leaflet consistent with our previous report (184, 489). This delay was considerably greater in Δ-s-tether cells where the MβCD-extracted ergosterol had an RSR of only ~0.15 after a 30-min chase (**Fig 2.19G**, Δ-s-tether). Expression of the ER-PM staple reduced the delay significantly such that the RSR increased to ~0.3 in Δ-s-tether cells chased for 30 min (**Fig 2.19G**, Δ-s-tether + staple). We conclude that (i) the transfer of ergosterol from its site of arrival at the cytoplasmic leaflet of the PM to the outer leaflet pool from which it can be extracted by MβCD is slower than the rate at which ergosterol exchanges between the ER and PM as a whole as reported previously (184), and (ii) the intra-PM movement of ergosterol, from the inner to the outer leaflet, is dramatically slower in Δ-s-tether cells compared with WT cells. Taken together with the fact that the abundance of characteristic PM lipids, e.g. inositol-P-ceramide (IPC), mannosyl-IPC (MIPC) and PS in Δ-s-tether cells differs significantly from WT cells (**Fig 2.5G**), it seems likely that the changes in ergosterol organization in the PM and the rate of exchange between ergosterol pools in the PM are an indirect consequence of changes in PM phospholipid and sphingolipid composition.

3.2.7. Membrane contacts between the ER and PM proliferate in response to sterol depletion

We have shown that membrane contact between the ER and PM impacts the abundance of PM lipids (sphingolipids, PE, PS (**Fig 2.5G**) and PI4P (**Fig 2.15C**) PM lipid organization (**Fig 2.19A, B, C, E**) and the intra-PM movement of ergosterol (**Fig 2.19G**). In turn, it is known that PM lipids play a role in the establishment of contact sites (**Fig 2.1A**): thus, phosphoinositides and PS in the PM provide anchors for ER-localized Tcb1p-Tcb3p, Ist2p, and Scs2p (30, 104, 130, 160, 163, 485, 494). As sterols represent a large fraction of PM lipids and are critical determinants of PM organization (486, 510), we analyzed the potential role of sterols in establishing contact sites between the ER and PM.

To test the dependence of MCS formation on ergosterol, we depleted yeast cells of sterols and visualized cER-PM association by both transmission electron microscopy and Tcb3p-GFP and RFP-ER distribution by fluorescence microscopy. Squalene synthase (Erg9p) represents the first sterol-specific enzymatic step in the production of all sterols, and inhibition of Erg9p specifically blocks sterol synthesis without directly affecting other isoprenoids (511). In *erg9*Δ P^{MET3}-*ERG9* cells, methionine addition to the growth medium represses Erg9p expression and *de novo* sterol synthesis stops. To our surprise, electron microscopy showed that sterol depletion in *erg9*Δ P^{MET3}-*ERG9* cells resulted in a dramatic expansion of cER (**Fig 2.21A**) such that the inner face of the PM was nearly completely covered with associated ER membrane (**Fig 2.21B**). This finding was confirmed by confocal fluorescence microscopy in live Tcb3p-GFP-expressing cells. In sterol-replete WT cells Tcb3p-GFP fluorescence exhibited a characteristic discontinuous stitched pattern around the cortex (**Fig 2.21C**) (38). In ~90% of sterol-depleted *erg9*Δ P^{MET3}-*ERG9* cells, however, cortical fluorescence was essentially contiguous (**Fig 2.21C**)**.** Although sterol-depleted cells accumulate as G1-arrested unbudded cells, G1-arrested *cdc42-101* cells did not induce any change in Tcb3p-GFP distribution, indicating that increased ER-PM contact is not due to G1 arrest *per se* (**Fig 2.22**). These results indicate that ER-PM membrane association is induced when cellular sterol synthesis is blocked.

Figure 3.21. Sterol depletion induces both ER-PM MCS formation and Tcb3p tether expression.

A. Electron micrographs of WT (CBY858) and *erg9*Δ P^{MET3}-*ERG9* (CBY745) cells before (- Met) and after (+ Met) methionine repression of P^{MET3}-*ERG9* synthesis of sterols (methionine was also added to WT). Inserts correspond to magnifications of boxed regions at the cell cortex showing PM-associated ER (arrowheads); cER is highlighted in magenta. Scale bar = 2 μm. B. Corresponding to panel A, quantification of cER length expressed as a percentage of the total circumference of the PM in each cell section counted (n = 25 cells for each strain; error bars show S.D.; $p = 7.6 \times 10^{-25}$ for the difference between WT and *erg9*Δ P^{MET3}-*ERG9* (+ Met)). C. WT (CBY5836) and *erg9*Δ (CBY5834) cells with integrated *TCB3*-GFP and P^{MET3}-*ERG9* constructs in the presence of methionine, which represses *ERG9* expression and sterol synthesis in *erg9*Δ cells. Scale bar = 2 μm. D. Corresponding to panel C, representative immunoblots probed with anti-GFP and anti-actin antibodies showing Tcb3-GFP levels in WT and sterol-depleted *erg9*Δ P^{MET3}-*ERG9* cells as compared to the actin (Act1) control. Relative to WT, Tcb3-GFP levels increased 5.6 ± 1.6 (mean ± S.D.; n = 5) fold in sterol-depleted *erg9*Δ P^{MET3}-*ERG9*. E. Continuous Tcb3-GFP and ER-RFP fluorescence along the PM (arrowheads) dissipated with the addition of exogenous cholesterol to sterol-depleted *hem1*Δ *erg9*Δ P^{MET3}-*ERG9* cells (CBY5995 and CBY5842 pCB1024, respectively). Intense ER-RFP nuclear fluorescence (arrows) also diminished after cholesterol addition. The normal discontinuous dashed line of Tcb3-GFP and ER-RFP around the cell cortex was unaffected in sterol-prototrophic *hem1*Δ cells (CBY5993 and CBY5844 pCB1024, respectively), Scale bar = 2 μm. F. Quantification of contiguous association between cER and the PM after cholesterol addition in *hem1*Δ, *TCB3*-GFP *hem1*Δ cells, and sterol-depleted *hem1*Δ *erg9*Δ P^{MET3}-*ERG9* cells and *TCB3*-GFP *hem1*Δ *erg9*Δ P^{MET3}-*ERG9* cells.

Following cholesterol addition to sterol-depleted *hem1*Δ *erg9*Δ P^{MET3}-*ERG9* cells, reductions in cortical Tcb3-GFP localization were detected 1 h after cholesterol addition, with reductions in cortical ER-RFP lagging slightly behind (*n* > 100).

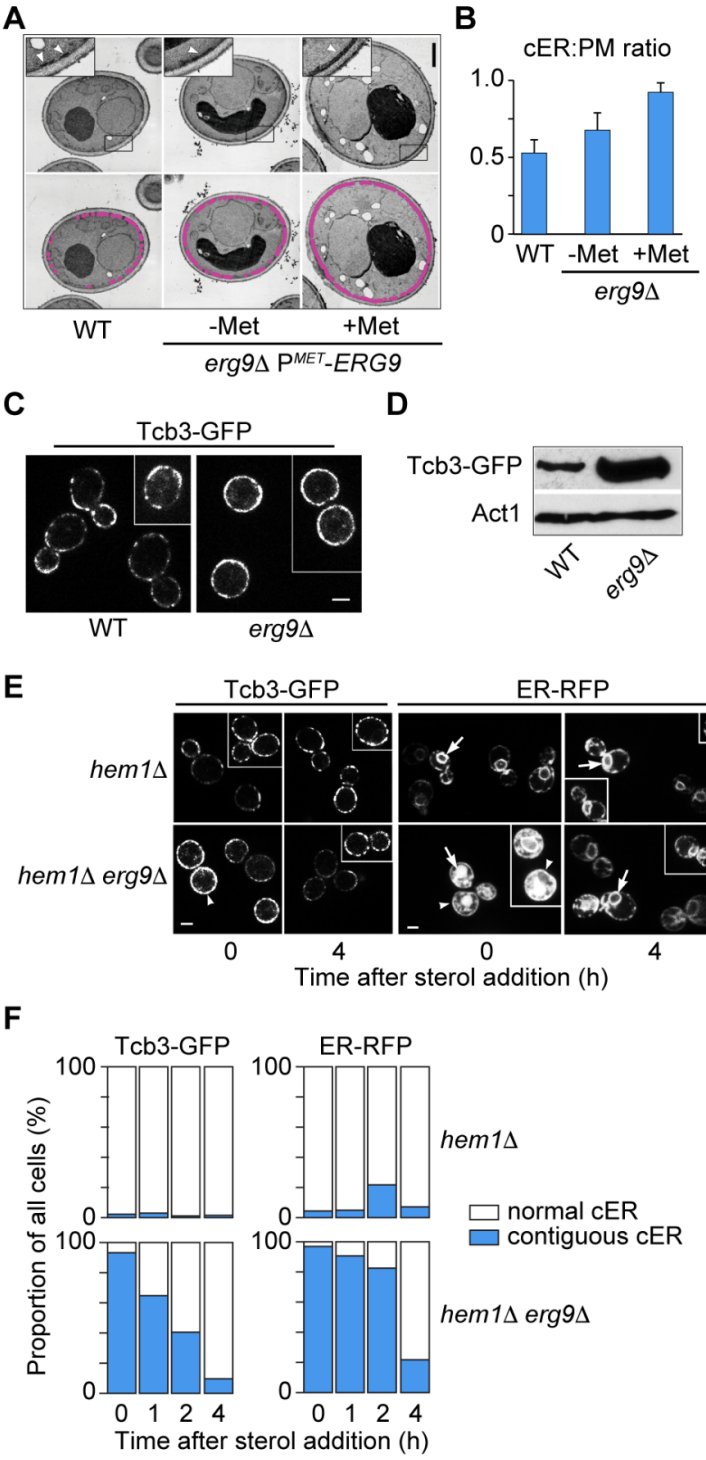

In addition to its altered distribution along the PM, Tcb3p-GFP fluorescence was generally greater in sterol-depleted cells relative to WT, suggesting an induction of Tcb3p protein levels in response to sterol reduction. This point was verified by analyzing cell extracts prepared from both WT and *erg9*Δ P^{MET3}-*ERG9* sterol-depleted cells expressing Tcb3p-GFP and determining relative levels of Tcb3p-GFP by SDS-PAGE/immunoblotting using anti-GFP antibodies. When normalized to levels of the actin (Act1p) internal control, Tcb3p-GFP protein levels were seen to be induced ~6-fold in sterol-depleted cells compared to similarly treated WT cells (**Fig 2.21D**). In genome-wide analyses of gene expression by DNA microarray, sterol depletion had no impact on transcript levels of any of the tether genes; relative to WT cells, methionine repression of de novo sterol synthesis in *erg9*Δ P^{MET3}-*ERG9* cells showed transcriptional changes between 0.93-1.05 ± 0.03 (mean ± S.D.; independent duplicate trials) for each of the seven tether protein genes. These results indicated that Tcb3 protein levels are post-transcriptionally regulated.

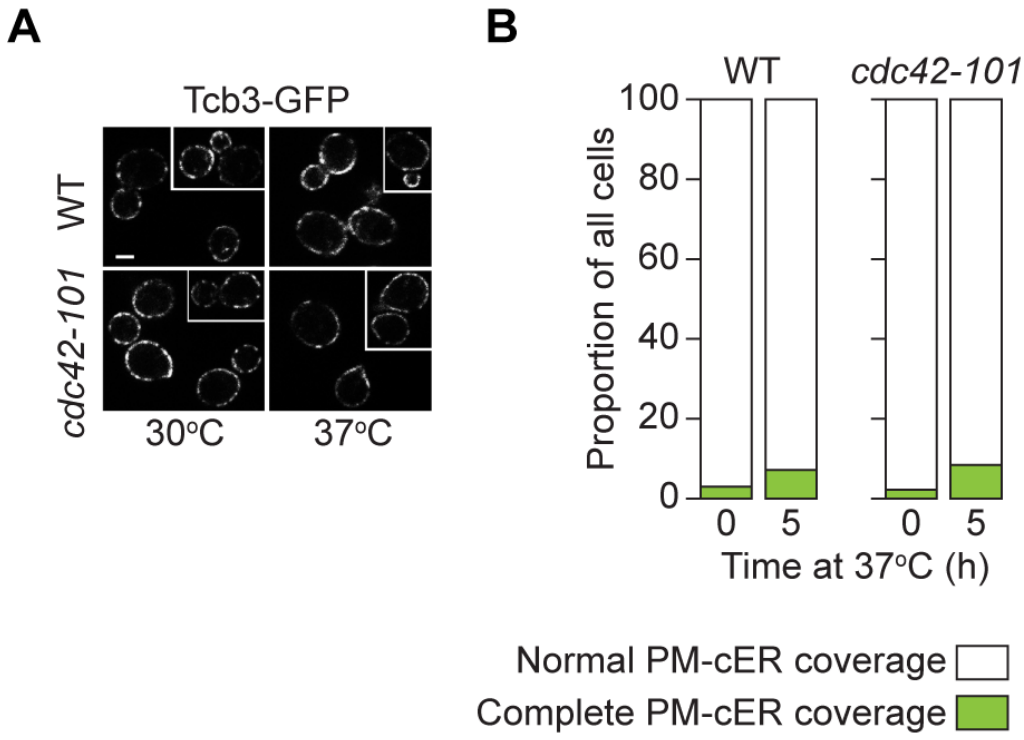

Figure 3.22. ER-PM MCSs do not increase in unbudded arrested cells.
A. Discontinuous cortical Tcb3-GFPp distribution was observed in WT (CBY5942) and cdc42-101ts (CBY5944) cells incubated 1 h at 37˚C, or at 30˚C. Scale bar = 2 μm.B. Percentage of cells with normal discontinuous Tcb3-GFP distribution versus continuous cortical localization along the PM in WT and cdc42-101ts cells. Even after G1-arrest for 5 h at 37˚C, Tcb3-GFP in cdc42-101ts cells was indistinguishable from WT.

Because of the long half-life of cellular sterols, an extended period is required after *ERG9* repression for complete sterol depletion. To determine how quickly sterol-depleted cells recover their normal distribution of ER-PM association, ER-RFP and Tcb3p-GFP redistribution was measured in response to exogenously added cholesterol. Under standard culture conditions yeast does not import sterols from the medium as discussed above (**Fig 2.9**), but the deletion of *HEM1* permits cholesterol uptake (429). A *hem1*Δ *erg9*Δ P^{MET3}-*ERG9* strain could grow after sterol depletion, but only when exogenous cholesterol (or δ-aminolevulinic acid (δ-ALA), the product of the Hem1p enzyme) was supplemented to the growth medium (**Fig 2.23**). In *hem1*Δ cells, ER-RFP and Tcb3-GFP distributions were the same with or without cholesterol supplementation (**Fig 2.21E**). In sterol-depleted *hem1*Δ *erg9*Δ P^{MET3}-*ERG9* cells, return to the normal discontinuous stitched fluorescence of cortical Tcb3p-GFP commenced 1 h after cholesterol addition, and the characteristic WT pattern was observed after ~4 h (**Fig 2.21E, F**). In these cells, recovery of normal ER-RFP morphology lagged behind the restoration of the normal Tcb3p-GFP distribution (**Fig 2.21F**), consistent with the idea that tethering complexes dictate changes in cER association. These results indicate that tethering between the ER and PM responds to cellular sterol pools.

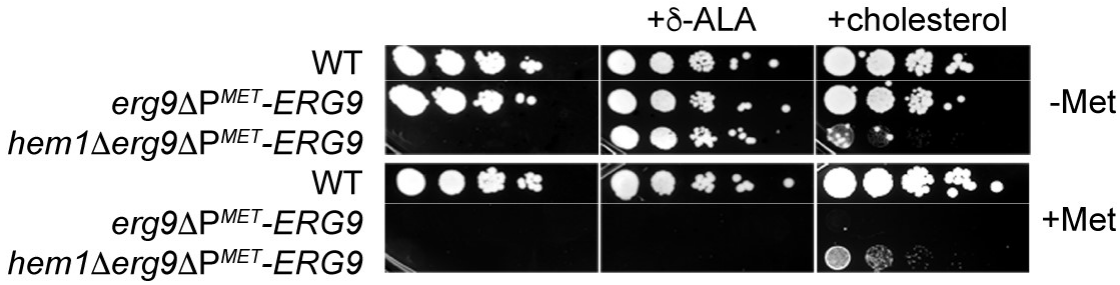

Figure 3.23. Rescue of sterol-depleted *hem1*Δ *erg9*Δ P^{MET}-*ERG9* cells with exogenous cholesterol.

Ten-fold serial dilutions of WT (with an integrated *P^{MET}-ERG9* construct; CBY918), *erg9*Δ *P^{MET}-ERG9* (CBY745), and *hem1*Δ *erg9*Δ P^{MET}-*ERG9* (CBY5844) cultures on synthetic solid medium with (+Met) or without (-Met) methionine, containing (as shown) cholesterol, or δ-aminolevulinic acid (+δ-ALA), or neither. In the absence of δ-ALA supplementation, all *hem1*Δ strains require methionine for growth and cholesterol uptake cannot occur under aerobic conditions without the *hem1*Δ mutation. In the presence of methionine, which represses PMET-ERG9 expression and sterol synthesis, *hem1*Δ *erg9*Δ P^{MET}-*ERG9* cells grow (albeit slowly) with 25 μg/ml cholesterol supplementation.

3.3. Discussion

Membrane contact sites are widely hypothesized to facilitate non-vesicular lipid exchange. We tested this hypothesis in the context of sterol exchange between the ER and PM in yeast by creating ∆-s-tether cells that lack ER-PM membrane contacts. We now report that these contact sites are not required for ER-PM sterol exchange but rather function as regulators of PM lipid homeostasis, controlling the organization and dynamics of sterols within the PM and acting redundantly with the OSBP homolog Osh4p in an essential pathway related to PI4P homeostasis. We also report our unexpected discovery that in the absence of sterol biosynthesis, ER-PM contact sites proliferate such that the entirety of the PM is associated with ER due to increased expression of tethers. These results invite a revision of current thinking about the role of contact sites as hubs for lipid transport and reveal a reciprocal relationship between the formation and function of contact sites on the one hand, and lipid homeostasis on the other.

3.3.1. Ice2 is an ER-PM tether.

To create ∆-s-tether cells we eliminated *ICE2* in the previously described ∆tether strain. The role of Ice2p in distributing ER along the PM between mother and daughter cells during mitosis is well established (125, 175), hinting that it may play a direct role in tethering ER to the PM. Ice2p is a polytopic ER membrane protein with a single prominent cytoplasmic loop that has been implicated in associating the ER with lipid droplets during the stationary phase of growth, and potentially channeling diacylglycerol to the phospholipid biosynthetic machinery in the ER as cells resume growth (178). In analogy to its proposed tethering role in stationary phase cells, we speculate that Ice2p may play a role in bridging the ER and PM in rapidly dividing cells. Indeed, fluorescence microscopy reveals that Ice2p is located at the cell cortex in ∆tether cells (**Fig 2.4**). As a potential tether protein, the cytoplasmic loop of Ice2p may interact directly *in trans* with the cytosolic face of the PM, or, similar to the Scs2p tether (16, 126), Ice2p might form a bridge across the ER-PM interface via an interaction with another protein. If the latter scenario is correct, then the mechanism of tethering by both Ice2p and Scs2p would differ from that of the autonomous membrane attachments conferred by Ist2p and the E-Syt homologs Tcb1p-Tcb3p (**Fig 2.1A**). Nevertheless, eliminating Ice2p in the context of

∆tether cells results in quantifiable reductions in ER-PM association beyond those previously reported for ∆tether cells (**Figs 2.1E and Fig 2.2**), leading to clear functional outcomes. For example, synthetic lethality of ∆-s-tether with *osh4*∆ or *sac1*∆ was not manifested in the progenitor ∆tether strain, and only occurred with the additional deletion of *ICE2*. Likewise, slowing of transport-coupled esterification of DHE (**Fig 2.9C**) and increased extractability of ergosterol by MβCD (**Fig 2.19E**) were observed only after deletion of *ICE2* in ∆tether cells. Taken together, these findings show that Ice2p is an important contributor to ER-PM tethering and associated functions.

3.3.2. Normal ER-PM sterol exchange in the absence of contact sites.

We found that bidirectional sterol exchange between the ER and PM occurs at the same rate in ∆-s-tether and WT cells indicating that ER-PM contact sites do not contribute quantitatively to the mechanism of sterol movement between these two membranes. If any elements of the sterol transport machinery are localized to ER-PM MCSs, then their function must be subsumed by other sterol transport mechanisms in ∆-s-tether cells. However, we show that in and of themselves, neither secretory vesicles (**Fig 2.11D**) nor the cytoplasmic sterol binding protein Osh4p (**Fig 2.15A, B**) or the ER-anchored Lam2 protein (**Fig 2.14**) provide this putative compensatory mechanism in ∆-s-tether cells. Our results also make it clear that yeast cells do not possess STPs with the ability to lower the energy barrier for sterol desorption to the point where transport becomes a diffusion-limited rather than desorption-limited process (488). Thus, non-vesicular sterol transport in yeast is likely mediated by unremarkable cytoplasmic STPs (i.e. STPs that are able to lower the energy barrier for sterol desorption by only 2-3 k_BT) present in a sufficient number per cell to account for the measured sterol exchange rate (488). The identification of these STPs is a focus of future work.

3.3.3. Altered sterol organization and dynamics in the PM of ∆-s-tether cells.

Even though ER-PM sterol exchange was unaffected by the lack of ER-PM contact sites, trafficking of exogenously supplied DHE to the ER was unexpectedly slow in ∆-s-tether cells compared with WT cells (**Fig 2.9C**). Careful analysis of the various mechanistic steps of the transport process (**Fig 2.9A**) revealed that the slow-down could be linked to a dramatic lowering of the rate at which sterols equilibrate between the inner and outer

leaflet of the PM in ∆-s-tether cells (**Fig 2.19F, G**). While this slow-down should not affect the equilibration of DHE with PM sterol pools during the extended hypoxic loading period used for this assay (**Fig 2.9A**, steps **1** and **2**), it would affect the rate at which newly synthesized ergosterol displaces DHE from the PM during the aerobic chase thereby resulting in a slower rate of transport-coupled DHE esterification. We previously reported that the appearance of newly synthesized ergosterol in the MβCD-extractable ergosterol pool in the outer leaflet of the PM lags behind its arrival at the PM in WT cells (**Fig 2.19D, E**), suggesting that equilibration of sterol across the yeast PM is considerably slower than seen for cholesterol flip-flop in synthetic, liquid crystalline membranes and in red blood cells (512–514). This may be a consequence of the unusual properties of the yeast PM, exemplified by the slow lateral diffusion of both lipids and proteins (508, 509) and the organization of PM proteins into a mosaic of domains (515). In the case of ∆-s-tether cells, the rate of transbilayer sterol equilibration was ~5-fold slower than for WT cells (**Fig 2.19G**), and this was reflected in changes in PM bilayer organization as manifested in the nystatin and edelfosine sensitivity of these cells, and the greater accessibility of sterols to MβCD extraction (**Fig 2.19A, B, E**). Quantification of cellular lipids revealed reductions in PE, PS, and the sphingolipids IPC and MIPC (**Fig 2.5G**). As these lipids generally reflect PM composition (516), we propose that relative changes in lipid levels are the underlying cause of the disturbance in the PM bilayer, resulting in a change in ergosterol dynamics.

3.3.4. PM phospholipid dysregulation in ∆-s-tether cells.

How do ER-PM contact sites affect PM lipid organization and intra-PM ergosterol dynamics? Because the growth defect of ∆-s-tether cells was rescued by choline supplementation (**Fig 2.5E**), which increases flux through phospholipid biosynthetic pathways (517) without inducing contact site formation (**Fig 2.5F**), the primary defect in cells lacking ER-PM contact sites appears to involve phospholipid regulation. Remarkably, both choline and the artificial staple corrected most defects inherent to ∆-s-tether cells (i.e. slow growth (**Fig 2.5B**); slow transport-coupled DHE esterification (**Fig 2.11D**); high MβCD-extractability of ergosterol (**Fig 2.19E**); slow rate of ergosterol exchange between PM pools (**Fig 2.19G**)). These results indicate that the function of the endogenous tethers, even those such as Tcb1p, Tcb2p and Tcb3p with lipid-transporting SMP domains (155), might be largely structural in this context, i.e. the tethers provide a

means of mechanical attachment of the ER to the PM, thereby enabling ER-localized proteins such as the PC-synthesizing phospholipid methyltransferase Opi3p to act *in trans*.

An exception to this general conclusion is that neither choline nor the artificial staple were able to re-establish normal PI4P polarization in ∆-s-tether cells (**Figs 2.15C, D and Fig 2.17**). PI4P dephosphorylation at the PM is proposed to be due to the ER-localized Sac1p phosphatase acting *in trans* at ER-PM contact sites (139), although the protein clearly also acts *in cis* (201). The inability of the artificial staple to facilitate PM access for Sac1p might stem from either (i) an insufficient number or improper positioning of membrane contacts established by the staple, and/or (ii) the inability of the staple to provide a specific requirement for Sac1p activation, which is otherwise provided by endogenous tethers (almost all tethers were identified by the virtue of specific interactions with Sac1p (16), whereas the artificial tether would lack this ability). Our data suggest that PM PI4P is reduced in the immediate vicinity of contact sites generated by the artificial staple (**Fig 2.17B**), indicating that Sac1p might access PI4P locally at those points. In contrast, endogenous tethers and their ancillary factors might further expand cER-associated regions of the PM that are accessible to Sac1p.

In yeast, all phospholipids are synthesized from phosphatidic acid (PA) via the CDP-diacylglycerol (CDP-DAG) pathway; PE and PC are also synthesized by the Kennedy pathway using diacylglycerol (DAG) and salvaged or exogenously supplied ethanolamine and choline (517, 518) (**Fig 2.24**). PA levels and the DAG:PA ratio are critical in determining the amount of CDP-DAG available for phospholipid synthesis (**Fig 2.24**). The mole percentage of PA in ∆-s-tether cells is 20% lower than that in WT cells, and the DAG:PA ratio is 2-fold greater (**Fig 2.5G**), indicating dysregulation of phospholipid synthesis in the absence of ER-PM contact sites. Consistent with this, levels of PS and PI-derived sphingolipids are much lower in ∆-s-tether than in WT cells (**Fig 2.5G**), although PI levels are unaffected (see below). As previously shown (177), *ice2*∆ *scs2*∆ cells have a diminished ability to convert PS to PC via Opi3p-mediated phospholipid methylation at ER-PM contact sites, necessitating choline supplementation for normal growth. In ∆-s-tether cells, choline supplementation would not only bypass the need for Opi3p, but also compensate for the lower overall rate of phospholipid synthesis resulting from decreased PA levels by generating PC via the Kennedy pathway for membrane growth. Lipidomic analysis of ∆-s-tether cells cultured with choline did in fact

show restoration of PC to levels comparable to WT (**Fig 2.8**). These results are also consistent with the choline-reversible synthetic growth defects observed when either *OPI3* or *CHO2* is deleted in Δ-s-tether cells (**Fig 2.6**). Thus, ER-PM contact sites may function as regulatory interfaces that coordinate the CDP-DAG and Kennedy pathways to balance convergent mechanisms for phospholipid synthesis.

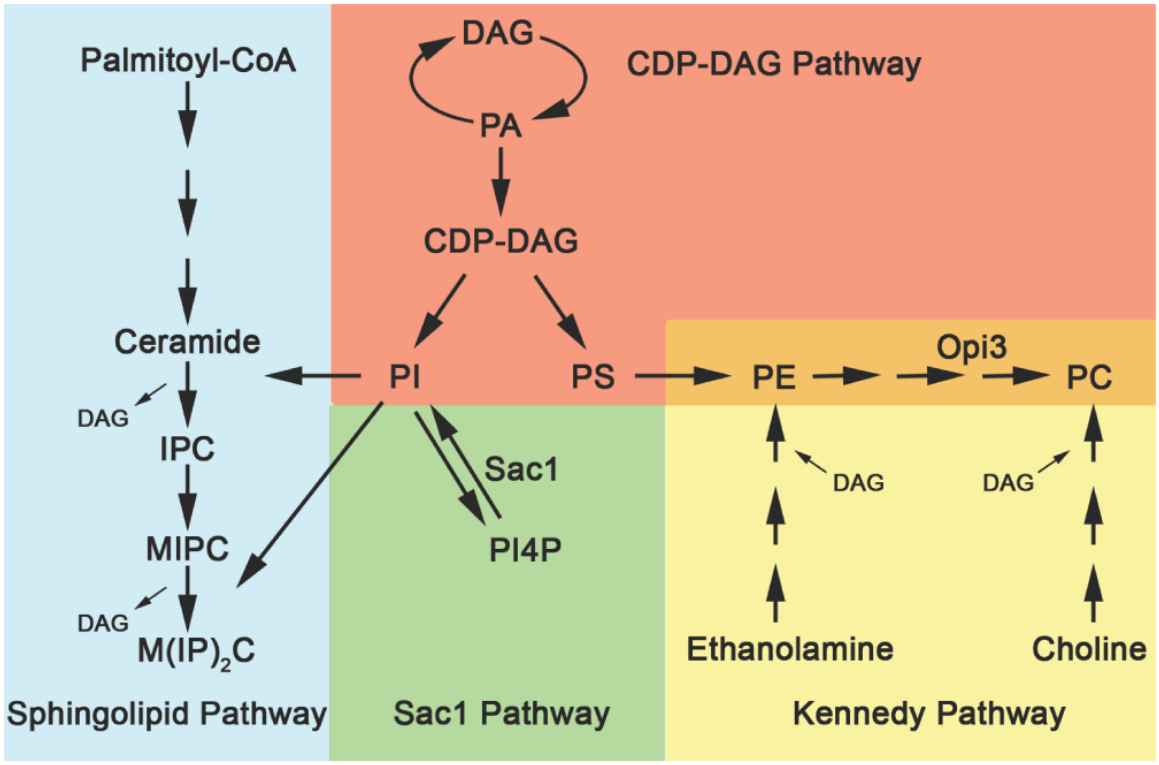

Figure 3.24. Glycerophospholipid and sphingolipid biosynthetic pathways in yeast.
See text for details

Δ-s-tether cells have a normal mole percentage of PI and increased PI4P, yet their content of inositol sphingolipids is ~60% lower than in WT cells (**Fig 2.5G**) indicating dysregulation of phosphoinositide homeostasis due to loss of ER-PM contacts. Total cellular PI is generated predominantly by the CDP-DAG pathway and Sac1-mediated dephosphorylation of PI4P (itself generated from PI) in separate cellular locations, with both routes providing the biosynthetic precursor for complex inositol sphingolipids (**Fig 2.24**). Brice et al. (404) reported that disruption of *SAC1* alone reduces PI levels dramatically, and IPC and MIPC levels by >70%. The Δ-s-tether mutations would reduce the Sac1p-mediated route for PI production by distancing the enzyme from its substrate in the PM (**Fig 2.15C**). However, *sac1*Δ and Δ-s-tether

mutations are lethal when combined, likely due to limiting PI levels, indicating that ∆-s-tether mutations must also inhibit PI production from the CDP-DAG pathway. Normal PI levels in ∆-s-tether cells may therefore be a consequence of preserving this lipid at the expense of inositol sphingolipid production. It should be noted that Sac1p is also a component of the SPOTS (SPT, Orm1p/2p, Tsc3p and Sac1p) complex that regulates early steps in sphingolipid synthesis (377, 519). However, levels of ceramide, an early precursor in sphingolipid synthesis, were essentially normal in ∆-s-tether cells (**Fig 2.5G**). It therefore seems unlikely that the SPOTS complex plays a direct role in ER-PM contact site regulation of inositol sphingolipids.

3.3.5. Intersection of Osh4, Sac1 and ER-PM MCSs in PI4P homeostasis.

While investigating whether normal ER-PM sterol transport in ∆-s-tether cells could be due to the compensatory activity of soluble or membrane-bound STPs, we discovered that the deletion of *OSH4* was synthetically lethal with ∆-s-tether mutations (**Fig 2.15A**). Lethality was not due to a sterol-related process because Osh6p, which does not bind sterols, could rescue *osh4*∆ ∆-s-tether growth defects (**Fig 2.15B**). Consistent with previous proposals that Osh proteins represent important regulators of PI4P (133, 139), the deletion of *SAC1* in ∆-s-tether cells also resulted in synthetic lethality (**Fig 2.15E**). Based on these findings we propose that Osh4p (and Sac1p) functions in a parallel pathway alongside ER-PM contact sites for PI4P regulation. However, expression of the soluble enzymatic domain of Sac1p did not suppress *osh4*∆ ∆-s-tether lethality (**Fig 2.18**), suggesting that the downstream regulation of Sac1p is not the only role Osh4 plays at ER-PM MCSs. The availability of ∆-s-tether cells now allows further interrogation of the mechanism by which ER-PM MCSs function as interfaces for regulating PI4P signaling and phospholipid metabolism.

Our results are consistent with the hypothesis that ER-PM contact sites constitute a regulatory nexus to balance sterol and phospholipid concentrations to maintain PM structure. In the absence of contact sites, the ratio of sterols to specific phospholipids and sphingolipids is uncoupled, which negatively impacts PM organization, intra-PM sterol dynamics, and PI4P levels. When sterols become limiting, post-transcriptional induction of Tcb3p increases the extent of ER-PM association, potentially facilitating compensatory changes to phospholipid synthesis to re-establish bilayer stability.

Although the mechanisms that control Tcb3p levels in sterol-replete or sterol-depleted cells are not known, it is interesting to speculate that the induction of a tether protein may represent a new homeostatic mechanism for regulating PM composition and structure.

3.4. Materials and Methods

3.4.1. Strains, plasmids, microbial and genetic techniques

Yeast strains and plasmids are listed in Supporting Information (**Table 2.1** and **2.2**, respectively). Unless otherwise stated, yeast cultures were grown in synthetic complete or YPD rich media at 30°C. All temperature-sensitive alleles were cultured at permissive growth temperatures (30°C unless otherwise stated) and shifted to the restrictive temperature of 37°C as specified. DNA cloning and bacterial and yeast transformations were carried out using standard techniques (520).

For the choline and ethanolamine supplementation growth assays, yeast strains were cultured in synthetic minimal media for 48 h, then streaked on to solid synthetic complete media containing 1 mM choline chloride or 1 mM ethanolamine (Sigma-Aldrich Chemicals, St. Louis, MO). Growth in response to inositol supplementation was tested on synthetic minimal media containing 75 µM myo-inositol (Sigma-Aldrich Chemicals). For the nystatin sensitivity plate assay, ten-fold serial dilutions of yeast cultures were spotted onto solid synthetic media containing 2.5 µM nystatin (Sigma-Aldrich Chemicals). Cell growth was also tested on solid rich media containing 60 µM edelfosine (Cayman Chemical, Ann Arbor, MI), 5 µM duramycin (Sigma-Aldrich Chemicals), or 0.5 µg/mL myriocin (Sigma-Aldrich Chemicals). To select against *URA3*-marked plasmids (e.g. pCB1183), yeast cultures were grown on rich growth media then streaked onto a synthetic solid growth medium containing 1 g/L 5-fluoroorotic acid (Gold Biotechnology, St. Louis, MO). For assays of cholesterol uptake by cells lacking *HEM1*, yeast cultures were spotted onto a solid synthetic medium lacking methionine, containing 25 µg/ml cholesterol in 1% (vol/vol) Tween 80–ethanol (1:1 [vol/vol]) and 50 µg/ml 5-aminolevulinic acid (δ-ALA; Sigma-Aldrich Chemicals). For sterol depletion assays, *erg9Δ* P^{MET3}-*ERG9* cells were grown at 30°C for 10 h in synthetic media lacking methionine and grown to mid-log phase before adding 100 mg/L methionine.

DNA cloning and bacterial and yeast transformations were carried out using standard techniques (520). The functional artificial tether fusion plasmids pCB1185 and pCB1188 were derived from pRS416-P^{YSP1}-eGFP-Myc-HMH-RitC, a kind gift from Tim Levine (UCL Institute of Ophthalmology). To construct pCB1185, coding sequences from pRS416-P^{YSP1}-eGFP-Myc-HMH-RitC were amplified using CACTCGAGTTATGGAGCAAAAGCTCATTTCTGAAGAG and CAGGTACCCTATACTGAATCCTTTTTCTTACGGAAT primers, and the product was digested with *Xho*I/*Kpn*I for subcloning in-frame with GFP under the control of an *ACT1* promoter in a YCplac111 vector. To construct pCB1188, coding sequences from pRS416-P^{YSP1}-eGFP-Myc-HMH-RitC were amplified using the primers: CATCCGGACTTATGGAGCAAAAGCTCATTTCTGAAGAG and CATCTAGACTATACTGAATCCTTTTTCTTACGGAATGG. The amplified product was digested with *Kpn*I/*Xba*I and subcloned in-frame with coding sequences for mCherry under the control of an *ACT1* promoter in a YCplac111 vector.

All genomic manipulations were performed by integration of PCR amplified product as previously described (521). All natMX4 and hphMX4 deletions were generated by homologous recombination into the yeast genome of targeted P4339 and pAG32 amplified products; transformants were selected for on YPD media containing 100 mg/L nourseothricin (Gold Biotechnology) and 400 mg/L hygromycin B (Toku-E, Bellingham, WA), respectively. For growth of *hem1*Δ::natMX4 cells, selective growth media contained 50 µg/ml δ-ALA. The *sec18-1:URA3* temperature-sensitive allele strains were isolated at 23°C after genomic recombination of the *sec18-1:URA3* gene cassette amplified from CBY2853 genomic DNA. All transformants were confirmed by genomic PCR or genetic complementation assays.

Table 3.1. Yeast strains.
Unless otherwise referenced, all strains were created as part of this study.

Strain	Genotype	Reference
ANDY198	*MAT*a *leu2-3,112 ura3-52 his3*Δ*200 trp1*Δ*901 lys2-801 suc2*Δ*9 ist2*Δ::hisMX6 *scs2*Δ::*TRP1 scs22*Δ::hisMX6 *tcb1*Δ::kanMX6 *tcb2*Δ::kanMX6 *tcb3*Δ::hisMX6	(16)
BY4741	*MAT*a *leu2*Δ0 *ura3*Δ0 *his3*Δ*0 met15*Δ*0*	
CBY745	*MAT*α *leu2*Δ0 *ura3*Δ0 *lys2*Δ0 *erg9*Δ::kanMX4 *HIS3*::P^{MET3}*-ERG9*	(443)

CBY858	*MAT*α *leu2*Δ0 *ura3*Δ0 *lys2*Δ0 *his3*Δ::kanMX4	(443)
CBY918	*MAT*α *leu2*Δ0 *ura3*Δ0 *lys2*Δ0 *ERG9 HIS3*::P^{MET3}-*ERG9*	
CBY2859	SEY6210 *sec18-1*:*URA3*	
CBY5194	BY4741 *lem3*Δ::kanMX4	
CBY5804	SEY6210 *ice2*Δ::natMX4	
CBY5834	CBY745 *TCB3*-GFP:*URA3*	
CBY5836	CBY918 *TCB3*-GFP:*URA3*	
CBY5838	ANDY198 *ice2*Δ::natMX4	
CBY5842	CBY745 *hem1*Δ::natMX4	
CBY5844	CBY918 *hem1*Δ::natMX4	
CBY5851	CBY5838 *sec18-1*:*URA3*	
CBY5940	ANDY198 *osh4*Δ::*URA3*	
CBY5942	*MAT*a *leu2-3,112 ura3-52 his3*Δ*200 lys2-801 CDC42*:*LEU2 TCB3*-GFP:*URA3*	
CBY5944	*MAT*a *leu2-3,112 ura3-52 his3*Δ*200 lys2-801 cdc42-101*:*LEU2 TCB3*-GFP:*URA3*	
CBY5980	ANDY198 *osh4*Δ::hphMX4 pCB1183	
CBY5988	ANDY198 *osh4*Δ::hphMX4 *ice2*Δ::natMX4 pCB1183	
CBY5993	CBY5844 *TCB3*-GFP*:URA3*	
CBY5995	CBY5842 *TCB3*-GFP*:URA3*	
CBY6031	ANDY198 *osh4*Δ::hphMX4 *ice2*Δ::natMX4 pCB1157	
CBY6140	ANDY198 *osh4*Δ::hphMX4 *ice2*Δ::natMX4 pCB1266	
CBY6142	ANDY198 *sac1*Δ::hphMX4	
CBY6146	ANDY198 *sac1*Δ::hphMX4 *ice2*Δ::natMX4 pCB1183	
CBY6150	ANDY198 *lam2*Δ::hphMX4	
CBY6153	ANDY198 *lam2*Δ::hphMX4 *ice2*Δ::natMX4	
CBY6220	ANDY198 *ICE2-GFP*:*URA3*	

CBY6267	ANDY198 *cho2*Δ::hphMX4 *ice2*Δ::natMX4	
CBY6271	ANDY198 *opi3*Δ::hphMX4 *ice2*Δ::natMX4	
HAB821	SEY6210 *osh4*Δ*::HIS3*	(522)
JRY6202	SEY6210 *osh3*Δ::*LYS2*	(192)
SEY6210	*MAT*α *leu2-3,112 ura3-52 his3*Δ*200 trp1*Δ*901 lys2-801 suc2*Δ*9*	(523)

Table 3.2. Plasmids
Unless otherwise referenced, all plasmids were created as part of this study.

Plasmid	Description	Source/Reference
p4339	pCRII-TOPO natMX4	C. Boone (University of Toronto)
pAG32	pFA6 hphMX4	
pCB598	YEplac181 *OSH4*	
pCB1024 (RFP-ER)	pRS416 P^{PHO5}-RFP-$SCS2^{220-244}$	(125)
pCB1157	YCplac111 *osh4-1*	
pCB1185	YCplac111 P^{ACT1}-GFP-Myc-HMH-RitC	
pCB1188	YCplac111 P^{ACT1}-mCherry-Myc-HMH-RitC	
pCB1204	YCplac111 RFP-*RAS2*	
pCB1266	YEplac181 *OSH6*	
pCB1277	YCplac111 P^{PHO5}-RFP-$SCS2^{220-244}$	
pGFP-Lam2	pRS416 GFP-*LAM2*	
pOPI3	pRS416 P^{PHO5}-Myc-*OPI3*	(177)
pRS416	*URA3 CEN*	(524)
pRS415 *SAC1*	pRS415 *SAC1*	(332)
pRS415 $SAC1^{1-522}$	pRS415 P^{CPS} -$SAC1^{1-522}$	(332)
pRS425 $SAC1^{1-522}$	pRS425 P^{CPS} -$SAC1^{1-522}$	(332)
pSCS2	pRS416 P^{PHO5}-Myc-*SCS2*	(177)
pTL511	pRS416 P^{CPY}-GFP-2xPH^{OSH2}	(138)
YCplac111	*LEU2 CEN*	(525)
YEplac181	*LEU2 2μ*	(525)

3.4.2. Transmission electron microscopy

Yeast cells were grown to mid-log phase and prepared (fixation, dehydration, infiltration/embedding) as previously described (526). Minor changes were made to the

infiltration schedule as follows: ethanol:resin (2:1) was incubated overnight while ethanol:resin (1:1) was incubated for 5 h. For calculations of cER abundance in electron micrographs, the ratio between PM and the length of PM associated with cER were determined using ImageJ (www. imagej.nih.gov/ij/index.html); cER was assigned as previously described (14).

3.4.3. FIB-SEM

The resin block was microtomed to expose a clean face and then attached to a metal SEM stub with carbon tape. The sides were coated with silver paint to increase conductivity. The block was then sputter coated with a thin coat of Au/Pd and inserted into the FIB/SEM. Areas of interest were identified by viewing with the electron beam at 25 keV. *Serial Blockface Imaging:* The area of interested was coated with 1 µm thick Pt in the microscope using the Pt deposition needle. The sample was tilted to 52 degrees and a ~30 µm trench was cut in front of the area. The FEI Slice and View G2 program was used for data collection, with the following parameters: Imaging at 2 keV; 50 pA current; 30 µs dwell time; horizontal field width 17.74 µm; tilt angle 60 degrees (cross-sectional viewing angle -30 degrees); working distance 2.5 mm; TLD detector set to -245V suction tube voltage for backscatter imaging. The slice thickness was set at 20 nm, so the final voxel size was 8.66 nm in X, 10 nm in Y and 20 nm in Z. *Image processing:* Raw images were aligned using the xfalign tool in IMOD (527). Images were then corrected for density gradients using ImageJ software (528). The aligned and corrected tiff images were imported into Amira for density-guided segmentation (FEI Software, Hillsboro, OR) and display.

3.4.4. Fluorescence microscopy and live-cell imaging

Confocal fluorescence microscopy was performed as previously described(529). For all experiments, yeast cells were grown to mid-log phase before visualization. GFP-Staple (pCB1185) and mCherry-Staple (pCB1188) fusion proteins were imaged using 150 and 750 ms exposures, respectively. RFP-ER (pCB1024 and pCB1277) and RFP-RAS2 (pCB1204) were imaged using a 750 ms exposure on the confocal. GFP-2xPH^{OSH2} (pTL511) was imaged by confocal microscopy using a 250 ms exposure. Tcb3p-GFP and Ice2p-GFP were imaged by confocal microscopy using 350 ms and 1.5 s exposures, respectively.

Widefield fluorescence microscopy was performed as previously described [94]. GFP-2xPH^{OSH2} (pTL511) imaged by widefield epifluorescence was acquired using a 200 ms exposure, 30% arc lamp intensity and analog gain set to full. Bleed-through between fluorescence channels was undetectable under the conditions used for image acquisition. All contrast enhancement was kept constant for each series of images.

3.4.5. Sterol transport assays

Transport of exogenously supplied DHE from the PM to the ER was determined as previously described (184, 497). Briefly, DHE was loaded into the PM of cells under hypoxic conditions and its transport to the ER upon subsequent aerobic chase was monitored by fluorescence microscopy and quantified by lipid extraction and HPLC to determine the extent of conversion to DHE-ester. To quantify the initial fluorescence of DHE-loaded cells, individual cells were outlined using ImageJ then the corresponding area and integrated density were measured to determine the Corrected Total Cell Fluorescence (CTCF), as previously described (530)[95]; CTCF = (integrated density - (area of selected cell x mean background fluorescence)). At least 40 cells were counted (from 4 individual fields) for each strain. The ACAT (Acyl-CoA:sterol acyltransferase) activity of the cells was assayed with microsomes using a modification of a published procedure (531) as described (184, 497).

Biosynthetic sterol transport was measured using a pulse-chase labeling procedure as previously described (184, 497). Briefly, cells were labeled with [^{3}H]-methyl-methionine for 4 min to generate a pulse of [^{3}H]ergosterol in the ER, and subsequently chased with unlabeled methionine. Transport was assessed after subcellular fractionation to isolate the PM, or methyl-β-cyclodextrin (MβCD) extraction to sample ergosterol in the outer leaflet of the PM. Ergosterol in cells, subcellular fractions, and MβCD extracts was solubilized using organic solvents and quantified by HPLC.

3.4.6. Lipidomics

For lipidomics analysis, cells were grown to OD_{600} ~0.8 and lipid were extracted with chloroform:methanol (2:1). Yeast lipid extracts were prepared using a standard chloroform-methanol mixture, spiked with appropriate internal standards, and analyzed using a 6490 Triple Quadrupole LC/MS system (Agilent Technologies, Santa Clara, CA)

(532). Glycerophospholipids and sphingolipids were separated with normal-phase HPLC as described before (532), with a few changes. An Agilent Zorbax Rx-Sil column (inner diameter 2.1 x 100 mm) was used under the following conditions: mobile phase A (chloroform:methanol:1 M ammonium hydroxide, 89.9:10:0.1, v/v) and mobile phase B (chloroform:methanol:water:ammonium hydroxide, 55:39.9:5:0.1, v/v); 95% A for 2 min, linear gradient to 30% A over 18 min and held for 3 min, and linear gradient to 95% A over 2 min and held for 6 min. Sterols and glycerolipids were separated with reverse-phase HPLC using an isocratic mobile phase as before (532) except with an Agilent Zorbax Eclipse XDB-C18 column (4.6 x 100 mm).

Quantification of lipid species was accomplished using multiple reaction monitoring (MRM) transitions (532, 533) in conjunction with referencing of appropriate internal standards: PA 17:0/14:1, PC 17:0/20:4, PE 17:0/14:1, PG 17:0/20:4, PI 17:0/20:4, PS 17:0/14:1, LPC 17:0, LPE 14:0, Cer d18:1/17:0, D7-cholesterol, cholesteryl ester (CE) 17:0, 4ME 16:0 diether DG, D5-TG 16:0/18:0/16:0 (Avanti Polar Lipids, Alabaster, AL). Quality and batch controls (534) were included to assess instrument stability and reproducibility, and allow for correction of drift and other systematic noise, e.g. biases correlated with analysis order and/or sample preparation. Values are represented as mole fraction with respect to total lipid (mole percentage) (532). All lipid species and subclasses were analyzed with one-way ANOVA followed by a post hoc Bonferroni test.

3.4.7. Immunoblots

For analysis of Tcb3 protein expression, 10 OD_{600} units of Tcb3p-GFP expressing cells post sterol depletion were prepared as described by Ohashi et al. (535). Pellets were resuspended in SDS sample buffer and boiled for 5 min before SDS-PAGE. Protein transfer to nitrocellulose membranes and immunoblot conditions were as previously described (536). To detect Tcb3p-GFP, immunoblots were incubated with a 1:1000 anti-GFP antibody (ThermoFisher Scientific Inc., Waltham, MA) followed with 1:10,000 anti-rabbit-HRP secondary antibody (Bio-Rad Laboratories, Mississauga, ON). Actin was detected using 1:1000 anti-actin antibody (Cedarlane, Burlington, ON) followed with 1:10000 anti-mouse-HRP secondary antibody (ThermoFisher Scientific Inc.).

For analysis of Ysp2 protein expression, 10 OD_{600} units of GFP-Ysp2 expressing cells were prepared and proteins extracted as above. To detect GFP-Ysp2, immunoblots were incubated with 1:2000 anti-GFP antibody (Sigma-Aldrich Chemicals) followed by 1:10,000 anti-rabbit-HRP secondary antibody (Promega, Madison, WI). GAPDH was detected using 1:10,000 anti-GAPDH antibody (ThermoFisher Scientific Inc.) followed with 1:10000 anti-mouse-HRP secondary antibody (Promega).

3.4.8. Estimate of the random chance of finding ER at the cell cortex in cells lacking tethers

We derive a rough estimate of the chance of finding cER at the cell cortex in yeast cells that lack the ability to tether the ER to the PM as follows. Assuming that a yeast cell has a volume of 65 μm^3 (radius = 2.5 μm)(537, 538), we estimate the volume of a cortical shell defined by the reported distance (30 nm) at which the ER is retained at the PM by tethers as 1.9 μm^3. As ~ 45% of the PM is associated with ER in WT cells (Fig. 1E and references (10, 16)), the volume of the cortical shell that is occupied by ER is 0.9 μm^3. If this amount of ER were to become untethered, then it could be found anywhere in the total volume of the cell. Approximately 65% of the total cell volume is available for this purpose, i.e. 42 μm^3, as the rest is occupied by the nucleus and organelles (539). Thus, the random chance of finding the dispersed complement of cER anywhere in the cell, including the cell cortex, is 0.9/42 = 0.02 or ~2%.

Chapter 4. Functionally defining Plasma Membrane-Endoplasmic reticulum membrane contact site secondary tether proteins

This chapter is adapted and expanded from a manuscript in preparation. The authors and their affiliations are listed below:

Evan Quon[1], Jesper Johansen[1], Christopher T. Beh[1,2]

[1]Department of Molecular Biology and Biochemistry, Simon Fraser University, Burnaby, British Columbia V5A 1S6, Canada

[2]Centre for Cell Biology, Development, and Disease, Simon Fraser University

I performed genetic manipulations to generate all recombinant yeast strains which served as the basis for this publication. I performed all experiments and analysis except for Figure 3.3B which was performed by Dr. Jesper Johansen and Figure 3.1A-D which were courteously provided by Dr. Anant Menon.

Dr. Christopher Beh contributed to writing and editing of the manuscript.

4.1. Introduction

Membrane Contact Sites (MCSs) are regions of close apposition between two organelles that serve as interfaces for both direct exchanges of membrane constituents and regulatory interactions. MCSs are seen within all eukaryotic cells and involve nearly all membrane compartments (16, 27–29, 38, 93, 97, 158, 540, 541). A wide variety of different tethering proteins bridge the gaps between membranes, including between the ER and the PM. As a major biosynthetic site for lipids, the ER represents the source of most membrane components. As the major resident site for lipids, the PM and the cell cortex represent the target destination for most cellular membrane constituents. In addition to vesicular transport from the ER, ER-PM MCSs provide another potential “non-vesicular” conduit for lipid transfer critical for maintaining cortical size. Apart from membrane transport, MCSs might also confer a "sensing nexus" wherein ER metabolic production and PM requirements are balanced.

In yeast, a large proportion of the cytoplasmic face of the PM is covered by closely associated ER membrane (10, 542). The physical attachment between these membranes is partly mediated by ER integral membrane proteins that interact with the cytoplasmic face of the PM, though for some tether proteins, the precise mechanism for PM binding has yet to be determined. Some of these ER-PM tether proteins were identified by Manford et al. (16), who postulated that tethers might directly interact with the phosphatidylinositol-4-phosphate (PI4P) phosphatase Sac1p and the VAP homolog Scs2p. Sac1p is an integral membrane protein normally restricted to the ER that may or may not regulate PM PI4P levels *in trans* at regions of close ER-PM apposition (139, 201, 543). Scs2p is also an ER membrane protein that had been previously implicated as a mediator of ER-PM contact (125, 139). It was reasoned that if Scs2p were the only ER-PM tether, then in *scs2*Δ cells Sac1p would be unable to reach across for PI4P turn-over in the PM, phenocopying *sac1*Δ defects (16). A modest decrease in PM PI4P was shown in cells lacking both *SCS2* and its homolog *SCS22*, but not as dramatic as observed in *sac1*Δ cells (16). These results suggested, in so far as ER regulation of PI4P is concerned, other tether proteins operate at ER-PM contact sites in addition to Scs2p (and Scs22p). On the premise that unidentified tethers would be at contact sites alongside Scs2p and Sac1p, where they might physically interact, a proteomic strategy was successfully applied to discover the other ER-PM tether proteins (16)

From a list of Sac1p- and Scs2p-interacting proteins determined by proteomic analysis, the three tricalbins Tcb1p-3p were identified along with Ist2p as potential tethers (16). All these integral membrane proteins had been independently found to reside at regions of cortical ER that associate *in trans* with PM phosphoinositides, which affirmed their involvement in ER-PM tethering (38, 161). Tricalbins represent yeast homologs of mammalian extended synaptotagmins (E-Syts), which seem to play dual roles in ER-PM lipid transfer and possibly in Ca2+ regulation (159, 544). Ist2p is a multispan ER transmembrane domain proteins and a representative member of the TMEM16-anoctamin family of ion channels and phospholipid scramblases (545). Because they interact with both Sac1p and Scs2p at ER-PM MCSs, Ist2p and the tricalbins could conceivably form one large protein complex with coupled functionalities. Alternatively, these Sac1p and Scs2p-binding tether proteins might represent independent complexes forming separate MCSs. Regardless, in yeast cells, the elimination of the primary tether proteins caused a drastic reduction in ER-PM MCSs.

Based on the work by Manford et al. and ourselves (16, 29), we classified the tricalbins, Ist2p, Ice2p, and Scs2p/22p as “primary tethers” (30) (Fig. 1.2). A primary tether protein must adhere to two criteria under normal growth conditions: i) a primary tether protein must localize to MCSs, ii) a primary tether protein is necessary for membrane association (i.e. deletion of a primary tether gene must significantly reduce membrane association). Elimination of any of these primary tethers reduces the frequency of MCS formation as compared to wild-type cells, as observed by electron microscopy or fluorescence microscopy using ER markers (**Fig. 3.1**). In ∆tether cells, which lack six of these primary tethers, ER-PM association is greatly reduced (16). It was noted, however, that ER-PM association does not entirely dissipate in ∆tether cells, suggesting the presence of additional tethers. Indeed, even if all ER-PM tether proteins are eliminated, random associations between untethered ER and the PM would still be predicted as freed ER drifts through the cytoplasm near the cell cortex. Through simple volumetric calculations, rough estimates can be made of residual stochastic ER-PM associations remaining in cells lacking all tethering proteins. Using the cytoplasmic volume determined for a prolate unbudded yeast cell (excluding volumes of major organelles), and the volume occupied by the ER-association with the PM (40% cortical coverage with a 35 nm thickness, corresponding to the average ER-PM gap distance), the ratio of cortical ER:cytoplasm volumes is ~0.02. In other words, if untethered cortical

ER disperses throughout the volume of the cytoplasm, 2% of this ER will be found anywhere within the cytoplasm including near the PM. In ∆tether cells, the coverage of PM with ER is significantly more than 2%, suggesting that some direct (non-stochastic) membrane tethering still remains. Based on our rough calculations and observations that ER-PM association remains in ∆tether cells, we searched for additional ER-PM tether(s).

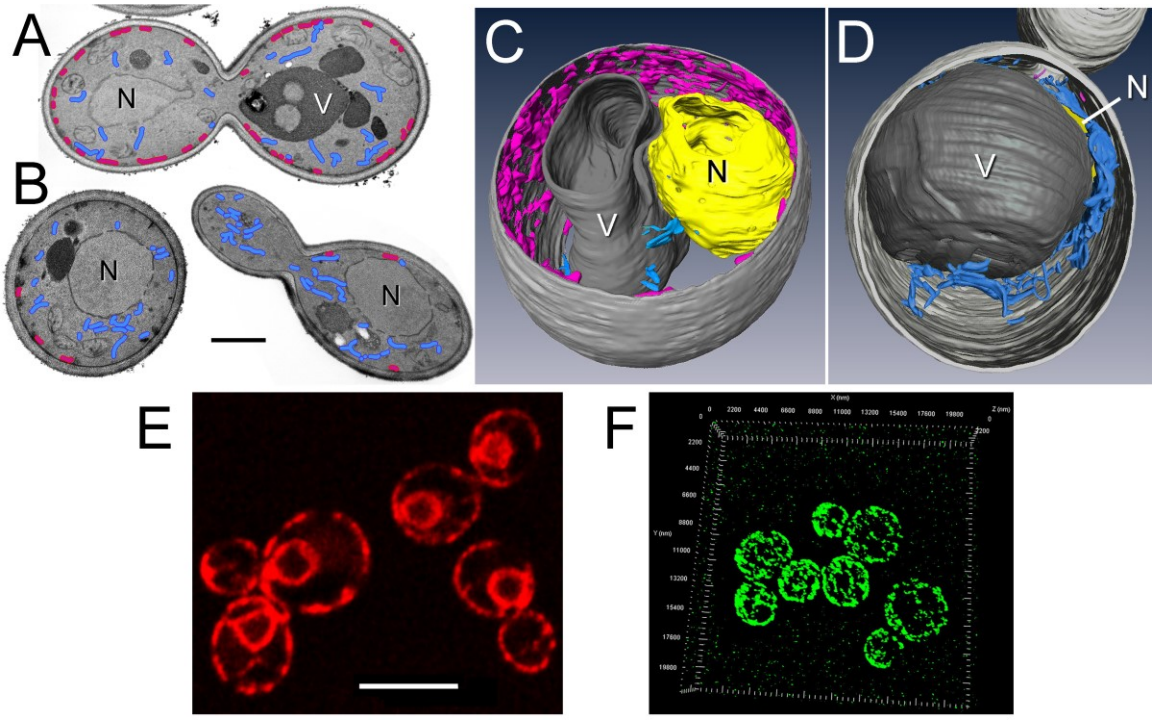

Figure 4.1. Primary membrane tether proteins adhere to cortical ER membrane to the cytoplasmic face of the PM

(**A**) Representative transmission electron microscopy (TEM) images of wild-type (SEY6210) and (**B**) ∆-s-tether cells (CBY5838) showing the distribution of cortical ER (magenta) lining the PM, and cytoplasmic ER (blue). N = nucleus, V = vacuole. (**C**) Representative wild-type and (**D**) ∆-s-tether cells modeled from 3-D constructions of sections imaged by focused-ion-beam tomography (FIB-SEM); cortical ER is shown in magenta, cytoplasmic ER in blue. V = vacuole, N = nucleus (yellow). Note that the nucleus is partially hidden underneath the vacuole in the 3-D image of the ∆-s-tether cell. (**E**) Super-resolution fluorescent microscopy of RFP-ER marking the nuclear, cytoplasmic, and cortical ER. (**F**) Super-resolution 3-D model showing Tcb3p-GFP fluorescence at ER-PM MCSs

As previously defined (30), secondary tethers might fortify or expand the association of membrane at pre-established contact sites, or they might induce membrane contact in response to specific stimuli. Unlike the primary tethers deleted in the ∆-s-tether strain, the elimination of secondary tethers from cells would not impact ER-PM contact site formation. In contrast to primary tethers, secondary tethers would be sufficient, but not necessary, to promote membrane association when overexpressed or

induced. Secondary tether overexpression may also suppress defects (i.e. growth) associated with the absence of MCSs. As demonstrated by the artificial membrane staple, ER-PM contact is relatively non-specific, so the mechanism of any presumptive secondary tether might also be quite general. To put flesh on the bones of this conceptual model, I tested two candidate ER proteins (Ysp2/Lam2p and Pah1p) previously implicated in MCS formation to determine if they meet the predicted criteria of secondary tethers.

4.2. Results

Ysp2/Lam2p (hereafter referred to as Ysp2p) is one of six StART domain homologs that are implicated in non-vesicular sterol transfer between the ER and other cellular compartments (211, 212). In particular, Ysp2p-GFP localizes to spots consistent with sites where the ER and PM are associated (**Fig 3.2**), though distinct from where established primary tethers are observed (211). The deletion of *YSP2* in wild-type, ∆tether or ∆-s-tether cells had no negative impact on growth relative to the corresponding parent strains, suggesting that Ysp2p is not functionally required for growth as a primary tether (29). Because these results suggest that Ysp2p is not necessary for ER-PM contact, Ysp2p does not meet the criterion of being a primary tether. Considering Ysp2 appears to be present at ER-PM interfaces despite being unnecessary for establishing membrane association, I hypothesize that Ysp2p may be a secondary tether. Because *YSP2* has a paralogue, *LAM4*, as well as four other *LAM* homologs that might be functionally redundant, it could be argued that *YSP2* would have to be deleted together with other *LAM* genes to manifest a growth defect in ∆tether or ∆-s-tether cells. However, all *LAM* genes are present in ∆-s-tether cells and only stochastic associations between the ER and PM are seen. Ysp2p and the rest of the Lam proteins are unlikely to play a major role in establishing ER-PM membrane contact, at least during conditions of normal cell growth.

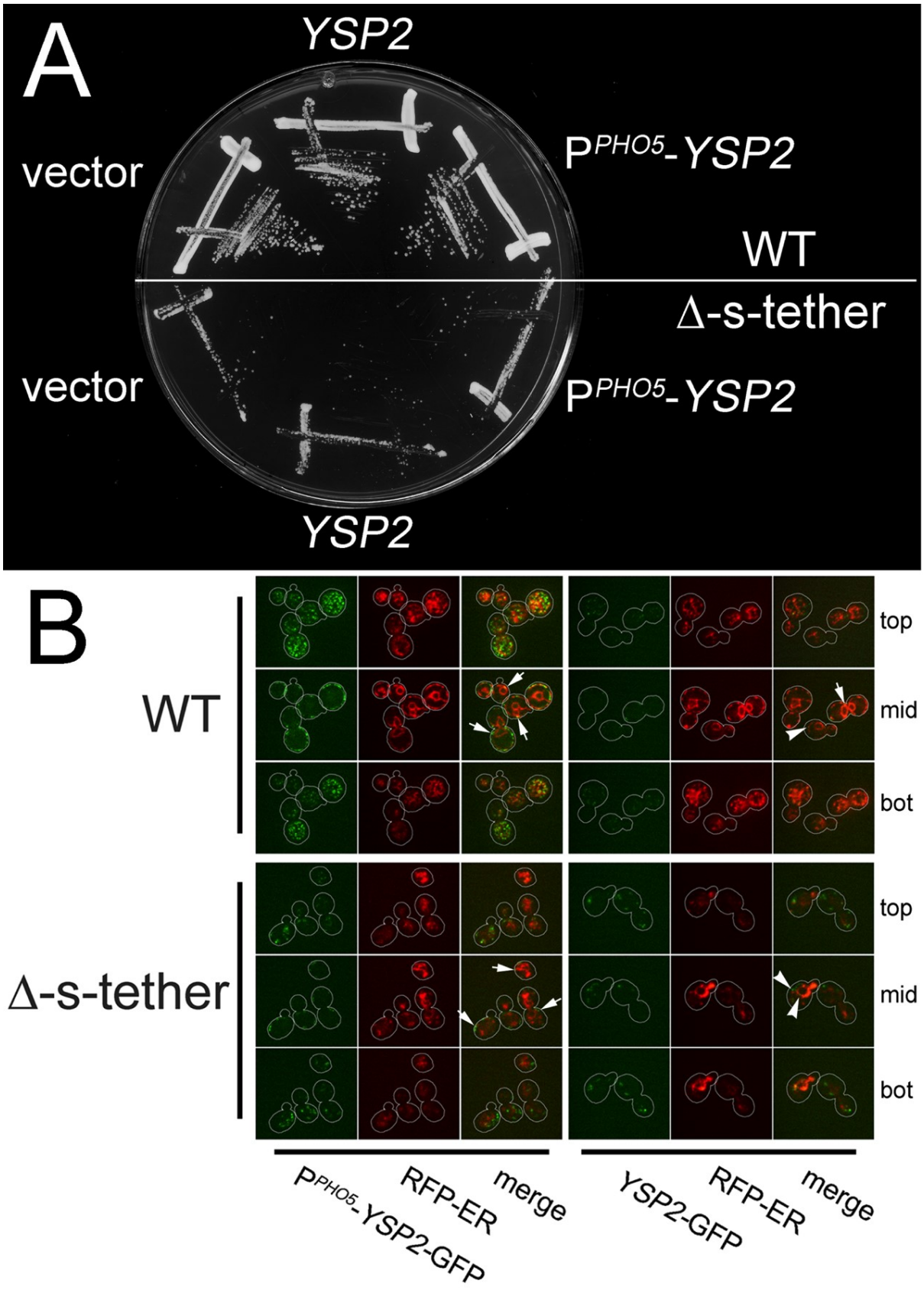
A
YSP2
vector
P PHO5 - YSP2
WT
Δ-s-tether
vector
P PHO5 - YSP2
YSP2
B
WT
Δ-s-tether
top
mid
bot
top
mid
bot
P PHO5 - YSP2-GFP
RFP-ER
merge
YSP2-GFP
RFP-ER
merge

Figure 4.2. Ysp2p localizes to the terminal ends of ER tubules.

(A) Wild-type (WT; SEY6210) and Δ-s-tether (CBY5838) cells transformed with vector alone (pRS416), YSP2 (P^{YSP2} GFP-*YSP2*), or YSP2 expressed from the strong PHO5 promoter (P^{PHO5}-GFP-*YSP2*) were streaked onto solid growth medium (without choline supplementation). Unlike the artificial membrane staple (or *PAH1*), *YSP2* overexpression did not suppress Δ-s-tether growth defects. (B) Confocal fluorescent microscopy images of WT and Δ-s-tether cells expressing RFP-ER and either P^{YSP2}-GFP-*YSP2* or P^{PHO5}-GFP-*YSP2* (overexpressed) shown at three different optical focal planes (top, middle, bottom). The cell cortex/cell membrane is traced corresponding to DIC images of the middle focal plane. Arrows represent Ysp2p at RFP-ER tubule ends at the cell cortex, and arrowheads represent Ysp2p within the cell body at ER tubule ends and branch points

YSP2 might not be necessary for establishing ER-PM contacts, but Ysp2p overexpression appears to be sufficient to increase membrane association. As shown in **Fig 3.2**, elevated expression of Ysp2p-GFP via transcription from a *PHO5* promoter increased the number of cortical Ysp2p-GFP spots, which correlated with an increase in ER association with the PM (as shown using the ER marker ER-RFP). Under these conditions Ysp2p can promote ER-PM association, however, this activity is dependent on pre-existing MCSs. In both Δtether and Δ-s-tether cells, the removal of primary tether proteins causes the frequency of Ysp2p-GFP puncta to dwindle to almost nothing (**Fig 3.2**) (29). Although these results meet other criteria predicted for secondary tethers, there is an alternative explanation for Ysp2p-GFP cortical localization that does not involve MCSs. Using 3-D fluorescence microscopy, I observed that ~60% of Ysp2p-GFP, when expressed from its endogenous promoter, localized to spots either the distal tips of ER tubules or to the junctions at branch points between ER tubules (12.2 ± 4.5 Ysp2p-GFP spots per each cell; n = 10 cells); consistent with findings reported in a previous study (211). Because the ER radiates from the nucleus out towards the PM, the distal ends of the ER would extend to the cell cortex, MCSs notwithstanding. If Ysp2p promotes ER tubule extension at its tips towards the PM, then Ysp2p might be a regulator of ER morphology and thereby an ancillary determinant of ER-PM contact, instead of a tether.

The yeast lipin homolog Pah1p is a phosphatidate phosphatase that converts phosphatidic acid into diacylglycerol (239, 240). The overexpression of Pah1p was previously found to suppress the partial choline auxotrophy of *scs2*Δ *ice2*Δ cells, and to restore their moderate reduction in ER-PM membrane contact back to normal (177). At first glance, this result suggested that membrane contact defects in *scs2*Δ *ice2*Δ cells might be corrected by changes in Pah1p-dependent lipid metabolism. However, it was

found that the Pah1p D398E substitution, a catalytically inactivate mutant, did not inhibit Pah1p suppression of *scs2*Δ *ice2*Δ defects (177). To test if Pah1p or its D398E catalytically inactive form can re-establish membrane association in a cell lacking all ER-PM contact sites, *PAH1* and *pah1*D398E were expressed in Δ-s-tether cells. Both Pah1p and its catalytically dead mutant rescued Δ-s-tether growth defects on solid medium lacking choline (**Fig. 3.3A**). Although Pah1p is mainly in the cytoplasm, when glucose is limiting Pah1p is associated at contact sites between the ER/nuclear membrane and the vacuole, and near ER-lipid droplet contact sites (244). In *scs2*Δ *ice2*Δ cells, overexpression of both active and catalytically inactive Pah1p increase the number of Tcb3p tethers between the cortical ER and the PM. Either Pah1p induces Tcb3p expression or Pah1p augments existing Tcb3p-dependent membrane contact (consistent with the role of a secondary tether). In Δ-s-tether cells, Tcb3p and all the other primary tethers are eliminated so the mode of Pah1p suppression cannot involve generating more pre-existing tether complexes. However, overexpression of Pah1p (or its catalytically dead mutant) did restore cortical ER association with the PM in Δ-s-tether cells (**Fig. 3.3B**). The most economical interpretation for this result is that Pah1p acts as a secondary ER-PM membrane tether, similar to its role in mediating the association between the ER and lipid droplets or the vacuole. However, it is also possible that Pah1p activates or induces the expression of another secondary tether that re-establishes ER-PM contact.

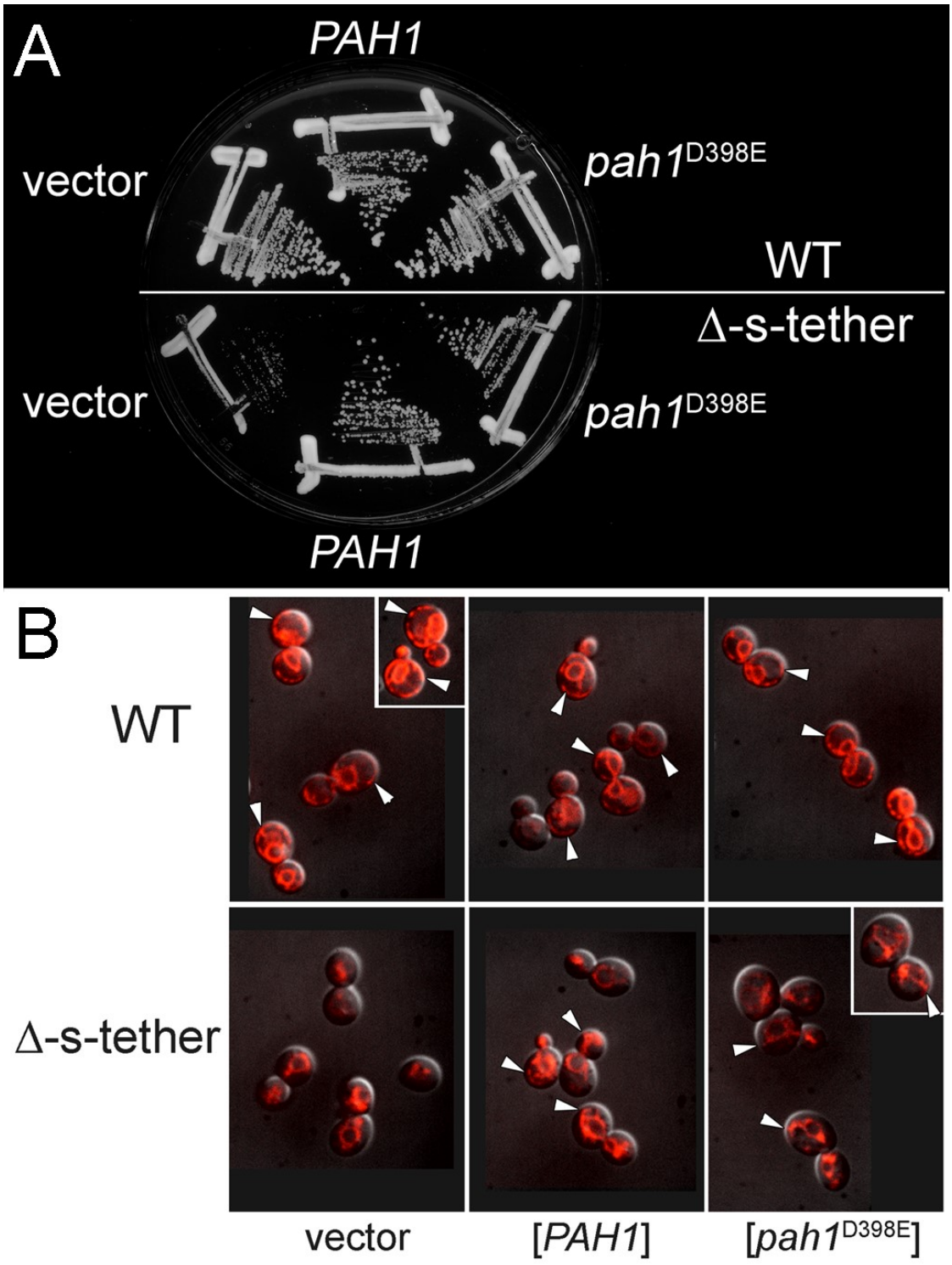

Figure 4.3. Pah1p confers ER-PM tethering in Δ-s-tether cells.
(A) Wild-type (WT; SEY6210) and Δ-s-tether (CBY5838) cells transformed with vector alone (YEplac181), *PAH1* (pGH312), or *pah1*D398E (enzymatically dead mutation) (pGH312-D398E) were streaked onto solid growth medium (without choline supplementation). Both *PAH1* and *pah1*D398E suppressed Δ-s-tether growth defects. (B) Merged DIC and spinning disc confocal fluorescent microscopy images of WT and Δ-s-tether expressing RFP-ER and either vector alone, *PAH1*, or *pah1*D398E. Arrowheads identify cortically localized RFP-ER.

4.3. Discussion

PM-ER MCSs are facilitated by a group of highly conserved tether proteins which anchor the ER to the PM. Under normal growth conditions, “Primary” tether proteins are required to mediate PM-ER membrane association. Based on work by Manford et al., and ourselves, I have classified the tricalbins, Ist2p, Scs2p/22p, and Ice2p as primary tether proteins in yeast (16). Elimination of any of these primary tethers reduces the frequency of MCS formation as compared to wild-type cells, as observed by electron microscopy or fluorescence microscopy using ER markers.

Recent research has suggested that many proteins are capable of reaching across the 15-60 nm gap between the ER and PM (16, 139, 177, 202, 211). I suggest that under non-standard conditions, some of these proteins may act as “Secondary” tether proteins and may be able to facilitate or augment membrane association when overexpressed or under specific growth conditions (i.e. stationary phase). Deletion of secondary tethers would not affect PM-ER MCSs under normal growth conditions, therefore they are not necessary for membrane association. To better understand secondary tether proteins, I conducted proof of principle experiments on previously suggested potential tethers.

4.3.1. Is Ysp2p a secondary tether protein?

Ysp2p is an ER protein consisting of two StART-link domains, a PH_{GRAM} domain, which belong to the PH domain superfamily, a polybasic region, and a transmembrane domain (211). These features have propagated speculations that Ysp2p is a tether protein and a sterol LTP (211). Considering Ysp2p is a cortically localized integral ER protein and contains two potential membrane binding domains (PH and polybasic region), makes Ysp2p being a tether protein an attractive hypothesis (211). Our analysis shows that GFP-Ysp2p cortically localizes and *YSP2* overexpression increased PM-ER membrane association, suggesting that Ysp2p may be a secondary tether (**Fig 3.2B**). However, overexpression of *YSP2* was unable to suppress growth defects in Δ-s-tether cells suggesting a lack of secondary tether functionality (**Fig 3.2A**). This does not exclude Ysp2p from acting as a secondary tether protein or regulator of PM-ER MCSs.

Under normal growth conditions the cortical localization of established primary tether proteins, such as GFP-Ist2p, GFP-Scs2p, Tcb3p-GFP, and Ice2p-GFP, primary tethers appear to localize along the length of ER tubule (16, 29, 38, 129, 161, 175, 546).

Comparatively, GFP-Ysp2p localizes to puncta adjacent to cortical ER junction and distal tips (**Fig 3.2B**). Overexpression of GFP-Ysp2 did not increase cortical localization along the ER tubule but did increase the number of puncta at the cortex. There are approximately 41 residues between the transmembrane domain and the polybasic region of Ysp2p, which may interact with the PM (202). This suggests that Ysp2p may have an approximate linker span of ~16 nm, which is close to the lower limit of observed PM-ER MCS gap width (10, 211). Ysp2 also contains a PH domain which is significantly further away from the transmembrane domain (507 residues) than the polybasic region and therefore may result in a significantly larger membrane gap (547). It has been hypothesized that some tethers may operate as local regions where MCS gap width matches the tether linker length (202). This is supported by evidence that shortening the linker of Ist2p from 130nm to 20nm, redistributes GFP-Ist2p from extended cortical tubular association to cortical puncta (548). Also, short linker length and cortical puncta localization do not exclude a protein from acting as a potential tether, as seen in the artificial membrane staple (29). Therefore, Ysp2p may function at discrete cortical microdomains associated with ER tubules. The primary tether proteins E-Syt1 has been shown to restrict the PM-ER MCS gap in response to extracellular calcium, suggesting a functional difference between MCS gap width (148). It is possible that the PH domain and polybasic region of Ysp2p may function similarly to modulate PM-ER MCS gap width. Another possibility is that Ysp2p functionality is depending on MCS gap width causing Ysp2p to preferentially localize to narrower PM-ER MCS microdomains.

The nature of this function remains to be discovered however several hypotheses have been proposed. Recent evidence suggests that the Ysp2p homolog Lam6p regulates ER-mitochondria MCSs, NVJ, and vacuole and mitochondria patches (vCLAMP; vacuole-mitochondria MCS) size and coordination (213). It is possible that Ysp2p may be functioning similarly to Lam6p and may be responsible for expanding and regulating existing PM-ER MCSs.

Alternatively, it has been hypothesized that Ysp2p is an ER to PM sterol LTP because it contains two StART-like domains (211). StART-like domain proteins represent a large protein family including the endosomal membrane protein STARD3, which capture cholesterol by its StART domain from the late endosome and transfer it to the ER (190). Because STARD3 is restricted to the endosomal membrane, the mechanism of transfer would necessitate cholesterol exchange where the ER and

endosomes are closely associated. Ysp2p is a Yeast StART Protein (Ysp) homolog and is therefore hypothesized to work similarly to STARD3 at ER-PM MCSs. Like STARD3 and other membrane-bound lipid transfer proteins, Ysp2p-mediated sterol transfer would require MCSs for exchange. Like Δ-s-tether cells, measuring DHE esterification in *ysp2*Δ mutants reveal retrograde sterol trafficking defects (211). However, whether the defect is caused by disruptions in PM sterol composition, like in Δ-s-tether cells, or by reduced bi-directional trafficking defects is unknown. I showed that *ysp2*Δ Δ–s-tether cells were viable with no additional growth defects relative to Δ–s-tether cells (29). Directed experiments testing the role of Ysp2p plays in the bi-directional transport of sterols between the ER and PM in the absence of vesicular trafficking has yet to be performed. However, I have shown that Δ-s-tether cells have minimal cortical GFP-Ysp2p cortical localization and have no sterol transfer defects in the absence of vesicular trafficking (**Fig 3.2**) (29). This suggests that Ysp2p may be functionally dependent on PM-ER MCSs and may be working redundantly with another sterol transfer mechanism.

4.3.2. Is Pah1p a secondary tether protein?

Previous reports have shown that overexpression of WT and catalytically dead *PAH1* can suppress PM-ER association defects in *scs2*Δ *ice2*Δ mutants and increase PM-ER association in WT cell (177). Here, I have shown that *PAH1* overexpression is capable of functionally suppressing Δ-s-tether growth defects and re-establishing PM-ER membrane association in Δ–s-tether cells (**Fig 3.3**). Under exponential growth conditions, Pah1p-GFP is primarily cytosolic then translocates to the NE during the post-diauxic shift and stationary phase (244). During the post-diauxic shift, Pah1p-GFP appears to localize to the NVJ, and shifts to NE-LD MCS during stationary phase (244). Although Pah1p seems to be associated with MCSs, it does not seem to associate with PM-ER MCSs under these conditions. Therefore, it is unknown if Pah1p directly re-establishes PM-ER membrane association or by regulating another secondary tether. As previously discussed, the Nem1p-Spo7p phosphatase complex activates Pah1p by dephosphorylation resulting in membrane association (242, 244). However, the catalytically dead Pah1p can bind membranes regardless of Nem1-Spo7p mediated dephosphorylation (549). Therefore, the secondary tether function of Pah1p is likely linked to its membrane association and not its phosphatase activity.

The function of *PAH1* is tightly regulated by the oppositional function of *DGK1* (246). In wild-type cells, Dgk1p-GFP localizes to the NE and ER (246, 550, 551). Recently evidence has shown that cells lacking the ability to generate TAG and SE (*dga*Δ *lro*Δ, *are1*Δ, *are2*Δ; 4Δ) have a significant expansion of the nuclear, cytoplasmic and cortical ER (244). However, all these phenotypes can be suppressed by deleting *DGK1* (244). This suggests that Dgk1p could also be a secondary tether and Pah1p could be affecting PM-ER membrane association through *DGK1* or vice versa. It has been shown that overexpression of *DGK1* causes increases membrane localization of WT and catalytically dead Pah1p (549). However, deletion of *PAH1* does not seem to affect Dgk1p-GFP localization (550), and it is not known if overexpression of *PAH1* causes increased Dgk1p membrane localization or *DGK1* expression. It should also be noted that overexpression of *DGK1* and deletion of *PAH1* causes proliferation of nuclear and cytoplasmic ER (241, 246). If *PAH1* overexpression causes a compensatory overexpression of *DKG1,* then it could re-establish membrane association by increasing ER volume, thereby increasing PM-ER stochastic association.

4.3.3. Definitions of secondary tether proteins

Unlike primary tether proteins, which directly contribute to membrane tethering, secondary tether proteins could facilitate membrane association directly or indirectly. For the direct model, specific growth, stress, or metabolic conditions would increase secondary tether expression, stabilization or recruitment leading to increased PM-ER membrane association. Additionally, many proteins play several roles depending on the growth conditions or the environment, therefore, depending on the cellular requirements, secondary tethers could be relocated, or re-purposed from other MCSs. An example would be the primary tether Ice2p which acts as a PM-ER MCS tether during exponential growth (30, 175) but acts as an ER-LD MCS tether during stationary phase (178).

It is possible that secondary tethers may not directly contribute to MCS initiation but contribute to MCS stabilization and expansion. A potential example of this is the ER-resident r-SNARE Sec22p which localizes to PM-ER MCSs and interact with the PM-resident t-SNARE Sso1 (187). It has been suggested that Sec22p contributes to PM-ER MCS expansion and stabilization (187). It should be noted that secondary tethers in this category would require pre-existing MCSs to function and may not be able to re-

establish membrane association on their own. It is possible that Ysp2p may fit into this category of secondary tether.

Indirect secondary tether models have a variety of mechanisms by which they could act. Some secondary tether may modulate tethering by transcriptionally activating other direct secondary tethers. For example, the zinc-regulated transcription factor Zap1 transcriptionally controls the expression of *PAH1,* which I have shown to be a secondary tether (552). However, these may be more accurately described as “tether regulators” as their mode of action becomes more removed from physical membrane association. An indirect secondary tether could facilitate membrane association by manipulating the morphology of the cell. For instance, *DGK1* can expand the ER volume which may increase stochastic association (246), or, the MECA tether protein, Num1p, may be able to compensate for the lack of PM-ER MCSs by increasing MECA junction points (97). Another model of indirect tethering would be to decrease direct secondary tether degradation or increase secondary tether stability. Last, changes to the lipid environment of the cell could affect membrane association. I previously showed that overexpressing of the phospholipid transferase *OPI3* can suppress ∆–s-tether synthetic growth defects (29). Opi3p is an ER resident protein and, like Sac1p, has been suggested to work *in trans* at the PM (177). Overexpression of *OPI3* may be suppressing membrane association defects through direct tethering. Alternatively, Opi3p could be modulating the ER and PM lipid environments, and which could support tethering indirectly. As will be discussed later, one would predict that PIP regulation may support membrane association, therefore PIP kinases or phosphatases may also appear to be indirect secondary tethers. Collectively, indirect secondary tethers are somewhat ambiguous and may require further or alternate definitions as their mechanisms of increasing membrane association become further removed from direct membrane tethering.

Another consideration which must be made is the difference between associated PM and ER membranes and functional PM-ER MCSs. As reviewed in Gatta et al (211), the linker between membranes varies depending on tether protein which may also correlate to function. Therefore, some proteins may require specific gap widths to function. Our previous results have shown that an artificial membrane staple can non-specifically function as a tether protein (29). It is possible that the artificial staple may only be functional with an approximate ~10 nm artificial MCS gap width. It is likely that

functional suppression is associated to MCS gap. Therefore, expanding the artificial MCS gap may not be able to functionally supress Δ-s-tether synthetic sickness.

4.3.4. Conclusion:

The discovery and characterization of primary PM-ER MCS tether proteins have been the major research focus for several years. However, the regulation of primary tether proteins and PM-ER MCSs remains largely a mystery. I propose that secondary tether proteins function in conjunction with primary tether proteins to regulate the PM-ER MCSs. Here I discuss two potential secondary tether proteins which have been shown to interact with PM-ER MCSs and may regulate membrane association by two seemingly different mechanisms. Further analysis into secondary tethers will not only expand our understanding of PM-ER MCS regulation but also the expanse of their functional implications.

4.4. Materials and Methods

4.4.1. Yeast Strain and Growth Conditions

Yeast strains and plasmids are listed in Supplementary **Tables 3.**1 and **3.2**, respectively. Unless otherwise stated, yeast cultures were grown in synthetic complete or YPD rich media at 30˚C. To test YSP2 and PAH1 suppression growth defects, cells were streaked onto solid synthetic complete media with and without 1 mM choline chloride (Sigma-Aldrich Chemicals) and incubated at 30°C for 48 h. To test s-tether growth defects on Ca2+ and Na+ media, cells were serial diluted and spotted onto solid synthetic complete media or YPD with and without 0.7 M sodium chloride (Sigma-Aldrich Chemicals) or 0.4 M calcium dichloride and incubated at 30°C for 48 h.

Table 4.1. Yeast strains.

Strain	Genotype	Source
ANDY198	*MAT*a *leu2-3,112 ura3-52 his3Δ200 trp1Δ901 lys2-801 suc2Δ9 ist2*Δ::hisMX6 *scs2*Δ::*TRP1 scs22*Δ::hisMX6 *tcb1*Δ::kanMX6 *tcb2*Δ::kanMX6 *tcb3*Δ::hisMX6	(16)
BY4741	*MAT*a *leu2Δ0 ura3Δ0 his3Δ0 met15Δ0*	
CBY5838	ANDY198 *ice2*Δ::natMX4	(29)
CBY6087	SEY6210 *TCB3*-GFP:*URA3*	

CBY6257	BY4741 *pmc1*Δ::KanMX4	Gift From Chris Loewen
CBY6258	BY4741 *pmr1*Δ::KanMX4	Gift From Chris Loewen
SEY6210	*MATα leu2-3,112 ura3-52 his3Δ200 trp1Δ901 lys2-801 suc2Δ9*	(523)

Unless otherwise referenced, all strains were created as part of this study.

Table 4.2. Plasmids

Plasmid	Description	Source
pCB1024 (ER-RFP)	pRS416 P^{PHO5}-RFP-$SCS2^{220-244}$	(125)
pCB1277 (ER-RFP)	YEplac181 P^{PHO5}-RFP-$SCS2^{220-244}$	(29)
pGH312	YEp351 HA-*PAH1*	(239)
pGH312-D398E	YEp351 HA-$PAH1^{D398E}$	(240)
pRS416 GFP-*YSP2*	pRS416 P^{YSP2}-GFP-*YSP2*	(29)
pRS416 GFP-*YSP2*	pRS416 P^{PHO5}-GFP-*YSP2*	(211)
pRS416	*URA3 CEN*	(524)
YEplac181	*LEU2 2μ*	(525)

Unless otherwise referenced, all plasmids were created as part of this study.

4.4.2. Fluorescent Microscopy and Live Cell Imaging

Confocal fluorescence microscopy was performed as previously described (529). For all experiments, yeast cells were grown to mid-log phase before visualization. The ER-RFP (pCB1024 and pCB1277) protein marker was imaged by confocal microscopy using 800 ms exposures. GFP-Ysp2p was imaged by confocal microscopy using a 1.5 s exposure. All contrast enhancement was kept constant for each series of images. Super-resolution fluorescent microscopy was performed on a Zeiss LSM 880 Confocal with Airyscan microscopy Plan-apochromat 63x/1.4 Oil. Images and Videos were made with Zen 2 (Blue edition) and exported as TIFF or uncompressed AVI files respectively.

4.4.3. Transmission Electron Microscopy

Yeast cells were grown to mid-log phase and were prepared (fixation, dehydration, infiltration/embedding) and imaged as previously described (29, 526). For calculations of cER abundance in electron micrographs, the ratio between PM and the length of PM associated with cER were determined using ImageJ (www.imagej.nih.gov/ij/index.html); cER was assigned as previously described (14)

4.4.4. FIB SEM

Yeast cells were grown to mid-log phase and were prepared (fixation, dehydration, infiltration/embedding) and blockface imaged as previously described (29). Raw images were aligned and processed as previously described (29).

Chapter 5. Discussion

Section 4.2 and 4.3 contain excerpts modified from a paper that has been published in Lipid Insights (Quon et al., 2016). The authors and their affiliations are listed below:

Evan Quon[1], Christopher T. Beh[1,2],

[1]Department of Molecular Biology and Biochemistry, Simon Fraser University, Burnaby, British Columbia V5A 1S6, Canada

[2]Centre for Cell Biology, Development, and Disease, Simon Fraser University

All conceptualization, writing, and editing were performed by Dr. Christopher Beh and me.

Membrane contact sites are well-established phenomena since their initial discovery in the early-1950's (27, 83–85), however, the expanse of their physiological roles has yet to be realized. Although MCSs exist between the ER and every organelle in the cell, the PM makes up most of the ER-associated membrane. Prior to the research performed in this thesis, the understanding of PM-ER MCSs and their role in regulating lipid biosynthesis and lipid transport had been hypothesized but never experimentally proven. Work previously performed by Manford et al defined the first six primary tether proteins in yeast, which are required for directed membrane association (16). However, in generating a strain lacking these six tether proteins (∆tether), it was discovered that not all directed membrane association had been eliminated. Here, I proved that Ice2p is also a primary tether protein and cells lacking all seven tethers (∆-s-tether) lack directed membrane association (29). Therefore, I used ∆-s-tether cell to directly test PM-ER MCS functions.

Using *in vivo* sterol transfer assays, ER-to-PM anterograde transport of pulse-chase labeled sterols was measured in ∆-s-tether cells (29). Compared to wild-type cells, no defect in transport of *de novo* synthesized sterol to the PM was detected. Ysp2/Lam2p or any other ER membrane-bound sterol transfer proteins would not be able to act *in trans* in ∆-s-tether cells that lack ER-PM association. However, if soluble sterol transfer proteins provide a redundant pathway for transfer, then anterograde transport might still proceed even in cells without ER-PM MCSs. Consistent with that premise, the eliminating the putative soluble sterol transfer protein Osh4p in ∆-s-tether cells caused cell lethality (29). This synthetic lethality seemed to suggest that all non-vesicular pathways for sterol transfer to the PM were inactivated in *osh4*∆ ∆-s-tether cells. To test if sterol trafficking was truly the basis of this defect, I overexpressed Osh6p in *osh4*∆ ∆-s-tether cells. Although Osh6p binds PI4P and PS, it can neither bind nor transfer sterols (136, 140). Nonetheless, Osh6p suppressed *osh4*∆ ∆-s-tether synthetic lethality indicating that the growth defect was unrelated to sterols. Apart from their other lipid-binding activities, both Osh4p and Osh6p bind PI4P and both activate Sac1p PI4P dephosphorylation. Based on this overlap in Osh protein functions, I tested if Sac1p and PI4P dysregulation are connected to ∆-s-tether defects by deleting *SAC1* in ∆-s-tether cells. Combining *sac1*∆ and ∆-s-tether mutations resulted in synthetic lethality, suggesting an integrated functional interaction between PI4P regulation, Osh proteins, and ER-PM tethers. It should be noted that sterols are carried within secretory vesicles

destined for the PM, but disrupting vesicular transport in *sec18-1*ts cells had no effect on sterol exchange between the ER and PM. Even if *sec18-1*ts and ∆-s-tether mutations were combined, no significant impact on sterol transport was detected. Overall these results indicated that ER-PM MCSs are in PI4P regulation, but they do not play a direct role in ER-to-PM sterol transport. However, other aspects of sterol trafficking are indirectly affected by ER-PM MCSs, and MCS formation is in turn regulated by sterol levels.

The non-vesicular transport of sterols between the ER and PM is a bi-directional equilibrium (133, 425). However, the PM has a higher concentration of sterols because sterol sequestration into sphingolipid-rich microdomains are not accessible for transport. Sterol-sphingolipid membrane domains within the PM represent a static pool of sterols, separable from the free sterol pool that can exchange with the ER. Nonetheless, the lack of ER-PM contact sites in ∆-s-tether cells slowed the retrograde trafficking exogenously supplied sterols from the PM back to the ER (29). The transport lag in ∆-s-tether cells seemed to be linked to lower rates of sterol equilibration between the inner and outer leaflet of the PM. This disruption in uptake and flipping sterols to the inner leaflet of the PM appears to limit subsequent equilibration steps for an intracellular PM to ER transfer. In ∆-s-tether cells, the rate of PM transbilayer sterol equilibration was ~5-fold slower than wild-type cells, which correlated with changes in PM bilayer organization. Indeed, the indirect effects on retrograde sterol transfer point to a direct consequence of eliminating MCSs on the composition of PM phospholipids.

Significant changes in PM-enriched phospholipids are apparent in ∆-s-tether cells, which would account for the observed organizational changes in the PM bilayer (29). Specifically, PS, PE, and the sphingolipid precursors inositol-phosphoceramide (IPC) and mannosyl-IPC (MIPC) were reduced whereas diacylglycerol (DAG) levels increased. These lipid changes and their effects on the PM are also consistent with the growth defect of ∆-s-tether cells on media lacking choline (a precursor of PC synthesis), the sensitivity of ∆-s-tether cells to the PM ergosterol-binding inhibitor nystatin, their resistance to the sphingolipid biosynthesis inhibitor myriocin, and their sensitivity to the cytotoxic PE analog edelfosine. Taken together these findings indicate that ER-PM MCSs are important interfaces to regulate ER lipid metabolism and PM bilayer organization, which in turn has indirect effects on non-vesicular sterol transport from the PM.

Despite the limited role ER-PM MCSs play in sterol trafficking, ER-PM tethering responds to sterol levels and thereby sterols regulate the extent of ER-PM association. Depletion of cellular sterols induces Tcb3p expression by almost 6-fold, resulting in a nearly absolute association of the PM inner surface with cortical ER (29). The increase of Tcb3p levels involves a post-transcriptional mechanism, suggesting an interesting possibility. The structural changes within the PM bilayer caused by sterol depletion might bolster PM contact by Tcb3p. In turn, the extended conformation of Tcb3p reaching across from the ER to the PM might enhance Tcb3p stability. Of course, I can not exclude an alternative model by which sterol depletion induces a secondary tether that in turn augments ER-PM contact. Nonetheless, the reciprocal dependence of tethers and membrane lipids underscores the role of ER-PM MCSs as membrane junctions not only for lipid exchange but for interfaces to coordinate membrane synthesis.

In addition to testing the physiological roles of PM-ER MCSs, I aimed to better define the regulators of MCSs. While these primary tethering proteins establish initial membrane contact, still other proteins might maintain membrane association at contact sites. For example, secondary tethering proteins or ancillary regulators might fortify or expand the association of membrane around the established contact sites. Such secondary tethering proteins and regulators would be predicted to be sufficient for promoting membrane contact, but not necessary. In other words, they would be dispensable for establishing contact but might enhance PM–ER membrane association if overexpressed. Membrane association conferred by these secondary tethering proteins and regulators may also be dependent on the primary tethering proteins. In this context, I examine both PM–ER membrane-tethering proteins and potential ancillary factors,

As proof of concept, I tested the ability of the ER-resident Yeast Start Homolog, Ysp2p, and the PA phosphatase Pah1p to suppress membrane association and growth defects in ∆-s-tether cells. Overexpression of *PAH1* was capable of suppressing growth and membrane association defects suggesting that it may be a secondary tether by an unknown mechanism. This suppression was not linked to the catalytic activity of Pah1p. Conversely, overexpression of *YSP2* was not able to suppress growth defects and had modest effects on cortical ER membrane association, suggesting that it may not be a secondary tether. However, observations that Ysp2p associates with cortical ER tips and junction suggest that it may play a role in regulating pre-existing PM-ER MCSs.

5.1. Is PI4P a regulator of PM-ER MCS formation, maintenance, and function?

The tethering proteins Tcb1p, Tcb2p, Tcb3p, and Ist2p bind to PI(4,5)P_2 in the PM to form a protein bridge between the PM and ER (**Fig 4.1**) (163). The affinity for PI(4,5)P_2 is shared by mammalian E-Syt tethering proteins (104), including the ER-localized STIM1 and STIM2 tethering proteins that regulate store-operated Ca^{2+} channels in the PM (162). Thus, the localization and activity of phosphoinositide kinases and phosphatases at PM–ER MCSs are likely to be ubiquitous regulators of tether protein recruitment.

Of all the defined primary tethering proteins, the elimination of the VAP ortholog Scs2p causes the greatest reduction in PM–ER membrane contact sites (16, 125). Scs2p may be of importance because of its direct interactions and recruitment of other tethering proteins, interactions with several lipid regulatory proteins, and physical interactions with several phosphoinositide species (16, 42, 102, 125, 130, 139, 312). Scs2p binds Sac1p, which in turn interacts with and is activated by specific yeast ORPs (139). Some of these ORPs also interact with Scs2p and bind PI(4,5)P_2 and/or PI4P (**Fig 4.1**) (133, 140, 193, 553). In addition, Tcb1p–3p and Ist2p tethering to PI(4,5)P_2 in the PM might be controlled by phosphoinositide regulation, similar to the E-Syts (554). In this regard, there is conflicting evidence that reductions in PI4P by Sac1p affect the PI(4,5)P_2 levels in such a way as to affect LTP and tethering protein binding to the PM (42, 301, 555). However, if PI(4,5)P_2 levels decrease at contact sites because of increased PI4P turnover by Sac1p, then Sac1p be a negative regulator of PM–tethering. Recent evidence has shown that mammalian cells overexpressing *SAC1* cause reductions in both PI4P and PI(4,5)P_2 at the PM (160). If Sac1 is a negative regulator of PM-ER MCS, then an experimental prediction cells lacking *SAC1* would have more PM–ER membrane association and less when *SAC1* is overexpressed. Recently, it has been shown that PI(4 5)P_2 is required for PM-ER MCS localization of Sac1p through interactions with E-Syt2 (160). Therefore, PI(4,5)P_2 may positively regulates PM-ER MCSs by increasing tether protein PM binding and negatively regulatie PM-ER MCSs by indirectly recruiting Sac1p and ultimately lowering PM PI(4,5)P_2 levels.

Inverse to Sac1p, PM PI4P pools are regulated by the PI4P kinase Stt4p. As previously discussed, Stt4p PM localization and kinase activity are regulated by the

conserved Efr3p, Ypp1p, and Sfk1p (198, 342–344). Both Stt4p and Sfk1p are cortically localized but it is unknown they co-localize with PM-ER MCSs (198, 343). It has been shown that Stt4p physically interacts with Scs2p, potentially through an unconventional FFAT motif (342, 556). Additionally, the main activator of Stt4p, Sfk1p, physically interacts with Tcb3p (557). This suggests that the regulation and activation of Stt4p may be linked to cortical localization with PM-ER MCSs.

Stt4p PM-ER MCSs localization and activation could be facilitating several functions: i) regulation of PM PS counter transport by counteracting the ER-PI4P sink, or ii) locally increasing PI4P and PI(4,5)P_2 concentrations to increase PM-ER membrane association; neither function is mutually exclusive. Cells lacking *STT4, SFK1, EFR3,* or *YPP1,* have decreased PI4P and PI(4,5)P_2 levels, demonstrating that Stt4p directly regulates PI4P and indirectly regulates PI(4,5)P_2 (198, 343). Therefore, Stt4p recruitment could be used to counteract the negating regulation of Sac1p. In this model Stt4p is operate as the gas pedal and Sac1p working as the break. Therefore, one would predict that *stt4* mutant cells would have less PM-ER MCSs and cells overexpressing *STT4* would have more. Considering the strict regulation of Stt4p, *SFK1* may also be required to facilitate full Stt4p activaiton. If these effects are caused by indirect regulation of PI(4,5)P_2, then the PM-ER MCS increased should be suppressed by also mutating *MSS4.* These experiments provide a model where PIP regulation dynamically balances PM-ER membrane association.

5.2. Lipid dynamics, membrane curvature, and composition regulate PM-ER MCSs

Based on proteomic interactions one can weave an “interactome” between these tethering proteins that might represent a single complex, but it seems more likely that there are several tethering complexes perhaps with subunit exchange between them (16, 147, 557, 558). As reviewed elsewhere, most identified tether proteins are conserved in mammalian cells and relatively well understood (541). Perhaps less understood, however, are the contributing mechanisms that facilitate the priming and propagation of PM-ER membrane association by tethering proteins. In terms of regulatory proteins, and membrane structure and composition, what is required to nucleate tether assembly at presumptive membrane contact sites? Do tethers require modulations in organelle morphology and bilayer curvature to bring membranes close

enough for initiating membrane capture? Following the establishment of membrane contact, what lipids and proteins affect the spread of membrane apposition around contacts sites, and what governs contact stability? If these contributing mechanisms are significant, I predict that yeast cells lacking known tether proteins might be hypersensitive to additional mutational defects in such ancillary lipid and protein regulators.

In addition to promoting lipid extraction from the bilayer by LTPs, membrane curvature and bilayer distortion can affect the plasticity of interacting membranes to bend them for closer apposition (559). Unlike the ER, the PM is inherently inflexible due to its relative enrichment in PC and PS, which preferentially form flat bilayers, and cholesterol, which fortifies lipid packing (560–562). In contrast, ER membrane structure is more malleable and ductile reflecting a lipid composition and organization that is more pliant for shaping (6, 88, 563). These divergent properties of the ER and PM suggest that different mechanisms operate to deform and bring these membranes in juxtaposition for tethers to establish contact (559). In addition to the physical effects of lipid composition and bilayer asymmetry on membrane architecture, a greater impact on membrane architecture seems to be conferred by protein regulators recruited to those membranes.

In yeast, the induction of membrane curvature in the ER is largely due to the action of the reticulons Rtn1p and Rtn2p, and the reticulon-like protein Yop1p (12, 564). These proteins insert wedge-like amphipathic helices into the cytosolic face of the ER membrane and thereby generate positive curvature (565). The yeast atlastin homolog Sey1p is a dynamin-like GTPase that also contributes to ER reticulation and membrane remodeling by facilitating ER-ER homotypic-membrane fusion (566, 567). Rtn1p/2p, Yop1p, and Sey1p are all cortically localized and their combined disruption causes increased cortical ER and the creation of a sheet of ER over the internal face of the PM, instead of the normal tubular lattice (10, 12, 564, 566, 567). The presence of Sey1p is also required for nuclear ER association during yeast mating because its ER remodeling activity is required to allow nuclear membranes to come close enough for tethering. (568) The reticulon genes *YOP1* and *SEY1* also genetically interact with genes encoding ERMES complex components, which reflects a role for reticulons in lipid exchange between the ER and mitochondria (95). Based on these findings, a reasonable prediction is that the reticulons together with Yop1p and Sey1p help shape the cortical ER along the PM so that tether proteins can then staple the membranes together (**Fig**

4.1). This model also predicts that ER-shaping by these proteins might play a role in the frequency and stability of PM-ER membrane contact. Consistent with this notion, Rtn1p/2p and Sey1p physically interact with Scs2p, a key tether protein (16). This interaction might represent a mechanism by which Scs2p recruits ER-remodeling regulators to expand or stabilize the zone of cortical ER association with the PM beyond the point of contact.

Given the comparative rigidity of the PM, gross changes in membrane architecture are less likely to play a significant role in its association with other organelles. Instead, PM interactions with other membranes appear to be governed by lipid domains within the lateral section of the bilayer, and the active control of bilayer asymmetry. Unlike in the ER membrane that contains small amounts of PS found mainly within the luminal bilayer leaflet (569, 570), in the PM PS is highly enriched and exclusively resides in the cytoplasmic face of its bilayer (560, 563), At the PM, PS promotes the recruitment of proteins through both specific (*e.g.* with discoidin-type C2 domains) and low-affinity interactions (*e.g.* lipidated polybasic proteins) (571). Likewise, another charged phospholipid, $PI(4,5)P_2$, is also enriched in the PM exclusively in the cytoplasmic bilayer leaflet (572, 573). This anionic charge density makes the PM a unique target for protein regulators, not least of which are tether proteins themselves.

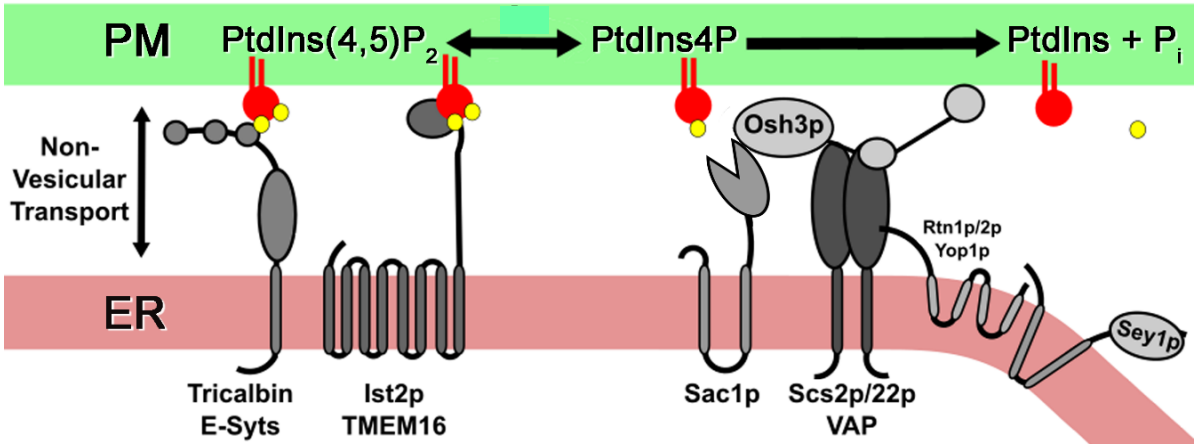

Figure 5.1. Tethers, membrane and lipid regulators of PM-ER membrane contact sites.

Regulation of $PI(4,5)P_2$ in the PM (green) is required to recruit tricalbins/E-Syts and Ist2p/TMEM16 tether proteins, which are anchored in the ER membrane (coral colored) and make contact with the PM. The $PI(4,5)P_2$ precursor PtdIns4P is dephosphorylated in the PM *in trans* by the ER-resident PtdIns4P phosphatase Sac1p. In yeast, Sac1p activity is regulated by its interactions with ORP homologs such as Osh3p, and the VAP homologs Scs2p/Scs22p. Scs2p is itself a tethering protein that interacts with other tethers, several ORPs, lipid regulators, and ER

membrane remodeling proteins. The reticulons Rtn1p and Rtn2p, the reticulon-like protein Yop1p, and the dynamin-like GTPase Sey1p are membrane-remodeling proteins that induce ER membrane plasticity, and potentially affect the juxtapositioning of the ER near the PM.

5.3. Are ORPs soluble lipid transfer proteins or lipid binding regulatory proteins?

As previously mentioned the yeast *OSHs* have a shared common essential function (192); however, what this essential function remains to be seen. The ORPs could be soluble lipid transfer proteins; lipid binding regulatory proteins; primary membrane tether adapters; lipid biosynthesis regulators; vesicular transport regulatory proteins; or all the above. What is clear, is that many of ORPs are mediating function at MCSs in yeast and mammals. In yeast, Osh1p-3p contain FFAT motifs and PH domains that localize them to specific membranes in an Scs2p-dependent manner (42, 43). The other Osh proteins (Osh4p-7p) also appear to be recruited to MCSs through a Scs2p-independent mechanism (62, 131, 191). In humans, 8 of the 12 ORPs have FFAT motifs while 11 of 12 ORPs contain PH domains (**Table S5**) (452). The PM-ER/ER mitochondria MCS resident ORP5 and ORP8 do not have FFAT motifs but do have transmembrane domains embedding them in the ER (137, 456, 574). Additionally, nearly all the human ORPs have been shown to co-localize to some species of MCSs (**Table S5**) (452).

It has been hypothesized that ORPs are LTPs, which seems to be the case for some (136, 195, 199), but the collective role ORPs play in non-vesicular lipid transfer remains to be solidified. The model depicting Osh4p as a sterol/PI4P co-transport is far from being proven *in vivo* (61, 62, 425). First, cells lacking *OSH4,* or all seven *OSHs,* have no sterol transfer defects (184). Seconds, Osh4p purified from the cytosol contains ergosterol in a 1:1 molar ratio with no evidence of a PI4P bound state, which would be predicted in a counter transport model (194). Third, a mutation blocking Osh4p sterol binding ($OSH4^{Y97F}$) causes hyperactivation, not depression (131). Fourth, cells lacking *SAC1* show PM PI4P accumulation which suggest a *trans* activity model (139). These pieces of evidence do not close the door on Osh4p being a soluble sterol LTP, however, they do beg for further experimentation.

Another function may be to regulate the PM lipid composition and organization. For example, the Osh proteins are dispensable for PM-ER intermembrane sterol

exchange, but cells lacking all OSHs show grossly altered PM sterol organization (184). There are two asymmetrically concentrated interchangeable pools of ergosterol within the PM. The MβCD extractable pool of ergosterol represent free ergosterol on the extracellular leaflet of the PM. The MβCD unextractable pool represent chemically inaccessible complexed ergosterol and ergosterol on the cytoplasmic leaflet of the PM (425). In the absence of yeast the *OSHs*, the MβCD extractable pool increases by 25-fold (184). This shift reflects a substantive change either in lateral domain organization in the PM sterol-sphingolipid-glycerophospholipid organization (i.e. lipid rafts) or in bilayer asymmetry causing an increase in sterols in the extracellular leaflet. This mirrors phenotypes observed in Δ-s-tether cells. A possible function of ORPs may be to regulate the PM lipid composition and organization and lipidomic analysis of cells lacking *OSH*s will provide insight into global lipid changes. One would predict that some of the changes may mirror phospholipid and sphingolipid defects observed in Δ-s-tether cells.

Another finding suggesting that *OSHs* regulate transbilayer asymmetry involves the antagonistic interaction between Osh4p and the P4-ATPase lipid flippase Drs2p (575). Drs2p flipping in the Golgi creates a PS and PE bilayer asymmetry that is preserved in post-Golgi vesicles destined to fuse with the PM (230, 576–578). Drs2p in the Golgi thereby contributes to lipid asymmetry in the PM. Apart from Osh4p, it is unclear if other yeast ORPs affect transbilayer asymmetry or if this function impacts membrane contact sites. However, it is noteworthy that Drs2p, despite its localization to the trans-Golgi, physically interacts with both Sac1p and the PM-ER tether protein Tcb3p (579). The Stt4p regulator Sfk1p may also act as a flippase and may affect membrane stability, permeability, and PM-ER membrane association (580). These findings hint at the possibility that PM–ER contact sites bring together LTPs, phosphoinositide regulators, and possibly transbilayer asymmetry regulators.

In addition to their lipid binding properties, it has been proposed that ORPs may act as membrane tether proteins themselves. Because of their ability to directly bind membranes and VAP proteins, it has been hypothesized that ORPs may act as adapters proteins to VAPs. This theory has yet to be directly tested. If this were the case, then one would predict that cells lacking all FFAT containing *OSHs* (osh1Δ osh2Δ osh3Δ), would have similar cortical ER association defects to scs2Δ scs22Δ mutant cells. It is possible that Osh proteins may work redundantly with other FFAT containing proteins, therefore only elimination of all FFAT adapter proteins would phenocopy VAP depletion.

Considering how many of the ORPs in humans and yeast co-localize with MCSs, it is very likely that ORPs play a role in the regulation of MCSs. The role ORPs play in PIP regulation suggest that they may also regulate MCS nucleation, expansion and stabilization. This highlighted by the fact that yeast cells lacking all *OSH* have similarly sterol, and PI4P defects observed in ∆−s-tether cells (29, 131, 184). Additionally, Osh proteins play a large role in the regulation of complex sphingolipids and LCB synthesis (29, 396, 404). However, it is unknown if these defects are caused by dysfunctional ORPs in ∆−s-tether cells or dysfunctional MCSs in *osh*∆ cells, neither of which are mutually exclusive. Considering the disease implications of both VAPs and ORPs, the functional relationship between ORPs and MCSs deserves further investigation.

5.4. ER-mediated MCSs across the cell orchestrate cell homeostasis

Many of the ORPs localize to several different cellular compartments depending on growth conditions (**Table S5 and S6**). Additionally, many of the ORPs have more than one lipid ligand, suggesting that they could work as Lipid counter-transporters or lipid sensing proteins. Considering again that Osh4p is extracted at a 1:1 molar ratio with ergosterol from the cytoplasm and abolishing sterol binding causes hyperactivation (131, 425), it seem unlikely that Osh4p is a LTP *in vivo*. Instead, Osh4p could be a sterol-sensing protein. When ergosterol levels drop below a certain level, ergosterol may be displaced from Osh4p and replaced with PI4P leading to activation. However, what activity Osh4p is performing remains a mystery.

OSH4 is functionally redundant with PM-ER MCSs suggesting that it is working in a compensatory or parallel pathway (29). This pathway could be the regulation of other MCSs or their activities. Considering Osh4p localizes to the Golgi, Osh4 may be working at ER-Golgi MCSs (131). Similarly, *SAC1* is also functionally redundant with PM-ER MCSs suggesting that it is working in a parallel pathway (29). Sac1p is predominately present in the ER but it has been suggested that it transiently localizes to the Golgi (465). *OSH4* is a known regulator of *SAC1* and cells lacking *sac1* can suppress Osh4^{Y97F} gain of function lethality (131). However, the inability of soluble *SAC1*$^{1-522}$ to suppress *osh4*∆ ∆−s-tether synthetic lethality suggests either that *OSH4* and *SAC1* are not working in the same pathway or *SAC1* epistatically precedes *OSH4* (29). If *SAC1*

epistatically precedes *OSH4*, then overexpression of *OSH4* would be predicted to suppress *sac1*Δ Δ–s-tether synthetic lethality. Alternatively, it is possible that a soluble *SAC1*$^{1-522}$ may not have enough membrane specific catalytic activity to suppress synthetic lethality. Therefore, *SAC1* may need to be tethered to either the PM or Golgi to suppress *osh4*Δ Δ–s-tether synthetic lethality.

Suppression of *osh4*Δ Δ–s-tether synthetic lethality by PM tethered *SAC1*$^{1-522}$ would be functionally distinct from Golgi tethered *SAC1*$^{1-522}$. PM tethered *SAC1*$^{1-522}$ suppression would strongly suggest that PM PI4P misregulation may be the cause of *osh4*Δ Δ–s-tether synthetic lethality. Considering that Δ–s-tether cells have morphological and polarization defects (29), lack of PM-ER MCSs and *OSH4* could result in misregulated vesicular trafficking, endocytosis, or cell signaling pathways, all of which are dependent on PI4P (131, 338, 529).

Golgi tethered *SAC1*$^{1-522}$ suppression may imply that vesicular transport, PI regulation, or sphingolipid biosynthesis may be the cause of *osh4*Δ Δ–s-tether synthetic lethality. Complex sphingolipids are essential and deletion or chemical inhibition of the IPC synthase *AUR1* is lethal in yeast (581, 582). Collectively it has been shown that *sac1*Δ, Δ–*s-tether*, and *osh*^{ts} cells all have significant reductions in complex sphingolipids (29, 396, 404). Complex sphingolipid defects in *sac1*Δ cells may cause decreased Golgi PI levels causing a decreased complex sphingolipid synthesis (404). Decreased complex sphingolipids in *osh*^{ts} cells may be caused by defective ER to Golgi ceramide transfer (396). The *OSHs* have also been shown to be regulators of the exocyst complex during post-Golgi vesicular trafficking which is also a PI4P dependent process (131, 339, 583). This would provide evidence that *OSHs* may functionally integrate PM-ER MCSs and ER-Golgi MCSs to regulate lipid homeostasis.

Sphingolipid defects in Δ-s-tether cells may give insight into a mechanism by which sterols regulate PM-ER MCSs. We showed that depletion of sterols resulted in increased PM-ER membrane association (29). Intuitively, if PM-ER MCSs play a role in sterol transport, PM-ER MCSs may be induced during sterol depletion to increase the flow of sterols to the PM from their source of *de novo* synthesis. PAMs are also enriched for sterol biosynthesis enzymes, such as Erg9p (103). Therefore, increased PM-ER MCS results in more ribosomal free ER at the PM-ER interface (10), and a potentially larger ergosterol biosynthesis platforms. This is supported by the fact that Sac1p and

Scs2p physically and genetically interact with several Erg proteins, including Erg9p (16). Drops in PM sterol levels have also been shown to stimulate sphingolipid biosynthesis and vice versa (377). Cells with various *ERG* mutants and do not produce ergosterol, have been shown to alter their lipidomic profile and increase complex sphingolipid biosynthesis (584). This may be a compensatory mechanism to maintain PM rigidity in the absence of sterols. Considering the significant change in free-sterol pools in Δ-s-tether cells, and the synergistic role sterols and sphingolipids have on one another, sterols may be sensing sphingolipid levels at the PM and *vice versa*. I propose that *OSH*s and *SAC1* act as a nexus to integrate sterols and sphingolipid levels by globally coordinating MCSs. Further experimental investigation must be performed to discern a plausible mechanistic model.

5.5. Conclusion

Membrane contact sites provide nucleating loci for the integrated regulation of several different lipid pathways. Lipid metabolic pathways, where the biosynthetic machinery is anchored on different organelles, necessitate lipid precursor exchange between different membranes at contact sites. Membrane contact sites are therefore centers for lipid biosynthesis, but also for lipid-dependent regulation of protein interactions and functions. At PM-ER membrane contact sites, PIPs appear to be the key regulators because of the dependence of LTPs and tethers on PtdIns4P and PI(4,5)P_2. As a result, I predict that phosphoinositide regulators like Sac1p might have a major impact on the establishment and propagation of PM-ER membrane association.

The response of Tcb3p expression to sterol depletion and the increase in ER-PM MCSs raises even more questions. Do changes in PM sterols affect Tcb3p levels directly, or does the post-transcriptional response on Tcb3p expression involve a pathway of sterol sensors and effectors? Does the response only impact Tcb3p and the other tricalbins or does the expression of other tethers also increase? Does Tcb3p expression respond specifically to sterols, or do other changes in lipid composition within the PM also elicit a response? Perhaps most interesting is the fact that ER-PM MCSs are not constitutive assemblies, but they undergo adaptive changes suggesting a dynamic mechanism for regulating ER-PM associations. Although ER defects in Δtether cells were shown to induce the “unfolded protein response” (4), cellular stresses might in turn impact tether expression and ER-PM MCS formation to change PM structure as a

protective mechanism. Indeed, the Arabidopsis tricalbin/E-Syt homolog SYT1 plays an important role in shielding plant cells from mechanical stresses (110). The genetic manipulations of yeast ER-PM tethers now pave the way to even a greater understanding of the mechanisms and roles of ER-PM MCSs during cell growth.

The creation of cells that lack ER-PM MCSs provides a new opportunity for testing the functional requirements for direct organelle membrane associations. These analyses have already resulted in some surprises, namely that ER-PM MCSs by themselves do not directly impact non-vesicular sterol trafficking. In general, the evidence I have presented here challenges a simplified mechanistic view of the roles played by LTPs and tether proteins. As opposed to being simple carriers involved in inter-membrane lipid transport, LTPs such as the yeast ORPs clearly affect the bilayer organization of their target membranes. These changes might facilitate lipid presentation at the membrane surface for capture and transfer by other LTPs, whether soluble or membrane-bound. Other potential LTPs like Lam6p have additional regulatory functions in controlling the extent of membrane association as secondary PM-ER membrane tethers (213). Even primary tether proteins are not just simple staples for adhering different membranes together.

Tether proteins such as Scs2p can serve as scaffolds for regulatory proteins, including membrane-anchored transcription factors and proteins that induce organelle shaping. Considering that nearly all ORPs in mammals and nearly half of the yeast *OSHs* have FFAT motifs, it is possible that this functional integration is mediated through VAPs. With that in consideration, ORPs are not the only FFAT containing proteins and the list of VAP binding proteins is ever-expanding (126). VAPs may provide a mechanism by which PIP regulation, lipid biosynthesis, lipid transport, lipid transcriptional regulation, and physical membrane association can all be integrated. Moving forward, the discovery and characterization of genes which integrate MCSs is essential to progressing our understanding of individual MCSs and MCSs as a functionally integrated network.

References

1. Westrate, L. M., Lee, J. E., Prinz, W. A., and Voeltz, G. K. (2015) Form Follows Function: The Importance of Endoplasmic Reticulum Shape. *Annu. Rev. Biochem.* **84**, 791–811

2. Rapoport, T. A. (2007) Protein translocation across the eukaryotic endoplasmic reticulum and bacterial plasma membranes. *Nature*. **450**, 663–669

3. Braakman, I., and Hebert, D. N. (2013) Protein Folding in the Endoplasmic Reticulum. *Cold Spring Harb. Perspect. Biol.* **5**, a013201–a013201

4. Fagone, P., and Jackowski, S. (2009) Membrane phospholipid synthesis and endoplasmic reticulum function. *J. Lipid Res.* **50**, S311–S316

5. Clapham, D. E. (2007) Calcium Signaling. *Cell*. **131**, 1047–1058

6. Voeltz, G. K., Rolls, M. M., and Rapoport, T. a. (2002) Structural organization of the endoplasmic reticulum. *EMBO Rep.* **3**, 944–950

7. Burke, B., and Ellenberg, J. (2002) Remodelling the walls of the nucleus. *Nat. Rev. Mol. Cell Biol.* **3**, 487–97

8. Hetzer, M. W., and Wente, S. R. (2009) Border control at the nucleus: biogenesis and organization of the nuclear membrane and pore complexes. *Dev. Cell*. **17**, 606–16

9. Bernales, S., McDonald, K. L., and Walter, P. (2006) Autophagy counterbalances endoplasmic reticulum expansion during the unfolded protein response. *PLoS Biol.* **4**, e423

10. West, M., Zurek, N., Hoenger, A., and Voeltz, G. K. (2011) A 3D analysis of yeast ER structure reveals how ER domains are organized by membrane curvature. *J. Cell Biol.* **193**, 333–346

11. Shibata, Y., Voeltz, G. K., and Rapoport, T. A. (2006) Rough Sheets and Smooth Tubules. *Cell*. **126**, 435–439

12. Voeltz, G. K., Prinz, W. A., Shibata, Y., Rist, J. M., and Rapoport, T. A. (2006) A class of membrane proteins shaping the tubular endoplasmic reticulum. *Cell*. **124**, 573–86

13. Shibata, Y., Shemesh, T., Prinz, W. A., Palazzo, A. F., Kozlov, M. M., and Rapoport, T. A. (2010) Mechanisms determining the morphology of the peripheral ER. *Cell*. **143**, 774–88

14. Prinz, W. A., Grzyb, L., Veenhuis, M., Kahana, J. A., Silver, P. A., and Rapoport,

T. A. (2000) Mutants affecting the structure of the cortical endoplasmic reticulum in Saccharomyces cerevisiae. *J. Cell Biol.* **150**, 461–474

15. Phillips, M. J., and Voeltz, G. K. (2016) Structure and function of ER membrane contact sites with other organelles. *Nat. Rev. Mol. Cell Biol.* **17**, 69–82

16. Manford, A. G., Stefan, C. J., Yuan, H. L., Macgurn, J. a, and Emr, S. D. (2012) ER-to-plasma membrane tethering proteins regulate cell signaling and ER morphology. *Dev. Cell*. **23**, 1129–40

17. Kornmann, B., Currie, E., Collins, S. R., Schuldiner, M., Nunnari, J., Weissman, J. S., and Walter, P. (2009) An ER-mitochondria tethering complex revealed by a synthetic biology screen. *Science*. **325**, 477–481

18. Lahiri, S., Chao, J. T., Tavassoli, S., Wong, A. K. O. O., Choudhary, V., Young, B. P., Loewen, C. J. R. R., and Prinz, W. a. (2014) A Conserved Endoplasmic Reticulum Membrane Protein Complex (EMC) Facilitates Phospholipid Transfer from the ER to Mitochondria. *PLoS Biol.* **12**, e1001969

19. Murley, A., Lackner, L. L., Osman, C., West, M., Voeltz, G. K., Walter, P., and Nunnari, J. (2013) ER-associated mitochondrial division links the distribution of mitochondria and mitochondrial DNA in yeast. *Elife*. **2013**, 1–16

20. Kurokawa, K., Okamoto, M., and Nakano, A. (2014) Contact of cis-Golgi with ER exit sites executes cargo capture and delivery from the ER. *Nat. Commun.* **5**, 3653

21. Pan, X., Roberts, P., Chen, Y., Kvam, E., Shulga, N., Huang, K., Lemmon, S., and Goldfarb, D. S. (2000) Nucleus-Vacuole Junctions in Saccharomyces cerevisiae Are Formed Through the Direct Interaction of Vac8p with Nvj1p. *Mol. Biol. Cell*. **11**, 2445–2457

22. Schuldiner, M., and Bohnert, M. (2017) A different kind of love – lipid droplet contact sites. *Biochim. Biophys. Acta - Mol. Cell Biol. Lipids*. **1862**, 1188–1196

23. Rocha, N., Kuijl, C., Van Der Kant, R., Janssen, L., Houben, D., Janssen, H., Zwart, W., and Neefjes, J. (2009) Cholesterol sensor ORP1L contacts the ER protein VAP to control Rab7-RILP-p150Gluedand late endosome positioning. *J. Cell Biol.* **185**, 1209–1225

24. Eden, E. R., White, I. J., Tsapara, A., and Futter, C. E. (2010) Membrane contacts between endosomes and ER provide sites for PTP1B-epidermal growth factor receptor interaction. *Nat. Cell Biol.* **12**, 267–272

25. Munck, J. M., Motley, A. M., Nuttall, J. M., and Hettema, E. H. (2009) A dual function for Pex3p in peroxisome formation and inheritance. *J. Cell Biol.* **187**, 463–471

26. Ungermann, C. (2015) vCLAMPs—an intimate link between vacuoles and mitochondria. *Curr. Opin. Cell Biol.* **35**, 30–36

27. Porter, K. R., and Palade, G. E. (1957) Studies on the endoplasmic reticulum. III. Its form and distribution in striated muscle cells. *J. Biophys. Biochem. Cytol.* **3**, 269–300

28. Henkart, M., Landis, D. M., and Reese, T. S. (1976) Similarity of junctions between plasma membranes and endoplasmic reticulum in muscle and neurons. *J. Cell Biol.* **70**, 338–347

29. Quon, E., Sere, Y. Y., Chauhan, N., Johansen, J., Sullivan, D. P., Dittman, J. S., Rice, W. J., Chan, R. B., di Paolo, G., Beh, C. T., and Menon, A. K. (2018) Endoplasmic reticulum-plasma membrane contact sites integrate sterol and phospholipid regulation. *PLOS Biol.* **16**, e2003864

30. Quon, E., and Beh, C. T. (2015) Membrane Contact Sites: Complex Zones for Membrane Association and Lipid Exchange. *Lipid Insights*. **8s1**, LPI.S37190

31. Li, S. C., and Kane, P. M. (2009) The yeast lysosome-like vacuole: endpoint and crossroads. *Biochim. Biophys. Acta*. **1793**, 650–63

32. Levine, T. P., and Munro, S. (2001) Dual Targeting of Osh1p, a Yeast Homologue of Oxysterol-binding Protein, to both the Golgi and the Nucleus-Vacuole Junction. *Mol. Biol. Cell*. **12**, 1633–1644

33. Roberts, P., Moshitch-Moshkovitz, S., Kvam, E., O'Toole, E., Winey, M., and Goldfarb, D. S. (2003) Piecemeal microautophagy of nucleus in Saccharomyces cerevisiae. *Mol. Biol. Cell*. **14**, 129–41

34. Kvam, E., and Goldfarb, D. S. (2007) Nucleus-vacuole junctions and piecemeal microautophagy of the nucleus in S. cerevisiae. *Autophagy*. **3**, 85–92

35. Hariri, H., Rogers, S., Ugrankar, R., Liu, Y. L., Feathers, J. R., and Henne, W. M. (2017) Lipid droplet biogenesis is spatially coordinated at ER–vacuole contacts under nutritional stress. *EMBO Rep.* **19**, e201744815

36. Kvam, E., and Goldfarb, D. S. (2004) Nvj1p is the outer-nuclear-membrane receptor for oxysterol-binding protein homolog Osh1p in Saccharomyces cerevisiae. *J. Cell Sci.* **117**, 4959–4968

37. Kvam, E., and Goldfarb, D. S. (2006) Structure and function of nucleus-vacuole junctions: outer-nuclear-membrane targeting of Nvj1p and a role in tryptophan uptake. *J. Cell Sci.* **119**, 3622–3633

38. Toulmay, A., and Prinz, W. a. (2012) A conserved membrane-binding domain targets proteins to organelle contact sites. *J. Cell Sci.* **125**, 49–58

39. Jeong, H., Park, J., Kim, H.-I., Lee, M., Ko, Y.-J., Lee, S., Jun, Y., and Lee, C. (2017) Mechanistic insight into the nucleus–vacuole junction based on the Vac8p–Nvj1p crystal structure. *Proc. Natl. Acad. Sci.* **114**, E4539–E4548

40. Kohlwein, S. D., Eder, S., Oh, C.-S., Martin, C. E., Gable, K., Bacikova, D., and Dunn, T. (2001) Tsc13p Is Required for Fatty Acid Elongation and Localizes to a Novel Structure at the Nuclear-Vacuolar Interface inSaccharomyces cerevisiae. *Mol. Cell. Biol.* **21**, 109–125

41. Kvam, E. (2005) Targeting of Tsc13p to Nucleus-Vacuole Junctions: A Role for Very-Long-Chain Fatty Acids in the Biogenesis of Microautophagic Vesicles. *Mol. Biol. Cell*. **16**, 3987–3998

42. Loewen, C. J. R., Roy, A., and Levine, T. P. (2003) A conserved ER targeting motif in three families of lipid binding proteins and in Opi1p binds VAP. *EMBO J.* **22**, 2025–2035

43. Weber-Boyvat, M., Kentala, H., Peränen, J., and Olkkonen, V. M. (2015) Ligand-dependent localization and function of ORP-VAP complexes at membrane contact sites. *Cell. Mol. Life Sci.* **72**, 1967–1987

44. Henne, W. M., Zhu, L., Balogi, Z., Stefan, C., Pleiss, J. A., and Emr, S. D. (2015) Mdm1/Snx13 is a novel ER-endolysosomal interorganelle tethering protein. *J. Cell Biol.* **210**, 541–551

45. Bryant, D., Liu, Y., Datta, S., Hariri, H., Seda, M., Anderson, G., Peskett, E., Demetriou, C., Sousa, S., Jenkins, D., Clayton, P., Bitner-Glindzicz, M., Moore, G. E., Henne, W. M., and Stanier, P. (2018) SNX14 mutations affect endoplasmic reticulum-associated neutral lipid metabolism in autosomal recessive spinocerebellar ataxia 20. *Hum. Mol. Genet.* **27**, 1927–1940

46. Kaksonen, M., and Roux, A. (2018) Mechanisms of clathrin-mediated endocytosis. *Nat. Rev. Mol. Cell Biol.* **19**, 313–326

47. Balderhaar, H. kleine, and Ungermann, C. (2013) CORVET and HOPS tethering complexes–coordinators of endosome and lysosome fusion. *J. Cell Sci.* **126**, 1307–1316

48. Friedman, J. R., Webster, B. M., Mastronarde, D. N., Verhey, K. J., and Voeltz, G. K. (2010) ER sliding dynamics and ER-mitochondrial contacts occur on acetylated microtubules. *J. Cell Biol.* **190**, 363–375

49. Raiborg, C., Wenzel, E. M., Pedersen, N. M., Olsvik, H., Schink, K. O., Schultz, S. W., Vietri, M., Nisi, V., Bucci, C., Brech, A., Johansen, T., and Stenmark, H. (2015) Repeated ER-endosome contacts promote endosome translocation and neurite outgrowth. *Nature*. **520**, 234–238

50. Friedman, J. R., DiBenedetto, J. R., West, M., Rowland, A. A., and Voeltz, G. K. (2013) Endoplasmic reticulum-endosome contact increases as endosomes traffic

and mature. *Mol. Biol. Cell*. **24**, 1030–1040

51. Rowland, A. A., Chitwood, P. J., Phillips, M. J., and Voeltz, G. K. (2014) ER contact sites define the position and timing of endosome fission. *Cell*. **159**, 1027–1041

52. Dong, R., Saheki, Y., Swarup, S., Lucast, L., Harper, J. W., De Camilli, P., and De Camilli, P. (2016) Endosome-ER Contacts Control Actin Nucleation and Retromer Function through VAP-Dependent Regulation of PI4P. *Cell*. **166**, 408–423

53. Alpy, F., Rousseau, A., Schwab, Y., Legueux, F., Stoll, I., Wendling, C., Spiegelhalter, C., Kessler, P., Mathelin, C., Rio, M.-C., Levine, T. P., and Tomasetto, C. (2013) STARD3 or STARD3NL and VAP form a novel molecular tether between late endosomes and the ER. *J. Cell Sci.* **126**, 5500–5512

54. Day, K. J., Staehelin, L. A., and Glick, B. S. (2013) A three-stage model of Golgi structure and function. *Histochem. Cell Biol.* **140**, 239–49

55. Papanikou, E., and Glick, B. S. (2009) The yeast Golgi apparatus: insights and mysteries. *FEBS Lett.* **583**, 3746–51

56. Wooding, S., and Pelham, H. R. (1998) The dynamics of golgi protein traffic visualized in living yeast cells. *Mol. Biol. Cell*. **9**, 2667–80

57. Funato, K., and Riezman, H. (2001) Vesicular and nonvesicular transport of ceramide from ER to the Golgi apparatus in yeast. *J. Cell Biol.* **155**, 949–59

58. Kannan, M., Riekhof, W. R., and Voelker, D. R. (2015) *Transport of Phosphatidylserine from the Endoplasmic Reticulum to the Site of Phosphatidylserine Decarboxylase2 in Yeast*, Wiley/Blackwell (10.1111), **16**, 123–134

59. De Matteis, M. A., and Rega, L. R. (2015) Endoplasmic reticulum-Golgi complex membrane contact sites. *Curr. Opin. Cell Biol.* **35**, 43–50

60. Hanada, K., Kumagai, K., Yasuda, S., Miura, Y., Kawano, M., Fukasawa, M., and Nishijima, M. (2003) Molecular machinery for non-vesicular trafficking of ceramide. *Nature*. **426**, 803–809

61. Mesmin, B., Bigay, J., Moser von Filseck, J., Lacas-Gervais, S., Drin, G., and Antonny, B. (2013) A Four-Step Cycle Driven by PI(4)P Hydrolysis Directs Sterol/PI(4)P Exchange by the ER-Golgi Tether OSBP. *Cell*. **155**, 830–843

62. Moser von Filseck, J., Vanni, S., Mesmin, B., Antonny, B., and Drin, G. (2015) A phosphatidylinositol-4-phosphate powered exchange mechanism to create a lipid gradient between membranes. *Nat. Commun.* **6**, 6671

63. Liu, L. K., Choudhary, V., Toulmay, A., and Prinz, W. A. (2017) An inducible ER-Golgi tether facilitates ceramide transport to alleviate lipotoxicity. *J. Cell Biol.* **216**, 131–147

64. Graef, M. (2018) Lipid droplet-mediated lipid and protein homeostasis in budding yeast. *FEBS Lett.* **592**, 1291–1303

65. Garbarino, J., Padamsee, M., Wilcox, L., Oelkers, P. M., D'Ambrosio, D., Ruggles, K. V., Ramsey, N., Jabado, O., Turkish, A., and Sturley, S. L. (2009) Sterol and diacylglycerol acyltransferase deficiency triggers fatty acid-mediated cell death. *J. Biol. Chem.* **284**, 30994–31005

66. Eisenberg, T., Büttner, S., and Buettner, S. (2014) Lipids and cell death in yeast. *FEMS Yeast Res.* **14**, 179–197

67. Choudhary, V., Ojha, N., Golden, A., and Prinz, W. A. (2015) A conserved family of proteins facilitates nascent lipid droplet budding from the ER. *J. Cell Biol.* **211**, 261–271

68. Jacquier, N., Choudhary, V., Mari, M., Toulmay, A., Reggiori, F., and Schneiter, R. (2011) Lipid droplets are functionally connected to the endoplasmic reticulum in Saccharomyces cerevisiae. *J. Cell Sci.* **124**, 2424–2437

69. Mishra, S., Khaddaj, R., Cottier, S., Stradalova, V., Jacob, C., and Schneiter, R. (2016) Mature lipid droplets are accessible to ER luminal proteins. *J. Cell Sci.* **129**, 3803–3815

70. Fei, W., Shui, G., Gaeta, B., Du, X., Kuerschner, L., Li, P., Brown, A. J., Wenk, M. R., Parton, R. G., and Yang, H. (2008) Fld1p, a functional homologue of human seipin, regulates the size of lipid droplets in yeast. *J. Cell Biol.* **180**, 473–82

71. Wang, C.-W., Miao, Y.-H., and Chang, Y.-S. (2014) Control of lipid droplet size in budding yeast requires the collaboration between Fld1 and Ldb16. *J. Cell Sci.* **127**, 1214–1228

72. Wang, H., Becuwe, M., Housden, B. E., Chitraju, C., Porras, A. J., Graham, M. M., Liu, X. N., Thiam, A. R., Savage, D. B., Agarwal, A. K., Garg, A., Olarte, M. J., Lin, Q., Frohlich, F., Hannibal-Bach, H. K., Upadhyayula, S., Perrimon, N., Kirchhausen, T., Ejsing, C. S., Walther, T. C., and Farese, R. V. (2016) Seipin is required for converting nascent to mature lipid droplets. *Elife*. **5**, 1–28

73. Salo, V. T., Belevich, I., Li, S., Karhinen, L., Vihinen, H., Vigouroux, C., Magré, J., Thiele, C., Hölttä-Vuori, M., Jokitalo, E., and Ikonen, E. (2016) Seipin regulates ER–lipid droplet contacts and cargo delivery. *EMBO J.* **35**, 2699–2716

74. Xu, N., Zhang, S. O., Cole, R. A., McKinney, S. A., Guo, F., Haas, J. T., Bobba, S., Farese, R. V., and Mak, H. Y. (2012) The FATP1-DGAT2 complex facilitates lipid droplet expansion at the ER-lipid droplet interface. *J. Cell Biol.* **198**, 895–911

75. Dimitrov, L., Lam, S. K., and Schekman, R. (2013) The role of the endoplasmic reticulum in peroxisome biogenesis. *Cold Spring Harb Perspect Biol*. **5**, a013243

76. Raychaudhuri, S., and Prinz, W. a (2008) Nonvesicular phospholipid transfer between peroxisomes and the endoplasmic reticulum. *Proc. Natl. Acad. Sci. U. S. A.* **105**, 15785–15790

77. David, C., Koch, J., Oeljeklaus, S., Laernsack, A., Melchior, S., Wiese, S., Schummer, A., Erdmann, R., Warscheid, B., and Brocard, C. (2013) A Combined Approach of Quantitative Interaction Proteomics and Live-cell Imaging Reveals a Regulatory Role for Endoplasmic Reticulum (ER) Reticulon Homology Proteins in Peroxisome Biogenesis. *Mol. Cell. Proteomics*. **12**, 2408–2425

78. Knoblach, B., Sun, X., Coquelle, N., Fagarasanu, A., Poirier, R. L., and Rachubinski, R. A. (2013) An ER-peroxisome tether exerts peroxisome population control in yeast. *EMBO J.* **32**, 2439–2453

79. Shai, N., Schuldiner, M., and Zalckvar, E. (2016) No peroxisome is an island - Peroxisome contact sites. *Biochim. Biophys. Acta - Mol. Cell Res.* **1863**, 1061–1069

80. Wang, S., Idrissi, F.-Z., Hermansson, M., Grippa, A., Ejsing, C. S., and Carvalho, P. (2018) Seipin and the membrane-shaping protein Pex30 cooperate in organelle budding from the endoplasmic reticulum. *Nat. Commun.* **9**, 2939

81. Hua, R., Cheng, D., Coyaud, É., Freeman, S., Di Pietro, E., Wang, Y., Vissa, A., Yip, C. M., Fairn, G. D., Braverman, N., Brumell, J. H., Trimble, W. S., Raught, B., and Kim, P. K. (2017) VAPs and ACBD5 tether peroxisomes to the ER for peroxisome maintenance and lipid homeostasis. *J. Cell Biol.* **216**, 367–377

82. Costello, J. L., Castro, I. G., Hacker, C., Schrader, T. A., Metz, J., Zeuschner, D., Azadi, A. S., Godinho, L. F., Costina, V., Findeisen, P., Manner, A., Islinger, M., and Schrader, M. (2017) ACBD5 and VAPB mediate membrane associations between peroxisomes and the ER. *J. Cell Biol.* **216**, 331–342

83. BERNHARD, W., HAGUENAU, F., GAUTIER, A., and OBERLING, C. (1952) [Submicroscopical structure of cytoplasmic basophils in the liver, pancreas and salivary gland; study of ultrafine slices by electron microscope]. *Z. Zellforsch. Mikrosk. Anat.* **37**, 281–300

84. BERNHARD, W., and ROUILLER, C. (1956) Close topographical relationship between mitochondria and ergastoplasm of liver cells in a definite phase of cellular activity. *J. Biophys. Biochem. Cytol.* **2**, 73–8

85. BERNHARD, W., and ROUILLER, C. (1956) Microbodies and the problem of mitochondrial regeneration in liver cells. *J. Biophys. Biochem. Cytol.* **2**, 355–60

86. Vance, J. E. (1990) Phospholipid synthesis in a membrane fraction associated with mitochondria . Phospholipid Mitochondria * Synthesis in a Membrane

Fraction Associated. *J. Biol. Chem.* **265**, 7248–7256

87. Rusiñol, A. E., Cui, Z., Chen, M. H., and Vance, J. E. (1994) A unique mitochondria-associated membrane fraction from rat liver has a high capacity for lipid synthesis and contains pre-Golgi secretory proteins including nascent lipoproteins. *J. Biol. Chem.* **269**, 27494–27502

88. Flis, V. V, and Daum, G. (2013) Lipid Transport between the Endoplasmic Reticulum and Mitochondria. *Cold Spring Harb. Perspect. Biol.* **5**, 1–22

89. Horvath, S. E., and Daum, G. (2013) Lipids of mitochondria. *Prog. Lipid Res.* **52**, 590–614

90. Prinz, W. A. (2010) Lipid trafficking sans Vesicles: where, why, how? *Cell*. **143**, 870–874

91. Yamano, K., Tanaka-Yamano, S., and Endo, T. (2010) Mdm10 as a dynamic constituent of the TOB/SAM complex directs coordinated assembly of Tom40. *EMBO Rep.* **11**, 187–193

92. Böckler, S., and Westermann, B. (2014) Mitochondrial ER contacts are crucial for mitophagy in yeast. *Dev. Cell*. **28**, 450–458

93. Lang, A., John Peter, A. T., and Kornmann, B. (2015) ER–mitochondria contact sites in yeast: beyond the myths of ERMES. *Curr. Opin. Cell Biol.* **35**, 7–12

94. Kopec, K. O., Alva, V., and Lupas, A. N. (2010) Homology of SMP domains to the TULIP superfamily of lipid-binding proteins provides a structural basis for lipid exchange between ER and mitochondria. *Bioinformatics*. **26**, 1927–1931

95. Voss, C., Lahiri, S., Young, B. P., Loewen, C. J., and Prinz, W. a. (2012) ER-shaping proteins facilitate lipid exchange between the ER and mitochondria in S. cerevisiae. *J. Cell Sci.* 10.1242/jcs.105635

96. Nguyen, T. T., Lewandowska, A., Choi, J. Y., Markgraf, D. F., Junker, M., Bilgin, M., Ejsing, C. S., Voelker, D. R., Rapoport, T. A., and Shaw, J. M. (2012) Gem1 and ERMES Do Not Directly Affect Phosphatidylserine Transport from ER to Mitochondria or Mitochondrial Inheritance. *Traffic*. **13**, 880–890

97. Lackner, L. L., Ping, H., Graef, M., Murley, A., and Nunnari, J. (2013) Endoplasmic reticulum-associated mitochondria-cortex tether functions in the distribution and inheritance of mitochondria. *Proc. Natl. Acad. Sci.* **110**, E458–E467

98. Ping, H. A., Kraft, L. M., Chen, W. T., Nilles, A. E., and Lackner, L. L. (2016) Num1 anchors mitochondria to the plasma membrane via two domains with different lipid binding specificities. *J. Cell Biol.* **213**, 513–524

99. Schmit, H. L., Kraft, L. M., Lee-Smith, C. F., and Lackner, L. L. (2018) The role of mitochondria in anchoring dynein to the cell cortex extends beyond clustering the anchor protein. *Cell Cycle*. 10.1080/15384101.2018.1480226

100. Hammermeister, M., Schödel, K., and Westermann, B. (2010) Mdm36 is a mitochondrial fission-promoting protein in Saccharomyces cerevisiae. *Mol. Biol. Cell*. **21**, 2443–52

101. Kormanec, J., Schaaff-Gerstenschläger, I., Zimmermann, F. K., Perečko, D., and Küntzel, H. (1991) Nuclear migration in Saccharomyces cerevisiae is controlled by the highly repetitive 313 kDa NUM1 protein. *MGG Mol. Gen. Genet.* **230**, 277–787

102. Chao, J. T., Wong, A. K. O., Tavassoli, S., Young, B. P., Chruscicki, A., Fang, N. N., Howe, L. J., Mayor, T., Foster, L. J., and Loewen, C. J. R. (2014) Polarization of the endoplasmic reticulum by ER-septin tethering. *Cell*. **158**, 620–632

103. Pichler, H., Gaigg, B., Hrastnik, C., Achleitner, G., Kohlwein, S. D., Zellnig, G., Perktold, A., and Daum, G. (2001) A subfraction of the yeast endoplasmic reticulum associates with the plasma membrane and has a high capacity to synthesize lipids. *Eur. J. Biochem.* **268**, 2351–2361

104. Giordano, F., Saheki, Y., Idevall-Hagren, O., Colombo, S. F., Pirruccello, M., Milosevic, I., Gracheva, E. O., Bagriantsev, S. N., Borgese, N., and De Camilli, P. (2013) PI(4,5)P(2)-dependent and Ca(2+)-regulated ER-PM interactions mediated by the extended synaptotagmins. *Cell*. **153**, 1494–509

105. Helle, S. C. J., Kanfer, G., Kolar, K., Lang, A., Michel, A. H., and Kornmann, B. (2013) Organization and function of membrane contact sites. *Biochim. Biophys. Acta - Mol. Cell Res.* **1833**, 2526–2541

106. López-Crisosto, C., Bravo-Sagua, R., Rodriguez-Peña, M., Mera, C., Castro, P. F., Quest, A. F. G., Rothermel, B. A., Cifuentes, M., and Lavandero, S. (2015) ER-to-mitochondria miscommunication and metabolic diseases. *Biochim. Biophys. Acta*. **1852**, 2096–105

107. Schneggenburger, R., and Rosenmund, C. (2015) Molecular mechanisms governing Ca(2+) regulation of evoked and spontaneous release. *Nat. Neurosci.* **18**, 935–41

108. Korzeniowski, M. K., Popovic, M. a., Szentpetery, Z., Varnai, P., Stojilkovic, S. S., and Balla, T. (2009) Dependence of STIM1/Orai1-mediated calcium entry on plasma membrane phosphoinositides. *J. Biol. Chem.* **284**, 21027–21035

109. Anderie, I., Schulz, I., and Schmid, A. (2007) Direct interaction between ER membrane-bound PTP1B and its plasma membrane-anchored targets. *Cell. Signal.* **19**, 582–592

110. Feske, S., Gwack, Y., Prakriya, M., Srikanth, S., Puppel, S.-H., Tanasa, B., Hogan, P. G., Lewis, R. S., Daly, M., and Rao, A. (2006) A mutation in Orai1

causes immune deficiency by abrogating CRAC channel function. *Nature*. **441**, 179–185

111. Zhou, Y., Meraner, P., Kwon, H. T., Machnes, D., Oh-hora, M., Zimmer, J., Huang, Y., Stura, A., Rao, A., and Hogan, P. G. (2010) STIM1 gates the store-operated calcium channel ORAI1 in vitro. *Nat. Struct. Mol. Biol.* **17**, 112–116

112. Haj, F. G., Sabet, O., Kinkhabwala, A., Wimmer-Kleikamp, S., Roukos, V., Han, H. M., Grabenbauer, M., Bierbaum, M., Antony, C., Neel, B. G., and Bastiaens, P. I. (2012) Regulation of signaling at regions of cell-cell contact by endoplasmic reticulum-bound protein-tyrosine phosphatase 1B. *PLoS One*. **7**, e36633

113. Hogan, P. G., Lewis, R. S., and Rao, A. (2010) Molecular Basis of Calcium Signaling in Lymphocytes: STIM and ORAI. *Annu. Rev. Immunol.* **28**, 491–533

114. Lewis, R. S. (2007) The molecular choreography of a store-operated calcium channel. *Nature*. **446**, 284–287

115. Liou, J., Kim, M. L., Heo, W. Do, Jones, J. T., Myers, J. W., James, E., Jr, F., and Meyer, T. (2005) STIM Is a Ca2+ Sensor Essential for Ca2+-Store-Depletion Triggered Ca2+ Influx. *Curr. Biol.* **15**, 1235–1241

116. Luik, R. M., Wang, B., Prakriya, M., Wu, M. M., and Lewis, R. S. (2008) Oligomerization of STIM1 couples ER calcium depletion to CRAC channel activation. *Nature*. **454**, 538–542

117. Wu, M. M., Buchanan, J., Luik, R. M., and Lewis, R. S. (2006) Ca2+ store depletion causes STIM1 to accumulate in ER regions closely associated with the plasma membrane. *J. Cell Biol.* **174**, 803–813

118. Park, C. Y., Hoover, P. J., Mullins, F. M., Bachhawat, P., Covington, D., Raunser, S., Walz, T., Garcia, K. C., E, R., and Lewis, R. S. (2009) STIM1 Clusters and Activates CRAC Channels via Direct Binding of a Cytosolic Domain to Orai1. *Cell*. **136**, 876–890

119. Zhang, S. L., Yu, Y., Roos, J., Kozak, J. A., Deerinck, T. J., Ellisman, M. H., Stauderman, K. A., and Cahalan, M. D. (2005) STIM1 is a Ca2+ sensor that activates CRAC channels and migrates from the Ca2+ store to the plasma membrane. *Nature*. **437**, 902–905

120. Woo, J. S., Srikanth, S., Nishi, M., Ping, P., Takeshima, H., and Gwack, Y. (2016) Junctophilin-4, a component of the endoplasmic reticulum-plasma membrane junctions, regulates Ca2+ dynamics in T cells. *Proc. Natl. Acad. Sci. U. S. A.* **113**, 2762–7

121. Takeshima, H., Hoshijima, M., and Song, L. S. (2015) Ca2+ microdomains organized by junctophilins. *Cell Calcium*. **58**, 349–356

122. Takeshima, H., Komazaki, S., Nishi, M., Iino, M., and Kangawa, K. (2000) Junctophilins. *Mol. Cell*. **6**, 11–22

123. Beavers, D. L., Landstrom, A. P., Chiang, D. Y., and Wehrens, X. H. T. (2014) Emerging roles of junctophilin-2 in the heart and implications for cardiac diseases. *Cardiovasc. Res.* **103**, 198–205

124. Garbino, A., van Oort, R. J., Dixit, S. S., Landstrom, A. P., Ackerman, M. J., and Wehrens, X. H. T. (2009) Molecular evolution of the junctophilin gene family. *Physiol. Genomics*. **37**, 175–186

125. Loewen, C. J. R., Young, B. P., Tavassoli, S., and Levine, T. P. (2007) Inheritance of cortical ER in yeast is required for normal septin organization. *J. Cell Biol.* **179**, 467–483

126. Murphy, S. E., and Levine, T. P. (2016) VAP, a Versatile Access Point for the Endoplasmic Reticulum: Review and analysis of FFAT-like motifs in the VAPome. *Biochim. Biophys. Acta - Mol. Cell Biol. Lipids*. **1861**, 952–961

127. Schauder, C. M., Wu, X., Saheki, Y., Narayanaswamy, P., Torta, F., Wenk, M. R., De Camilli, P., and Reinisch, K. M. (2014) Structure of a lipid-bound extended synaptotagmin indicates a role in lipid transfer. *Nature*. **510**, 552–5

128. Kaiser, S. E., Brickner, J. H., Reilein, A. R., Fenn, T. D., Walter, P., and Brunger, A. T. (2005) Structural Basis of FFAT Motif-Mediated ER Targeting. *Structure*. **13**, 1035–1045

129. Loewen, C. J. R., and Levine, T. P. (2005) A highly conserved binding site in vesicle-associated membrane protein-associated protein (VAP) for the FFAT motif of lipid-binding proteins. *J. Biol. Chem.* **280**, 14097–14104

130. Kagiwada, S., and Hashimoto, M. (2007) The yeast VAP homolog Scs2p has a phosphoinositide-binding ability that is correlated with its activity. *Biochem. Biophys. Res. Commun.* **364**, 870–876

131. Alfaro, G., Johansen, J., Dighe, S. a, Duamel, G., Kozminski, K. G., and Beh, C. T. (2011) The sterol-binding protein Kes1/Osh4p is a regulator of polarized exocytosis. *Traffic*. **12**, 1521–36

132. de Saint-Jean, M., Delfosse, V., Douguet, D., Chicanne, G., Payrastre, B., Bourguet, W., Antonny, B., and Drin, G. (2011) Osh4p exchanges sterols for phosphatidylinositol 4-phosphate between lipid bilayers. *J. Cell Biol.* **195**, 965–978

133. Beh, C. T., McMaster, C. R., Kozminski, K. G., and Menon, A. K. (2012) A detour for yeast oxysterol binding proteins. *J. Biol. Chem.* **287**, 11481–8

134. Tong, J., Manik, M. K., Yang, H., and Im, Y. J. (2016) Structural insights into nonvesicular lipid transport by the oxysterol binding protein homologue family.

Biochim. Biophys. Acta - Mol. Cell Biol. Lipids. **1861**, 928–939

135. Kentala, H., Weber-Boyvat, M., and Olkkonen, V. M. (2016) OSBP-Related Protein Family: Mediators of Lipid Transport and Signaling at Membrane Contact Sites. in *International Review of Cell and Molecular Biology*, pp. 299–340, **321**, 299–340

136. Moser von Filseck, J., Opi, A., Delfosse, V., Vanni, S., Jackson, C. L., Bourguet, W., and Drin, G. (2015) Phosphatidylserine transport by ORP/Osh proteins is driven by phosphatidylinositol 4-phosphate. *Science (80-.).* **349**, 432–436

137. Chung, J., Torta, F., Masai, K., Lucast, L., Czapla, H., Tanner, L. B., Narayanaswamy, P., Wenk, M. R., Nakatsu, F., and De Camilli, P. (2015) PI4P/phosphatidylserine countertransport at ORP5- and ORP8-mediated ER-plasma membrane contacts. *Science (80-.).* **349**, 428–432

138. Roy, A., and Levine, T. P. (2004) Multiple pools of phosphatidylinositol 4-phosphate detected using the pleckstrin homology domain of Osh2p. *J. Biol. Chem.* **279**, 44683–44689

139. Stefan, C. J., Manford, A. G., Baird, D., Yamada-Hanff, J., Mao, Y., and Emr, S. D. (2011) Osh Proteins Regulate Phosphoinositide Metabolism at ER-Plasma Membrane Contact Sites. *Cell*. **144**, 389–401

140. Tong, J., Yang, H., Yang, H., Eom, S. H., and Im, Y. J. (2013) Structure of Osh3 reveals a conserved mode of phosphoinositide binding in oxysterol-binding proteins. *Structure*. **21**, 1203–1213

141. Weber-Boyvat, M., Kentala, H., Lilja, J., Vihervaara, T., Hanninen, R., Zhou, Y., Peränen, J., Nyman, T. A., Ivaska, J., and Olkkonen, V. M. (2015) OSBP-related protein 3 (ORP3) coupling with VAMP-associated protein A regulates R-Ras activity. *Exp. Cell Res.* **331**, 278–291

142. Kentala, H., Pfisterer, S. G., Olkkonen, V. M., and Weber-Boyvat, M. (2015) Sterol liganding of OSBP-related proteins (ORPs) regulates the subcellular distribution of ORP-VAPA complexes and their impacts on organelle structure. *Steroids*. **99**, 248–258

143. Encinar del Dedo, J., Idrissi, F.-Z., Fernandez-Golbano, I. M., Garcia, P., Rebollo, E., Krzyzanowski, M. K., Grötsch, H., and Geli, M. I. (2017) ORP-Mediated ER Contact with Endocytic Sites Facilitates Actin Polymerization. *Dev. Cell*. 10.1016/j.devcel.2017.10.031

144. Craven, R. J., and Petes, T. D. (2001) The Saccharomyces cerevisiae suppressor of choline sensitivity (SCS2) gene is a multicopy suppressor of mec1 telomeric silencing defects. *Genetics*. **158**, 145–154

145. Riekhof, W. R., Wu, W. I., Jones, J. L., Nikrad, M., Chan, M. M., Loewen, C. J. R., and Voelker, D. R. (2014) An assembly of proteins and lipid domains regulates

transport of phosphatidylserine to phosphatidylserine decarboxylase 2 in Saccharomyces cerevisiae. *J. Biol. Chem.* **289**, 5809–5819

146. Groer, G. J., Haslbeck, M., Roessle, M., and Gessner, A. (2008) Structural characterization of soluble E-Syt2. *FEBS Lett.* **582**, 3941–3947

147. Creutz, C. E., Snyder, S. L., and Schulz, T. A. (2004) Characterization of the yeast tricalbins: membrane-bound multi-C2-domain proteins that form complexes involved in membrane trafficking. *Cell. Mol. Life Sci.* **61**, 1208–20

148. Fernández-Busnadiego, R., Saheki, Y., and De Camilli, P. (2015) Three-dimensional architecture of extended synaptotagmin-mediated endoplasmic reticulum–plasma membrane contact sites. *Proc. Natl. Acad. Sci.* **112**, E2004–E2013

149. Min, S.-W., Chang, W.-P., and Südhof, T. C. (2007) E-Syts, a family of membranous Ca2+-sensor proteins with multiple C2 domains. *Proc. Natl. Acad. Sci. U. S. A.* **104**, 3823–8

150. Rizo, J., and Südhof, T. C. (1998) C2-domains, structure and function of a universal Ca2+-binding domain. *J. Biol. Chem.* **273**, 15879–82

151. Chang, C.-L., Hsieh, T.-S., Yang, T. T., Rothberg, K. G., Azizoglu, D. B., Volk, E., Liao, J.-C., and Liou, J. (2013) Feedback Regulation of Receptor-Induced Ca2+ Signaling Mediated by E-Syt1 and Nir2 at Endoplasmic Reticulum-Plasma Membrane Junctions. *Cell Rep.* **5**, 813–825

152. Idevall-Hagren, O., Lü, A., Xie, B., and De Camilli, P. (2015) Triggered Ca2+ influx is required for extended synaptotagmin 1-induced ER-plasma membrane tethering. *EMBO J.* **34**, 1–15

153. Sclip, A., Bacaj, T., Giam, L. R., and Südhof, T. C. (2016) Extended Synaptotagmin (ESyt) triple knock-out mice are viable and fertile without obvious endoplasmic reticulum dysfunction. *PLoS One*. **11**, 1–17

154. Tremblay, M. G., and Moss, T. (2016) Loss of all 3 Extended Synaptotagmins does not affect normal mouse development, viability or fertility. *Cell Cycle*. **15**, 2360–2366

155. Reinisch, K. M., and De Camilli, P. (2016) SMP-domain proteins at membrane contact sites: Structure and function. *Biochim. Biophys. Acta - Mol. Cell Biol. Lipids*. **1861**, 924–927

156. Yu, H., Liu, Y., Gulbranson, D. R., Paine, A., Rathore, S. S., and Shen, J. (2016) Extended synaptotagmins are Ca^{2+}-dependent lipid transfer proteins at membrane contact sites. *Proc. Natl. Acad. Sci.* **113**, 4362–4367

157. Saheki, Y., Bian, X., Schauder, C. M., Sawaki, Y., Surma, M. A., Klose, C., Pincet,

F., Reinisch, K. M., and De Camilli, P. (2016) Control of plasma membrane lipid homeostasis by the extended synaptotagmins. *Nat. Cell Biol.* **18**, 504–515

158. Saheki, Y., and De Camilli, P. (2017) Endoplasmic reticulum-Plasma Membrane Contact Sites. *Annu. Rev. Biochem.* **86**, 659–684

159. Saheki, Y., and De Camilli, P. (2017) The Extended-Synaptotagmins. *Biochim. Biophys. Acta - Mol. Cell Res.* **1864**, 1490–1493

160. Dickson, E. J., Jensen, J. B., Vivas, O., Kruse, M., Traynor-Kaplan, A. E., and Hille, B. (2016) Dynamic formation of ER-PM junctions presents a lipid phosphatase to regulate phosphoinositides. *J. Cell Biol.* **213**, 33–48

161. Wolf, W., Kilic, A., Schrul, B., Lorenz, H., Schwappach, B., and Seedorf, M. (2012) Yeast Ist2 recruits the endoplasmic reticulum to the plasma membrane and creates a ribosome-free membrane microcompartment. *PLoS One*. 10.1371/journal.pone.0039703

162. Ercan, E., Momburg, F., Engel, U., Temmerman, K., Nickel, W., and Seedorf, M. (2009) A conserved, lipid-mediated sorting mechanism of yeast Ist2 and mammalian STIM proteins to the peripheral ER. *Traffic*. **10**, 1802–1818

163. Fischer, M. A., Temmerman, K., Ercan, E., Nickel, W., and Seedorf, M. (2009) Binding of plasma membrane lipids recruits the yeast integral membrane protein Ist2 to the cortical ER. *Traffic*. **10**, 1084–1097

164. Maass, K., Fischer, M. A., Seiler, M., Temmerman, K., Nickel, W., and Seedorf, M. (2009) A signal comprising a basic cluster and an amphipathic alpha-helix interacts with lipids and is required for the transport of Ist2 to the yeast cortical ER. *J. Cell Sci.* **122**, 625–635

165. Hartzell, H. C., Yu, K., Xiao, Q., Chien, L. T., and Qu, Z. (2009) Anoctamin/TMEM16 family members are Ca2+-activated Cl- channels. *J. Physiol.* **587**, 2127–2139

166. Kunzelmann, K., Cabrita, I., Wanitchakool, P., Ousingsawat, J., Sirianant, L., Benedetto, R., and Schreiber, R. (2016) Modulating Ca2+ signals: a common theme for TMEM16, Ist2, and TMC. *Pflugers Arch. Eur. J. Physiol.* **468**, 475–490

167. Malvezzi, M., Chalat, M., Janjusevic, R., Picollo, A., Terashima, H., Menon, A. K., and Accardi, A. (2013) Ca2+-dependent phospholipid scrambling by a reconstituted TMEM16 ion channel. *Nat. Commun.* **4**, 1–9

168. Brunner, J. D., Lim, N. K., Schenck, S., Duerst, A., and Dutzler, R. (2014) X-ray structure of a calcium-activated TMEM16 lipid scramblase. *Nature*. **516**, 207–212

169. Schroeder, B. C., Cheng, T., Jan, Y. N., and Jan, L. Y. (2008) Expression Cloning of TMEM16A as a Calcium-Activated Chloride Channel Subunit. *Cell*. **134**, 1019–

1029

170. Caputo, A., Caci, E., Ferrera, L., Pedemonte, N., Barsanti, C., Sondo, E., Pfeffer, U., Ravazzolo, R., Zegarra-Moran, O., and Galietta, L. J. V. (2008) TMEM16A, A Membrane Protein Associated with Calcium-Dependent Chloride Channel Activity. *Science (80-.).* **322**, 590–594

171. Yang, Y. D., Cho, H., Koo, J. Y., Tak, M. H., Cho, Y., Shim, W.-S., Park, S. P., Lee, J., Lee, B., Kim, B.-M., Raouf, R., Shin, Y. K., and Oh, U. (2008) TMEM16A confers receptor-activated calcium-dependent chloride conductance. *Nature*. **455**, 1210–1215

172. Yang, H., Kim, A., David, T., Palmer, D., Jin, T., Tien, J., Huang, F., Cheng, T., Coughlin, S. R., Jan, Y. N., and Jan, L. Y. (2012) TMEM16F forms a Ca2+-activated cation channel required for lipid scrambling in platelets during blood coagulation. *Cell*. **151**, 111–22

173. Yu, K., Whitlock, J. M., Lee, K., Ortlund, E. A., Yuan Cui, Y., and Hartzell, H. C. (2015) Identification of a lipid scrambling domain in ANO6/TMEM16F. *Elife*. **4**, e06901

174. Wanitchakool, P., Ousingsawat, J., Sirianant, L., Cabrita, I., Faria, D., Schreiber, R., and Kunzelmann, K. (2017) Cellular defects by deletion of ANO10 are due to deregulated local calcium signaling. *Cell. Signal.* **30**, 41–49

175. de Martin, P. E., Du, Y., Novick, P., and Ferro-Novick, S. (2005) Ice2p is important for the distribution and structure of the cortical ER network in *Saccharomyces cerevisiae*. *J. Cell Sci.* **118**, 65–77

176. Toulmay, A., and Prinz, W. A. (2011) Lipid transfer and signaling at organelle contact sites: the tip of the iceberg. *Curr. Opin. Cell Biol.* **23**, 458–63

177. Tavassoli, S., Chao, J. T., Young, B. P., Cox, R. C., Prinz, W. a, de Kroon, A. I. P. M., and Loewen, C. J. R. (2013) Plasma membrane--endoplasmic reticulum contact sites regulate phosphatidylcholine synthesis. *EMBO Rep.* **14**, 434–40

178. Markgraf, D. F., Klemm, R. W., Junker, M., Hannibal-Bach, H. K., Ejsing, C. S., and Rapoport, T. A. (2014) An ER protein functionally couples neutral lipid metabolism on lipid droplets to membrane lipid synthesis in the ER. *Cell Rep.* **6**, 44–55

179. Rogers, J. V, McMahon, C., Baryshnikova, A., Hughson, F. M., and Rose, M. D. (2014) ER-associated retrograde SNAREs and the Dsl1 complex mediate an alternative, Sey1p-independent homotypic ER fusion pathway. *Mol. Biol. Cell*. **25**, 3401–12

180. Levine, T. (2004) Short-range intracellular trafficking of small molecules across endoplasmic reticulum junctions. *Trends Cell Biol.* **14**, 483–90

181. Lev, S. (2010) Non-vesicular lipid transport by lipid-transfer proteins and beyond. *Nat. Rev. Mol. Cell Biol.* **11**, 739–750

182. Lev, S. (2012) Nonvesicular lipid transfer from the endoplasmic reticulum. *Cold Spring Harb. Perspect. Biol.* **4**, 1–16

183. McLean, L. R., and Phillips, M. C. (1981) Mechanism of cholesterol and phosphatidylcholine exchange or transfer between unilamellar vesicles. *Biochemistry*. **20**, 2893–2900

184. Georgiev, A. G., Sullivan, D. P., Kersting, M. C., Dittman, J. S., Beh, C. T., and Menon, A. K. (2011) Osh proteins regulate membrane sterol organization but are not required for sterol movement between the ER and PM. *Traffic*. **12**, 1341–55

185. Ferrell, J. E., Lee, K. J., and Huestis, W. H. (1985) Lipid transfer between phosphatidylcholine vesicles and human erythrocytes: exponential decrease in rate with increasing acyl chain length. *Biochemistry*. **24**, 2857–2864

186. Phillips, M. C., Johnson, W. J., and Rothblat, G. H. (1987) Mechanisms and consequences of cellular cholesterol exchange and transfer. *Biochim. Biophys. Acta - Rev. Biomembr.* **906**, 223–276

187. Petkovic, M., Jemaiel, A., Daste, F., Specht, C. G., Izeddin, I., Vorkel, D., Verbavatz, J.-M., Darzacq, X., Triller, A., Pfenninger, K. H., Tareste, D., Jackson, C. L., and Galli, T. (2014) The SNARE Sec22b has a non-fusogenic function in plasma membrane expansion. *Nat. Cell Biol.* **16**, 434–44

188. Merklinger, E., Schloetel, J.-G., Spitta, L., Thiele, C., and Lang, T. (2016) No Evidence for Spontaneous Lipid Transfer at ER–PM Membrane Contact Sites. *J. Membr. Biol.* **249**, 41–56

189. Yamaji, T., Kumagai, K., Tomishige, N., and Hanada, K. (2008) Two sphingolipid transfer proteins, CERT and FAPP2: Their roles in sphingolipid metabolism. *IUBMB Life*. **60**, 511–518

190. Alpy, F., and Tomasetto, C. (2014) START ships lipids across interorganelle space. *Biochimie*. **96**, 85–95

191. Schulz, T. a., Choi, M. G., Raychaudhuri, S., Mears, J. a., Ghirlando, R., Hinshaw, J. E., and Prinz, W. a. (2009) Lipid-regulated sterol transfer between closely apposed membranes by oxysterol-binding protein homologues. *J. Cell Biol.* **187**, 889–903

192. Beh, C. T., Cool, L., Phillips, J., and Rine, J. (2001) Overlapping functions of the yeast oxysterol-binding protein homologues. *Genetics*. **157**, 1117–40

193. Im, Y. J., Raychaudhuri, S., Prinz, W. a, and Hurley, J. H. (2005) Structural mechanism for sterol sensing and transport by OSBP-related proteins. *Nature*.

437, 154–8

194. Maeda, K., Anand, K., Chiapparino, A., Kumar, A., Poletto, M., Kaksonen, M., and Gavin, A. C. (2013) Interactome map uncovers phosphatidylserine transport by oxysterol-binding proteins. *Nature*. **501**, 257–261

195. Sohn, M., Korzeniowski, M., Zewe, J. P., Wills, R. C., Hammond, G. R. V, Humpolickova, J., Vrzal, L., Chalupska, D., Veverka, V., Fairn, G. D., Boura, E., and Balla, T. (2018) PI(4,5)P2 controls plasma membrane PI4P and PS levels via ORP5/8 recruitment to ER – PM contact sites. *J. Cell Biol.* **217**, 1797–1813

196. van Meer, G., Voelker, D. R., and Feigenson, G. W. (2008) Membrane lipids: where they are and how they behave. *Nat. Rev. Mol. Cell Biol.* **9**, 112–124

197. Menon, A. K., and Levine, T. P. (2015) Countercurrents in lipid flow. *Nature*. **525**, 191–192

198. Audhya, A., and Emr, S. D. (2002) Stt4 PI 4-kinase localizes to the plasma membrane and functions in the Pkc1-mediated MAP kinase cascade. *Dev. Cell*. **2**, 593–605

199. Manik, M. K., Yang, H., Tong, J., and Im, Y. J. (2017) Structure of Yeast OSBP-Related Protein Osh1 Reveals Key Determinants for Lipid Transport and Protein Targeting at the Nucleus-Vacuole Junction. *Structure*. **25**, 617–629.e3

200. Drin, G., Moser von Filseck, J., Čopič, A., von Filseck, J. M., and Čopič, A. (2016) New molecular mechanisms of inter-organelle lipid transport. *Biochem. Soc. Trans.* **44**, 486–492

201. Zewe, J. P., Wills, R. C., Sangappa, S., Goulden, B. D., and Hammond, G. R. V. (2018) SAC1 degrades its lipid substrate Ptdins4P in the endoplasmic reticulum to maintain a steep chemical gradient with donor membranes. *Elife*. **7**, 1–25

202. Gatta, A. T., and Levine, T. P. (2017) Piecing Together the Patchwork of Contact Sites. *Trends Cell Biol.* **27**, 214–229

203. Stocco, D. M., and Clark, B. J. (1996) Role of the steroidogenic acute regulatory protein (StAR) in steroidogenesis. *Biochem. Pharmacol.* **51**, 197–205

204. Stocco, D. M. (2001) StAR protein and the regulation of steroid hormone biosynthesis. *Annu. Rev. Physiol.* **63**, 193–213

205. Soccio, R. E., and Breslow, J. L. (2003) StAR-related Lipid Transfer (START) Proteins: Mediators of Intracellular Lipid Metabolism. *J. Biol. Chem.* **278**, 22183–22186

206. Alpy, F., Stoeckel, M. E., Dierich, a, Escola, J. M., Wendling, C., Chenard, M. P., Vanier, M. T., Gruenberg, J., Tomasetto, C., and Rio, M. C. (2001) The

steroidogenic acute regulatory protein homolog MLN64, a late endosomal cholesterol-binding protein. *J. Biol. Chem.* **276**, 4261–9

207. Alpy, F., Latchumanan, V. K., Kedinger, V., Janoshazi, A., Thiele, C., Wendling, C., Rio, M. C., and Tomasetto, C. (2005) Functional characterization of the MENTAL domain. *J. Biol. Chem.* **280**, 17945–17952

208. Murcia, M., Faráldo-Gómez, J. D., Maxfield, F. R., and Roux, B. (2006) Modeling the structure of the StART domains of MLN64 and StAR proteins in complex with cholesterol. *J. Lipid Res.* **47**, 2614–30

209. Kishida, T., Kostetskii, I., Zhang, Z., Martinez, F., Liu, P., Walkley, S. U., Dwyer, N. K., Blanchette-Mackie, E. J., Radice, G. L., and Strauss, J. F. (2004) Targeted mutation of the MLN64 START domain causes only modest alterations in cellular sterol metabolism. *J. Biol. Chem.* **279**, 19276–85

210. Romanowski, M. J., Soccio, R. E., Breslow, J. L., and Burley, S. K. (2002) Crystal structure of the Mus musculus cholesterol-regulated START protein 4 (StarD4) containing a StAR-related lipid transfer domain. *Proc. Natl. Acad. Sci. U. S. A.* **99**, 6949–54

211. Gatta, A. T., Wong, L. H., Sere, Y. Y., Calderón-Noreña, D. M., Cockcroft, S., Menon, A. K., and Levine, T. P. (2015) A new family of StART domain proteins at membrane contact sites has a role in ER-PM sterol transport. *Elife*. **4**, 1–21

212. Murley, A., Sarsam, R. D., Toulmay, A., Yamada, J., Prinz, W. a, and Nunnari, J. (2015) Ltc1 is an ER-localized sterol transporter and a component of ER-mitochondria and ER-vacuole contacts. *J. Cell Biol.* **1**, 539–548

213. Elbaz-Alon, Y., Eisenberg-Bord, M., Shinder, V., Stiller, S. B., Shimoni, E., Wiedemann, N., Geiger, T., and Schuldiner, M. (2015) Lam6 Regulates the Extent of Contacts between Organelles. *Cell Rep.* **12**, 7–14

214. Lee, I., and Hong, W. (2006) Diverse membrane-associated proteins contain a novel SMP domain. *FASEB J.* **20**, 202–6

215. AhYoung, A. P., Jiang, J., Zhang, J., Khoi Dang, X., Loo, J. A., Zhou, Z. H., and Egea, P. F. (2015) Conserved SMP domains of the ERMES complex bind phospholipids and mediate tether assembly. *Proc. Natl. Acad. Sci. U. S. A.* 10.1073/pnas.1422363112

216. Sud, M., Fahy, E., Cotter, D., Brown, A., Dennis, E. A., Glass, C. K., Merrill, A. H., Murphy, R. C., Raetz, C. R. H., Russell, D. W., and Subramaniam, S. (2007) LMSD: LIPID MAPS structure database. *Nucleic Acids Res.* **35**, D527–D532

217. Klug, L., and Daum, G. (2014) Yeast lipid metabolism at a glance. *FEMS Yeast Res.* **14**, 369–388

218. Henry, S. a., Kohlwein, S. D., and Carman, G. M. (2012) Metabolism and regulation of glycerolipids in the yeast Saccharomyces cerevisiae. *Genetics*. **190**, 317–349

219. Tehlivets, O., Scheuringer, K., and Kohlwein, S. D. (2007) Fatty acid synthesis and elongation in yeast. *Biochim. Biophys. Acta - Mol. Cell Biol. Lipids*. **1771**, 255–270

220. Ejsing, C. S., Sampaio, J. L., Surendranath, V., Duchoslav, E., Ekroos, K., Klemm, R. W., Simons, K., and Shevchenko, A. (2009) Global analysis of the yeast lipidome by quantitative shotgun mass spectrometry. *Proc. Natl. Acad. Sci. {U.S.A.}*. **106**, 2136–2141

221. Hoja, U., Marthol, S., Hofmann, J., Stegner, S., Schulz, R., Meier, S., Greiner, E., and Schweizer, E. (2004) HFA1 Encoding an Organelle-specific Acetyl-CoA Carboxylase Controls Mitochondrial Fatty Acid Synthesis in Saccharomyces cerevisiae. *J. Biol. Chem.* **279**, 21779–21786

222. Hasslacher, M., Ivessa, A. S., Paltauf, F., and Kohlwein, S. D. (1993) Acetyl-CoA carboxylase from yeast is an essential enzyme and is regulated by factors that control phospholipid metabolism. *J. Biol. Chem.* **268**, 10946–52

223. Leibundgut, M., Maier, T., Jenni, S., and Ban, N. (2008) The multienzyme architecture of eukaryotic fatty acid synthases. *Curr. Opin. Struct. Biol.* **18**, 714–725

224. Toke, D. A., and Martin, C. E. (1996) Isolation and characterization of a gene affecting fatty acid elongation in Saccharomyces cerevisiae. *J. Biol. Chem.* **271**, 18413–22

225. Oh, C. S., Toke, D. A., Mandala, S., and Martin, C. E. (1997) ELO2 and ELO3, homologues of the Saccharomyces cerevisiae ELO1 gene, function in fatty acid elongation and are required for sphingolipid formation. *J. Biol. Chem.* **272**, 17376–84

226. Stukey, J. E., McDonough, V. M., and Martin, C. E. (1989) Isolation and characterization of OLE1, a gene affecting fatty acid desaturation from Saccharomyces cerevisiae. *J. Biol. Chem.* **264**, 16537–44

227. Jouhet, J. (2013) Importance of the hexagonal lipid phase in biological membrane organization. *Front. Plant Sci.* **4**, 1–5

228. Stachowiak, J. C., Schmid, E. M., Ryan, C. J., Ann, H. S., Sasaki, D. Y., Sherman, M. B., Geissler, P. L., Fletcher, D. a., and Hayden, C. C. (2012) Membrane bending by protein–protein crowding. *Nat. Cell Biol.* **14**, 944–949

229. Panatala, R., Hennrich, H., and Holthuis, J. C. M. (2015) Inner workings and biological impact of phospholipid flippases. *J. Cell Sci.* **128**, 2021–32

230. Pomorski, T., and Menon, a. K. (2006) Lipid flippases and their biological functions. *Cell. Mol. Life Sci.* **63**, 2908–2921

231. Daleke, D. L. (2007) Phospholipid flippases. *J. Biol. Chem.* **282**, 821–825

232. Klose, C., Surma, M. A., Gerl, M. J., Meyenhofer, F., Shevchenko, A., and Simons, K. (2012) Flexibility of a eukaryotic lipidome - insights from yeast lipidomics. *PLoS One*. 10.1371/journal.pone.0035063

233. Zinser, E., Sperka-Gottlieb, C. D. M., Fasch, E. V., Kohlwein, S. D., Paltauf, F., and Daum, G. (1991) Phospholipid synthesis and lipid composition of subcellular membranes in the unicellular eukaryote Saccharomyces cerevisiae. *J. Bacteriol.* **173**, 2026–2034

234. Murate, M., Abe, M., Kasahara, K., Iwabuchi, K., Umeda, M., and Kobayashi, T. (2015) Transbilayer distribution of lipids at nano scale. *J. Cell Sci.* **128**, 1627–1638

235. Carman, G. M., and Henry, S. A. (2007) Phosphatidic acid plays a central role in the transcriptional regulation of glycerophospholipid synthesis in Saccharomyces cerevisiae. *J. Biol. Chem.* **282**, 37293–37297

236. Zaremberg, V., and McMaster, C. R. (2002) Differential partitioning of lipids metabolized by separate yeast glycerol-3-phosphate acyltransferases reveals that phospholipase D generation of phosphatidic acid mediates sensitivity to choline-containing lysolipids and drugs. *J. Biol. Chem.* **277**, 39035–44

237. Benghezal, M., Roubaty, C., Veepuri, V., Knudsen, J., and Conzelmann, A. (2007) SLC1 and SLC4 encode partially redundant acyl-coenzyme A 1-acylglycerol-3-phosphate O-acyltransferases of budding yeast. *J. Biol. Chem.* **282**, 30845–55

238. Faulkner, A., Chen, X., Rush, J., Horazdovsky, B., Waechter, C. J., Carman, G. M., and Sternweis, P. C. (1999) The LPP1 and DPP1 gene products account for most of the isoprenoid phosphate phosphatase activities in Saccharomyces cerevisiae. *J. Biol. Chem.* **274**, 14831–7

239. Han, G. S., Wu, W. I., and Carman, G. M. (2006) The Saccharomyces cerevisiae lipin homolog is a Mg2+-dependent phosphatidate phosphatase enzyme. *J. Biol. Chem.* **281**, 9210–9218

240. Han, G. S., Siniossoglou, S., and Carman, G. M. (2007) The cellular functions of the yeast lipin homolog Pah1p are dependent on its phosphatidate phosphatase activity. *J. Biol. Chem.* **282**, 37026–37035

241. Adeyo, O., Horn, P. J., Lee, S. K., Binns, D. D., Chandrahas, A., Chapman, K. D., and Goodman, J. M. (2011) The yeast lipin orthologue Pah1p is important for biogenesis of lipid droplets. *J. Cell Biol.* **192**, 1043–1055

242. Hsieh, L. S., Su, W. M., Han, G. S., and Carman, G. M. (2016) Phosphorylation of yeast Pah1 phosphatidate phosphatase by casein kinase II regulates its function in lipid metabolism. *J. Biol. Chem.* **291**, 9974–9990

243. Rahman, M. A., Mostofa, M. G., and Ushimaru, T. (2018) The Nem1/Spo7-Pah1/lipin axis is required for autophagy induction after TORC1 inactivation. *FEBS J.* **285**, 1840–1860

244. Barbosa, A. D., Sembongi, H., Su, W.-M., Abreu, S., Reggiori, F., Carman, G. M., and Siniossoglou, S. (2015) Lipid partitioning at the nuclear envelope controls membrane biogenesis. *Mol. Biol. Cell*. **26**, 3641–3657

245. Pascual, F., and Carman, G. M. (2013) Phosphatidate phosphatase, a key regulator of lipid homeostasis. *Biochim. Biophys. Acta - Mol. Cell Biol. Lipids*. **1831**, 514–522

246. Han, G.-S. S., O'Hara, L., Carman, G. M., and Siniossoglou, S. (2008) An unconventional diacylglycerol kinase that regulates phospholipid synthesis and nuclear membrane growth. *J. Biol. Chem.* **283**, 20433–20442

247. McMaster, C. R., and Bell, R. M. (1994) Phosphatidylcholine biosynthesis via the CDP-choline pathway in Saccharomyces cerevisiae. Multiple mechanisms of regulation. *J. Biol. Chem.* **269**, 14776–83

248. Fernández-Murray, J. P., and McMaster, C. R. (2016) Lipid synthesis and membrane contact sites: a crossroads for cellular physiology. *J. Lipid Res.* **57**, 1789–1805

249. Carter, J. R., and Kennedy, E. P. (1966) Enzymatic synthesis of cytidine diphosphate diglyceride. *J. Lipid Res.* **7**, 678–83

250. Kelley, M. J., and Carman, G. M. (1987) Purification and characterization of CDP-diacylglycerol synthase from Saccharomyces cerevisiae. *J. Biol. Chem.* **262**, 14563–70

251. Shen, H., Heacock, P. N., Clancey, C. J., and Dowhan, W. (1996) The *CDS1* Gene Encoding CDP-diacylglycerol Synthase In *Saccharomyces cerevisiae* Is Essential for Cell Growth. *J. Biol. Chem.* **271**, 789–795

252. Atkinson, K. D., Jensen, B., Kolat, A. I., Storm, E. M., Henry, S. A., and Fogel, S. (1980) Yeast mutants auxotrophic for choline or ethanolamine. *J. Bacteriol.* **141**, 558–64

253. Letts, V. A., Klig, L. S., Bae-Lee, M., Carman, G. M., and Henry, S. A. (1983) Isolation of the yeast structural gene for the membrane-associated enzyme phosphatidylserine synthase. *Proc. Natl. Acad. Sci. U. S. A.* **80**, 7279–83

254. Clancey, C. J., Chang, S. C., and Dowhan, W. (1993) Cloning of a gene (PSD1)

encoding phosphatidylserine decarboxylase from Saccharomyces cerevisiae by complementation of an Escherichia coli mutant. *J. Biol. Chem.* **268**, 24580–90

255. Trotter, P. J., Pedretti, J., Yates, R., and Voelker, D. R. (1995) Phosphatidylserine decarboxylase 2 of Saccharomyces cerevisiáe. Cloning and mapping of the gene, heterologous expression, and creation of the null allele. *J. Biol. Chem.* **270**, 6071–80

256. Trotter, P. J., and Voelker, D. R. (1995) Identification of a non-mitochondrial phosphatidylserine decarboxylase activity (PSD2) in the yeast Saccharomyces cerevisiae. *J. Biol. Chem.* **270**, 6062–70

257. Kodaki, T., and Yamashita, S. (1987) Yeast phosphatidylethanolamine methylation pathway. Cloning and characterization of two distinct methyltransferase genes. *J. Biol. Chem.* **262**, 15428–35

258. Summers, E. F., Letts, V. A., McGraw, P., and Henry, S. A. (1988) Saccharomyces cerevisiae cho2 mutants are deficient in phospholipid methylation and cross-pathway regulation of inositol synthesis. *Genetics*. **120**, 909–22

259. KODAKI, T., and YAMASHITA, S. (1989) Characterization of the methyltransferases in the yeast phosphatidylethanolamine methylation pathway by selective gene disruption. *Eur. J. Biochem.* **185**, 243–251

260. McGraw, P., and Henry, S. A. (1989) Mutations in the Saccharomyces cerevisiae opi3 gene: effects on phospholipid methylation, growth and cross-pathway regulation of inositol synthesis. *Genetics*. **122**, 317–30

261. Nikawa, J., Hosaka, K., Tsukagoshi, Y., and Yamashita, S. (1990) Primary structure of the yeast choline transport gene and regulation of its expression. *J. Biol. Chem.* **265**, 15996–6003

262. Hosaka, K., Kodaki, T., and Yamashita, S. (1989) Cloning and characterization of the yeast CKI gene encoding choline kinase and its expression in Escherichia coli. *J. Biol. Chem.* **264**, 2053–9

263. Tsukagoshi, Y., Nikawa, J., and Yamashita, S. (1987) Molecular cloning and characterization of the gene encoding cholinephosphate cytidylyltransferase in Saccharomyces cerevisiae. *Eur. J. Biochem.* **169**, 477–86

264. Hjelmstad, R. H., and Bell, R. M. (1987) Mutants of Saccharomyces cerevisiae defective in sn-1,2-diacylglycerol cholinephosphotransferase. Isolation, characterization, and cloning of the CPT1 gene. *J. Biol. Chem.* **262**, 3909–17

265. Kim, K., Kim, K. H., Storey, M. K., Voelker, D. R., and Carman, G. M. (1999) Isolation and characterization of the Saccharomyces cerevisiae EKI1 gene encoding ethanolamine kinase. *J. Biol. Chem.* **274**, 14857–66

266. Min-Seek, R., Kawamata, Y., Nakamura, H., Ohta, A., and Takagi, M. (1996) Isolation and Characterization of ECTl Gene Encoding CTP: Phosphoethanolamine Cytidylyltransferase of Saccharomyces cerevisiae. *J. Biochem.* **120**, 1040–1047

267. Morash, S. C., McMaster, C. R., Hjelmstad, R. H., and Bell, R. M. (1994) Studies employing Saccharomyces cerevisiae cpt1 and ept1 null mutants implicate the CPT1 gene in coordinate regulation of phospholipid biosynthesis. *J. Biol. Chem.* **269**, 28769–76

268. Patton-Vogt, J. L., Griac, P., Sreenivas, A., Bruno, V., Dowd, S., Swede, M. J., and Henry, S. A. (1997) Role of the Yeast Phosphatidylinositol/Phosphatidylcholine Transfer Protein (Sec14p) in Phosphatidylcholine Turnover and INO1 Regulation. *J. Biol. Chem.* **272**, 20873–20883

269. Ella, K. M., Dolan, J. W., and Meier, K. E. (1995) Characterization of a regulated form of phospholipase D in the yeast Saccharomyces cerevisiae. *Biochem. J.* **307**, 799–805

270. Waksman, M., Eli, Y., Liscovitch, M., and Gerst, J. E. (1996) Identification and Characterization of a Gene Encoding Phospholipase D Activity in Yeast. *J. Biol. Chem.* **271**, 2361–2364

271. Xie, Z., Fang, M., Rivas, M. P., Faulkner, A. J., Sternweis, P. C., Engebrecht, J., and Bankaitis, V. A. (1998) Phospholipase D activity is required for suppression of yeast phosphatidylinositol transfer protein defects. *Proc. Natl. Acad. Sci.* **95**, 12346–12351

272. Fischl, A. S., and Carman, G. M. (1983) Phosphatidylinositol biosynthesis in Saccharomyces cerevisiae: Purification and properties of microsome-associated phosphatidylinositol synthase. *J. Bacteriol.* **154**, 304–311

273. NIKAWA, J. -i, and YAMASHITA, S. (1984) Molecular cloning of the gene encoding CDPdiacylglycerol–inositol 3-phosphatidyl transferase in Saccharomyces cerevisiae. *Eur. J. Biochem.* **143**, 251–256

274. Nikawa, J., Tsukagoshi, Y., and Yamashita, S. (1991) Isolation and characterization of two distinct myo-inositol transporter genes of Saccharomyces cerevisiae. *J. Biol. Chem.* **266**, 11184–91

275. Donahue, T. F., and Henry, S. A. (1981) myo-Inositol-1-phosphate synthase. Characteristics of the enzyme and identification of its structural gene in yeast. *J. Biol. Chem.* **256**, 7077–85

276. Klig, L. S., and Henry, S. A. (1984) Isolation of the yeast INO1 gene: located on an autonomously replicating plasmid, the gene is fully regulated. *Proc. Natl. Acad. Sci.* **81**, 3816–3820

277. Murray, M., and Greenberg, M. L. (2002) Expression of yeast INM1 encoding inositol monophosphatase is regulated by inositol, carbon source and growth stage and is decreased by lithium and valproate. *Mol. Microbiol.* **36**, 651–661

278. Janitor, M., and Šubík, J. (1993) Molecular cloning of the PEL1 gene of Saccharomyces cerevisiae that is essential for the viability of petite mutants. *Curr. Genet.* **24**, 307–312

279. Osman, C., Haag, M., Wieland, F. T., Brügger, B., and Langer, T. (2010) A mitochondrial phosphatase required for cardiolipin biosynthesis: the PGP phosphatase Gep4. *EMBO J.* **29**, 1976–87

280. Chang, S. C., Heacock, P. N., Clancey, C. J., and Dowhan, W. (1998) The PEL1 gene (renamed PGS1) encodes the phosphatidylglycero-phosphate synthase of Saccharomyces cerevisiae. *J. Biol. Chem.* **273**, 9829–36

281. Beranek, A., Rechberger, G., Knauer, H., Wolinski, H., Kohlwein, S. D., and Leber, R. (2009) Identification of a cardiolipin-specific phospholipase encoded by the gene CLD1 (YGR110W) in yeast. *J. Biol. Chem.* **284**, 11572–8

282. Lee, K. S., Patton, J. L., Fido, M., Hines, L. K., Kohlwein, S. D., Paltauf, F., Henry, S. A., and Levin, D. E. (1994) The Saccharomyces cerevisiae PLB1 gene encodes a protein required for lysophospholipase and phospholipase B activity. *J. Biol. Chem.* **269**, 19725–30

283. Fyrst, H., Oskouian, B., Kuypers, F. A., and Saba, J. D. (1999) The PLB2 gene of Saccharomyces cerevisiae confers resistance to lysophosphatidylcholine and encodes a phospholipase B/lysophospholipase. *Biochemistry*. **38**, 5864–71

284. Merkel, O., Fido, M., Mayr, J. A., Prüger, H., Raab, F., Zandonella, G., Kohlwein, S. D., and Paltauf, F. (1999) Characterization and function in vivo of two novel phospholipases B/lysophospholipases from Saccharomyces cerevisiae. *J. Biol. Chem.* **274**, 28121–7

285. Murray, J. P. F., and McMaster, C. R. (2005) Nte1p-mediated deacylation of phosphatidylcholine functionally interacts with Sec14p. *J. Biol. Chem.* **280**, 8544–52

286. Fernández-Murray, J. P., and McMaster, C. R. (2005) Glycerophosphocholine catabolism as a new route for choline formation for phosphatidylcholine synthesis by the Kennedy pathway. *J. Biol. Chem.* **280**, 38290–6

287. Yoko-o, T., Matsui, Y., Yagisawa, H., Nojima, H., Uno, I., and Toh-e, A. (1993) The putative phosphoinositide-specific phospholipase C gene, PLC1, of the yeast Saccharomyces cerevisiae is important for cell growth. *Proc. Natl. Acad. Sci.* **90**, 1804–1808

288. Engelberg, D., Perlman, R., and Levitzki, A. (2014) Transmembrane signaling in Saccharomyces cerevisiae as a model for signaling in metazoans: State of the art

after 25years. *Cell. Signal.* **26**, 2865–2878

289. Oelkers, P., Tinkelenberg, A., Erdeniz, N., Cromley, D., Billheimer, J. T., and Sturley, S. L. (2000) A lecithin cholesterol acyltransferase-like gene mediates diacylglycerol esterification in yeast. *J. Biol. Chem.* **275**, 15609–12

290. Oelkers, P., Cromley, D., Padamsee, M., Billheimer, J. T., and Sturley, S. L. (2002) The DGA1 gene determines a second triglyceride synthetic pathway in yeast. *J. Biol. Chem.* **277**, 8877–81

291. Sorger, D., and Daum, G. (2002) Synthesis of Triacylglycerols by the Acyl-Coenzyme A:Diacyl-Glycerol Acyltransferase Dga1p in Lipid Particles of the Yeast Saccharomyces cerevisiae. *J. Bacteriol.* **184**, 519–524

292. Kohlwein, S. D. (2010) Obese and anorexic yeasts: experimental models to understand the metabolic syndrome and lipotoxicity. *Biochim. Biophys. Acta*. **1801**, 222–9

293. Horvath, S. E., Wagner, A., Steyrer, E., and Daum, G. (2011) Metabolic link between phosphatidylethanolamine and triacylglycerol metabolism in the yeast Saccharomyces cerevisiae. *Biochim. Biophys. Acta - Mol. Cell Biol. Lipids*. **1811**, 1030–1037

294. Athenstaedt, K., Zweytick, D., Jandrositz, A., Kohlwein, S. D., and Daum, G. (1999) Identification and characterization of major lipid particle proteins of the yeast Saccharomyces cerevisiae. *J. Bacteriol.* **181**, 6441–8

295. Yang, H., Bard, M., Bruner, D. A., Gleeson, A., Deckelbaum, R. J., Aljinovic, G., Pohl, T. M., Rothstein, R., and Sturley, S. L. (1996) Sterol Esterification in Yeast: A Two-Gene Process. *Science (80-.).* **272**, 1353–1356

296. Zweytick, D., Leitner, E., Kohlwein, S. D., Yu, C., Rothblatt, J., and Daum, G. (2000) Contribution of Are1p and Are2p to steryl ester synthesis in the yeast Saccharomyces cerevisiae. *Eur. J. Biochem.* **267**, 1075–82

297. Sorger, D., Athenstaedt, K., Hrastnik, C., and Daum, G. (2004) A yeast strain lacking lipid particles bears a defect in ergosterol formation. *J. Biol. Chem.* **279**, 31190–6

298. Santiago, T. C., and Mamoun, C. Ben (2003) Genome expression analysis in yeast reveals novel transcriptional regulation by inositol and choline and new regulatory functions for Opi1p, Ino2p, and Ino4p. *J. Biol. Chem.* **278**, 38723–30

299. Henry, S. A., Gaspar, M. L., and Jesch, S. A. (2014) The response to inositol: regulation of glycerolipid metabolism and stress response signaling in yeast. *Chem. Phys. Lipids*. **180**, 23–43

300. Jesch, S. A., Zhao, X., Wells, M. T., and Henry, S. A. (2005) Genome-wide

analysis reveals inositol, not choline, as the major effector of Ino2p-Ino4p and unfolded protein response target gene expression in yeast. *J. Biol. Chem.* **280**, 9106–18

301. Loewen, C. J. R., Gaspar, M. L., Jesch, S. a, Delon, C., Ktistakis, N. T., Henry, S. a, and Levine, T. P. (2004) Phospholipid metabolism regulated by a transcription factor sensing phosphatidic acid. *Science*. **304**, 1644–1647

302. Gaspar, M. L., Chang, Y.-F. F., Jesch, S. A., Aregullin, M., and Henry, S. A. (2017) Interaction between repressor Opi1p and ER membrane protein Scs2p facilitates transit of phosphatidic acid from the ER to mitochondria and is essential for INO1 gene expression in the presence of choline. *J. Biol. Chem.* **292**, jbc.M117.809970

303. Greenberg, M. L., and Lopes, J. M. (1996) Genetic regulation of phospholipid biosynthesis in Saccharomyces cerevisiae. *Microbiol. Rev.* **60**, 1–20

304. Hirsch, J. P., and Henry, S. A. (1986) Expression of the Saccharomyces cerevisiae inositol-1-phosphate synthase (INO1) gene is regulated by factors that affect phospholipid synthesis. *Mol. Cell. Biol.* **6**, 3320–8

305. Carman, G. M., and Henry, S. A. (1999) Phospholipid biosynthesis in the yeast Saccharomyces cerevisiae and interrelationship with other metabolic processes. *Prog. Lipid Res.* **38**, 361–399

306. Loewy, B. S., and Henry, S. A. (1984) The INO2 and INO4 loci of Saccharomyces cerevisiae are pleiotropic regulatory genes. *Mol. Cell. Biol.* **4**, 2479–85

307. Schwank, S., Ebbert, R., Rautenstrauβ, K., Schweizer, E., and Schüller, H.-J. (1995) Yeast transcriptional activator *INO2* interacts as an Ino2p/Ino4p basic helix-loop-helix heteromeric complex with the inositol/choline-responsive element necessary for expression of phospholipid biosynthetic genes in *Saccharomyces cerevisiae*. *Nucleic Acids Res.* **23**, 230–237

308. Wagner, C., Blank, M., Strohmann, B., and Schüller, H. J. (1999) Overproduction of the Opi1 repressor inhibits transcriptional activation of structural genes required for phospholipid biosynthesis in the yeast Saccharomyces cerevisiae. *Yeast*. **15**, 843–54

309. Henry, S. A., and Patton-Vogt, J. L. (1998) Genetic regulation of phospholipid metabolism: yeast as a model eukaryote. *Prog. Nucleic Acid Res. Mol. Biol.* **61**, 133–79

310. Kagiwada, S., Hosaka, K., Murata, M., Nikawa, J. I., and Takatsuki, A. (1998) The Saccharomyces cerevisiae SCS2 gene product, a homolog of a synaptobrevin-associated protein, is an integral membrane protein of the endoplasmic reticulum and is required for inositol metabolism. *J. Bacteriol.* **180**, 1700–1708

311. Kagiwada, S., and Zen, R. (2003) Role of the yeast VAP homolog, Scs2p, in INO1

expression and phospholipid metabolism. *J. Biochem.* **133**, 515–522

312. Wilson, J. D., Thompson, S. L., and Barlowe, C. (2011) Yet1p-Yet3p interacts with Scs2p-Opi1p to regulate ER localization of the Opi1p repressor. *Mol. Biol. Cell*. **22**, 1430–1439

313. Walter, P., and Ron, D. (2011) The unfolded protein response: From stress pathway to homeostatic regulation. *Science (80-.).* **334**, 1081–1086

314. Han, J., and Kaufman, R. J. (2016) The role of ER stress in lipid metabolism and lipotoxicity. *J. Lipid Res.* **57**, 1329–1338

315. Shamu, C. E., and Walter, P. (1996) Oligomerization and phosphorylation of the Ire1p kinase during intracellular signaling from the endoplasmic reticulum to the nucleus. *EMBO J.* **15**, 3028–39

316. Cox, J. S., Shamu, C. E., and Walter, P. (1993) Transcriptional induction of genes encoding endoplasmic reticulum resident proteins requires a transmembrane protein kinase. *Cell*. **73**, 1197–1206

317. Cox, J. S., and Walter, P. (1996) A Novel Mechanism for Regulating Activity of a Transcription Factor That Controls the Unfolded Protein Response. *Cell*. **87**, 391–404

318. Jonikas, M. C., Collins, S. R., Denic, V., Oh, E., Quan, E. M., Schmid, V., Weibezahn, J., Schwappach, B., Walter, P., Weissman, J. S., and Schuldiner, M. (2009) Comprehensive characterization of genes required for protein folding in the endoplasmic reticulum. *Science (80-.).* **323**, 1693–1697

319. Ariyama, H., Kono, N., Matsuda, S., Inoue, T., and Arai, H. (2010) Decrease in membrane phospholipid unsaturation induces unfolded protein response. *J. Biol. Chem.* **285**, 22027–35

320. Minville-Walz, M., Pierre, A.-S., Pichon, L., Bellenger, S., Fèvre, C., Bellenger, J., Tessier, C., Narce, M., and Rialland, M. (2010) Inhibition of Stearoyl-CoA Desaturase 1 Expression Induces CHOP-Dependent Cell Death in Human Cancer Cells. *PLoS One*. **5**, e14363

321. Fu, J., Mares, C., Lizcano, A., Liu, Y., and Wickes, B. L. (2011) Insertional mutagenesis combined with an inducible filamentation phenotype reveals a conserved STE50 homologue in Cryptococcus neoformans that is required for monokaryotic fruiting and sexual reproduction. *Mol. Microbiol.* **79**, 990–1007

322. Cox, J. S., Chapman, R. E., and Walter, P. (1997) The unfolded protein response coordinates the production of endoplasmic reticulum protein and endoplasmic reticulum membrane. *Mol. Biol. Cell*. **8**, 1805–1814

323. Nikawa, J.-I., and Yamashita, S. (1992) IRE1 encodes a putative protein kinase

containing a membrane-spanning domain and is required for inositol phototrophy in Saccharomyces cerevisiae. *Mol. Microbiol.* **6**, 1441–1446

324. Nikawa, J. (1996) Saccharomyces cerevisiae IRE2/HAC1 is involved in IRE1-mediated KAR2 expression. *Nucleic Acids Res.* **24**, 4222–4226

325. Jesch, S. A., Liu, P., Zhao, X., Wells, M. T., and Henry, S. A. (2006) Multiple endoplasmic reticulum-to-nucleus signaling pathways coordinate phospholipid metabolism with gene expression by distinct mechanisms. *J. Biol. Chem.* **281**, 24070–83

326. Thibault, G., Ismail, N., and Ng, D. T. W. (2011) The unfolded protein response supports cellular robustness as a broad-spectrum compensatory pathway. *Proc. Natl. Acad. Sci. U. S. A.* **108**, 20597–602

327. Strahl, T., and Thorner, J. (2007) Synthesis and function of membrane phosphoinositides in budding yeast, Saccharomyces cerevisiae. *Biochim. Biophys. Acta*. **1771**, 353–404

328. De Craene, J. O., Bertazzi, D. L., Bär, S., and Friant, S. (2017) Phosphoinositides, major actors in membrane trafficking and lipid signaling pathways. *Int. J. Mol. Sci.* 10.3390/ijms18030634

329. Itoh, T., and Takenawa, T. (2002) Phosphoinositide-binding domains: Functional units for temporal and spatial regulation of intracellular signalling. *Cell. Signal.* **14**, 733–743

330. Putney, J. W., and Tomita, T. (2012) Phospholipase C signaling and calcium influx. *Adv. Biol. Regul.* **52**, 152–64

331. D'Angelo, G., Vicinanza, M., Di Campli, A., and De Matteis, M. A. (2008) The multiple roles of PtdIns(4)P - not just the precursor of PtdIns(4,5)P2. *J. Cell Sci.* **121**, 1955–1963

332. Foti, M., Audhya, A., and Emr, S. D. (2001) Sac1 lipid phosphatase and Stt4 phosphatidylinositol 4-kinase regulate a pool of phosphatidylinositol 4-phosphate that functions in the control of the actin cytoskeleton and vacuole morphology. *Mol. Biol. Cell*. **12**, 2396–411

333. Audhya, A., Foti, M., and Emr, S. D. (2000) Distinct Roles for the Yeast Phosphatidylinositol 4-Kinases, Stt4p and Pik1p, in Secretion, Cell Growth, and Organelle Membrane Dynamics. *Mol. Biol. Cell*. **11**, 2673–2689

334. Han, G. S., Audhya, A., Markley, D. J., Emr, S. D., and Carman, G. M. (2002) The Saccharomyces cerevisiae LSB6 gene encodes phosphatidylinositol 4-kinase activity. *J. Biol. Chem.* **277**, 47709–47718

335. Hama, H., Schnieders, E. A., Thorner, J., Takemoto, J. Y., and DeWald, D. B.

(1999) Direct involvement of phosphatidylinositol 4-phosphate in secretion in the yeast Saccharomyces cerevisiae. *J. Biol. Chem.* **274**, 34294–34300

336. Whitters, E. A., Cleves, A. E., McGee, T. P., Skinner, H. B., and Bankaitis, V. A. (1993) SAC1p is an integral membrane protein that influences the cellular requirement for phospholipid transfer protein function and inositol in yeast. *J. Cell Biol.* **122**, 79–94

337. Mizuno-Yamasaki, E., Medkova, M., Coleman, J., and Novick, P. (2010) Phosphatidylinositol 4-phosphate controls both membrane recruitment and a regulatory switch of the Rab GEF Sec2p. *Dev. Cell*. **18**, 828–40

338. Johansen, J., Ramanathan, V., and Beh, C. T. (2012) Vesicle trafficking from a lipid perspective: Lipid regulation of exocytosis in Saccharomyces cerevisiae. *Cell. Logist.* **2**, 151–160

339. Ling, Y., Hayano, S., and Novick, P. (2014) Osh4p is needed to reduce the level of phosphatidylinositol-4-phosphate on secretory vesicles as they mature. *Mol. Biol. Cell*. **25**, 3389–3400

340. Donovan, K. W., and Bretscher, A. (2015) Tracking individual secretory vesicles during exocytosis reveals an ordered and regulated process. *J. Cell Biol.* **210**, 181–9

341. Chang, F. S., Han, G.-S., Carman, G. M., and Blumer, K. J. (2005) A WASp-binding type II phosphatidylinositol 4-kinase required for actin polymerization-driven endosome motility. *J. Cell Biol.* **171**, 133–42

342. Nakatsu, F., Baskin, J. M., Chung, J., Tanner, L. B., Shui, G., Lee, S. Y., Pirruccello, M., Hao, M., Ingolia, N. T., Wenk, M. R., De Camilli, P., Camilli, P. De, and De Camilli, P. (2012) Ptdins4P synthesis by PI4KIIIα at the plasma membrane and its impact on plasma membrane identity. *J. Cell Biol.* **199**, 1003–1016

343. Baird, D., Stefan, C., Audhya, A., Weys, S., and Emr, S. D. (2008) Assembly of the PtdIns 4-kinase Stt4 complex at the plasma membrane requires Ypp1 and Efr3. *J. Cell Biol.* **183**, 1061–1074

344. Wu, X., Chi, R. J., Baskin, J. M., Lucast, L., Burd, C. G., De Camilli, P., and Reinisch, K. M. (2014) Structural Insights into Assembly and Regulation of the Plasma Membrane Phosphatidylinositol 4-Kinase Complex. *Dev. Cell*. **28**, 19–29

345. Chung, J., Nakatsu, F., Baskin, J. M., and De Camilli, P. (2015) Plasticity of PI4KIIIα interactions at the plasma membrane. *EMBO Rep.* **16**, 312–320

346. Córcoles-Sáez, I., Hernández, M. L., Martínez-Rivas, J. M., Prieto, J. A., and Randez-Gil, F. (2016) Characterization of the S. cerevisiae inp51 mutant links phosphatidylinositol 4,5-bisphosphate levels with lipid content, membrane fluidity and cold growth. *Biochim. Biophys. Acta - Mol. Cell Biol. Lipids*. **1861**, 213–226

347. Liu, Y., and Bankaitis, V. A. (2010) Phosphoinositide phosphatases in cell biology and disease. *Prog. Lipid Res.* **49**, 201–217

348. Stefan, C. J., Audhya, A., and Emr, S. D. (2002) The yeast synaptojanin-like proteins control the cellular distribution of phosphatidylinositol (4,5)-bisphosphate. *Mol. Biol. Cell*. **13**, 542–57

349. Homma, K., Terui, S., Minemura, M., Qadota, H., Anraku, Y., Kanaho, Y., and Ohya, Y. (1998) Phosphatidylinositol-4-phosphate 5-Kinase Localized on the Plasma Membrane Is Essential for Yeast Cell Morphogenesis. *J. Biol. Chem.* **273**, 15779–15786

350. Desrivières, S., Cooke, F. T., Parker, P. J., and Hall, M. N. (1998) MSS4, a phosphatidylinositol-4-phosphate 5-kinase required for organization of the actin cytoskeleton in Saccharomyces cerevisiae. *J. Biol. Chem.* **273**, 15787–93

351. Sun, Y., and Drubin, D. G. (2012) The functions of anionic phospholipids during clathrin-mediated endocytosis site initiation and vesicle formation. *J. Cell Sci.* **125**, 6157–65

352. Yamamoto, W., Wada, S., Nagano, M., Aoshima, K., Siekhaus, D. E., Toshima, J. Y., and Toshima, J. (2018) Distinct roles for plasma membrane PtdIns(4)P and PtdIns(4,5)P2 during receptor-mediated endocytosis in yeast. *J. Cell Sci.* **131**, jcs207696

353. Martin, T. F. J. (2012) Role of PI(4,5)P(2) in vesicle exocytosis and membrane fusion. *Subcell. Biochem.* **59**, 111–30

354. Mendonsa, R., and Engebrecht, J. (2009) Phosphatidylinositol-4,5-bisphosphate and phospholipase D-generated phosphatidic acid specify SNARE-mediated vesicle fusion for prospore membrane formation. *Eukaryot. Cell*. **8**, 1094–105

355. Guillas, I., Vernay, A., Vitagliano, J.-J. J.-J., and Arkowitz, R. A. (2013) Phosphatidylinositol 4,5-bisphosphate is required for invasive growth in Saccharomyces cerevisiae. *J. Cell Sci.* **126**, 3602–3614

356. Flick, J. S., and Thorner, J. (1993) Genetic and biochemical characterization of a phosphatidylinositol-specific phospholipase C in Saccharomyces cerevisiae. *Mol. Cell. Biol.* **13**, 5861–76

357. Hawkins, P. T., and Stephens, L. R. (2015) PI3K signalling in inflammation. *Biochim. Biophys. Acta - Mol. Cell Biol. Lipids*. **1851**, 882–897

358. Burd, C. G., and Emr, S. D. (1998) Phosphatidylinositol(3)-phosphate signaling mediated by specific binding to RING FYVE domains. *Mol. Cell*. **2**, 157–162

359. Schu, P., Takegawa, K., Fry, M., Stack, J., Waterfield, M., and Emr, S. (1993) Phosphatidylinositol 3-kinase encoded by yeast VPS34 gene essential for protein

sorting. *Science (80-.).* **260**, 88–91

360. Stack, J. H. (1995) Vesicle-mediated protein transport: regulatory interactions between the Vps15 protein kinase and the Vps34 PtdIns 3-kinase essential for protein sorting to the vacuole in yeast. *J. Cell Biol.* **129**, 321–334

361. Morel, E., Chamoun, Z., Lasiecka, Z. M., Chan, R. B., Williamson, R. L., Vetanovetz, C., Dall'Armi, C., Simoes, S., Point Du Jour, K. S., McCabe, B. D., Small, S. A., and Di Paolo, G. (2013) Phosphatidylinositol-3-phosphate regulates sorting and processing of amyloid precursor protein through the endosomal system. *Nat. Commun.* **4**, 2250

362. Dall'Armi, C., Devereaux, K. A., and Di Paolo, G. (2013) The role of lipids in the control of autophagy. *Curr. Biol.* **23**, R33-45

363. Parrish, W. R., Stefan, C. J., and Emr, S. D. (2004) Essential Role for the Myotubularin-related Phosphatase Ymr1p and the Synaptojanin-like Phosphatases Sjl2p and Sjl3p in Regulation of Phosphatidylinositol 3-Phosphate in Yeast. *Mol. Biol. Cell*. **15**, 3567–3579

364. Gary, J. D., Wurmser, A. E., Bonangelino, C. J., Weisman, L. S., and Emr, S. D. (1998) Fab1p Is Essential for PtdIns(3)P 5-Kinase Activity and the Maintenance of Vacuolar Size and Membrane Homeostasis. *J. Cell Biol.* **143**, 65–79

365. McEwen, R. K., Dove, S. K., Cooke, F. T., Painter, G. F., Holmes, A. B., Shisheva, A., Ohya, Y., Parker, P. J., and Michell, R. H. (1999) Complementation Analysis in PtdIns *P* Kinase-deficient Yeast Mutants Demonstrates That *Schizosaccharomyces pombe* and Murine Fab1p Homologues Are Phosphatidylinositol 3-Phosphate 5-Kinases. *J. Biol. Chem.* **274**, 33905–33912

366. Gary, J. D., Sato, T. K., Stefan, C. J., Bonangelino, C. J., Weisman, L. S., and Emr, S. D. (2002) Regulation of Fab1 phosphatidylinositol 3-phosphate 5-kinase pathway by Vac7 protein and Fig4, a polyphosphoinositide phosphatase family member. *Mol. Biol. Cell*. **13**, 1238–51

367. Rudge, S. A., Anderson, D. M., and Emr, S. D. (2004) Vacuole size control: regulation of PtdIns(3,5)P2 levels by the vacuole-associated Vac14-Fig4 complex, a PtdIns(3,5)P2-specific phosphatase. *Mol. Biol. Cell*. **15**, 24–36

368. Duex, J. E., Nau, J. J., Kauffman, E. J., and Weisman, L. S. (2006) Phosphoinositide 5-phosphatase Fig 4p is required for both acute rise and subsequent fall in stress-induced phosphatidylinositol 3,5-bisphosphate levels. *Eukaryot. Cell*. **5**, 723–31

369. Hasegawa, J., Strunk, B. S., and Weisman, L. S. (2017) PI5P and PI(3,5)P2: Minor, but Essential Phosphoinositides. *Cell Struct. Funct.* **42**, 49–60

370. Jefferies, H. B. J., Cooke, F. T., Jat, P., Boucheron, C., Koizumi, T., Hayakawa, M., Kaizawa, H., Ohishi, T., Workman, P., Waterfield, M. D., and Parker, P. J.

(2008) A selective PIKfyve inhibitor blocks PtdIns(3,5)P(2) production and disrupts endomembrane transport and retroviral budding. *EMBO Rep.* **9**, 164–70

371. Botelho, R. J., Efe, J. A., Teis, D., and Emr, S. D. (2008) Assembly of a Fab1 phosphoinositide kinase signaling complex requires the Fig4 phosphoinositide phosphatase. *Mol. Biol. Cell*. **19**, 4273–86

372. Takatori, S., Tatematsu, T., Cheng, J., Matsumoto, J., Akano, T., and Fujimoto, T. (2016) Phosphatidylinositol 3,5-Bisphosphate-Rich Membrane Domains in Endosomes and Lysosomes. *Traffic*. **17**, 154–67

373. Jin, N., Chow, C. Y., Liu, L., Zolov, S. N., Bronson, R., Davisson, M., Petersen, J. L., Zhang, Y., Park, S., Duex, J. E., Goldowitz, D., Meisler, M. H., and Weisman, L. S. (2008) VAC14 nucleates a protein complex essential for the acute interconversion of PI3P and PI(3,5)P(2) in yeast and mouse. *EMBO J.* **27**, 3221–34

374. Alghamdi, T. A., Ho, C. Y., Mrakovic, A., Taylor, D., Mao, D., and Botelho, R. J. (2013) Vac14 protein multimerization is a prerequisite step for Fab1 protein complex assembly and function. *J. Biol. Chem.* **288**, 9363–72

375. Duex, J. E., Tang, F., and Weisman, L. S. (2006) The Vac14p-Fig4p complex acts independently of Vac7p and couples PI3,5P2 synthesis and turnover. *J. Cell Biol.* **172**, 693–704

376. Chow, C. Y., Zhang, Y., Dowling, J. J., Jin, N., Adamska, M., Shiga, K., Szigeti, K., Shy, M. E., Li, J., Zhang, X., Lupski, J. R., Weisman, L. S., and Meisler, M. H. (2007) Mutation of FIG4 causes neurodegeneration in the pale tremor mouse and patients with CMT4J. *Nature*. **448**, 68–72

377. Breslow, D. K., and Weissman, J. S. (2010) Membranes in Balance: Mechanisms of Sphingolipid Homeostasis. *Mol. Cell*. **40**, 267–279

378. Megyeri, M., Riezman, H., Schuldiner, M., and Futerman, A. H. (2016) Making Sense of the Yeast Sphingolipid Pathway. *J. Mol. Biol.* **428**, 4765–4775

379. Montefusco, D. J., Matmati, N., and Hannun, Y. A. (2014) *The yeast sphingolipid signaling landscape*, NIH Public Access, **177**, 26–40

380. Huang, J., and Feigenson, G. W. (1999) A microscopic interaction model of maximum solubility of cholesterol in lipid bilayers. *Biophys. J.* **76**, 2142–57

381. Simons, K., and Ikonen, E. (1997) Functional rafts in cell membranes. *Nature*. **387**, 569–72

382. Lingwood, D., Kaiser, H.-J., Levental, I., and Simons, K. (2009) Lipid rafts as functional heterogeneity in cell membranes. *Biochem. Soc. Trans.* **37**, 955–960

383. Lingwood, D., and Simons, K. (2010) Lipid Rafts As a Membrane- Organizing Principle. *Science (80-.).* **327**, 46–50

384. Lippincott-Schwartz, J., and Phair, R. D. (2010) Lipids and Cholesterol as Regulators of Traffic in the Endomembrane System. *Annu. Rev. Biophys.* **39**, 559–578

385. Nagiec, M. M., Baltisberger, J. A., Wells, G. B., Lester, R. L., and Dickson, R. C. (1994) The LCB2 gene of Saccharomyces and the related LCB1 gene encode subunits of serine palmitoyltransferase, the initial enzyme in sphingolipid synthesis. *Proc. Natl. Acad. Sci.* **91**, 7899–7902

386. Gable, K., Slife, H., Bacikova, D., Monaghan, E., and Dunn, T. M. (2000) Tsc3p Is an 80-Amino Acid Protein Associated with Serine Palmitoyltransferase and Required for Optimal Enzyme Activity. *J. Biol. Chem.* **275**, 7597–7603

387. Chen, J. K., Lane, W. S., and Schreiber, S. L. (1999) The identification of myriocin-binding proteins. *Chem. Biol.* **6**, 221–235

388. Breslow, D. K., Collins, S. R., Bodenmiller, B., Aebersold, R., Simons, K., Shevchenko, A., Ejsing, C. S., and Weissman, J. S. (2010) Orm family proteins mediate sphingolipid homeostasis. *Nature*. **463**, 1048–1053

389. Beeler, T., Bacikova, D., Gable, K., Hopkins, L., Johnson, C., Slife, H., and Dunn, T. (1998) The Saccharomyces cerevisiae TSC10/YBR265w gene encoding 3-ketosphinganine reductase is identified in a screen for temperature-sensitive suppressors of the Ca2+-sensitive csg2Delta mutant. *J. Biol. Chem.* **273**, 30688–94

390. Haak, D., Gable, K., Beeler, T., and Dunn, T. (1997) Hydroxylation of Saccharomyces cerevisiae ceramides requires Sur2p and Scs7p. *J. Biol. Chem.* **272**, 29704–10

391. Nagiec, M. M., Skrzypek, M., Nagiec, E. E., Lester, R. L., and Dickson, R. C. (1998) The LCB4 (YOR171c) and LCB5 (YLR260w) genes of Saccharomyces encode sphingoid long chain base kinases. *J. Biol. Chem.* **273**, 19437–42

392. Kondo, N., Ohno, Y., Yamagata, M., Obara, T., Seki, N., Kitamura, T., Naganuma, T., and Kihara, A. (2014) Identification of the phytosphingosine metabolic pathway leading to odd-numbered fatty acids. *Nat. Commun.* **5**, 1–11

393. Schorling, S., Vallée, B., Barz, W. P., Riezman, H., and Oesterhelt, D. (2001) Lag1p and Lac1p Are Essential for the Acyl-CoA–dependent Ceramide Synthase Reaction in *Saccharomyces cerevisae*. *Mol. Biol. Cell*. **12**, 3417–3427

394. Vallée, B., and Riezman, H. (2005) Lip1p: a novel subunit of acyl-CoA ceramide synthase. *EMBO J.* **24**, 730–741

395. Perry, R. J., and Ridgway, N. D. (2006) Oxysterol-binding Protein and Vesicle-associated Membrane Protein–associated Protein Are Required for Sterol-dependent Activation of the Ceramide Transport Protein. *Mol. Biol. Cell*. **17**, 2604–2616

396. Kajiwara, K., Ikeda, A., Aguilera-Romero, A., Castillon, G. A., Kagiwada, S., Hanada, K., Riezman, H., Muniz, M., Funato, K., Muñiz, M., and Funato, K. (2014) Osh proteins regulate COPII-mediated vesicular transport of ceramide from the endoplasmic reticulum in budding yeast. *J. Cell Sci.* **127**, 376–387

397. Nagiec, M. M., Nagiec, E. E., Baltisberger, J. A., Wells, G. B., Lester, R. L., and Dickson, R. C. (1997) Sphingolipid synthesis as a target for antifungal drugs. Complementation of the inositol phosphorylceramide synthase defect in a mutant strain of Saccharomyces cerevisiae by the AUR1 gene. *J. Biol. Chem.* **272**, 9809–17

398. Reggiori, F., and Conzelmann, A. (1998) Biosynthesis of inositol phosphoceramides and remodeling of glycosylphosphatidylinositol anchors in Saccharomyces cerevisiae are mediated by different enzymes. *J. Biol. Chem.* **273**, 30550–9

399. Levine, T. P., Wiggins, C. A., and Munro, S. (2000) Inositol phosphorylceramide synthase is located in the Golgi apparatus of Saccharomyces cerevisiae. *Mol. Biol. Cell*. **11**, 2267–2281

400. Sato, K., Noda, Y., and Yoda, K. (2009) Kei1: a novel subunit of inositolphosphorylceramide synthase, essential for its enzyme activity and Golgi localization. *Mol. Biol. Cell*. **20**, 4444–57

401. Uemura, S., Kihara, A., Inokuchi, J.-I., and Igarashi, Y. (2003) Csg1p and newly identified Csh1p function in mannosylinositol phosphorylceramide synthesis by interacting with Csg2p. *J. Biol. Chem.* **278**, 45049–55

402. Dickson, R. C., Nagiec, E. E., Skrzypek, M., Tillman, P., Wells, G. B., and Lester, R. L. (1997) Sphingolipids are potential heat stress signals in Saccharomyces. *J. Biol. Chem.* **272**, 30196–200

403. Sawai, H., Okamoto, Y., Luberto, C., Mao, C., Bielawska, A., Domae, N., and Hannun, Y. A. (2000) Identification of ISC1 (YER019w) as inositol phosphosphingolipid phospholipase C in Saccharomyces cerevisiae. *J. Biol. Chem.* **275**, 39793–8

404. Brice, S. E., Alford, C. W., and Cowart, L. A. (2009) Modulation of sphingolipid metabolism by the phosphatidylinositol-4-phosphate phosphatase Sac1p through regulation of phosphatidylinositol in Saccharomyces cerevisiae. *J. Biol. Chem.* **284**, 7588–7596

405. Jesch, S. A., Gaspar, M. L., Stefan, C. J., Aregullin, M. A., and Henry, S. A. (2010) Interruption of inositol sphingolipid synthesis triggers Stt4p-dependent

protein kinase C signaling. *J. Biol. Chem.* **285**, 41947–60

406. Yano, T., Inukai, M., and Isono, F. (2004) Deletion of OSH3 gene confers resistance against ISP-1 in Saccharomyces cerevisiae. *Biochem. Biophys. Res. Commun.* **315**, 228–234

407. Dickson, R. C. (1998) SPHINGOLIPID FUNCTIONS IN *SACCHAROMYCES CEREVISIAE* : Comparison to Mammals. *Annu. Rev. Biochem.* **67**, 27–48

408. Yetukuri, L., Ekroos, K., Vidal-Puig, A., and Orešič, M. (2008) Informatics and computational strategies for the study of lipids. *Mol. BioSyst.* **4**, 121–127

409. Shevchenko, A., and Simons, K. (2010) Lipidomics: coming to grips with lipid diversity. *Nat. Rev. Mol. Cell Biol.* **11**, 593–598

410. Wullschleger, S., Loewith, R., and Hall, M. N. (2006) TOR signaling in growth and metabolism. *Cell*. **124**, 471–84

411. Huber, A., Bodenmiller, B., Uotila, A., Stahl, M., Wanka, S., Gerrits, B., Aebersold, R., and Loewith, R. (2009) Characterization of the rapamycin-sensitive phosphoproteome reveals that Sch9 is a central coordinator of protein synthesis. *Genes Dev.* **23**, 1929–43

412. Soulard, A., Cremonesi, A., Moes, S., Schütz, F., Jenö, P., and Hall, M. N. (2010) The rapamycin-sensitive phosphoproteome reveals that TOR controls protein kinase A toward some but not all substrates. *Mol. Biol. Cell*. **21**, 3475–86

413. Helliwell, S. B., Howald, I., Barbet, N., and Hall, M. N. (1998) TOR2 is part of two related signaling pathways coordinating cell growth in Saccharomyces cerevisiae. *Genetics*. **148**, 99–112

414. Aronova, S., Wedaman, K., Aronov, P. A., Fontes, K., Ramos, K., Hammock, B. D., and Powers, T. (2008) Regulation of ceramide biosynthesis by TOR complex 2. *Cell Metab.* **7**, 148–58

415. Dickson, R. C. (2008) More chores for TOR: de novo ceramide synthesis. *Cell Metab.* **7**, 99–100

416. Shimobayashi, M., Oppliger, W., Moes, S., Jenö, P., and Hall, M. N. (2013) TORC1-regulated protein kinase Npr1 phosphorylates Orm to stimulate complex sphingolipid synthesis. *Mol. Biol. Cell*. **24**, 870–881

417. Roelants, F. M., Breslow, D. K., Muir, A., Weissman, J. S., and Thorner, J. (2011) Protein kinase Ypk1 phosphorylates regulatory proteins Orm1 and Orm2 to control sphingolipid homeostasis in Saccharomyces cerevisiae. *Proc. Natl. Acad. Sci. U. S. A.* **108**, 19222–7

418. Sun, Y., Miao, Y., Yamane, Y., Zhang, C., Shokat, K. M., Takematsu, H.,

Kozutsumi, Y., and Drubin, D. G. (2012) Orm protein phosphoregulation mediates transient sphingolipid biosynthesis response to heat stress via the Pkh-Ypk and Cdc55-PP2A pathways. *Mol. Biol. Cell*. **23**, 2388–98

419. Muir, A., Ramachandran, S., Roelants, F. M., Timmons, G., and Thorner, J. (2014) TORC2-dependent protein kinase Ypk1 phosphorylates ceramide synthase to stimulate synthesis of complex sphingolipids. *Elife*. **3**, 1–34

420. Muir, A., Roelants, F. M., Timmons, G., Leskoske, K. L., and Thorner, J. (2015) Down-regulation of TORC2-Ypk1 signaling promotes MAPK-independent survival under hyperosmotic stress. *Elife*. 10.7554/eLife.09336

421. Powers, T., Aronova, S., and Niles, B. (2010) TORC2 and Sphingolipid Biosynthesis and Signaling: Lessons from Budding Yeast. *Enzym.* **27**, 177–197

422. Costanzo, M., Baryshnikova, A., Bellay, J., Kim, Y., Spear, E. D., Sevier, C. S., Ding, H., Koh, J. L. Y., Toufighi, K., Mostafavi, S., Prinz, J., St Onge, R. P., VanderSluis, B., Makhnevych, T., Vizeacoumar, F. J., Alizadeh, S., Bahr, S., Brost, R. L., Chen, Y., Cokol, M., Deshpande, R., Li, Z., Lin, Z.-Y., Liang, W., Marback, M., Paw, J., San Luis, B.-J., Shuteriqi, E., Tong, A. H. Y., van Dyk, N., Wallace, I. M., Whitney, J. a, Weirauch, M. T., Zhong, G., Zhu, H., Houry, W. a, Brudno, M., Ragibizadeh, S., Papp, B., Pál, C., Roth, F. P., Giaever, G., Nislow, C., Troyanskaya, O. G., Bussey, H., Bader, G. D., Gingras, A.-C., Morris, Q. D., Kim, P. M., Kaiser, C. a, Myers, C. L., Andrews, B. J., and Boone, C. (2010) The genetic landscape of a cell. *Science*. **327**, 425–31

423. Lange, Y., and Steck, T. L. (1997) Quantitation of the pool of cholesterol associated with Acyl-CoA. Cholesterol acyltransferase in human fibroblasts. *J. Biol. Chem.* **272**, 13103–13108

424. Maxfield, F. R., and Wüstner, D. (2002) Intracellular cholesterol transport. *J. Clin. Invest.* **110**, 891–898

425. Menon, A. K. (2018) Sterol gradients in cells. *Curr. Opin. Cell Biol.* **53**, 37–43

426. Burg, J. S., and Espenshade, P. J. (2011) Regulation of HMG-CoA reductase in mammals and yeast. *Prog. Lipid Res.* **50**, 403–10

427. Lorenz, R. T., Rodriguez, R. J., Lewis, T. A., and Parks, L. W. (1986) Characteristics of sterol uptake in Saccharomyces cerevisiae. *J. Bacteriol.* **167**, 981–5

428. Lorenz, R. T., and Parks, L. W. E. O. W. (1987) Regulation of Ergosterol Biosynthesis and Sterol Uptake in Sterol-Auxotrophic Yeast. *J. Bacteriol.* **169**, 3707–3711

429. Lewis, T. A., Taylor, F. R., and Parks, L. W. (1985) Involvement of heme biosynthesis in control of sterol uptake by Saccharomyces cerevisiae. *J. Bacteriol.* **163**, 199–207

430. Andreasen, A. A., and Stier, T. J. B. (1953) Anaerobic nutrition of Saccharomyces cerevisiae. I. Ergosterol requirement for growth in a defined medium. *J. Cell. Comp. Physiol.* **41**, 23–36

431. Volland, C., and Felix, F. (1984) Isolation and properties of 5-aminolevulinate synthase from the yeast Saccharomyces cerevisiae. *Eur. J. Biochem.* **142**, 551–7

432. Zavrel, M., Hoot, S. J., and White, T. C. (2013) Comparison of sterol import under aerobic and anaerobic conditions in three fungal species, Candida albicans, Candida glabrata, and Saccharomyces cerevisiae. *Eukaryot. Cell*. **12**, 725–38

433. Li, Y., and Prinz, W. a. (2004) ATP-binding Cassette (ABC) Transporters Mediate Nonvesicular, Raft-modulated Sterol Movement from the Plasma Membrane to the Endoplasmic Reticulum. *J. Biol. Chem.* **279**, 45226–45234

434. Kohut, P., Wüstner, D., Hronska, L., Kuchler, K., Hapala, I., and Valachovic, M. (2011) The role of ABC proteins Aus1p and Pdr11p in the uptake of external sterols in yeast: Dehydroergosterol fluorescence study. *Biochem. Biophys. Res. Commun.* **404**, 233–238

435. Clayton, R. B. (1964) The Utilization of Sterols By Insects. *J. Lipid Res.* **15**, 3–19

436. Maxfield, F. R. (2014) Role of Endosomes and Lysosomes in Human Disease. *Cold Spring Harb. Perspect. Biol.* **6**, a016931–a016931

437. Stewart, P. R., and Rudney, H. (1966) The biosynthesis of beta-hydroxy-beta-methylglutaryl coenzyme A in yeast. IV. The origin of the thioester bond of beta-hydroxy-beta-methylglutaryl coenzyme A. *J. Biol. Chem.* **241**, 1222–5

438. Dequin, S., Gloeckler, R., Herbert, C. J., and Boutelet, F. (1988) Cloning, sequencing and analysis of the yeast S. uvarum ERG10 gene encoding acetoacetyl CoA thiolase. *Curr. Genet.* **13**, 471–8

439. Espenshade, P. J., and Hughes, A. L. (2007) Regulation of Sterol Synthesis in Eukaryotes. *Annu. Rev. Genet.* **41**, 401–427

440. Kuranda, K., François, J., and Palamarczyk, G. (2010) The isoprenoid pathway and transcriptional response to its inhibitors in the yeast *Saccharomyces cerevisiae*. *FEMS Yeast Res.* **10**, 14–27

441. Jennings, S. M., Tsay, Y. H., Fisch, T. M., and Robinson, G. W. (1991) Molecular cloning and characterization of the yeast gene for squalene synthetase. *Proc. Natl. Acad. Sci. U. S. A.* **88**, 6038–42

442. Daum, G., Lees, N. D., Bard, M., and Dickson, R. (1998) Biochemistry, cell biology and molecular biology of lipids ofSaccharomyces cerevisiae. *Yeast*. **14**, 1471–1510

443. Beh, C. T., and Rine, J. (2004) A role for yeast oxysterol-binding protein homologs in endocytosis and in the maintenance of intracellular sterol-lipid distribution. *J. Cell Sci.* **117**, 2983–96

444. Jandrositz, A., Turnowsky, F., and Högenauer, G. (1991) The gene encoding squalene epoxidase from Saccharomyces cerevisiae: cloning and characterization. *Gene*. **107**, 155–60

445. Corey, E. J., Matsuda, S. P., and Bartel, B. (1994) Molecular cloning, characterization, and overexpression of ERG7, the Saccharomyces cerevisiae gene encoding lanosterol synthase. *Proc. Natl. Acad. Sci. U. S. A.* **91**, 2211–5

446. Espenshade, P. J. (2006) SREBPs: sterol-regulated transcription factors. *J. Cell Sci.* **119**, 973–6

447. Zhang, L., and Hach, A. (1999) Molecular mechanism of heme signaling in yeast: the transcriptional activator Hap1 serves as the key mediator. *Cell. Mol. Life Sci.* **56**, 415–26

448. Hampton, R. Y., Gardner, R. G., and Rine, J. (1996) Role of 26S proteasome and HRD genes in the degradation of 3-hydroxy-3-methylglutaryl-CoA reductase, an integral endoplasmic reticulum membrane protein. *Mol. Biol. Cell*. **7**, 2029–2044

449. Hampton, R. Y., and Bhakta, H. (1997) Ubiquitin-mediated regulation of 3-hydroxy-3-methylglutaryl-CoA reductase. *Proc. Natl. Acad. Sci. U. S. A.* **94**, 12944–8

450. Vik A, Åshild, and Rine, J. (2001) Upc2p and Ecm22p, dual regulators of sterol biosynthesis in Saccharomyces cerevisiae. *Mol. Cell. Biol.* **21**, 6395–405

451. Lev, S., Halevy, D. Ben, Peretti, D., and Dahan, N. (2008) The VAP protein family: from cellular functions to motor neuron disease. *Trends Cell Biol.* **18**, 282–290

452. Pietrangelo, A., and Ridgway, N. D. (2018) Bridging the molecular and biological functions of the oxysterol-binding protein family. *Cell. Mol. Life Sci.* **75**, 1–20

453. Ross, C. A., and Poirier, M. A. (2004) Protein aggregation and neurodegenerative disease. *Nat. Med.* **10**, S10–S17

454. Area-Gomez, E., de Groof, A., Bonilla, E., Montesinos, J., Tanji, K., Boldogh, I., Pon, L., and Schon, E. A. (2018) A key role for MAM in mediating mitochondrial dysfunction in Alzheimer disease. *Cell Death Dis.* **9**, 335

455. Gómez-Suaga, P., Bravo-San Pedro, J. M., González-Polo, R. A., Fuentes, J. M., and Niso-Santano, M. (2018) ER–mitochondria signaling in Parkinson's disease. *Cell Death Dis.* **9**, 337

456. Du, X., Kumar, J., Ferguson, C., Schulz, T. A., Ong, Y. S., Hong, W., Prinz, W. A.,

Parton, R. G., Brown, A. J., and Yang, H. (2011) A role for oxysterol-binding protein-related protein 5 in endosomal cholesterol trafficking. *J. Cell Biol.* **192**, 121–135

457. Nishimura, A. L., Mitne-Neto, M., Silva, H. C. A., Richieri-Costa, A., Middleton, S., Cascio, D., Kok, F., Oliveira, J. R. M., Gillingwater, T., Webb, J., Skehel, P., and Zatz, M. (2004) A Mutation in the Vesicle-Trafficking Protein VAPB Causes Late-Onset Spinal Muscular Atrophy and Amyotrophic Lateral Sclerosis. *Am. J. Hum. Genet.* **75**, 822–831

458. Teuling, E., Ahmed, S., Haasdijk, E., Demmers, J., Steinmetz, M. O., Akhmanova, A., Jaarsma, D., and Hoogenraad, C. C. (2007) Motor Neuron Disease-Associated Mutant Vesicle-Associated Membrane Protein-Associated Protein (VAP) B Recruits Wild-Type VAPs into Endoplasmic Reticulum-Derived Tubular Aggregates. *J. Neurosci.* **27**, 9801–9815

459. Kanekura, K., Nishimoto, I., Aiso, S., and Matsuoka, M. (2006) Characterization of amyotrophic lateral sclerosis-linked P56S mutation of vesicle-associated membrane protein-associated protein B (VAPB/ALS8). *J. Biol. Chem.* **281**, 30223–30233

460. Kuijpers, M., van Dis, V., Haasdijk, E. D., Harterink, M., Vocking, K., Post, J. A., Scheper, W., Hoogenraad, C. C., and Jaarsma, D. (2014) Amyotrophic lateral sclerosis (ALS)-associated VAPB-P56S inclusions represent an ER quality control compartment. *Acta Neuropathol. Commun.* **2**, 1

461. Moustaqim-Barrette, A., Lin, Y. Q., Pradhan, S., Neely, G. G., Bellen, H. J., and Tsuda, H. (2014) The amyotrophic lateral sclerosis 8 protein, VAP, is required for ER protein quality control. *Hum. Mol. Genet.* **23**, 1975–89

462. Darbyson, A., and Ngsee, J. K. (2016) Oxysterol-binding protein ORP3 rescues the Amyotrophic Lateral Sclerosis-linked mutant VAPB phenotype. *Exp. Cell Res.* **341**, 18–31

463. Mochizuki, S., Miki, H., Zhou, R., Kido, Y., Nishimura, W., Kikuchi, M., and Noda, Y. (2018) Oxysterol-binding protein-related protein (ORP) 6 localizes to the ER and ER-plasma membrane contact sites and is involved in the turnover of PI4P in cerebellar granule neurons. *Exp. Cell Res.* **370**, 601–612

464. Herold, C., Hooli, B. V, Mullin, K., Liu, T., Roehr, J. T., Mattheisen, M., Parrado, A. R., Bertram, L., Lange, C., and Tanzi, R. E. (2016) Family-based association analyses of imputed genotypes reveal genome-wide significant association of Alzheimer's disease with OSBPL6, PTPRG, and PDCL3. *Mol. Psychiatry*. **21**, 1608–1612

465. Del Bel, L. M., and Brill, J. A. (2018) Sac1, a lipid phosphatase at the interface of vesicular and nonvesicular transport. *Traffic*. **19**, 301–318

466. Rao, M., Song, W., Jiang, A., Shyr, Y., Lev, S., Greenstein, D., Brantley-Sieders,

D., and Chen, J. (2012) VAMP-Associated Protein B (VAPB) Promotes Breast Tumor Growth by Modulation of Akt Activity. *PLoS One*. **7**, e46281

467. Tokuda, E., Itoh, T., Hasegawa, J., Ijuin, T., Takeuchi, Y., Irino, Y., Fukumoto, M., and Takenawa, T. (2014) Phosphatidylinositol 4-phosphate in the Golgi apparatus regulates cell-cell adhesion and invasive cell migration in human breast cancer. *Cancer Res.* **74**, 3054–66

468. Guo, X., Zhang, L., Fan, Y., Zhang, D., Qin, L., Dong, S., and Li, G. (2017) Oxysterol-Binding Protein-Related Protein 8 Inhibits Gastric Cancer Growth Through Induction of ER Stress, Inhibition of Wnt Signaling, and Activation of Apoptosis. *Oncol. Res. Featur. Preclin. Clin. Cancer Ther.* **25**, 799–808

469. Zhong, W., Qin, S., Zhu, B., Pu, M., Liu, F., Wang, L., Ye, G., Yi, Q., and Yan, D. (2015) Oxysterol-binding protein-related protein 8 (ORP8) increases sensitivity of hepatocellular carcinoma cells to Fas-mediated apoptosis. *J. Biol. Chem.* **290**, 8876–87

470. Koga, Y., Ishikawa, S., Nakamura, T., Masuda, T., Nagai, Y., Takamori, H., Hirota, M., Kanemitsu, K., Baba, Y., and Baba, H. (2008) Oxysterol binding protein-related protein-5 is related to invasion and poor prognosis in pancreatic cancer. *Cancer Sci.* **99**, 2387–2394

471. Nagano, K., Imai, S., Zhao, X., Yamashita, T., Yoshioka, Y., Abe, Y., Mukai, Y., Kamada, H., Nakagawa, S., Tsutsumi, Y., and Tsunoda, S. I. (2015) Identification and evaluation of metastasis-related proteins, oxysterol binding protein-like 5 and calumenin, in lung tumors. *Int. J. Oncol.* **47**, 195–203

472. Luo, X., Cheng, C., Tan, Z., Li, N., Tang, M., Yang, L., and Cao, Y. (2017) Emerging roles of lipid metabolism in cancer metastasis. *Mol. Cancer*. **16**, 76

473. Altan-Bonnet, N., and Balla, T. (2012) Phosphatidylinositol 4-kinases: hostages harnessed to build panviral replication platforms. *Trends Biochem. Sci.* **37**, 293–302

474. Lee, C. (2012) Roles of phosphoinositides and phosphoinositides kinases in hepatitis C virus RNA replication. *Arch. Pharm. Res.* **35**, 1701–11

475. Li, H., Yang, X., Yang, G., Hong, Z., Zhou, L., Yin, P., Xiao, Y., Chen, L., Chung, R. T., and Zhang, L. (2014) Hepatitis C virus NS5A hijacks ARFGAP1 to maintain a phosphatidylinositol 4-phosphate-enriched microenvironment. *J. Virol.* **88**, 5956–66

476. Amako, Y., Sarkeshik, A., Hotta, H., Yates, J., and Siddiqui, A. (2009) Role of oxysterol binding protein in hepatitis C virus infection. *J. Virol.* **83**, 9237–46

477. Park, I.-W., Ndjomou, J., Wen, Y., Liu, Z., Ridgway, N. D., Kao, C. C., and He, J. J. (2013) Inhibition of HCV Replication by Oxysterol-Binding Protein-Related Protein 4 (ORP4) through Interaction with HCV NS5B and Alteration of Lipid

Droplet Formation. *PLoS One*. **8**, e75648

478. Ishikawa-Sasaki, K., Nagashima, S., Taniguchi, K., and Sasaki, J. (2018) A model of OSBP-mediated cholesterol supply to Aichi virus RNA replication sites involving protein-protein interactions among viral proteins, ACBD3, OSBP, VAP-A/B, and SAC1. *J. Virol.* **92**, JVI.01952-17

479. El Kasmi, I., Khadivjam, B., Lackman, M., Duron, J., Bonneil, E., Thibault, P., and Lippé, R. (2018) Extended Synaptotagmin 1 Interacts with Herpes Simplex Virus 1 Glycoprotein M and Negatively Modulates Virus-Induced Membrane Fusion. *J. Virol.* **92**, 1–19

480. Barajas, D., Xu, K., Sharma, M., Wu, C. Y., and Nagy, P. D. (2014) Tombusviruses upregulate phospholipid biosynthesis via interaction between p33 replication protein and yeast lipid sensor proteins during virus replication in yeast. *Virology*. **471**–**473**, 72–80

481. Barajas, D., Xu, K., de Castro Martín, I. F., Sasvari, Z., Brandizzi, F., Risco, C., and Nagy, P. D. (2014) Co-opted Oxysterol-Binding ORP and VAP Proteins Channel Sterols to RNA Virus Replication Sites via Membrane Contact Sites. *PLoS Pathog.* **10**, e1004388

482. Holthuis, J. C. M., and Levine, T. P. (2005) Lipid traffic: floppy drives and a superhighway. *Nat. Rev. Mol. Cell Biol.* **6**, 209–220

483. Holthuis, J. C. M., and Menon, A. K. (2014) Lipid landscapes and pipelines in membrane homeostasis. *Nature*. **510**, 48–57

484. Gallo, A., Vannier, C., and Galli, T. (2016) Endoplasmic Reticulum–Plasma Membrane Associations:Structures and Functions. *Annu. Rev. Cell Dev. Biol.* **32**, 279–301

485. Eisenberg-Bord, M., Shai, N., Schuldiner, M., and Bohnert, M. (2016) A Tether Is a Tether Is a Tether: Tethering at Membrane Contact Sites. *Dev. Cell*. **39**, 395–409

486. Maxfield, F. R., and Menon, A. K. (2006) Intracellular sterol transport and distribution. *Curr. Opin. Cell Biol.* **18**, 379–385

487. Maxfield, F. R., and van Meer, G. (2010) Cholesterol, the central lipid of mammalian cells. *Curr. Opin. Cell Biol.* **22**, 422–429

488. Dittman, J. S., and Menon, A. K. (2017) Speed Limits for Nonvesicular Intracellular Sterol Transport. *Trends Biochem. Sci.* **42**, 90–97

489. Baumann, N. A., Sullivan, D. P., Ohvo-Rekilä, H., Simonot, C., Pottekat, A., Klaassen, Z., Beh, C. T., and Menon, A. K. (2005) Transport of newly synthesized sterol to the sterol-enriched plasma membrane occurs via nonvesicular

equilibration. *Biochemistry*. [online] http://pubs.acs.org/doi/abs/10.1021/bi048296z (Accessed September 24, 2014)

490. Wong, L. H., and Levine, T. P. (2016) Lipid transfer proteins do their thing anchored at membrane contact sites… but what is their thing? *Biochem. Soc. Trans.* **44**, 517–527

491. Raychaudhuri, S., Im, Y. J., Hurley, J. H., and Prinz, W. A. (2006) Nonvesicular sterol movement from plasma membrane to ER requires oxysterol-binding protein-related proteins and phosphoinositides. *J. Cell Biol.* **173**, 107–19

492. Tong, J., Manik, M. K., and Im, Y. J. (2018) Structural basis of sterol recognition and nonvesicular transport by lipid transfer proteins anchored at membrane contact sites. *Proc. Natl. Acad. Sci. U. S. A.* **115**, E856–E865

493. Wilhelm, L. P., Wendling, C., Védie, B., Kobayashi, T., Chenard, M.-P., Tomasetto, C., Drin, G., and Alpy, F. (2017) STARD3 mediates endoplasmic reticulum-to-endosome cholesterol transport at membrane contact sites. *EMBO J.* **36**, 1412–1433

494. Raiborg, C., Wenzel, E. M., Pedersen, N. M., and Stenmark, H. (2016) Phosphoinositides in membrane contact sites. *Biochem. Soc. Trans.* **44**, 425–30

495. Schuldiner, M., Collins, S. R., Thompson, N. J., Denic, V., Bhamidipati, A., Punna, T., Ihmels, J., Andrews, B., Boone, C., Greenblatt, J. F., Weissman, J. S., and Krogan, N. J. (2005) Exploration of the Function and Organization of the Yeast Early Secretory Pathway through an Epistatic Miniarray Profile. *Cell*. **123**, 507–519

496. Franz, A., Maass, K., and Seedorf, M. (2007) A complex peptide-sorting signal, but no mRNA signal, is required for the Sec-independent transport of Ist2 from the yeast ER to the plasma membrane. *FEBS Lett.* **581**, 401–5

497. Georgiev, A. G., Johansen, J., Ramanathan, V. D., Sere, Y. Y., Beh, C. T., and Menon, A. K. (2013) Arv1 Regulates PM and ER Membrane Structure and Homeostasis But is Dispensable for Intracellular Sterol Transport. *Traffic*. **14**, 912–921

498. Maxfield, F. R., and Wüstner, D. (2012) Analysis of Cholesterol Trafficking with Fluorescent Probes. in *Methods in cell biology*, pp. 367–393, **108**, 367–393

499. Kaplan, M. R., and Simoni, R. D. (1985) Transport of cholesterol from the endoplasmic reticulum to the plasma membrane. *J. Cell Biol.* **101**, 446–53

500. Graham, T. R., and Emr, S. D. (1991) Compartmental organization of Golgi-specific protein modification and vacuolar protein sorting events defined in a yeast sec18 (NSF) mutant. *J. Cell Biol.* **114**, 207–18

501. Eakle, K., Bernstein, M., and Emr, S. (1988) Characterization of a component of the yeast secretion machinery: identification of the SEC18 gene product. *Mol. Cell. Biol.* 10.1128/MCB.8.10.4098.Updated

502. Puoti, A., Desponds, C., and Conzelmann, A. (1991) Biosynthesis of mannosylinositolphosphoceramide in Saccharomyces cerevisiae is dependent on genes controlling the flow of secretory vesicles from the endoplasmic reticulum to the Golgi. *J. Cell Biol.* **113**, 515–25

503. Ghaemmaghami, S., Huh, W.-K., Bower, K., Howson, R. W., Belle, A., Dephoure, N., O'Shea, E. K., and Weissman, J. S. (2003) Global analysis of protein expression in yeast. *Nature*. **425**, 737–741

504. Fei, W., Alfaro, G., Muthusamy, B.-P., Klaassen, Z., Graham, T. R., Yang, H., and Beh, C. T. (2008) Genome-Wide Analysis of Sterol-Lipid Storage and Trafficking in *Saccharomyces cerevisiae*. *Eukaryot. Cell*. **7**, 401–414

505. Hanson, P. K., Malone, L., Birchmore, J. L., and Nichols, J. W. (2003) Lem3p Is Essential for the Uptake and Potency of Alkylphosphocholine Drugs, Edelfosine and Miltefosine. *J. Biol. Chem.* **278**, 36041–36050

506. Zaremberg, V., Gajate, C., Cacharro, L. M., Mollinedo, F., and McMaster, C. R. (2005) Cytotoxicity of an anti-cancer lysophospholipid through selective modification of lipid raft composition. *J. Biol. Chem.* **280**, 38047–58

507. Aresta-Branco, F., Cordeiro, A. M., Marinho, H. S., Cyrne, L., Antunes, F., and de Almeida, R. F. M. (2011) Gel domains in the plasma membrane of Saccharomyces cerevisiae: highly ordered, ergosterol-free, and sphingolipid-enriched lipid rafts. *J. Biol. Chem.* **286**, 5043–54

508. Greenberg, M. L., and Axelrod, D. (1993) Anomalously slow mobility of fluorescent lipid probes in the plasma membrane of the yeast Saccharomyces cerevisiae. *J. Membr. Biol.* **131**, 115–27

509. Pelham, J. V.-T. and H. R. B. (2003) Slow Diffusion of Proteins in the Yeast Plasma Membrane Allows Polarity to Be Maintained by Endocytic Cycling. *Curr. Biol.* **13**, 1636–1640

510. Maxfield, F. R., and van Meer, G. (2011) Cholesterol, the central lipid of mammalian cells. *Mol. Cell. Biol.* **22**, 422–429

511. Daum, G., Lees, N. D., Bard, M., and Dickson, R. (1998) Biochemistry, cell biology and molecular biology of lipids of Saccharomyces cerevisiae. *Yeast*. **14**, 1471–510

512. John, K., Kubelt, J., Müller, P., Wüstner, D., and Herrmann, A. (2002) Rapid transbilayer movement of the fluorescent sterol dehydroergosterol in lipid membranes. *Biophys. J.* **83**, 1525–34

513. Leventis, R., and Silvius, J. R. (2001) Use of cyclodextrins to monitor transbilayer movement and differential lipid affinities of cholesterol. *Biophys. J.* **81**, 2257–67

514. Steck, T. L., Ye, J., and Lange, Y. (2002) Probing red cell membrane cholesterol movement with cyclodextrin. *Biophys. J.* **83**, 2118–25

515. Schuberth, C., and Wedlich-Söldner, R. (2015) Building a patchwork — The yeast plasma membrane as model to study lateral domain formation. *Biochim. Biophys. Acta - Mol. Cell Res.* **1853**, 767–774

516. Schneiter, R., Brügger, B., Sandhoff, R., Zellnig, G., Leber, A., Lampl, M., Athenstaedt, K., Hrastnik, C., Eder, S., Daum, G., Paltauf, F., Wieland, F. T., and Kohlwein, S. D. (1999) Electrospray ionization tandem mass spectrometry (ESI-MS/MS) analysis of the lipid molecular species composition of yeast subcellular membranes reveals acyl chain-based sorting/remodeling of distinct molecular species en route to the plasma membrane. *J. Cell Biol.* **146**, 741–54

517. Carman, G. M., and Han, G.-S. (2009) Regulation of phospholipid synthesis in yeast. *J. Lipid Res.* **50 Suppl**, S69-73

518. Carman, G. M., and Han, G.-S. (2011) Regulation of Phospholipid Synthesis in the Yeast *Saccharomyces cerevisiae*. *Annu. Rev. Biochem.* **80**, 859–883

519. Liu, M., Huang, C., Polu, S. R., Schneiter, R., and Chang, a. (2012) Regulation of sphingolipid synthesis through Orm1 and Orm2 in yeast. *J. Cell Sci.* **125**, 2428–2435

520. Amberg, D. C., Burke, D. J., and Strathern, J. N. (2005) *Methods in Yeast Genetics: A Cold Spring Harbor Laboratory Course Manual, 2005 Edition*

521. Longtine, M. S., Iii, A. M. K., Demarini, D. J., and Shah, N. G. (1998) Additional Modules for Versatile and Economical PCR-based Gene Deletion and Modification in Saccharomyces cerevisiae. *Yeast*. **961**, 953–961

522. Jiang, B., Brown, J. L., Sheraton, J., Fortin, N., and Bussey, H. (1994) A new family of yeast genes implicated in ergosterol synthesis is related to the human oxysterol binding protein. *Yeast*. **10**, 341–353

523. Robinson, J. S., Klionsky, D. J., Banta, L. M., and Emr, S. D. (1988) Protein sorting in Saccharomyces cerevisiae: isolation of mutants defective in the delivery and processing of multiple vacuolar hydrolases. *Mol. Cell. Biol.* **8**, 4936–48

524. Sikorski, R. S., and Hieter, P. (1989) A system of shuttle vectors and yeast host strains designed for efficient manipulation of DNA in Saccharomyces cerevisiae. *Genetics*. **122**, 19–27

525. Gietz, R. D., and Sugino, A. (1988) New yeast-Escherichia coli shuttle vectors constructed with in vitro mutagenized yeast genes lacking six-base pair restriction

sites. *Gene*. **74**, 527–34

526. Wright, R. (2000) Transmission electron microscopy of yeast. *Microsc. Res. Tech.* **51**, 496–510

527. Kremer, J. R., Mastronarde, D. N., and McIntosh, J. R. (1996) Computer Visualization of Three-Dimensional Image Data Using IMOD. *J. Struct. Biol.* **116**, 71–76

528. Schneider, C. A., Rasband, W. S., and Eliceiri, K. W. (2012) NIH Image to ImageJ: 25 years of image analysis. *Nat. Methods*. **9**, 671–5

529. Johansen, J., Alfaro, G., and Beh, C. T. (2016) Polarized Exocytosis Induces Compensatory Endocytosis by Sec4p-Regulated Cortical Actin Polymerization. *PLoS Biol.* **14**, 1–24

530. Ansari, N., Müller, S., Stelzer, E. H. K., and Pampaloni, F. (2013) Quantitative 3D Cell-Based Assay Performed with Cellular Spheroids and Fluorescence Microscopy. in *Methods in cell biology*, pp. 295–309, **113**, 295–309

531. Billheimer, J. T., Tavani, D., and Nes, W. R. (1981) Effect of a dispersion of cholesterol in Triton WR-1339 on acyl CoA: cholesterol acyltransferase in rat liver microsomes. *Anal. Biochem.* **111**, 331–5

532. Chan, R. B., Oliveira, T. G., Cortes, E. P., Honig, L. S., Duff, K. E., Small, S. A., Wenk, M. R., Shui, G., and Di Paolo, G. (2012) Comparative Lipidomic Analysis of Mouse and Human Brain with Alzheimer Disease. *J. Biol. Chem.* **287**, 2678–2688

533. Guan, X. L., Riezman, I., Wenk, M. R., and Riezman, H. (2010) Yeast Lipid Analysis and Quantification by Mass Spectrometry. in *Methods in enzymology*, pp. 369–391, **470**, 369–391

534. Vorkas, P. A., Isaac, G., Anwar, M. A., Davies, A. H., Want, E. J., Nicholson, J. K., and Holmes, E. (2015) Untargeted UPLC-MS Profiling Pipeline to Expand Tissue Metabolome Coverage: Application to Cardiovascular Disease. *Anal. Chem.* **87**, 4184–4193

535. Ohashi, A., Gibson, J., Gregor, I., and Schatz, G. (1982) Import of proteins into mitochondria. The precursor of cytochrome c1 is processed in two steps, one of them heme-dependent. *J. Biol. Chem.* **257**, 13042–7

536. Beh, C. T., Brizzio, V., and Rose, M. D. (1997) KAR5 encodes a novel pheromone-inducible protein required for homotypic nuclear fusion. *J. Cell Biol.* **139**, 1063–76

537. Sullivan, D. P., Ohvo-Rekilä, H., Baumann, N. A., Beh, C. T., and Menon, A. K. (2006) Sterol trafficking between the endoplasmic reticulum and plasma membrane in yeast. *Biochem. Soc. Trans.* **34**, 356–358

538. Sherman, F. (2002) Getting started with yeast. *Methods Enzymol.* **350**, 3–41

539. Yamaguchi, M., Namiki, Y., Okada, H., Mori, Y., Furukawa, H., Wang, J., Ohkusu, M., and Kawamoto, S. (2011) Structome of Saccharomyces cerevisiae determined by freeze-substitution and serial ultrathin-sectioning electron microscopy. *Microscopy*. **60**, 321–335

540. Hönscher, C., and Ungermann, C. (2014) A close-up view of membrane contact sites between the endoplasmic reticulum and the endolysosomal system: From yeast to man. *Crit. Rev. Biochem. Mol. Biol.* **9238**, 1–7

541. Henne, W. M., Liou, J., and Emr, S. D. (2015) Molecular mechanisms of inter-organelle ER-PM contact sites. *Curr. Opin. Cell Biol.* **35**, 123–30

542. Schuck, S., Prinz, W. A., Thorn, K. S., Voss, C., and Walter, P. (2009) Membrane expansion alleviates endoplasmic reticulum stress independently of the unfolded protein response. *J. Cell Biol.* **187**, 525–536

543. Manford, A., Xia, T., Saxena, A. K., Stefan, C., Hu, F., Emr, S. D., and Mao, Y. (2010) Crystal structure of the yeast Sac1: implications for its phosphoinositide phosphatase function. *EMBO J.* **29**, 1489–1498

544. Giordano, F., Saheki, Y., Idevall-Hagren, O., Colombo, S. F., Pirruccello, M., Milosevic, I., Gracheva, E. O., Bagriantsev, S. N., Borgese, N., and De Camilli, P. (2013) PI(4,5)P2-Dependent and Ca2+-Regulated ER-PM interactions mediated by the extended synaptotagmins. *Cell*. **153**, 1494–1509

545. Jin, N., Mao, K., Jin, Y., Tevzadze, G., Kauffman, E. J., Park, S., Bridges, D., Loewith, R., Saltiel, A. R., Klionsky, D. J., and Weisman, L. S. (2014) Roles for PI(3,5)P2 in nutrient sensing through TORC1. *Mol. Biol. Cell*. **25**, 1171–85

546. Wolf, W., Meese, K., and Seedorf, M. (2014) Ist2 in the yeast cortical endoplasmic reticulum promotes trafficking of the amino acid transporter Bap2 to the plasma membrane. *PLoS One*. **9**, 1–13

547. Horenkamp, F. A., Valverde, D. P., Nunnari, J., and Reinisch, K. M. (2018) Molecular basis for sterol transport by StART-like lipid transfer domains. *EMBO J.* **37**, 1–15

548. Kralt, A., Carretta, M., Mari, M., Reggiori, F., Steen, A., Poolman, B., and Veenhoff, L. M. (2015) Intrinsically Disordered Linker and Plasma Membrane-Binding Motif Sort Ist2 and Ssy1 to Junctions. *Traffic*. **16**, 135–147

549. Karanasios, E., Han, G.-S., Xu, Z., Carman, G. M., and Siniossoglou, S. (2010) A phosphorylation-regulated amphipathic helix controls the membrane translocation and function of the yeast phosphatidate phosphatase. *Proc. Natl. Acad. Sci.* **107**, 17539–17544

550. Miner, G. E., Starr, M. L., Hurst, L. R., and Fratti, R. A. (2017) Deleting the DAG kinase Dgk1 augments yeast vacuole fusion through increased Ypt7 activity and altered membrane fluidity. *Traffic*. **18**, 315–329

551. Wolinski, H., Hofbauer, H. F., Hellauer, K., Cristobal-Sarramian, A., Kolb, D., Radulovic, M., Knittelfelder, O. L., Rechberger, G. N., and Kohlwein, S. D. (2015) Seipin is involved in the regulation of phosphatidic acid metabolism at a subdomain of the nuclear envelope in yeast. *Biochim. Biophys. Acta - Mol. Cell Biol. Lipids*. **1851**, 1450–1464

552. Soto-Cardalda, A., Fakas, S., Pascual, F., Choi, H.-S., and Carman, G. M. (2012) Phosphatidate phosphatase plays role in zinc-mediated regulation of phospholipid synthesis in yeast. *J. Biol. Chem.* **287**, 968–77

553. LeBlanc, M. A., and McMaster, C. R. (2010) Lipid binding requirements for oxysterol-binding protein Kes1 inhibition of autophagy and endosome-trans-Golgi trafficking pathways. *J. Biol. Chem.* **285**, 33875–84

554. Jozsef Maleth, Seok Choi, Shmuel Muallem, M. A. (2014) Translocation between PI(4,5)P2-poor and PI(4,5)P2-rich microdomains during store depletion determines STIM1 conformation and Orai1 gating. *Nat. Commun.* **5**, 1–10

555. Hammond, G. R. V., Fischer, M. J., Anderson, K. E., Holdich, J., Koteci, A., Balla, T., and Irvine, R. F. (2012) PI4P and PI(4,5)P2 Are Essential But Independent Lipid Determinants of Membrane Identity. *Science (80-.).* **337**, 727–730

556. Gavin, A.-C., Bösche, M., Krause, R., Grandi, P., Marzioch, M., Bauer, A., Schultz, J., Rick, J. M., Michon, A.-M., Cruciat, C.-M., Remor, M., Höfert, C., Schelder, M., Brajenovic, M., Ruffner, H., Merino, A., Klein, K., Hudak, M., Dickson, D., Rudi, T., Gnau, V., Bauch, A., Bastuck, S., Huhse, B., Leutwein, C., Heurtier, M.-A., Copley, R. R., Edelmann, A., Querfurth, E., Rybin, V., Drewes, G., Raida, M., Bouwmeester, T., Bork, P., Seraphin, B., Kuster, B., Neubauer, G., and Superti-Furga, G. (2002) Functional organization of the yeast proteome by systematic analysis of protein complexes. *Nature*. **415**, 141–147

557. Tarassov, K., Messier, V., Landry, C. R., Radinovic, S., Serna Molina, M. M., Shames, I., Malitskaya, Y., Vogel, J., Bussey, H., and Michnick, S. W. (2008) An in vivo map of the yeast protein interactome. *Science*. **320**, 1465–70

558. Babu, M., Vlasblom, J., Pu, S., Guo, X., Graham, C., Bean, B. D. M., Burston, H. E., Vizeacoumar, F. J., Snider, J., Phanse, S., Fong, V., Tam, Y. Y. C., Davey, M., Hnatshak, O., Bajaj, N., Chandran, S., Punna, T., Christopolous, C., Wong, V., Yu, A., Zhong, G., Li, J., Stagljar, I., Conibear, E., Wodak, S. J., Emili, A., and Greenblatt, J. F. (2012) Interaction landscape of membrane-protein complexes in Saccharomyces cerevisiae. *Nature*. **489**, 585–589

559. Elbaz, Y., and Schuldiner, M. (2011) Staying in touch: the molecular era of organelle contact sites. *Trends Biochem. Sci.* **36**, 616–23

560. Zachowski, a (1993) Phospholipids in animal eukaryotic membranes: transverse asymmetry and movement. *Biochem. J.* **294**, 1–14

561. Pomorski, T., Holthuis, J. C. M., Herrmann, A., and van Meer, G. (2004) Tracking down lipid flippases and their biological functions. *J. Cell Sci.* **117**, 805–13

562. Simons, K., and Sampaio, J. L. (2011) Membrane organization and lipid rafts. *Cold Spring Harb. Perspect. Biol.* **3**, a004697

563. van Meer, G., and Sprong, H. (2004) Membrane lipids and vesicular traffic. *Curr. Opin. Cell Biol.* **16**, 373–378

564. Hu, J., Shibata, Y., Voss, C., Shemesh, T., Li, Z., Coughlin, M., Kozlov, M. M., Rapoport, T. a, and Prinz, W. a (2008) Membrane proteins of the endoplasmic reticulum induce high-curvature tubules. *Science*. **319**, 1247–1250

565. Yang, Y. S., and Strittmatter, S. M. (2007) The reticulons: a family of proteins with diverse functions. *Genome Biol.* **8**, 234

566. Hu, J., Shibata, Y., Zhu, P. P., Voss, C., Rismanchi, N., Prinz, W. a., Rapoport, T. a., and Blackstone, C. (2009) A Class of Dynamin-like GTPases Involved in the Generation of the Tubular ER Network. *Cell*. **138**, 549–561

567. Anwar, K., Klemm, R. W., Condon, A., Severin, K. N., Zhang, M., Ghirlando, R., Hu, J., Rapoport, T. a., and Prinz, W. a. (2012) The dynamin-like GTPase Sey1p mediates homotypic ER fusion in S. cerevisiae. *J. Cell Biol.* **197**, 209–217

568. Rogers, J. V, Arlow, T., Inkellis, E. R., Koo, T. S., and Rose, M. D. (2013) ER-associated SNAREs and Sey1p mediate nuclear fusion at two distinct steps during yeast mating. *Mol. Biol. Cell*. **24**, 3896–908

569. Bollen, I. C., and Higgins, J. A. (1980) Phospholipid asymmetry in rough- and smooth-endoplasmic-reticulum membranes of untreated and phenobarbital-treated rat liver. *Biochem. J.* **189**, 475–80

570. Fairn, G. D., Schieber, N. L., Ariotti, N., Murphy, S., Kuerschner, L., Webb, R. I., Grinstein, S., and Parton, R. G. (2011) High-resolution mapping reveals topologically distinct cellular pools of phosphatidylserine. *J. Cell Biol.* **194**, 257–275

571. Leventis, P. A., and Grinstein, S. (2010) The Distribution and Function of Phosphatidylserine in Cellular Membranes. *Annu. Rev. Biophys.* **39**, 407–427

572. McLaughlin, S., and Murray, D. (2005) Plasma membrane phosphoinositide organization by protein electrostatics. *Nature*. **438**, 605–611

573. Sun, Y., Thapa, N., Hedman, A. C., and Anderson, R. A. (2013) Phosphatidylinositol 4,5-bisphosphate: targeted production and signaling.

BioEssays. **35**, 513–22

574. Ghai, R., Du, X., Wang, H., Dong, J., Ferguson, C., Brown, A. J., Parton, R. G., Wu, J.-W., and Yang, H. (2017) ORP5 and ORP8 bind phosphatidylinositol-4, 5-biphosphate (PtdIns(4,5)P 2) and regulate its level at the plasma membrane. *Nat. Commun.* **8**, 757

575. Baby-Periyanayaki Muthusamy, Sumana Raychaudhuri, Paramasivam Natarajan, F. A., Ke Liu, W. A. P., Graham, and T. R., Muthusamy, B.-P., Raychaudhuri, S., Natarajan, P., Abe, F., Liu, K., Prinz, W. A., and Graham, T. R. (2009) Control of protein and sterol trafficking by antagonistic activities of a type IV P-type ATPase and oxysterol binding protein homologue. *Mol. Biol. Cell*. **20**, 2920–31

576. Menon, A K. (1995) Flippases. *Trends Cell Biol.* **5**, 355–60

577. van Meer, G., Halter, D., Sprong, H., Somerharju, P., and Egmond, M. R. (2006) ABC lipid transporters: Extruders, flippases, or flopless activators? *FEBS Lett.* **580**, 1171–1177

578. Devaux, P. F., Herrmann, A., Ohlwein, N., and Kozlov, M. M. (2008) How lipid flippases can modulate membrane structure. *Biochim. Biophys. Acta - Biomembr.* **1778**, 1591–1600

579. Puts, C. F., Lenoir, G., Krijgsveld, J., Williamson, P., and Holthuis, J. C. M. (2010) A P 4 -ATPase Protein Interaction Network Reveals a Link between Aminophospholipid Transport and Phosphoinositide Metabolism research articles. *J. Proteome Res.* **9**, 833–842

580. Mioka, T., Fujimura-Kamada, K., Mizugaki, N., Kishimoto, T., Sano, T., Nunome, H., Williams, D. E., Andersen, R. J., and Tanaka, K. (2018) Phospholipid flippases and Sfk1p, a novel regulator of phospholipid asymmetry, contribute to low permeability of the plasma membrane. *Mol. Biol. Cell*. **29**, 1203–1218

581. Hashida-Okado, T., Ogawa, A., Endo, M., Yasumoto, R., Takesako, K., and Kato, I. (1996) AUR1, a novel gene conferring aureobasidin resistance on Saccharomyces cerevisiae: a study of defective morphologies in Aur1p-depleted cells. *Mol. Gen. Genet.* **251**, 236–44

582. Heidler, S. A., and Radding, J. A. (1995) The AUR1 gene in Saccharomyces cerevisiae encodes dominant resistance to the antifungal agent aureobasidin A (LY295337). *Antimicrob. Agents Chemother.* **39**, 2765–2769

583. Grote, E., Carr, C., and Novick, P. (2000) Ordering the final events in yeast exocytosis. *J. Cell Biol.* **151**, 439–52

584. Guan, X. L., Souza, C. M., Pichler, H., et al., (2009) Functional Interactions between Sphingolipids and Sterols in Biological Membranes Regulating Cell Physiology. *Mol. Biol. Cell*. **20**, 2083–2095

Appendix

Table S.1. List of Saccharomyces cerevisiae and mammalian membrane contact site tether proteins and a brief description of their function

Membrane Interface	Yeast	Mammalian
PM-ER	Scs2p/22p	VAPA/VAPB
	Tcb1p-3p	E-Syt1-3
	Ist2p	TMEM16
	Ice2p	
		Junctophilins (JP1-4)
ER-mitochondria	ERMES (Mmm1p, Mdm10p, Mdm34p, Mdm12p)	
	EMC (Emc1p-6p)	
		PTPIP51 (RMD3)
		Mitofusin-2
MECA	Num1p	
	Mdm6p	
ER-Golgi	Nvj2p	
		OSBP/VAP
NVJ	Nvj1p-Vac8p	
	Mdm1p	Snx14
	Osh1p/Scs2p?	
ER-Early/Late Endosome		ORP1L
		STARD3, STARD3L
		Protrudin
		Rab3
		SNX2
LD to ER	Sei1p, Ldb16p	BSCL2
		FATP1 DGAT2 (C. Elegans)
Peroxisome to ER	Inp1p, Pex3p, Pex30p	
		ACBD5/VAPA

Table S.2. List of yeast glycerophospholipid biosynthesis genes with their corresponding enzymatic name and function

Yeast Gene	Enzyme	Function
ACC1/HFA1	Acetyl-CoA Carboxylase	Fatty Acid Synthesis
FAS1-2	Fatty Acid Synthase (Cytosolic)	Fatty Acid Synthesis
CEM1/OAR1/HTD2/ETR1/PPT2	Fatty Acid Synthase(mitochondrial)	Fatty Acid Synthesis
ELO1-3	Fatty Acid elongase	Fatty Acid Synthesis
OLE1	the acyl-CoA Δ9-desaturase	Fatty Acid Synthesis
SCT1/GPT2	Glycerol-3-Phosphate acyltransferases	PA synthesis
SLC1/ALE1	lysophospholipid acyltransferase	PA synthesis
DGK1	DAG Kinase	PA synthesis
PAH1/LPP1/DPP1	PA phosphatase	DAG synthesis
PHO85/PHO80	Protein Kinase complex	DAG synthesis
CDC28	Cyclin-dependent kinase	DAG synthesis
NEM1/SPO7	Pah1 Phosphatase complex	DAG synthesis
CDS1	CDP-DAG Synthase	CDP-DAG Pathway
CHO1	CDP-DAG-serine phosphatidyltransferase	CDP-DAG Pathway (PS synthesis)
PSD1-2	phosphatidylserine decarboxylase	CDP-DAG Pathway (PE synthesis)
CHO2	phosphatidylethanolamine N-methyltransferase	CDP-DAG Pathway (PC synthesis)
OPI3	phospholipid methyltransferase	CDP-DAG Pathway (PC synthesis)
HNM1	PM Cho/Eth Transporter	Kennedy Pathway
CKI1	choline kinase	Kennedy Pathway (PC Synthesis)
PCT1	phosphocholine cytidylyltransferase	Kennedy Pathway (PC Synthesis)
CPT1	choline phosphotransferase	Kennedy Pathway (PC Synthesis)
EKI1	ethanolamine kinase	Kennedy Pathway (PE Synthesis)
ECT1	phosphoethanolamine cytidylyltransferase	Kennedy Pathway (PE Synthesis)
EPT1	ethanolaminephosphotransferase	Kennedy Pathway (PE Synthesis)
PIS1	Phosphoinositol synthase	PI synthesis
ITR1-2	Myo-inositol transporter	PI synthesis
INO1	Inositol-3 phosphate synthase	PI synthesis
INM1	Inositol monophosphatase	PI synthesis
PLB1-3/NTE1	Phospholipase B	Phospholipid turnover
GDE1	GroPCho-phosphodiesterase	Phospholipid turnover
PLC1	Phospholipase C	PI45P2 turnover (Signaling)

SPO14 (PLD1)	Phospholipase D	PC turnover
FMP30	Phospholipase D	NAPE turnover
DGA1/LRO1	DAG Acyltransferase	TAG synthesis
ARE1/ARE2	Sterol Acyltransferase	Sterol Esterification
TGL3-5	TAG Lipase	TAG metabolism (DAG synthesis)
YJU3	MAG lipase	TAG metabolism
YEH1-2/TGL1	Sterol Ester Hydrolase	Sterol metabolism
INO2/INO4	UASino Transcription factor	Phospholipid transcriptional regulation
OPI1	UASino transcriptional repressor	Phospholipid transcriptional regulation
YET1/YET3	UASino transcriptional Activator	Phospholipid transcriptional regulation
IRE1	Ser/Thr Kinase-endoribonuclease	UPR activation
HAC1	Transcription Factor	UPR activation

Table S.3. List of yeast and human phosphoinositide kinase and phosphatase genes with their corresponding functions and preferred substrates.

Yeast Gene	Human Gene	Enzymatic Function	Preferred substrate
Kinases			
STT4	PI4KIIIα	PI 4-kinase	PI
PIK1	PI4KIIIβ	PI 4-kinase	PI
LSB6	PI4KII	PI 4-kinase	PI
MSS4	Type I PI4P5Kα,β,γ	PI4P 5-kinase	PI4P
	Type II PI5P4Kα,β,γ	PI5P 4-kinase	PI5P (humans only)
	Type II PI4P3K	PI4P 3-kinase	PI4P (humans only)
VAP34	hVSP34	PI 3-kinase	PI
FAB1	PIKfyve	PIP 5-kinase	PI3P, PI (humans only)
	PI3KI (p100/p85)	$PI(4,5)P_2$ 3-kinase	$PI(4,5)P_2$
Phosphatases			
SAC1	SAC1	PIP phosphatase	PI4P, PI3P (yeast: in vitro)
INP51-53 (SJL1-3)	Synaptojanin 1,2	PIP phosphatase	PI4P, PI3P, $PI(4,5)P_2$, $PI(3,5)P_2$
INP54	INPP5B	PI 5P-phosphatase	$PI(4,5)P_2$, $PI(3,4,5)P_3$
	OCRL1	PI 5P-phosphatase	$PI(4,5)P_2$, $PI(3,4,5)P_3$
	SHIP1/2 (INPP5D/INPPL1)	PI 5P-phosphatase	$PI(3,4,5)P_3$
	TPIPα,β,γ	PI 3P-phosphatase	$PI(3,4,5)P_3$
TEP1 (no phosphotase activity)	PTEN	PI 3P-phosphatase	PI3P, $PI(3,4,5)P_3$
FIG4	hFIG4	PI 5P-phosphatase	$PI(3,5)P_2$
YMR1	MTM1, MTMR1-4,6-8	PI 3P-phosphatase	PI3P, $PI(3,5)P_2$ (human only)
	INPP4A,B	PI 4P-phosphatase	$PI(3,4)P_2$

Table S.4. List of yeast sphingolipid biosynthesis genes with their corresponding enzymatic name and function

Yeast Gene	Enzyme	Function
LCB1/2,TSC3 (SPT Complex)	Serine palmitolstransferase	LCB synthesis
ORM1/2	SPT inhibitor	SPT inhibitor
SAC1	PI4P phosphatase	PIP phosphatase and regulator of Orm1p/2p
TSC10	3-ketosphinganine reductase	LCB synthesis
SUR2	Sphinganine C4-hydroxylase	LCB synthesis/Ceramide synthesis
LAG1	Ceramide synthase	Ceramide synthesis
LAC1	Ceramide synthase	Ceramide synthesis
LIP1	Ceramide synthase	Ceramide synthesis
AUR1	Phosphatidylinositol:ceramide phosphoinositol transferase	Complex sphingolipid synthesis
KEI1	Phosphatidylinositol:ceramide phosphoinositol transferase	Complex sphingolipid synthesis
CSG1/2	Mannosylinositol phosphorylceramide synthase	Complex sphingolipid synthesis
CSH1	Mannosylinositol phosphorylceramide synthase	Complex sphingolipid synthesis
IPT1	mannose-(inositol-P)2-ceramide phosphoinositol transferase	Complex sphingolipid synthesis
LCB4/5	LCB Kinase	LCB turnover
DPL1	Dihydrosphingosine phosphate lyase	LCB turnover
LCB3/YSR3	Dihydrosphingosine 1-phosphate phosphatase	LCB synthesis
ISC1	Inositol phosphosphingolipid phospholipase C	Complex sphingolipid turnover

Table S.5. List of human ORP and their corresponding domains, cellular localization, lipid ligand, and diseases associations

Data modified and summarized from Pietrangelo and Ridgeway 2018 (452).

ORP	Domains	Localization	Ligand	Disease Association
OSBP	PH, FFAT, ORD	ER-trans-Golgi MCS	25OHC and other oxysterols, cholesterol, PI4P	ALS8
ORP1	ANK, PH, FFAT, ORD (ORP1L) ORD (ORP1S)	ER-endosome MCS (ORP1L) Cytosol and nucleus (ORP1S)	24(S)OHC, 22(R)OHC, 25OHC, 7KC, cholesterol	Dyslipidemia
ORP2	FFAT, ORD	ER-LD MCS, Golgi	22(R)OHC, 7KC, 25OHC, cholesterol	Autosomal Dominant non-syndromic hearing loss, Dyslipidemia, ALS8
ORP3,	PH, FFAT, ORD	PM-ER MCS (Mochizuki et al 2018), Cytosol, ER, PM	Photo-25OH, photo-cholesterol	Glioblastoma, Breast Cancer, Dyslipidemia, Pancreatic ductal carcinoma, metastasis, ALS8
ORP4	PH, FFAT, ORD (ORP4L) FFAT, ORD (ORP4M) ORD (ORP4S)	Cytosol (ORP4L) vimentin (ORP4S/M/L)	25OHC, 7KC 20OHC, 22 (R)OHC, 22(S)OHC, 7OHC, cholesterol	T-Cell acute lymphoblastic leukemia Chronic myeloid leukemia, Spermatogenesis Cholangiocarcinoma, Pancreatic cancer
ORP5	PH ORD TM	PM-ER MCS, ER-Mitochondria MCS (Soha et al 2018)	PS, PI4P, dehydroergosterol, cholesterol?	Metastatic lung cancer, Alcohol dependence, Dyslipidemia
ORP6	PH, FFAT, ORD	PM-ER MCS (Mochizuki et al 2018) ER-endosome MCS, NE, Cytosol, ER, PM	Photo-25OH, PI4P? (Mochizuki et al 2018)	Dyslipidemia, Alzheimer's syndrome
ORP7	PH, FFAT, ORD	Cytosol ER PM	Photo-25OH	Cholangiocarcinoma, Dyslipidemia, Gastric cancer,
ORP8	PH, ORD, TM	PM-ER MCS, ER-Mitochondria MCS (Soha et al 2018)	PS, PI4P, Cholesterol, 25OHC?	Cholangiocarcinoma, Dyslipidemia, Gastric cancer, hepatocellular carcinoma
ORP9	PH, FFAT, ORD (ORP9L) FFAT, ORD (ORP9S)	ER-trans-Golgi MCS (ORP9L), ER (ORP9S)	Cholesterol, PI4P	Colorectal cancer dyslipidemia
ORP10	PH, ORD (ORP10L) ORD (ORP10S)	Microtubule, Golgi (ORP10L) Nuclear (ORP10S)	PS, PI4P cholesterol?	Dyslipidemia, prostate cancer, hypertension
ORP11	PH, ORD	Golgi-Late endosome MCS	?	Dyslipidemia

Table S.6. List of yeast OSHs and their corresponding domains, localization, and lipid ligand.

OSH Gene	Domains	Localization	Ligand
OSH1	ANK, PH, FFAT, ORD	NVJ	Sterols, PI4P
OSH2	ANK, PH, FFAT, ORD	PM-ER MCS, cytosol	Sterols, PI4P
OSH3	GOLD, PH, FFAT, ORD	PM-ER MCS, cytosol	PI4P
OSH4	ORD	Golgi, vesicles, cytosol	Sterols, PI4P
OSH5	ORD	Vacuole?	Sterols
OSH6	ORD	PM-ER MCS, cytosol	PS, PI4P
OSH7	ORD	PM-ER MCS, cytosol	PS, PI4P

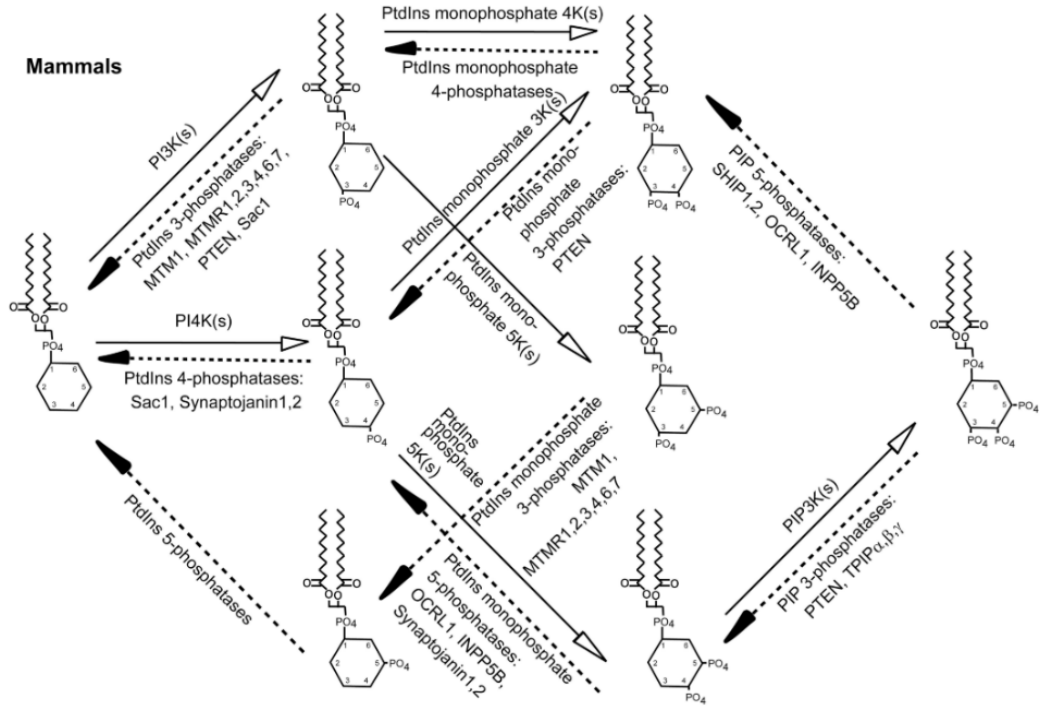

Figure S.1. Phosphatidylinositol phosphates (PIP) synthesized in humans and the corresponding phosphatases and kinases.

Phosphoinositide metabolism in human cells. The execution points of the mammalian PI kinases and PI phosphatases that regulate the synthesis and turnover of PIPs, respectively, are identified. Reprinted by permission from Elsevier, Progress in Lipid Research, Phosphoinositide phosphatases in cell biology and disease, Liu Y., and Bankaitis V. A., 2010.